

Exploring the glycosylation potential of glucanases

From enzyme to product

Tim Devlamynck

Cover design: Marta Martínez García

Printed by: University Press

ISBN: 9789463570428

Tim Devlamynck was supported by a fellowship of the Ubbo Emmius Fund (University of Groningen) and the Special Research Fund (Ghent University).





university of
 groningen



Exploring the glucosylation potential of glucansucrases

From enzyme to product

PhD thesis

to obtain the degree of PhD at the
 University of Groningen
 on the authority of the
 Rector Magnificus Prof. E. Sterken
 and in accordance with
 the decision by the College of Deans

and

to obtain the degree of PhD at
 Ghent University
 on the authority of the
 Rector Prof. R. Van de Walle
 and in accordance with
 the decision by the Faculty Doctoral Commission

Double PhD degree

This thesis will be defended in public on

Friday 27 October 2017 at 14.30

by

Tim Nick Devlamynck

born on 12 January 1990
 in Torhout, Belgium

Supervisors

Prof. L. Dijkhuizen
Prof. W. Soetaert

Copromotor

Dr. E. M. te Poele

Assessment committee

Prof. R. M. Boom
Prof. G. J. W. Euverink
Prof. D. B. Janssen
Prof. J. Van Camp

Table of contents

Chapter 1	General introduction	7
Chapter 2	Glucansucrase Gtf180-ΔN of <i>Lactobacillus reuteri</i> 180: suppressing α-glucan synthesis results in improved glycosylation yields	49
Chapter 3	Improving the low operational stability of Gtf180-ΔN from <i>Lactobacillus reuteri</i> 180 by means of its immobilization	89
Chapter 4	Glucansucrase (mutant) enzymes from <i>Lactobacillus reuteri</i> 180 efficiently transglucosylate <i>Stevia</i> component rebaudioside A, resulting in a superior taste	107
Chapter 5	Glucosylation of stevioside by Gtf180-ΔN-Q1140E improves its taste profile	139
Chapter 6	Biocatalytic production of novel steviol glycosides with improved taste: scale-up, downstream processing and cost analysis	169
Chapter 7	Glucosylation of neohesperidin dihydrochalcone from citrus fruits: glucansucrase Gtf180-ΔN-Q1140E as biocatalyst for the glycodiversification of sweet glycosides	201
Chapter 8	Summary and future prospects	225
Samenvatting		233
References		243
Dankwoord		261

Chapter 1

General introduction

Introduction

For many centuries, micro-organisms (and their enzymes) have been employed for the production of bread, beer, vinegar, etc. without any understanding of the underlying biochemical principles. At present, we know that enzymes are nature's highly efficient and specific catalysts, performing a diverse array of reactions. Enzymes catalyze all processes essential for life such as DNA replication and transcription, protein synthesis, metabolism, etc. Conventional enzyme applications include the addition of proteases and lipases to laundry detergents, the clarification of fruit juices by pectinases or denim washing by cellulases (bio-stonewashing).

More recently, enzymes have gained interest as industrial biocatalysts, due to their ability to perform highly specific chemical reactions in aqueous media with low energy inputs, which makes biocatalysis more cost effective and eco-friendly than conventional chemical synthesis^{1,2}. Moreover, the advent of recombinant DNA technology made it possible to produce enzymes in relatively large quantities, in order to meet the constantly increasing demand³. Initial drawbacks of biocatalysts, such as low operational stabilities and limited substrate specificities, can be overcome by enzyme engineering technologies, such as directed evolution, high-throughput screening of mutant libraries and *in silico* rational design⁴. In 2014, the global market for industrial enzymes was estimated to have a value of roughly \$4.2 billion. A compound annual growth rate (CAGR) of approximately 7% was predicted, reaching a market of nearly \$6.2 billion by 2020⁵.

A fine example of a biocatalytic process with industrial potential is the enzymatic glycosylation of small molecules. *In vivo*, glycosylation is a way to structurally diversify natural products, such as alkaloids, steroids, flavonoids and antibiotics. Glycosylated molecules typically display different physicochemical and biological properties than their non-glycosylated aglycons⁶. The most obvious effect of glycosylation is the improved solubility of hydrophobic compounds, which has a

direct impact on their bio-availability. Moreover, the stability of labile molecules against light and oxidation can be enhanced. For example, glycosylated ascorbic acid is much more stable against oxidative degradation than the aglycon, making high-value applications of ascorbic acid in cosmetics possible⁷. Interestingly, the flavor of many food ingredients is modified by glycosylation. For example, steviol glycosides, the molecules which give the leaves of *Stevia rebaudiana* its sweet taste, display different degrees of sweetness, bitterness and other off-flavors depending on the number, location and configuration of the attached glycosyl moieties⁸. Glycosylation, more specifically galactosylation, offers the possibility to target compounds towards the liver as a way of site-specific drug delivery⁹. Furthermore, it has been demonstrated that glycosylation is an effective tool for the modulation of the activity spectrum of glycopeptide antibiotics, a process known as “glycorandomization”¹⁰. These examples illustrate the need for cheap and efficient glycosylation technologies, useful both in the laboratory and in industry. This PhD study focused on the optimization of glycosylation reactions catalyzed by glucansucrase Gtf180 from *Lactobacillus reuteri* 180 and the characterization of its glycoside products, with an important emphasis on the glycosylation of steviol glycosides. This introductory chapter explores the state of the art glycosylation technologies after which glucansucrase-mediated glycoside synthesis is further elaborated. The scope of the thesis is presented at the end of this chapter.

Synthesis of glycosides: state of the art technologies

A wide diversity of glycosides occurs in nature and could in theory be extracted from their production host (mostly plants). However, extraction is a labor-intensive, low-yielding process, restricting its application to highly priced compounds such as anthocyanins¹¹ and certain polyphenol glycosides¹². The quest for alternative approaches has led to the development of chemical, enzymatic –and *in vivo* (bioconversion and fermentation) synthesis of glycosides, each briefly discussed below.

Chemical glycosylation

Although a large variety of chemical glycosylation protocols has been developed over the years, chemical glycoside synthesis still largely relies on four reactions, differing in the glycosyl donors and the activation agents applied¹³ (Figure 1).

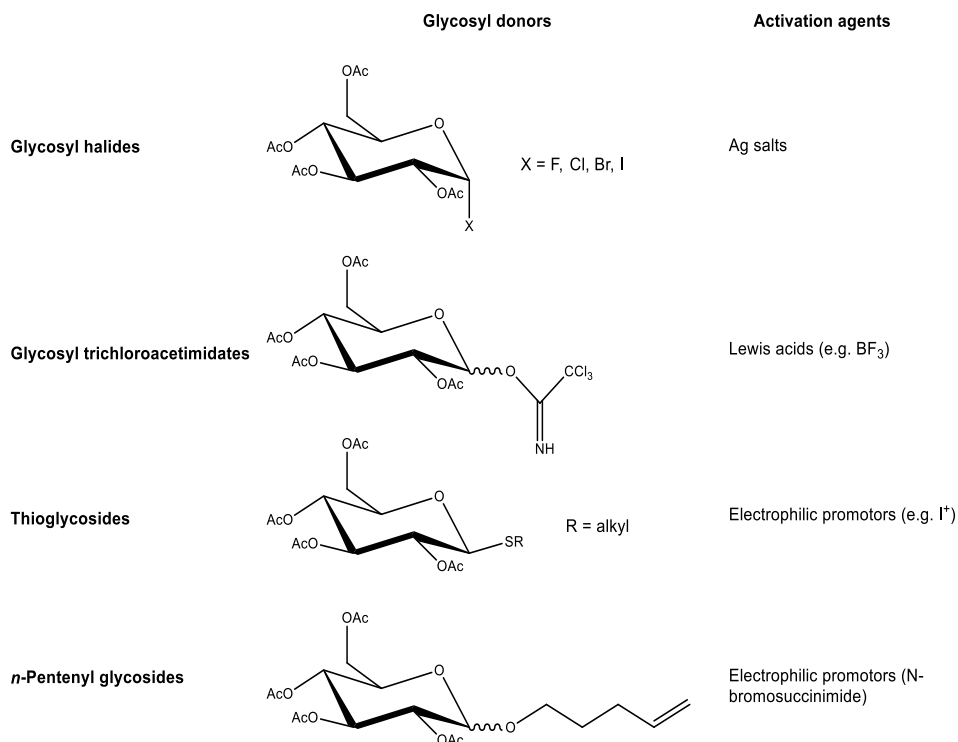


Figure 1. Glycosyl donors and corresponding activation agents applied in chemical glycoside synthesis. Ac = acetyl.

Chemical glycosylations generally follow a unimolecular S_N1 mechanism (unimolecular nucleophilic substitution). The activation agent assists in the departure of the leaving group, resulting in the formation of an oxocarbenium ion which is then attacked by the nucleophilic acceptor substrate¹⁴. Chemists face two big challenges when developing chemical glycosylation reactions: regio –and linkage (α or β linkage) selectivity. The former is adequately dealt with by the application of appropriate protective groups. The latter is determined by the nature of the protecting group on the C-2 of the donor substrate, i.e. by

anchimeric assistance or neighboring-group participation. In short: a participating group, traditionally an acyl moiety, sterically hinders one face of the glycosyl ring, which results in the stereoselective formation of a 1,2-trans –or 1,2-cis linkage. Depending on the nature of the donor substrate (e.g. glucose or mannose), this stereoselectivity is translated into α –or β -selectivity^{15,16}.

The chemical synthesis of glycosides typically includes multiple steps (resulting in low overall yields), time-consuming activation and protection procedures, the use of toxic catalysts and solvents and the production of a considerable amount of waste¹⁵. Alternatively, several carbohydrate-active enzymes (CAZymes; <http://www.cazy.org>) can be applied for glycoside synthesis, without the limitations associated with chemical glycosylation. CAZymes display a high regio –and stereospecificity, which makes labor-intensive protection steps unnecessary, and act in eco-friendly, aqueous media. This results in a remarkable improvement in efficiency, as 5-fold less waste is generated and a 15-fold higher space-time yield is obtained, compared to chemical glycoside synthesis¹⁷.

Enzymatic glycosylation

Four classes of CAZymes, each displaying different advantages and drawbacks, are applied in glycosylation reactions (Figure 2).

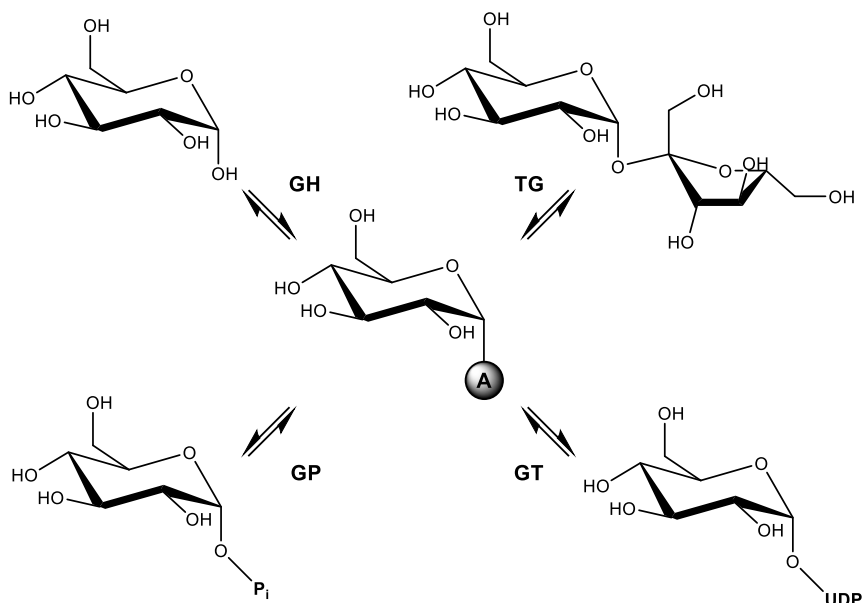


Figure 2. CAZymes and corresponding donor substrates used for enzymatic glycoside synthesis. **GH** Glycoside hydrolases; **TG** Transglycosidases; **GP** Glycoside phosphorylases; **GT** “Leloir” Glycosyl transferases.

Nature’s glycosylation catalysts are known as “Leloir” glycosyl transferases (GT, EC 2.4)¹⁸. Despite their high specificity and efficiency, their industrial breakthrough is hampered by their use of expensive nucleotide-activated sugars (mostly UDP-sugars) as donor substrates. GT-mediated glycosylation with *in situ* regeneration of nucleotide-activated sugars by sucrose synthase has been proposed as most interesting solution, and was demonstrated for the synthesis of a number of glycosides, e.g. curcumin glucosides¹⁹ and quercetin glycosides²⁰. This strategy not only permits the use of catalytic amounts of UDP, also the glycosylation yields are increased as reverse glycosylation and inhibition of GT by high concentrations of UDP are suppressed. Nevertheless, product concentrations (~ 5 mM) and space-time yields (~ 0.1 g L⁻¹ h⁻¹) are still very low, complicating scale-up to an industrial level. Heterologous enzyme expression (in e.g. *Escherichia coli*), the poor water solubility of many acceptor substrates, and the inhibition of GTs by substrates and products have been identified as most

important bottlenecks, with an urgent need for adequate reaction –and enzyme engineering²¹.

Glycoside phosphorylases (GP, EC 2.4), on the other hand, utilize glycosyl phosphates (e.g. glucose-1-phosphate) for the transfer of a glycosyl moiety, compounds that are easily synthesized in large quantities. Sucrose phosphorylase (SP) can even use inexpensive sucrose as glucose donor substrate for the synthesis of glycosides. Moreover, SP displays activity towards a wide array of acceptor substrates, which makes it the most interesting GP for glycoside synthesis^{22,23}. The main disadvantage of GP is that their glycosylation yields are significantly lower than those of “Leloir” glycosyl transferases, which is caused by their low affinity for alternative acceptor substrates²⁴. Recently, improved glycosylation yields were achieved by the construction of two SP mutants with a better accessibility of the active site, allowing the efficient synthesis of e.g. resveratrol glycosides^{25,26}.

Glycoside hydrolases (GH, EC 3.2.1), *in vivo* catalyzing the hydrolysis of carbohydrates, can be manipulated by dynamic or kinetic control to perform glycosylation reactions *in vitro*. The former strategy, also called reverse hydrolysis, consists of shifting the reaction equilibrium towards glycoside synthesis by increasing the donor and acceptor substrate concentrations, or by lowering the water content²⁷. This approach is typically used for the glycosylation of primary and secondary alcohols by exploiting the high operational stability and robustness of GH towards acceptor substrates and solvents²⁸. For example, allyl- β -D-glucoside was synthesized by almond β -glucosidase in a 90% allyl alcohol solution with high yield²⁹. Kinetic control implies that the donor substrate is activated by a leaving group, e.g. a *para*-nitrophenyl moiety. The leaving group is released, yielding an activated anomeric center which is then attacked by the acceptor substrate. The resulting yield is consequently higher than the equilibrium yield. However, the reaction has to be stopped on time, otherwise the thermodynamically favored hydrolytic reaction takes over²⁸. To cope with the inherent hydrolytic nature of GH, many successful enzyme engineering strategies have been developed over the past years, most notably resulting in the

development of glycosynthases³⁰. These enzymes constitute a class of GH mutants that promote glycosidic bond formation, provided a suitable activated glycosyl donor is supplied, but do not hydrolyze the newly formed glycosidic linkage. A famous example is the E197S mutant of cellulase Cel7B from *Humicola insolens*, capable of efficiently glycosylating several flavonoids with reaction rates that are comparable with those of “Leloir” glycosyltransferases³¹.

Last but not least, transglycosidases (TG, EC 2.4) constitute an interesting class of glycosylation biocatalysts. They only require readily available, non-activated carbohydrates (e.g. sucrose) as donor substrates for glycoside synthesis. TG are in fact retaining glycoside hydrolases that are able to avoid water as acceptor substrate, instead catalyzing the glycosylation of carbohydrates by an intra- or intermolecular substitution at the anomeric position of a certain glycoside³². In addition, they can also be applied for glycoside synthesis. Cyclodextrin glucanotransferases (CGTase, family GH13) have for example been used for the glycosylation of resveratrol into α -glycosylated products with a conversion degree of 50%³³. Another interesting group of TG are glucansucrase enzymes (family GH70). The glucansucrase Gtf180- Δ N (an N-terminally truncated version of the Gtf180 enzyme) from *L. reuteri* 180 was the glycosylation biocatalyst studied in this PhD project, therefore glucansucrases are discussed in more detail below.

***In vivo* glycosylation**

The third option to glycosylate small molecules is *in vivo* synthesis, either by bioconversion (resting cells) or fermentation (actively growing cells). Most technologies are based on the overexpression of UDP-glycosyl transferases (UGTs) in a micro-organism, consequently making use of its intracellular UDP-sugar pool. As such, this technology intends to exploit the high specificity of UGTs while circumventing their main constraint for application *in vitro* (i.e. high cost of UDP-sugars)³⁴.

Three major types can be distinguished, differing by the number of micro-organisms used and whether the aglycon is added or not: bacterial coupling,

single cell glycosylation and *de novo* fermentation. As the name suggests, the bacterial coupling strategy consists of combining different hosts, each fulfilling one of three steps in the formation of glycosides (i.e. UTP formation, UDP-sugar formation and UGT-mediated glycosylation).³⁵ Although successfully applied for the production of oligosaccharides^{35,36}, the inherent complexity of this system (separate fermentations to obtain high cell densities of each host involved) makes it an instable and relatively costly process. The development of single cell glycosylations, merging all steps in one organism, thus is a logical next step. Depending on the metabolic state of the cell, bioconversion (resting cells) and fermentation (actively growing cells) can be distinguished. Of the two, fermentation is preferred as it omits some of the disadvantages associated with bioconversion. Indeed, the latter often requires permeabilization of the host and suffers from decreasing productivities over time, caused by cell decay. In contrast, actively growing cells display enhanced productivities over time³⁴. Later on, the advances in the field of metabolic engineering even resulted in the development of *de novo* fermentation of glycosides, thereby eliminating the need for the addition of acceptor substrates. A limited number of successful examples, applying the traditional hosts *E. coli* and *Saccharomyces cerevisiae*, are reported, e.g. vanillin glucoside³⁷, resveratrol glucosides³⁸ and steviol glycosides^{8,39}.

In general, the currently developed *in vivo* glycosylation processes all suffer from very low product concentrations (~ 1 g/L), which can partly be explained by the low solubility and toxicity of many of the target compounds³⁷⁻⁴². On the other hand, the described processes lack the ability to efficiently (re)generate UDP-sugars, which results in their rapid depletion and, hence, low product yields. Much effort is thus still required to turn *in vivo* glycosylation, in whatever form, into an economically feasible process.

Case study: Glycosylation of steviol glycosides

The various advantages and disadvantages of the previously discussed glycosylation technologies are nicely illustrated by using the glycosylation of *Stevia* glycosides as case study. The steviol glycosides of the plant *Stevia rebaudiana*, native in Paraguay and Brazil, were approved for use as high-intensity sweetener (HIS) in food products by the European Commission in 2011⁴³. Although the share of HIS in the global sweetener market, estimated at US\$ 68 billion annually, is currently not significant (Figure 3), the HIS market is predicted to grow significantly over the next years, due to increased consumption of low-calorie food products, fueled by increased consumer awareness of diet-related diseases. Stevia is currently the fastest growing HIS and is expected to reach a value of US\$ 565 million by 2020, reflecting a CAGR of 8.5% during 2014-2020, a significantly faster growth than the total sweetener market, registering a CAGR of 5.7% during the forecast period. The volume consumption of stevia is expected to reach 8507 tons on an annual basis by the end of 2020, the majority of which will be used in beverages and table top sweeteners, collectively accounting for around 72% of the global stevia market⁴⁴. Stevia is projected by the World Health Organization to eventually replace 20% of the sugar segment, equaling a US\$ 10 billion industry⁴⁵. This is significantly greater than 2014 sales, estimated at around US\$ 347 million⁴⁴.

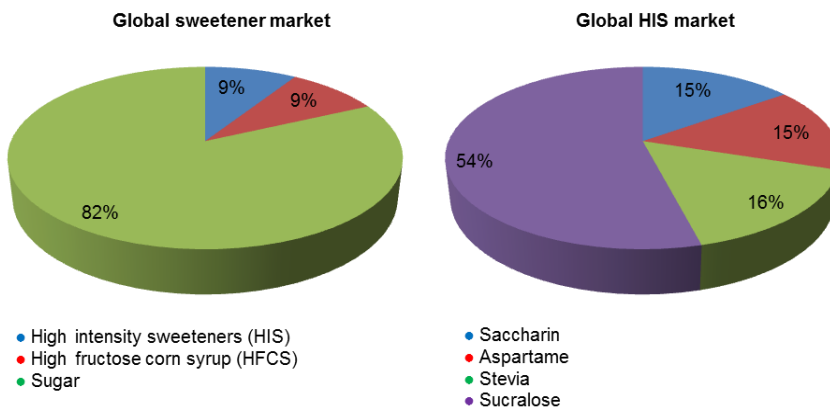
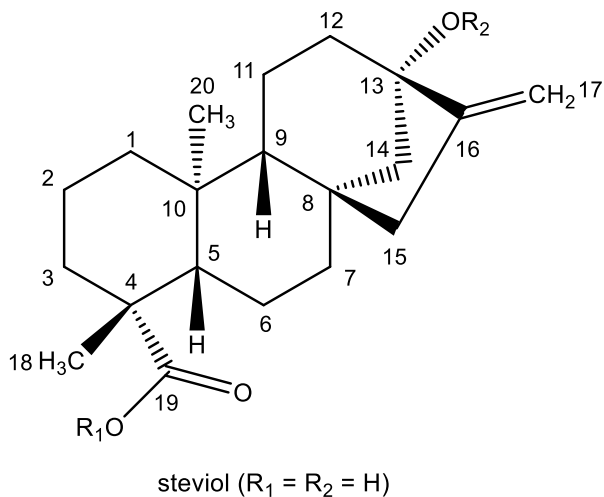


Figure 3. Global sweetener market, estimated at \$68 billion, and global high-intensity sweetener (HIS) market in 2014⁴⁴.



Steviol glycoside	R_1 (C-19)	R_2 (C-13)
Stevioside	Glc(β 1 \rightarrow)	Glc(β 1 \rightarrow 2)Glc(β 1 \rightarrow)
Steviolbioside	H	Glc(β 1 \rightarrow 2)Glc(β 1 \rightarrow)
Rebaudioside A	Glc(β 1 \rightarrow)	Glc(β 1 \rightarrow 2)[Glc(β 1 \rightarrow 3)]Glc(β 1 \rightarrow)
Rebaudioside B	H	Glc(β 1 \rightarrow 2)[Glc(β 1 \rightarrow 3)]Glc(β 1 \rightarrow)
Rebaudioside C	Glc(β 1 \rightarrow)	Rha(α 1 \rightarrow 2)[Glc(β 1 \rightarrow 3)]Glc(β 1 \rightarrow)
Rebaudioside D	Glc(β 1 \rightarrow 2)Glc(β 1 \rightarrow)	Glc(β 1 \rightarrow 2)[Glc(β 1 \rightarrow 3)]Glc(β 1 \rightarrow)
Rebaudioside E	Glc(β 1 \rightarrow 2)Glc(β 1 \rightarrow)	Glc(β 1 \rightarrow 2)Glc(β 1 \rightarrow)
Rebaudioside F	Glc(β 1 \rightarrow)	Xyl(β 1 \rightarrow 2)[Glc(β 1 \rightarrow 3)]Glc(β 1 \rightarrow)
Rebaudioside M	Glc(β 1 \rightarrow 2)[Glc(β 1 \rightarrow 3)]Glc(β 1 \rightarrow)	Glc(β 1 \rightarrow 2)[Glc(β 1 \rightarrow 3)]Glc(β 1 \rightarrow)
Rubusoside	Glc(β 1 \rightarrow)	Glc(β 1 \rightarrow)
Dulcoside A	Glc(β 1 \rightarrow)	Rha(α 1 \rightarrow 2)Glc(β 1 \rightarrow)

Figure 4. Chemical structures of the most prevalent steviol glycosides found in the leaves of *Stevia rebaudiana*. They are, without exception, glycosides of steviol, a diterpene compound. Glucose (Glc), xylose (Xyl) and rhamnose (Rha) occur in the pyranose ring form. Glc and Xyl have the D configuration and Rha the L configuration.

Stevia extract mainly consists of the steviol glycosides rebaudioside A (RebA, 2-4 % of leaf dry weight) and stevioside (5-10% of leaf dry weight) (Figure 4). As most steviol glycosides, they display a lingering bitterness which has limited their successful commercialization⁴⁶. Solving the taste issue of *Stevia* holds the potential to greatly expand its use, for example by allowing the creation of zero-calorie stevia soft drinks. Although the correlation between the structure of steviol glycosides and their taste quality is still not fully understood, it is clear that the latter depends on the number, location and configuration of the glycosyl moieties⁸. In general, the bitterness is correlated with the total number of attached glycosyl units: steviol glycosides with fewer glycosyl residues are more bitter than steviol glycosides with more glycosyl residues⁴⁶. Glycosylation of steviol glycosides has consequently been proposed multiple times as bitterness-eliminating and taste-improving process.

Chemical glycosylation of steviol glycosides

Chemical glycosylation of steviol glycosides has – unsurprisingly – not been widely reported since this strategy is characterized by a vast complexity of (de)protection steps and the use of many toxic chemical reagents, which is undesired for food applications. The importance of these studies is therefore merely academic⁸. However, one patent application, reporting the chemical synthesis of rebaudioside D (RebD) from RebA, has to be noted^{47,48}. RebD is considered the “holy grail” of *Stevia* glycosides due to its superior taste profile compared to RebA and stevioside. Unfortunately, its low presence in the *Stevia* plant (around 0.3% of leaf dry weight or 2.5% of total steviol glycosides) makes RebD extraction impractical and costly, urging the need for its synthesis⁴⁹. In short, the reported chemical synthesis of RebD included 4 main steps (Figure 5): **1** conversion of RebA into rebaudioside B by alkaline treatment, **2** acetylation of the free hydroxyl groups at the C-13 site, **3** glycosylation of the free C-19 carboxyl group with acetylated α -sophorosyl bromide by activation with silver carbonate, and **4** deacetylation yielding RebD, resulting in a low overall yield of 8.1%, illustrative for chemical glycosylations in general^{47,48}.

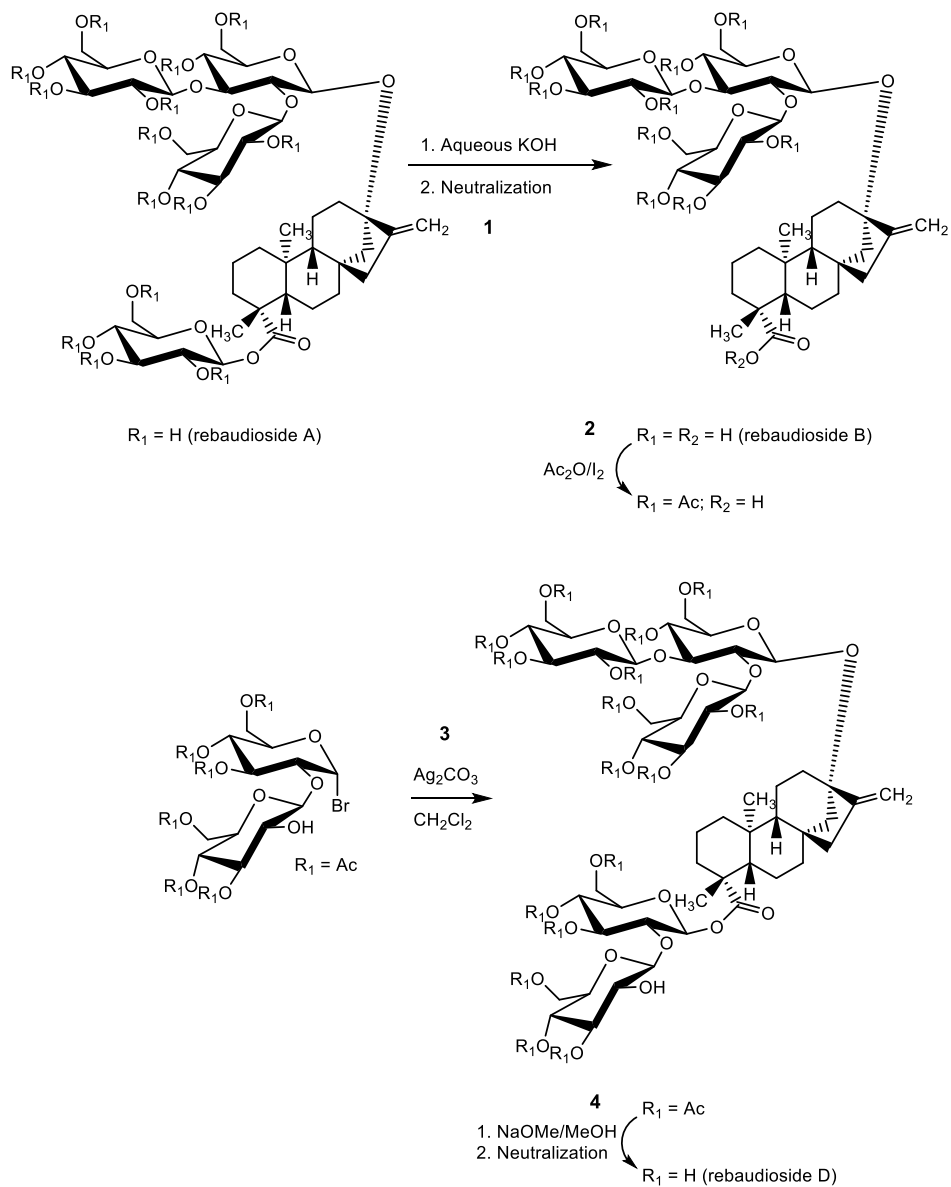


Figure 5. Chemical synthesis of rebaudioside D from rebaudioside A⁴⁷.

Enzymatic glycosylation of steviol glycosides

Due to the many disadvantages of chemical glycosylation routes, enzymatic glycosylation has been applied – with and without success - to improve the taste

profile of steviol glycosides, mainly by using cyclodextrin glucanotransferases (CGTases)⁵⁰⁻⁵⁶, UDP-glycosyltransferases (UGTs)⁵⁷⁻⁵⁹ and glycoside hydrolases (GHs)⁶⁰⁻⁶⁵. Although CGTase-catalyzed glycosylations often result in high yields, a poor C-13/C-19-regiospecificity is obtained⁵¹, which has been shown to be of major influence for the taste quality of the glycosylated products. For example, (α 1 \rightarrow 4)-glycosylation of stevioside and rubusoside at the C-13 steviol position yielded products with improved intensity and quality of sweetness, whereas (α 1 \rightarrow 4)-glycosylation at the C-19 position resulted in an increased bitterness⁵²⁻⁵⁴. Moreover, several studies reported that the many multiglycosylated products synthesized by CGTases were perceived as more bitter than their monoglycosylated counterparts^{50,53}. This lack of selectivity resulted in a complicated and costly purification process to obtain the monoglycosylated product with improved taste, limiting the industrial application of CGTases for the glycosylation of steviol glycosides. Some progress has been made by using micro-wave assisted glycosylation with a CGTase from *Bacillus firmus* (from 46% to 66% monoglycosylation)⁵⁵ and, more recently, by application of a CGTase found in a *Paenibacillus* sp. isolated from *Stevia* farmland, yielding a single monoglycosylated product but, unfortunately, also displaying a low total conversion⁵⁶. To this date, the shortcomings of CGTase-catalyzed glycosylation of steviol glycosides largely remain. Improvement of the product specificity by mutational engineering is consequently strongly required.

Few studies report the glycosylation of steviol glycosides by UGTs *in vitro*⁵⁷⁻⁵⁹. Of industrial interest is the application of UGT76G1 from *S. rebaudiana* in combination with sucrose synthase from *Arabidopsis thaliana*, regenerating the costly UDP-glucose, for the conversion of stevioside into the better-tasting RebA. Although a reasonably high conversion degree was obtained (78%), the productivity was very low: less than 2 mM RebA was synthesized in 30 h⁵⁹. Similarly, UGT91D2 from *S. rebaudiana* has been used for the synthesis of RebD from RebA, however, only a 4.7% conversion was obtained⁵⁷. In order to circumvent the usage of UDP-glucose as donor substrate, UGT76G1 and UGT91D2 have been applied *in vivo* for the synthesis of RebD and rebaudioside M (RebM), as described in detail below.

The substrate promiscuity of glycoside hydrolases has been exploited for the glycosylation of various alternative acceptor substrates, including steviol glycosides. For example, incubation of stevioside with maltose in the presence of Biozyme L, a commercially available β -amylase preparation, resulted in the ($\alpha 1 \rightarrow 6$)-glycosylation at the C-19 site and the ($\alpha 1 \rightarrow 6$) –and ($\alpha 1 \rightarrow 3$)-glycosylation at the C-13 site. Only the former product displayed an improved taste profile, again illustrating the importance of regio –and linkage specificity on the sensory properties⁶⁰. More recently, an α -amylase from *B. amyloliquefaciens* was applied as biocatalyst for the glycosylation of stevioside, using soluble starch as donor substrate (38% conversion)⁶¹. Remarkably, RebA turned out to be a much poorer acceptor substrate (1% conversion), results that were repeated with an α -amylase from *A. oryzae*⁶². A biocatalyst capable of glycosylating stevioside and RebA holds great commercial potential since it could be applied for the glycosylation of *Stevia* extract instead of the more expensive high-purity steviol glycosides. To date, no biocatalyst has been shown to efficiently glycosylate both steviol glycosides.

Also of great potential value is the application of β -glucosidases for the glycosylation of steviol glycosides, as these enzymes introduce the naturally occurring β -linkages. However, the currently described processes suffer from several drawbacks, including low conversions, the use of rare donor substrates (e.g. curdlan, a ($\beta 1 \rightarrow 3$)-glucan), very long incubation times, but most importantly, the hydrolysis of the steviol glycoside substrates⁶³⁻⁶⁵. For example, the cell-free extract from the fungus *Gibberella fujikuroi* used stevioside as acceptor substrate and as donor substrate, resulting not only in the formation of RebA but also of steviolbioside, steviolmonoside and finally even steviol, all of which are unwanted side-products with an inferior taste profile⁶⁵. Despite their own shortcomings, UGTs are therefore more suitable for the β -glycosylation of steviol glycosides, as they display mainly transglycosylation activity.

The presented examples illustrate that industrial biocatalysts for the glycosylation of steviol glycosides need to combine an adequate regio –and linkage specificity with high conversion degrees and product yields. This PhD research therefore

studied in more detail the potential of glucansucrase Gtf180- Δ N (mutants) of *L. reuteri* 180 to glycosylate RebA and stevioside, and the sensory properties of the glycosylated products (Chapters 4, 5 and 6). To date, only two studies have reported the glycosylation of stevioside with glucansucrases, whereas RebA glycosylation with glucansucrases has only been described once⁸. A dextransucrase from *Leuconostoc citreum* converted stevioside with a high conversion degree (94%), but its volumetric productivity was low (< 2 g/L/h), despite the addition of 4500 U/mL enzyme⁶⁶. Additionally, glycosylation of stevioside was achieved with an alternansucrase from *L. citreum*, displaying an insufficient conversion degree of 44%⁶⁷. In contrast, the patented *L. reuteri* glucansucrase Gtf180- Δ N based process appears to be much more promising (Chapters 4, 5 and 6)⁶⁸⁻⁷⁰.

***In vivo* production of steviol glycosides**

In addition, *de novo* fermentation of RebD and RebM, steviol glycosides with improved taste compared to RebA and stevioside, has been reported. The patented process applies *S. cerevisiae* to express the complete steviol glycoside pathway, using (mutants of) UGT76G1 as key enzyme^{39,58,71}. One of the main challenges faced is that RebD and RebM are not formed in a linear pathway from steviol, but result from a metabolic glycosylation grid. Their formation is directly dependent on the promiscuous “chameleon” enzyme UGT76G1, not only involved in the synthesis of RebD and RebM, but also catalyzing the formation of many side products, e.g. 1,3-bioside (Figure 6). Homology modelling of UGT76G1 followed by docking of RebD and RebM into the active site of the obtained 3D model, revealed 38 amino acid residues which may play a role in UGT76G1’s acceptor substrate specificity. A site-saturation library of these residues was generated in order to create mutants favoring the synthesis of RebD and RebM. Several mutants indeed displayed an increased accumulation of e.g. RebD, however, this was typically accompanied with a decrease of RebM, and *vice versa*. Moreover, these same mutants often displayed an increased accumulation of e.g. stevioside, which is obviously undesired⁷¹. In addition, the product concentrations reported in the patent application are in the range of 0.5

to 3 g/L, which should be improved in order for the process to reach a viable scale⁵⁸. Nevertheless, a joint-venture of Switzerland-based Evolva, the patent holder, and Cargill, offering its facilities, has announced to launch fermentation-based RebD and RebM (EverSweet™) in 2018 (<http://www.evolva.com>). It should be noted that the initial launching date was set back several times since 2013. The joint venture has indicated that the production costs are still problematic, due to inadequate strain characteristics and too high fermentation and downstream processing costs.

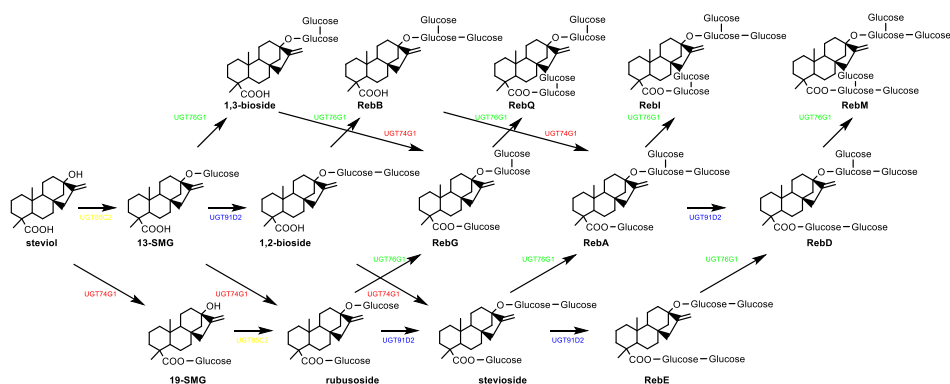


Figure 6. Steviol and the metabolic grid of glycosylation reactions resulting in the synthesis of rebaudioside D and rebaudioside M⁷¹.

Conclusions

From the discussion it is clear that the glycosylation of steviol glycosides holds great commercial potential, resulting in an ongoing development of novel and improved glycosylation processes, enzymatic as well as fermentation-based. The main advantage of *de novo* fermentation over most enzymatic glycosylation reactions is that nature-identical steviol glycosides, i.e. RebD and RebM, are synthesized. On the other hand, these processes may suffer from disputes concerning their GMO nature, possibly resulting in their (partial) rejection by consumers⁷². In contrast, many enzymatic glycosylation reactions yield products which will be classified as novel food, requiring additional regulatory approval by

e.g. the European Food Safety Agency (EFSA). To their advantage, biocatalysts are generally classified as a processing aid, omitting the obligation for labelling.

Glucansucrases

Glucansucrases are glycoside hydrolase enzymes (GH70) from bacterial origin with an average molecular weight of approximately 160 kDa. They catalyze the conversion of sucrose into α -glucan polysaccharides, linking the α -D-glucopyranosyl units by (α 1 \rightarrow 2), (α 1 \rightarrow 3), (α 1 \rightarrow 4), or (α 1 \rightarrow 6) bonds, depending on the enzyme specificity^{73,74}. In addition, they catalyze the so called acceptor reaction, thereby glycosylating a wide array of carbohydrate and non-carbohydrate acceptor molecules, using sucrose as donor substrate. As such, they form a cheaper alternative for “Leloir” glycosyltransferases, which require rare and expensive nucleotide-activated sugars as donor substrate. Their promiscuity towards different acceptor substrates and their use of inexpensive sucrose as donor substrate have attracted interest from industry for the application of glucansucrases as glycosylation biocatalyst. This section discusses their distribution, structure, reaction mechanism and in particular the acceptor reaction and the optimization thereof.

Distribution of glucansucrases

Glucansucrases have only been isolated from Gram-positive lactic acid bacteria (LAB), such as *Lactobacillus*, *Leuconostoc*, *Streptococcus* and *Weissella*⁷⁵. As their name suggests, LAB produce lactic acid as the major metabolic end product of carbohydrate metabolism. For centuries, this trait has been exploited for the fermentation of food products, such as yogurt and sour beer. The importance of LAB for the food industry is further evidenced by their use as probiotics, as such conferring health benefits on the consumer⁷⁶. More recently, LAB have attracted interest for their production of various exopolysaccharides, compounds attributed with health-enhancing properties. Many of these LAB exopolysaccharides are

produced by glucansucrases, extracellular enzymes which are, depending on the bacterial source, either cell wall-attached, free or both⁷⁷.

Up until the beginning of 2017, 63 GH70 glucansucrases had been characterized, representing a wide variety of linkage specificities, and are listed in the CAZy database (<http://www.cazy.org>). Most of them were obtained from the genera *Leuconostoc* (24 of 63) and *Streptococcus* (21 of 63) and a minority from *Lactobacillus* (13 of 63) and *Weissella* (5 of 63). Some LAB strains express more than one glucansucrase. For example, *L. citreum* NRRL B-1299 (originally *L. mesenteroides* NRRL B-1299) is known to produce six different glucansucrases⁷⁸ whereas *Streptococcus mutans* produces three⁷⁹.

Structure of glucansucrases

The primary structure of all glucansucrase proteins can be divided in four distinct regions: 1) signal peptide (SP), 2) N-terminal variable region (VR), 3) conserved catalytic domain (CD) and 4) C-terminal glucan-binding domain (GBD)⁸⁰. As glucansucrases are extracellular enzymes, their N-terminus contains a signal peptide, typical for Gram-positive bacteria, of 36 to 40 amino acids. Adjacent to SP is a highly variable region which contains between 200 and 700 amino acids, depending on the glucansucrase. Exception to the rule is glucansucrase DsrA from *L. citreum* NRRL B-1299 which has no VR, suggesting that this region is not essential for glucansucrase activity⁸¹. Deleting the VR of several glucansucrases confirmed this hypothesis, since no effect on the enzyme activity nor structure of the α -glucans synthesized could be determined. For example, deleting the VR (residues 0-742) of Gtf180 from *L. reuteri* 180 resulted in an enzyme (Gtf180- Δ N) with nearly identical biochemical characteristics. Moreover, the N-terminally truncated enzyme could be produced in *E. coli* with a higher yield, compared to production of the WT enzyme^{80,82}.

The crystal structures of four GH70 glucansucrases are currently available (Figure 7): Gtf180- Δ N from *L. reuteri* 180⁸³, GtfA- Δ N from *L. reuteri* 121⁸⁴, Gtf-SI (amino acid residues 244-1163) from *S. mutans*⁸⁵ and the Δ N₁₂₃-glucan-binding

domain-catalytic domain 2, a truncated form of DsrE from *L. citreum* NRRL B-1299⁸⁶. They all share a common domain organization and a common architecture. Interestingly, the elucidation of these crystal structures revealed a different domain organization than the one predicted by sequence alignment: all crystal structures represent a U-shape, composed of five domains (A, B, C, IV and V). Domains A, B, IV and V are formed by discontinuous N- and C-terminal stretches of the polypeptide chain, while domain C consists of a contiguous polypeptide chain, forming the bottom part of the tertiary U-shape structure.

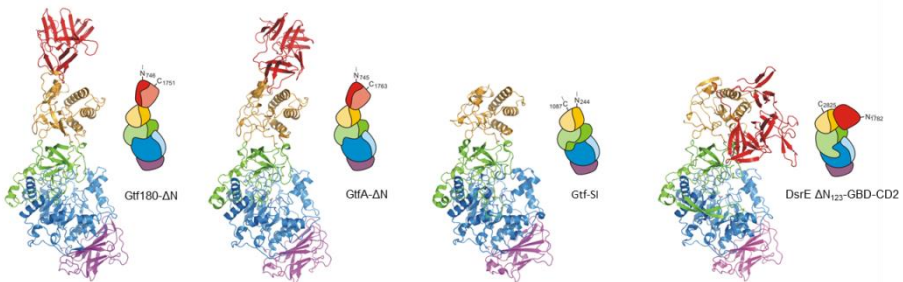


Figure 7. Three-dimensional structures and schematic domain organization of GH70 glucansucrases (Gtf180- Δ N (PDB: 3KLN, 1.65 Å), GtfA- Δ N (PDB: 4AMC, 3.60 Å), Gtf-SI (PDB: 3AIE, 2.1 Å) and DsrE Δ N₁₂₃-GBD-CD2 (PDB: 3TTQ, 1.90 Å). Domains are colored in blue (A), green (B), magenta (C), yellow (IV) and red (V). This figure has been adapted from Leemhuis et al. 2013⁷⁵.

Similarly to GH13 enzymes, domains A, B and C form the catalytic core. In contrast, enzymes from family GH13, including amylosucrases, lack domains IV and V. Their role in GH70 glucansucrases has remained largely unknown, however, it was proposed that domain IV acts as a hinge, supporting the rotation of domain V, thereby allowing the latter to bring the bound glucan chain in proximity of the catalytic site⁸⁵. This hypothesis is supported by the positional variability of domain V among the different crystal structures⁸³⁻⁸⁶. Moreover, the flexibility of domain V was demonstrated by the elucidation of an alternative crystal structure of Gtf180- Δ N: a 120° rotation of domain V was observed compared to the previously elucidated crystal structure⁸⁷. Deletion of Gtf180- Δ N's domain V also heavily impaired its polysaccharide forming ability, confirming the

hinge hypothesis yet again⁸⁸. Domain A adopts a circularly permuted (β/α)₈-barrel fold, as predicted by sequence alignment with GH13 enzymes⁸⁹, containing the three catalytic residues (nucleophile, acid/base catalyst and transition state stabilizer) at loops following β -strands β 4, β 5 and β 7, respectively. The complete active site is located in a pocket-shaped cavity at the interface of domains A and B. In fact, several amino acids belonging to domain B assist in shaping the substrate binding sites, consequently influencing the reaction specificity⁸³. Additionally, some amino acids between domains A and B form a calcium binding site near the nucleophilic residue; the Ca^{2+} ion is absolutely essential for glucansucrase activity⁷⁵. The function of domain C is not known yet, although it is widely distributed within G13 and G70 enzymes. It is composed out of an eight-stranded β -sheet with a Greek key motif⁸³.

Catalytic mechanism of glucansucrases

According to the CAZy classification system which is based on amino acid sequence similarity⁹⁰, glucansucrases are classified as glycoside hydrolase family GH70. Structurally, mechanistically and evolutionary, they are closely related to enzymes of the GH13 and GH77 families, together forming the GH-H clan⁹¹. Typical for members of the GH-H clan is their use of the α -retaining double-displacement reaction mechanism, involving 3 catalytic residues: a nucleophile, an acid/base catalyst and a transition state stabilizer^{74,92} (Figure 8). Firstly, the glycosidic linkage of donor substrate sucrose is cleaved by the nucleophile. Simultaneously, the acid/base catalyst protonates the fructosyl moiety, resulting in the release of fructose. An β -glucosyl enzyme intermediate, stabilized by the transition state stabilizing residue, is consequently formed. In the next step, this β -glucosyl enzyme intermediate is attacked by the non-reducing end of the acceptor substrate (i.e. sucrose, or a growing oligosaccharide or polysaccharide chain), resulting in product formation with retention of the α -anomeric configuration.

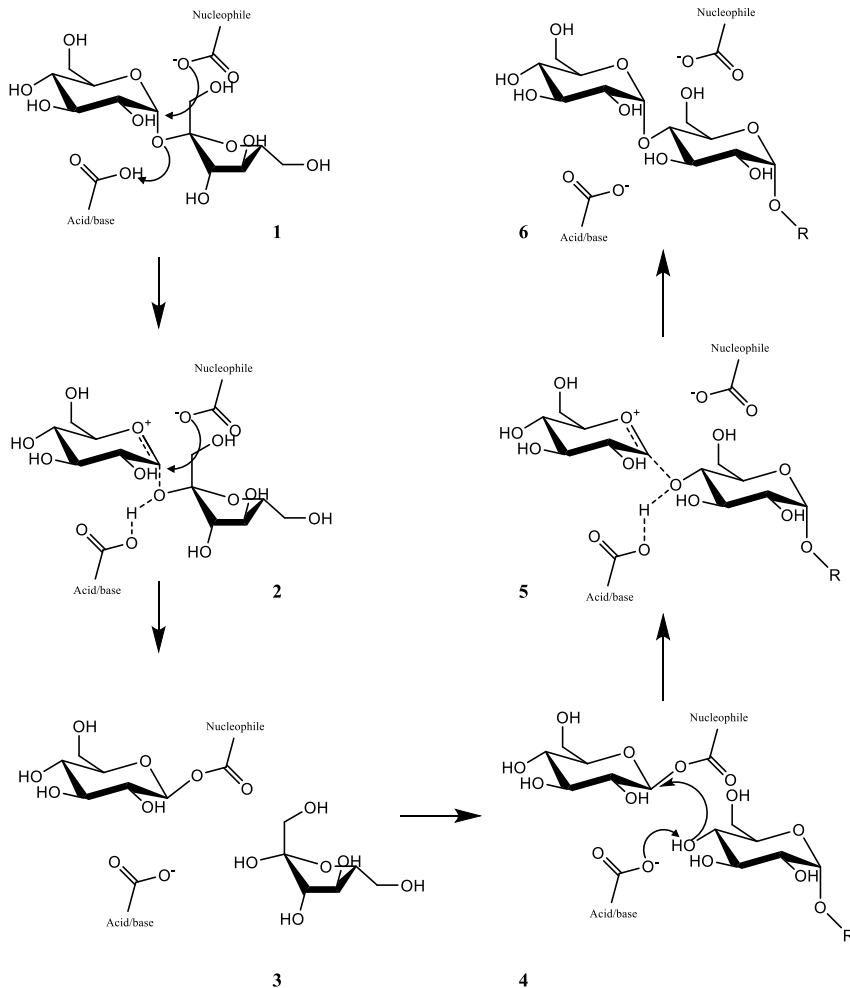


Figure 8. Reaction mechanism used by glucansucrases for α -glucan synthesis. **1** Donor substrate binding, **2** Transition state, **3** β -glucosyl intermediate, **4** Acceptor substrate binding, **5** Transition state, **6** Product formation.

This reaction mechanism is supported by the observed interactions of the catalytic triad (D1025, E1063 and D1136) of the inactive mutant Gtf180- Δ N-D1025N from *L. reuteri* 180 with donor substrate sucrose⁸³. The latter is bound in subsites -1 and +1, which results in the adoption of a distorted half-chair conformation by the -1 glucosyl ring. The seven strictly conserved residues found in subsite -1 (R1023, D1025, H1135, D1136, E1063, Y1465 and Q1509) all interact with the glucosyl moiety of sucrose, orienting the substrate in such

manner that the formation of the covalent intermediate is favored. The anomeric C1 carbon of the glucosyl unit is attacked by the nucleophilic residue (D1025), resulting in the formation of the covalent β -glucosyl enzyme intermediate via an oxocarbenium ion-like transition state. Residue E1063 serves as the acid/base catalyst initially donating a proton to activate fructose as leaving group and subsequently deprotonating the acceptor substrate to increase its nucleophilicity. The partly planar transition state is stabilized by interactions with the transition state stabilizer (D1136), an arginine residue (R1023) and a glutamine residue (Q1509).

The active site of Gtf180- Δ N stretches no further than subsite -1 due to adequate “blocking” by residues Q1140, N1411 and D1458. This creates a pocket-like shape which is also observed in *Neisseria polysaccharea* amylosucrase (belonging to GH13) and is the reason why glucansucrases can only transfer one single glucose moiety per catalytic cycle, while GH13 α -amylases, which have a longer binding groove, can also transfer oligosaccharides. In contrast to subsite -1, the residues found in subsite +1 are much less conserved, which is reflected in the different product specificities that are displayed by glucansucrases and which can be exploited for the glycosylation of alternative acceptor substrates.

Reactions catalyzed by glucansucrases

The β -glucosyl enzyme intermediate, formed in the first step of the catalytic cycle, can not only react with a growing glucan chain to form polysaccharides but also with the hydroxyl group of several carbohydrate and non-carbohydrate acceptor substrates, resulting in the synthesis of oligosaccharides and α -D-glucosides, respectively. Furthermore, also water can act as acceptor substrate, with the hydrolysis of sucrose into glucose and fructose as result^{73,75} (Figure 9).

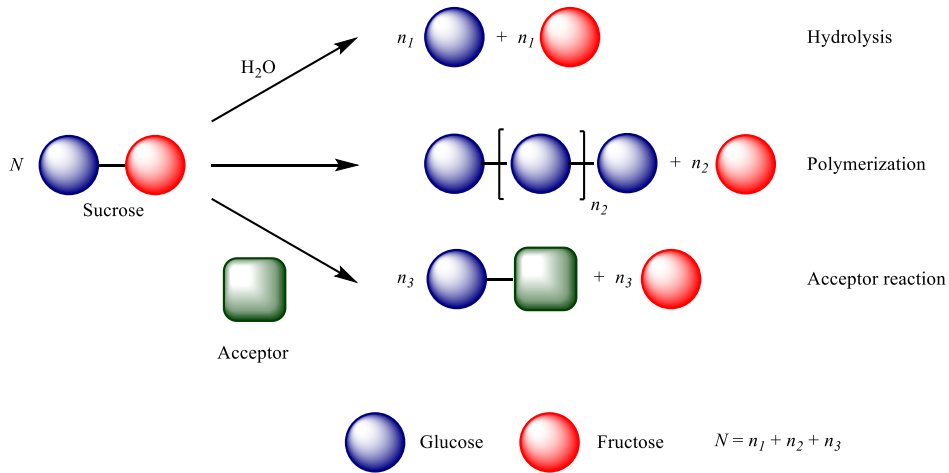


Figure 9. Reactions catalyzed by glucansucrases using sucrose as donor substrate.

α -Glucan synthesis

The dominant reaction of glucansucrases is α -glucan synthesis, also referred to as polymerization reaction. Glucansucrases synthesize a remarkably large diversity of α -glucans, differing in the type of α -glycosidic linkages connecting the glucose moieties (1 \rightarrow 2, 1 \rightarrow 3, 1 \rightarrow 4 or 1 \rightarrow 6), the types and degrees of branching and the molecular mass. Furthermore, the ratios of α -glycosidic bonds and the frequency and length of the branches also vary greatly⁷⁵. The α -glucan structures are classified according to their predominant linkage type. Dextran contains mainly α (1 \rightarrow 6) bonds, mutan mainly α (1 \rightarrow 3) and reuteran mainly α (1 \rightarrow 4). As the name suggests, alternan is composed of alternating α (1 \rightarrow 3) and α (1 \rightarrow 6) bonds. Except for the latter, the different glycosidic linkages are more or less randomly distributed within the polymers^{93,94}. Very often glucansucrases are also named after the product they synthesize, e.g. dextransucrase (EC 2.4.1.5) or alternansucrase (EC 2.4.1.140). The above mentioned parameters have an impact on the physicochemical properties of the α -glucans, such as viscosity, stickiness, solubility, mass, etc.⁷⁵.

Despite the elucidation of several glucansucrase crystal structures and the structural characterization of their α -glucan products, it is still not entirely clear

how glucansucrases synthesize such a wide array of α -glucans. Essentially, α -glucan synthesis is the step-wise addition of glucose moieties to a growing α -glucan chain⁷⁴. Every catalytic cycle starts with the cleavage of the glycosidic bond of sucrose which results in the covalent attachment of the glucosyl moiety at subsite -1, forming the so called β -glucosyl enzyme intermediate. Which type of glycosidic linkage is subsequently formed depends on the orientation of the acceptor substrate. Hence, it is the architecture of the active site, and in particular that of acceptor subsite +1, that determines the glycosidic linkage specificity⁹⁵. Indeed, it has repeatedly been shown that mutations in residues of subsite +1 and +2 lead to the synthesis of α -glucans with altered ratios of glycosidic linkages⁹⁶⁻¹⁰². Unfortunately, there is still little understanding about how the glycosidic linkage specificity is affected by such mutations. Rational design of glucansucrase mutants for the synthesis of pre-defined α -glucan products is thus still very complicated.

For many years, it remained unclear how α -glucan synthesis is initiated, or in other words, which molecule acts as primer. Several studies have since been performed on the structural characterization of the initially formed products, revealing that the formation of α -glucans most typically starts with the glycosylation of sucrose^{103,104}. The latter is thus not only the donor substrate of glucansucrases but at the same time also the acceptor substrate. The consequence is that the glycosylation of alternative acceptor substrates will unavoidably face competition from the synthesis of α -glucans, unless the latter is adequately suppressed by reaction –or enzyme engineering. It has to be noted that one study, investigating the mechanism of DsrS from *L. mesenteroides*, has proposed both sucrose and glucose as primers for α -glucan synthesis, however, it is still unknown if this can be extended to other glucansucrases¹⁰⁵. During the initial phase of α -glucan synthesis, hydrolysis of sucrose into fructose and glucose is the dominant reaction, as the affinity of glucansucrases for sucrose as acceptor substrate is relatively low. Once the preferred acceptor substrates, i.e. α -glucan oligosaccharides, have been formed in sufficient quantities, the hydrolytic activity is suppressed in favor of α -glucan synthesis and α -glucan polysaccharides are efficiently synthesized¹⁰³.

Whether glucansucrases function as a processive or non-processive enzyme has been subject to considerable debate. A number of studies revealed that high-molecular-mass (HMM) glucans reached maximum size after a relatively short time, suggesting that glucansucrases act processively^{103,105,106}. However, also oligosaccharides could be detected in the reaction mixture, indicating a non-processive mode of action¹⁰⁵. Interestingly, no intermediate size α -glucan products were detected. Taking into account all the available information, Remaud-Siméon et al. suggested that glucansucrases follow a semi-processive mechanism: in the initial phase of the reaction, oligosaccharides are synthesized non-processively. When the oligosaccharides reach a certain size, polysaccharides are formed in a processive mode¹⁰⁵. The structural basis of this mechanism is proposed to lie in both domain V and the acceptor binding sites, representing remote and close binding sites for glucan chains, respectively. This was nicely illustrated for Gtf180- Δ N: the truncation of its domain V heavily impaired polysaccharide synthesis in favor of oligosaccharide formation⁸⁸. However, mutations of residues located in the acceptor binding sites (in particular L940 mutants) partially restored the polysaccharide synthesis of the Δ V-truncated enzyme^{98,106}. The elucidation of glucansucrase crystal structures with HMM glucan chains bound to the enzyme is necessary to shed more light on the mechanism of α -glucan synthesis and will without doubt offer new opportunities to engineer the reaction specificity of glucansucrases. The following study serves as good example: the crystal structure of amylosucrase, a special glucansucrase belonging to family GH13, bound with maltoheptaose revealed the absence of domains IV and V but the presence of three oligosaccharide binding sites (OB1, OB2 and OB3)^{107,108}. Molecular modeling and mutational studies confirmed the importance of OB1 and OB2 for polysaccharide synthesis, suggesting that OB2 provides an anchoring platform for the polysaccharide^{107,109}.

Additionally, the elucidation of several glucansucrase crystal structures has revealed that their acceptor substrate binding region is reasonably spacious^{83,84}. Indeed, the synthesis of branched α -glucans demands an acceptor substrate binding region which is capable of accommodating bulky α -glucan chains. As a consequence, glucansucrases display a broad acceptor substrate specificity,

which is exploited in the glycosylation of alternative acceptor substrates such as phenolic compounds, sugar alcohols, etc. Here again, it is still not clear how the formation of branches is triggered in favor of chain elongation.

Hydrolysis

Glucansucrases also are able to catalyze the hydrolysis of sucrose into glucose and fructose, basically acting as a hydrolase enzyme. Especially at low acceptor substrate concentrations, hydrolysis is the dominant reaction. When oligosaccharide products become available, glucansucrases preferentially transfer the glucosyl moiety to these growing α -glucan chains¹⁰³. The crystal structure of the inactive mutant Gtf180- Δ N-D1025N revealed that residue W1065, located at subsite +2, is an important structural determinant for hydrolysis, interacting with the carbohydrate acceptor substrate through hydrophobic stacking. The mutation of W1065 to non-aromatic residues resulted in a significantly increased hydrolysis¹⁰². Also the mutations of residues N1029, providing a direct hydrogen bond to carbohydrate acceptor substrates at subsite +1, and L981, strictly conserved in all glucansucrases, substantially enhanced hydrolysis⁹⁹. The application of these mutants for the glycosylation of non-carbohydrates (such as catechol or hexanol) resulted in improved (mono)-glycosylation yields (Chapter 2)¹¹⁰.

Acceptor reaction

Glucansucrases are not only able to utilize growing α -glucan chains and water as acceptor substrate. Due to their rather wide acceptor substrate binding region, they show a relatively high promiscuity towards several other acceptor substrates¹¹¹⁻¹¹³. This promiscuity can be exploited for the glycosylation of carbohydrates and non-carbohydrates, resulting in the synthesis of oligosaccharides and α -D-glucosides, respectively. Enzymes are particularly suited for glycosylation reactions as they display a high regio- and stereospecificity, a feature that is hard to achieve by chemical synthesis¹³. In nature, glycosylation is performed by “Leloir” glycosyltransferase enzymes (EC

2.4.-). Their industrial use is hampered by the high price of their donor substrates, nucleotide-activated sugars²¹. Glucansucrases offer a cheaper alternative, since they only require the energy stored in the glycosidic linkage of sucrose (~ 27.6 kJ.mol⁻¹) to synthesize their glycosylated products¹¹⁴. In 1953, this so called acceptor reaction was first reported by Koepsell et al¹¹⁵. Their study demonstrated the glycosylation of a large number of sugars and sugar derivatives such as maltose, isomaltose, glucose, and methyl glucoside by a dextransucrase from *L. mesenteroides* NRRL B-512F. Since then, many other carbohydrates were added to the list of acceptor substrates. This makes glucansucrase-mediated glycosylation an effective tool for the production of a wide array of interesting oligosaccharides. Isomalto-oligosaccharides (IMO) of controlled size are produced from sucrose plus maltose or glucose, using a dextransucrase from *L. mesenteroides* NRRL B-512F¹¹⁶. They are attributed with prebiotic properties (i.e. altering the composition and/or activity of the gastrointestinal microflora, as such conferring health benefits upon the consumer) and used as a low calorie sweetener in a variety of foods like bakery and cereal products¹¹⁷. Also lactulosucrose, another prebiotic oligosaccharide, is effectively synthesized by this dextransucrase enzyme, using lactulose as acceptor substrate¹¹⁸. Another example is the glycosylation of the bitter prebiotic gentiobiose with alternansucrase, producing several oligosaccharides with reduced or even eliminated bitterness¹¹⁹.

Glycosylation of non-carbohydrate compounds

The glycosylation of non-carbohydrates, such as aromatic or aliphatic compounds, is a valuable tool for the glycodiversification of these molecules (for examples, see 1. Introduction). A wide range of (poly)phenolic and aliphatic compounds are glycosylated by glucansucrases. The highest conversions are obtained with phenolic compounds with two vicinal (*ortho*-substituted) hydroxyl groups as acceptor substrate (Figure 10). *Meta* –and *para*-substituted phenolics as well as aliphatic compounds are typically not very well glycosylated^{110,120}. Examples of compounds that are glycosylated by glucansucrases are listed in Table I. To obtain insight into the economic viability of these glycosylation

processes, the respective conversion degrees and product yields are given. Although medium to high conversions are obtained, the product yields are usually low. This is partly due to a lack of reaction engineering: the water solubilities of many acceptor substrates are low, which could be improved by the addition of cosolvents.

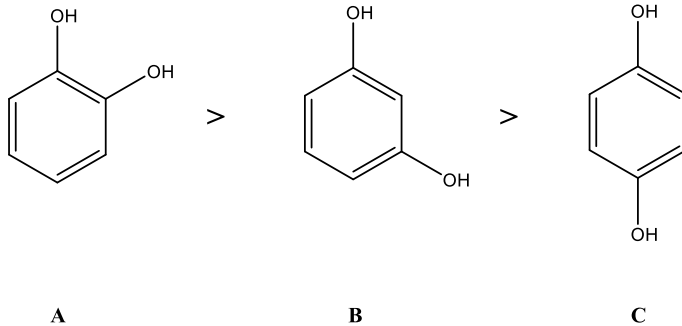


Figure 10. Phenolic compounds with two vicinal hydroxyl groups (*ortho*-substituted) are preferred over meta –and para-substituted phenolic compounds. **A** catechol, **B** resorcinol, **C** hydroquinone.

Engineering glucanucrase reaction specificity

Glucanucrases are capable of catalyzing three reactions, using sucrose as donor substrate: α -glucan synthesis, hydrolysis and glycosylation of acceptor substrates. The ratio between these reactions is first of all dependent on the enzyme specificity but can be altered by reaction engineering and enzyme engineering. The former strategy consists of optimizing the reaction conditions (donor/acceptor ratio, cosolvent concentration, agitation rate, etc.) whereas the latter strategy alters the enzyme specificity by mutational engineering. In case the glycosylation of acceptor substrates is targeted, α -glucan synthesis and hydrolysis become unwanted side reactions, lowering the yield of the glycosylated acceptor substrates and complicating their downstream processing.

Reaction engineering

Dealing with the low affinity for alternative acceptor substrates

Although many alternative acceptor substrates are indeed glycosylated by glucansucrases, very often incomplete conversions, with low to moderate yields, are obtained. Alternative acceptor substrates are per definition not the natural acceptor substrates of glucansucrases and, hence, they generally have rather high K_m values (Chapter 2)¹¹⁰. High concentrations of acceptor substrate are consequently required to outcompete α -glucan synthesis and hydrolysis as possible glucansucrase reactions. In this way, the relative balance between the 3 reactions may shift towards the acceptor reaction, as was already shown in 1993 by Su and Robyt¹³². Moreover, high volumetric productivities (space-time yields), which greatly reduce production costs, can only be achieved if the acceptor substrate concentrations are sufficiently high. However, glucansucrases may be inhibited by high concentrations of non-carbohydrate acceptor substrates. Phenolic compounds, such as catechol, displayed inhibitory effects on glucansucrase GtfD from *S. mutans* GS-5 at a concentration of 200 mM but not at a concentration of 40 mM¹²⁵. A similar effect was obtained for the glycosylation of catechol by Gtf180 from *L. reuteri* 180, which was inhibited at concentrations of catechol higher than 400 mM (Chapter 2)¹¹⁰. The inhibition of amylosucrase from *N. polysaccharea* by several flavonoids was also reported¹²⁴.

Many (poly)phenolic and aliphatic acceptor substrates have limited water solubilities, which complicates their glycosylation. A common strategy to increase the solubility of the acceptor substrate is the addition of organic solvents such as DMSO, ethanol, acetone, etc. Since the 1980s it has been repeatedly shown that enzymes can be used in solvent systems with great efficiency¹³³. However, enzyme activity and stability typically decrease with increasing solvent concentration. Hence, a compromise between substrate solubility and enzyme activity needs to be found for each individual case. The determination of the initial activity of the dextransucrase from *L. mesenteroides* NRRL B-512F in the presence of organic solvents, revealed a 50% loss in activity in 20% DMSO, 15%

ethanol, 15% acetone, 10% DMF and 7% acetonitrile¹³⁴. Diglyme or bis(2-methoxyethyl) ether (MEE) displayed lower inhibitory effects on glucansucrases: the dextranucrase from *L. mesenteroides* NRRL B-512F and the alternansucrase from *L. mesenteroides* NRRL B-23192 retained more than 50% of their activity at a MEE concentration of 30%¹²⁰. It is clear that the combined use of high concentrations of certain acceptor substrates and high solvent concentrations will be even more detrimental for glucansucrase activity. Hence, the optimal balance between acceptor substrate concentration, solvent concentration and enzyme activity will differ for every individual case.

Dealing with unwanted side reactions

Applying glucansucrases for the glycosylation of alternative acceptor substrates usually requires high concentrations of donor substrate sucrose to drive the glycosylation reaction. This is not without negative consequences: the unavoidable accumulation of relatively high concentrations of fructose results in competitive inhibition of the desired glycosylation reaction by fructose. In other words, fructose is under these circumstances used by glucansucrases as acceptor substrate, resulting in the synthesis of sucrose isomers such as leucrose and trehalulose¹³⁵. For example, a K_i value (inhibitor constant) for fructose as low as 9.3 mM has been observed for GtfD from *S. mutans*. Surprisingly, in the same study, glucose did not act as an inhibitor¹²³. It is clear from the reaction mechanism of glucansucrases that formation of fructose is inevitable. The solution to this problem is therefore found externally, i.e. by the addition of a micro-organism that removes fructose from the reaction mixture and consequently reduces its inhibiting effect. In order for this strategy to work properly, it is essential that sucrose itself is not metabolized by the micro-organism. The methylotrophic yeast *Pichia pastoris* and the mutant *S. cerevisiae* T2-3D¹³⁶ are viable options as both strains are incapable of fermenting sucrose. In addition, these micro-organisms should not be inhibited themselves by the presence of acceptor substrates nor metabolize the glycosylated product. The incubation of *P. pastoris* and *S. cerevisiae* T2-3D in a (+)-catechin glycosylation reaction mixture revealed that their fructose consumption resulted in a

prolongation of the transglucosylation activity of GtfD. However, the (+)-catechin glucoside yield was only slightly improved, indicating that the conversion of alternative acceptor substrates is dependent on other factors as well¹²³.

The main glucansucrase catalyzed reaction, i.e. the synthesis of α -glucan oligo – and polysaccharides from sucrose, is the most important side reaction and strongly impedes the efficient glycosylation of alternative acceptor substrates. As previously discussed, sucrose acts as primer for α -glucan synthesis, and increased concentrations of sucrose will result in the formation of more (growing chains of) α -glucan oligosaccharides, the preferred acceptor substrates of glucansucrases^{103,104,135}. Their generation initiates a vicious circle of increased α -glucan synthesis and, hence, needs to be avoided. Suppressing α -glucan synthesis can be accomplished by performing a “fed-batch” reaction, in which the donor substrate sucrose is gradually added to the reaction mixture. In this way, an excess of acceptor substrate relative to sucrose is maintained throughout the complete reaction, conditions which theoretically favor the glycosylation of the acceptor substrate by suppressing the synthesis of α -glucans. Successful attempts include the glycosylation of stevioside with dextransucrase from *L. citreum*⁶⁶ and the glycosylation of rebaudioside A with the Q1140E-mutant of Gtf180- Δ N from *L. reuteri*⁷⁰. However, performing glucansucrase-catalyzed glycosylation reactions in fed-batch mode is mostly limited to the glycosylation of highly soluble compounds, which in addition display very little inhibitory effects on the enzyme. High ratios of non-carbohydrate acceptor substrate over sucrose are indeed known to strongly inhibit glucansucrases, as described previously^{110,125}.

Furthermore, te Poele et al. have demonstrated that, upon sucrose depletion, glucansucrases from *L. reuteri* use several phenolic glucosides as donor substrate for the synthesis of α -glucans and the further glycosylation of these phenolic glucosides into multiglycosylated products¹³⁷. Hence, the incubation time and enzyme loading (U/mL) of glucansucrase catalyzed glycosylations need to be carefully selected in order to prevent suboptimal conversion degrees. Another remarkable characteristic displayed by glucansucrases is their ability to add multiple α -D-glucosyl moieties to one acceptor substrate, forming α -D-

glucosides of different sizes and structures. A prominent example concerns GtfA- Δ N of *L. reuteri* 121⁸⁰: after incubation with catechol and sucrose, several glycosylated catechol products up to DP5, differing in their combination of (α 1 \rightarrow 4) and (α 1 \rightarrow 6) linkages, were characterized¹³⁸. From an industrial point of view, the synthesis of only one glycoside, typically the monoglycosylated product, is desired in order to facilitate downstream processing. Indeed, the monoglycosylated product often displays better functional properties than multiglycosylated products. A comprehensive study on the anti-oxidant activities of various phenolic glucosides revealed that an increasing level of glycosylation results in reduced radical-scavenging abilities¹³⁹. The number of glycosyl moieties attached to steviol glycosides is also known to have pronounced effects on their taste⁸.

Dealing with low operational stability: Enzyme immobilization

Immobilization is an established strategy to increase the operational activity and stability of enzymes. In this way, immobilization may compensate for the decrease of enzyme activity and stability provoked by high solvent and acceptor substrate concentrations¹⁴⁰. An additional advantage is the reusability of the immobilized biocatalyst, which can drastically lower the economic cost of the enzymatic process¹⁴¹. A number of immobilization methods can be distinguished: reversible methods (adsorption and affinity binding) and irreversible methods (entrapment, aggregation and covalent binding). Reversible immobilization methods typically result in enzyme leaching, preventing biocatalyst reuse and representing economic loss. On the contrary, irreversible immobilization methods minimize enzyme leaching due to much stronger interactions between enzyme and support, which also stabilizes the enzyme more effectively. On the downside, enzyme activity may decrease due to active site occlusion and inherent diffusion limitations¹⁴².

Glucansucrases have been described as difficult to covalently immobilize, mainly due to inactivation of the enzyme, e.g. by the participation of a lysine residue in the active site. Typical immobilization yields (ratio of activity of immobilized

enzyme to the activity of enzyme prior immobilization) range from 3% to 22%¹⁴³⁻¹⁴⁶. In contrast, encapsulation of glucansucrases in alginate beads has been more successfully applied as immobilization method. Several studies report immobilization yields up to 90%^{147,148}. However, this method cannot be used for the production of α -glucan polysaccharides as their accumulation in alginate results in rupture of the beads.

Enzyme engineering

Although of value, applying reaction engineering to optimize the acceptor reaction of glucansucrases is faced with limitations. Enzyme engineering offers an alternative, more direct optimization method, by altering the reaction specificity of the enzyme itself. Over the years, many studies have reported successful attempts to engineer the specificity of enzymes. For example, the affinity of sucrose phosphorylase (SP) for glucose as acceptor substrate could be dramatically enhanced by a double mutation, resulting in the efficient synthesis of the rare disaccharide kojibiose¹⁴⁹. Additionally, SP has been engineered twice towards the more efficient synthesis of polyphenolic glycosides. The first study attributed the enhanced yields to a better accessibility of the active site, caused by a single mutation removing a sterically hindering active site loop, more specifically by the mutation of an arginine residue into an alanine residue (R134A mutant)²⁵. As such, it forms a good example of loop engineering, i.e. the alteration of loops, a diverse class of very flexible secondary structures comprising turns, random coils, and strands connecting the main secondary protein structures (α -helices and β -strands) and which very often play a vital role in the catalytic function of the enzyme¹⁵⁰. Also the single mutation used in the second study yielded a loop shift in the active site of SP, as revealed by analysis of the crystal structure of the mutant. It was argued that the loop shift resulted from a cascade of structural changes arising from the Q345F exchange, ultimately causing a widened access channel²⁶. This nicely illustrates how substantial the effect can be of a – at first sight – simple single mutation, demonstrating the great power of enzyme engineering, but also revealing one of the difficulties to rationally design biocatalysts.

To date, only a few enzyme engineering studies on glucansucrases have been dedicated to the glycosylation of non-carbohydrate acceptor substrates. This is partly due to the lack of available crystal structures (and consequently lack of docking experiments) with bound acceptor substrates, complicating rational design of glucansucrase mutants for the synthesis of glycosides. In theory, glucansucrases can be engineered towards a more efficient acceptor reaction in three distinguishable ways: lowering their affinity to catalyze side-reactions (in particular α -glucan synthesis), enhancing their affinity for alternative acceptor substrates, or both simultaneously. In 2016, Liang et al. expanded the acceptor substrate promiscuity of GtfD from *S. mutans* by simultaneous site saturation mutagenesis of residues Y418 and N469. Significant improvements in glycosylation yield of several flavonoids were obtained with the best double mutant (Y418R and N469C), the major products being monoglycosylated. Docking studies based on the crystal structure of Gtf180- Δ N from *L. reuteri* 180 suggested that the mutant enzyme formed three additional hydrogen bonds with the flavonoid acceptor substrate, resulting in an increased catalytic efficiency of the mutant enzyme compared to the wild type¹⁵¹. Another study reported that the I228A mutant of the amylosucrase (EC 2.4.1.4) from *N. polysaccharea* displayed a significant improvement in luteolin monoglycosylation, compared to the wild-type enzyme. Docking studies revealed that the introduction of the alanine residue reduced the steric hindrance, resulting in a better positioning of luteolin in the catalytic pocket¹²⁹. Finally, Devlamynck et al. reported that applying Gtf180- Δ N mutants with an impaired α -glucan synthesis resulted in an improved glycosylation of several non-carbohydrate acceptor substrates (Chapter 2)¹¹⁰.

Other enzyme engineering studies with glucansucrases have focused on the formation of oligosaccharides. Their synthesis is of considerable interest for the food industry, which already produces prebiotic oligosaccharides such as isomaltooligosaccharides (IMO)¹⁵², leucrose¹⁵³ and isomaltulose (palatinose)¹⁵⁴. Random mutagenesis of the most conserved motif around the transition state stabilizer in glucansucrases (RAHDSEV motif) yielded variants of GtfR from *Streptococcus oralis* with altered reaction specificity. In particular the S628D mutant displayed a drastic 25-fold increase of conversion degrees for the

synthesis of isomaltose and leucrose, using glucose and fructose as acceptor substrate, respectively. In contrast, this variant lost most of its ability to synthesize α -glucan polysaccharides. Unfortunately, the absence of the GtfR crystal structure prevented a rational explanation of the obtained results¹⁵⁵. The mutational improvement of Gtf180- Δ N for the glycosylation of rebaudioside A, with the steviol glycoside here considered as an oligosaccharide, has also been reported^{8,68-70}. The increased conversion degree from approximately 50% to 95% was attributed to the improved deprotonation of the HO-6 of the C-19 glucosyl moiety of rebaudioside A, caused by the mutation of a glutamine residue into a glutamate residue (Q1140E mutant)^{68,70}.

Although some progress has been made in the rational design of enzymes, enzyme engineering still mostly relies on directed evolution, i.e. mimicking natural selection through random mutagenesis and subsequent screening of the resulting enzyme libraries¹⁵⁶⁻¹⁵⁸. High-throughput screening for the identification of improved variants is thus a key factor. For glucansucrases, glycosylation reactions can in theory be screened by measuring the release of fructose from sucrose. However, no distinction can then be made between the glycosylation of the desired acceptor substrate and α -glucan synthesis, possibly resulting in an overestimation of the glycosylation potential. Directly screening the formation of α -D-glucosides is thus preferred. For example, Seibel et al. identified new acceptor specificities of GtfR with the aid of substrate microarrays. Firstly, the acceptor substrates were immobilized on the surface of a microtiter plate. After incubation of GtfR with sucrose and subsequent removal of the reaction mixture, fluorescein-labelled (FITC) concanavalin A, a glucose-specific lectin, was added. Hence, successful glycosylation reactions could be detected by an increase of fluorescence¹⁵⁹.

Conclusions

The broad acceptor substrate specificity of glucansucrases offers a good starting point to engineer their reaction specificity towards the synthesis of

oligosaccharides and α -D-glucosides, using carbohydrates and non-carbohydrates as acceptor substrate, respectively. The structural diversity of alternative acceptor substrates requires a similar diversity of optimal reaction conditions and optimal (mutant) glucansucrases. The combination of reaction – and enzyme engineering is thus essential to meet the industrial requirements of high conversion degrees and product yields. The operational stability of enzymes is an equally crucial factor for industrial applications. Glycosylation biocatalysts in particular need to be sufficiently robust to withstand the harsh conditions that are typically applied: high temperatures of 55-60 °C to avoid microbial contamination and the presence of organic cosolvents, added to the reaction mixture to solubilize hydrophobic acceptor substrates.

Scope of the thesis

As discussed in this chapter, GH70 glucansucrases have been repeatedly shown to glycosylate several carbohydrate and non-carbohydrate molecules with low to moderate yields. From the discussion, it was clear that an important impediment to the efficient glycosylation of these molecules is the competition from the main glucansucrase catalyzed reaction, i.e. α -glucan synthesis. Furthermore, it was illustrated that another drawback in the use of GH70 glucansucrases as glycosylation biocatalyst is their relatively low operational stability. **Chapters 2 and 3** of this PhD thesis address these issues by applying a combination of reaction –and enzyme engineering. In order to select a GH70 glucansucrase enzyme from our in-house collection (Gtf180- Δ N from *L. reuteri* 180, GtfA- Δ N from *L. reuteri* 121 and GtfO- Δ N from *L. reuteri* ATCC 55730), their potential to glycosylate catechol was examined (Figure 11). Based on the obtained results, Gtf180- Δ N was preferred since it demonstrated a higher operational stability (deactivated by catechol concentrations higher than 400 mM, compared to 300 and 200 mM for GtfA- Δ N and GtfO- Δ N, respectively) and a higher glycosylation productivity, compared to the other enzymes.

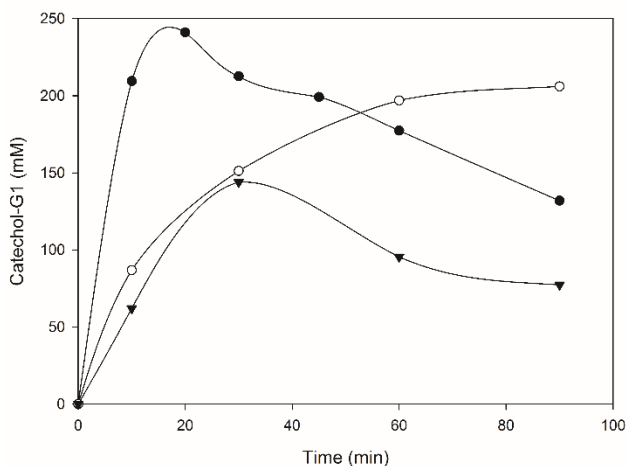


Figure 11. Time-course synthesis of monoglycosylated catechol (catechol-G1) by ● Gtf180-ΔN (400 mM catechol), ○ GtfA-ΔN (300 mM catechol) and ▼ GtfO-ΔN (200 mM catechol). 1000 mM sucrose, 4 U/mL enzyme (total activity), T = 37 °C, pH = 4.7.

This introductory chapter also illustrated the commercial potential of glycosylating steviol glycosides to improve their sensory characteristics. Therefore, our in-house collection of GH70 glucansucrases was screened for their ability to glycosylate the most prevalent steviol glycosides, rebaudioside A (RebA) and stevioside. Once again, Gtf180-ΔN demonstrated most potential. In fact, it was the only GH70 glucansucrase of our collection capable of glycosylating RebA. The second part of this PhD thesis (**Chapters 4, 5 and 6**) consequently focusses on the use of Gtf180-ΔN and derived mutants to glycosylate RebA and stevioside. **Chapter 7** is another illustration of the relatively high acceptor substrate promiscuity of Gtf180-ΔN; also the high-intensity sweetener neohesperidin dihydrochalcone (NHDC) was glycosylated in order to improve its sensory –and physicochemical properties. Conclusively, this PhD thesis describes the improvement of glucansucrase Gtf180-ΔN from *L. reuteri* 180 as glycosylation biocatalyst by applying mutational engineering, optimization of reaction conditions and development of downstream processing. Furthermore, the sensory properties of the glycosylated products were determined by a trained panel.

Chapter 1 discusses the state of the art glycosylation technologies, illustrating their respective advantages and drawbacks by using the glycosylation of steviol glycosides as case study. Secondly, it reviews current knowledge of GH70 glucansucrases and in particular their use as biocatalyst for the glycosylation of non-carbohydrate compounds, such as (+)-catechin, and *Stevia* glycosides, such as stevioside and rebaudioside A. Conclusively, reaction –and enzyme engineering are discussed as strategies to improve the glycosylation potential of GH70 glucansucrases.

Chapter 2 demonstrates that suppressing α -glucan synthesis by mutational engineering of the Gtf180- Δ N enzyme of *Lactobacillus reuteri* 180 resulted in the improved glycosylation of several non-carbohydrate acceptor substrates, such as catechol and butanol. Three mutants (L938F, L981A and N1029M) were selected from a previously constructed library of 61 mutants with single amino acid residue changes, targeting 10 amino acid residues of the Gtf180- Δ N acceptor binding sites +1 and +2^{93,94}. Kinetic analysis revealed that impairing α -glucan synthesis resulted in a higher affinity of the mutant enzymes for the model acceptor substrate catechol, explaining the improved monoglycosylation yields. Finally, the chemical structures of the glycosylated acceptor substrates were elucidated by NMR spectroscopy.

Chapter 3 discusses solvent engineering strategies (biphasic and cosolvents systems) for the glycosylation of poorly soluble acceptor substrates by Gtf180- Δ N of *L. reuteri* 180. Also the immobilization of this enzyme onto mesoporous silica particles is described. The covalently immobilized WT enzyme retained most of its activity at 60 °C, whereas the free WT enzyme lost all activity at temperatures above 50 °C. Moreover, the covalently immobilized WT enzyme was much more active at high DMSO concentrations and high acceptor substrate concentrations than the free WT enzyme, allowing the glycosylation at higher acceptor substrate concentrations of poorly soluble acceptor substrates, such as ethyl gallate, gallic acid and (+)-catechin.

Chapter 4 reports the glycosylation of rebaudioside A (RebA), a natural high-intensity sweetener obtained from the leaves of *Stevia rebaudiana*, by Gtf180- Δ N and its Q1140E-mutant, which was selected from a mutant library^{99,100} in view of its reduced α -glucan synthesis, enhanced RebA glycosylation potential and introduction of a single extra glucose unit. Structural analysis of the main product showed that both enzymes exclusively glucosylate RebA at the Glc(β 1 \rightarrow C-19 position, with the formation of an (α 1 \rightarrow 6) linkage. This result was explained by docking of RebA in the enzyme's active site, using its high resolution 3D structure⁷⁸: only the steviol C-19 β -D-glucosyl moiety is available for glycosylation. The reaction conditions for the batch process were optimized by response surface methodology (RSM), revealing the importance of the ratio of donor substrate sucrose over acceptor substrate RebA to obtain high RebA conversions. The product yield could be further enhanced by developing a fed-batch reaction, which further suppressed the remaining and competing α -glucan synthesis still present in mutant Q1140E. Sensory analysis of the glycosylated RebA product by a trained taste panel revealed a near complete removal of bitterness, compared to RebA. In other words, an efficient process for the synthesis of a novel steviol glycoside (RebA-G1), displaying a superior taste profile, was developed.

Chapter 5 continues the work on *Stevia* glycosides by reporting the glycosylation of stevioside, the most abundant steviol glycoside extracted from the leaves of *Stevia rebaudiana*, with the Gtf180- Δ N-Q1140E enzyme. The chemical structures of the glycosylated stevioside products were elucidated by NMR spectroscopy, revealing an identical regiospecificity as with RebA glycosylation. Surprisingly, a minor diglycosylated product with an (α 1 \rightarrow 4) linkage was isolated from the glycosylation reaction mixture, a specificity that is normally not displayed by the Gtf180- Δ N enzyme. The reaction conditions for the batch process were again optimized using RSM, indicating that stevioside glycosylation is significantly less productive than RebA glycosylation. Analysis of the sensory properties of the glycosylated stevioside product by a trained taste panel revealed a substantial decrease in bitterness compared to stevioside and RebA.

Equally important, its taste profile was nearly identical to that of the glycosylated RebA product.

Chapter 6 discusses the scale-up of the Gtf180- Δ N- Δ V-Q1140E-catalyzed glycosylation of RebA and stevioside. Firstly, the enzyme production was investigated. It was shown that the N- and V-terminally truncated Gtf180- Δ N- Δ V-Q1140E protein was more efficiently produced than the N-terminally truncated enzyme, whereas its biocatalytic potential was identical. Secondly, an eco-friendly and efficient downstream processing of the glycosylated products was developed and demonstrated at pilot-plant scale, allowing the production of 200 g glycosylated RebA product. A cost analysis demonstrated the economic feasibility of the process and pointed out the steviol glycoside substrate (RebA, stevioside) cost as major factor in the total production cost. The use of low-grade stevia extract, half the price of high-purity RebA, was therefore proposed as cost reducing strategy. In this context, the simultaneous glycosylation of stevioside and RebA was demonstrated, a technology which holds strong commercial potential.

Chapter 7 illustrates the potential of Gtf180- Δ N-Q1140E to glycosylate neohesperidin dihydrochalcone (NHDC), a high-intensity sweetener obtained from citrus fruits. NHDC finds many applications as flavor enhancer (E959) in the food- and pharmaceutical industry due to its ability to suppress bitterness and astringency, but also draws interest due to its strong anti-oxidant capacity. The main drawback of NHDC, its low water solubility, was overcome by its glycosylation, while the glycosides retained strong anti-oxidant capacities. Sensory analysis of the flavor enhancing effects of NHDC and the NHDC glycosides on RebA by a trained panel revealed a slight decrease of bitterness and an increased sweetness. Although the obtained conversion degree of roughly 65% was not of the same order as for RebA and stevioside glycosylation (95%), it forms a good starting point for a profound optimization of the reaction conditions.

Chapter 8 summarizes and discusses the results presented in this PhD thesis.

Table I. Examples of compounds, shown in Figure 10, that are glycosylated by glucansucrases. The specific glucansucrase, microbial source, conversion degree (ratio of converted acceptor substrate to total acceptor substrate added) and yield (amount of glycosylated product synthesized) are given. ¹In vivo synthesis. ²Mutant enzyme.

Compound	Glucansucrase	Micro-organism	Conversion (%)	Yield (mM)	Reference
Ampelopsin	dextransucrase	<i>L. mesenteroides</i>	94	65.8	121
Astragalín	dextransucrase	<i>L. mesenteroides</i>	ND	ND	122
(+)-Catechin	dextransucrase	<i>S. mutans</i>	90	9.0	123
(±)-Catechin	dextransucrase ¹	<i>S. oralis</i>	85	8.5	124
Catechol	dextransucrase	<i>S. mutans</i>	65	26.0	125
(-)-Epicatechin	dextransucrase ¹	<i>S. oralis</i>	59	5.9	124
Epigallocatechin gallate	glucansucrase	<i>L. mesenteroides</i>	25	1.0	126
Hydroquinone	dextransucrase	<i>L. mesenteroides</i>	< 1	2.0	127
L-DOPA	dextransucrase	<i>L. mesenteroides</i>	n.a.	n.a.	128
Luteolin	amylosucrase ²	<i>N. polysaccharaea</i>	65	3.2	129
Luteolin	dextransucrase	<i>L. mesenteroides</i>	44	4.0	120
Myricetin	alternansucrase	<i>L. mesenteroides</i>	49	4.4	120
Quercetin	glucansucrase	<i>L. mesenteroides</i>	23	< 1	130
(±)-Taxifolin	amylosucrase	<i>N. polysaccharaea</i>	5	< 1	131
(±)-Taxifolin	dextransucrase	<i>S. oralis</i>	74	7.4	131

Chapter 2

Glucansucrase Gtf180- Δ N of *Lactobacillus reuteri* 180: suppressing α -glucan synthesis results in improved glycosylation yields

This chapter is published as:

Tim Devlamynck, Evelien M. te Poele, Xiangfeng Meng, Sander S. van Leeuwen, Lubbert Dijkhuizen (2016) Glucansucrase Gtf180- Δ N of *Lactobacillus reuteri* 180: enzyme and reaction engineering for improved glycosylation of non-carbohydrate molecules. *Appl Microbiol Biotechnol* 100:7529-7539.

Abstract

Glucansucrases have a broad acceptor substrate specificity and receive increased attention as biocatalysts for the glycosylation of small non-carbohydrate molecules using sucrose as donor substrate. However, the main glucansucrase catalyzed reaction results in synthesis of α -glucan polysaccharides from sucrose and this strongly impedes the efficient glycosylation of non-carbohydrate molecules and complicates downstream processing of glucosylated products. This chapter reports that suppressing α -glucan synthesis by mutational engineering of the Gtf180- Δ N enzyme of *Lactobacillus reuteri* 180 results in the construction of more efficient glycosylation biocatalysts. Gtf180- Δ N mutants (L938F, L981A and N1029M) with an impaired α -glucan synthesis displayed a substantial increase in monoglycosylation yields for several phenolic and alcoholic compounds. Kinetic analysis revealed that these mutants possess a higher affinity for the model acceptor substrate catechol but a lower affinity for its mono- α -D-glucoside product, explaining the improved monoglycosylation yields. Analysis of the available high resolution 3D crystal structure of the Gtf180- Δ N protein provided a clear understanding of how mutagenesis of residues L938, L981 and N1029 impaired α -glucan synthesis, thus yielding mutants with an improved glycosylation potential.

1. Introduction

Glycosylation is a versatile tool to enhance the physicochemical and biological properties of small non-carbohydrate molecules¹³. This may result in an increased solubility of hydrophobic compounds³³ and an improved stability of labile molecules against light and oxidation⁷. Furthermore, glycosylating medium- and long-chain alcohols yields alkyl glycosides or alkyl polyglycosides, a class of eco-friendly and non-ionic surfactants displaying a high surface activity and good biodegradability¹⁶⁰.

The chemical synthesis of glycosides requires the use of toxic catalysts and involves many protection and deprotection steps, resulting in low overall yields. Biocatalysis offers an alternative method circumventing multistep-synthesis and generating 5-fold less waste¹⁷. In nature, glycosylation is catalyzed by Leloir glycosyltransferase enzymes (EC 2.4.-.-), using nucleotide-activated sugars as donor substrates. Despite their high efficiency and specificity, the breakthrough as glycosylation catalysts is hampered by the high price of their donor substrates¹⁸. Glycosidases (EC 3.2.-.-) in turn suffer from low yields when applied in the synthetic direction¹⁶¹.

Glycoside hydrolase enzymes such as glucansucrases (GS) provide an excellent alternative for enzymatic glycoside synthesis. These enzymes belong to glycoside hydrolase family 70 (GH70)⁹⁰ and catalyze the conversion of the cheap donor substrate sucrose into α -glucan polysaccharides, thereby linking the α -D-glucopyranosyl units by (α 1 \rightarrow 2), (α 1 \rightarrow 3), (α 1 \rightarrow 4) or (α 1 \rightarrow 6) bonds, depending on the enzyme specificity^{73,74}. Moreover, GS are promiscuous towards a wide range of acceptor substrates^{75,162}. They can use saccharides such as maltose as acceptor substrate to catalyze the synthesis of various oligosaccharides¹⁶³. Glycosylation of non-carbohydrate acceptor substrates, such as L-ascorbic acid¹⁶⁴ and luteolin¹²⁰, also has been reported. The usefulness of GS enzymes as a glycosylation biocatalyst is further demonstrated by a number of patent

applications by Auriol et al. (2012), in which the synthesis of a wide array of phenolic compounds with *Leuconostoc* glucansucrases is claimed¹⁶⁵.

A remarkable characteristic shared by all GS is their ability to add multiple α -D-glucopyranosyl moieties to one acceptor substrate, forming α -D-glucosides of different sizes and structures. A prominent example concerns the glycosylation of acceptor substrates by the GtfA enzyme of *Lactobacillus reuteri* 121⁸⁰: after incubation with catechol and sucrose, several glycosylated catechol products up to DP5, differing in their combination of (α 1 \rightarrow 4) and (α 1 \rightarrow 6) linkages, were characterized¹³⁸. From an industrial perspective, the synthesis of only one glycoside is desired in order to facilitate downstream processing. In addition to the production of a mixture of α -D-glucosides, glucansucrases also synthesize rather large amounts of α -glucan polysaccharides from sucrose under these conditions. This is in fact their main reaction but in this case an unwanted side reaction lowering the yield of the glycosylated acceptor substrates and complicating their downstream processing. In this chapter, a combination of reaction- and enzyme engineering was applied to explore the potential of the N-terminally truncated glucansucrase Gtf180 from *Lactobacillus reuteri* 180 (Gtf180- Δ N, retaining wild type activity and specificity)⁸² as a glycosylation biocatalyst, aiming to suppress the competing α -glucan synthesis reaction as much as possible. Screening of a previously constructed mutant library, targeting 10 amino acid residues involved in the acceptor substrate binding subsites +1 and +2^{99,100}, yielded mutants with an impaired α -glucan synthesis. As will be demonstrated, this substantially enhanced the conversion of a wide range of phenolic and alcoholic molecules into their α -D-glucosides, and also shifted the glycoside distribution pattern towards monoglycosylation.

2. Materials and methods

2.1. Production and purification of recombinant Gtf180- Δ N (mutants)

Recombinant, N-terminally truncated Gtf180- Δ N from *Lactobacillus reuteri* 180 and derived mutant enzymes (Table S1) were produced and purified as described previously^{80,99}.

2.2. Glucansucrase activity assays

Enzyme activity assays were performed at 37°C with 100 mM sucrose in 25 mM sodium acetate (pH 4.7) and 1 mM CaCl₂ unless stated otherwise. Samples of 100 μ l were taken every min over a period of 8 min and immediately inactivated with 20 μ l 1 M NaOH for 30 min. The released glucose and fructose were quantified enzymatically by monitoring the reduction of NADP with the hexokinase and glucose-6-phosphate dehydrogenase/phosphoglucose isomerase assay (Roche) as described previously^{166,167}, allowing the determination of the total- (fructose release) and hydrolytic (glucose release) activities, and calculation of the transglycosylation activity. The α -glucan synthesis potential (α -GSP) is defined as the ratio of transglycosylation activity over total activity.

One unit (U) of total activity corresponds to the release of 1 μ mole fructose from 100 mM sucrose in 25 mM sodium acetate (pH 4.7) and 1 mM CaCl₂ at 37 °C. For the comparison of different reaction conditions and mutants, 4 U/mL enzyme was added to the incubations, unless stated otherwise.

2.3. Production and purification of glycoside products

The glycosylation of catechol, resorcinol, hydroquinone and butanol was carried out at 100 mL scale, by incubating 1 U/mL Gtf180- Δ N at 37°C in 25 mM sodium acetate (pH 4.7) and 1 mM CaCl₂ with 400 mM acceptor substrate and 1000 mM

sucrose for 2 h. Alternatively, hexanol and octanol were glycosylated in a biphasic system consisting of 20% alcohol, 25 mM sodium acetate (pH 4.7), 1 mM CaCl_2 and 1000 mM sucrose, while stirring was achieved in a shaker at 100 rpm. The reactions were terminated by incubating the reaction mixture at 95°C for 10 min. Most of the fermentable sugars were subsequently removed by fermentation with the yeast *Saccharomyces cerevisiae* (Fermentis Ethanol Red®) at pH 4.0 and 30°C¹⁶⁸. Twenty g/L peptone and 10 g/L yeast extract were added to support growth. After 24 h incubation the yeast cells were removed by centrifugation (10000 x g, 4 °C, 10 min) after which the supernatant was concentrated by evaporating *in vacuo*. The glycoside products were subsequently purified from the residue by column chromatography using silica gel (pore size 60 Å, particle size 230-400 mesh) as the stationary phase. The eluent consisted of ethyl acetate-methanol-water (30:5:4 by volume) in case monoglucosides were purified and ethyl acetate-methanol-water (30:6:4 by volume) for the purification of diglucosides.

2.4. HPLC analysis

HPLC analysis of phenolic acceptor molecules and their α -D-glucosides was performed on an Adsorbil amine column (250 mm \times 4.6 mm, 10 μm) with acetonitrile (solvent A) and 50 mM ammonium formate (pH 4.4, solvent B) as the mobile phase. The flow rate and temperature were set at 1.0 mL/min and 35°C, respectively. The following gradient elution was used: 95% of solvent A (0–5 min), 5–40% solvent B (5–22 min), 80% solvent B (22–25 min) and again 95% of solvent A (25–29 min). Detection of the phenolic acceptor substrates and their α -D-glucosides was achieved with an UV detector (276 nm). Before being subjected to HPLC analysis the samples were diluted 200 times in 80% methanol. Calibration of the obtained peaks was accomplished using standard curves of the purified glycosides. All HPLC analyses were performed in duplicate.

2.5. TLC analysis

TLC analysis was performed on silica gel 60 F₂₅₄ plates (Merck). The eluent consisted of ethyl acetate-methanol-water (30:5:4 by volume). Detection was achieved by UV absorption (254 nm) and/or staining with 10% (v/v) H₂SO₄ containing 2 g/L orcinol. The concentration of the alkyl α -D-glucosides was determined by scanning the charred plates with a ChemiDoc™ MP imaging system and subsequently analyzing the spots with Image Lab 4.0 software. Calibration of the obtained spots was accomplished using standard curves of the purified alkyl α -D-glucosides. There was a linear response in the range of 1-10 mM alkyl glucoside (determined experimentally). All TLC analyses were performed in triplicate.

2.6. Kinetic analysis of Gtf180- Δ N (mutants)

Kinetic analysis of the Gtf180- Δ N (mutants) was based upon the method described by Dirks-Hofmeister et al. (2015) for the glycosylation of resveratrol with sucrose phosphorylase²⁵. Kinetic parameters (K_m and k_{cat} values) for the acceptor substrates catechol and the mono- α -D-glucoside of catechol (catechol-G1), purified as described above, were determined using 10 different catechol(-G1) concentrations (ranging from 6.25 to 400 mM), while the concentration of the donor substrate sucrose had a constant value of 1000 mM. One U/mL of Gtf180- Δ N (mutants) was added. Four samples were taken over a period of 3 min and immediately inactivated by incubating for 10 min at 95 °C. All samples were subjected to TLC analysis as described above. The charred plates were scanned with a ChemiDoc™ MP imaging system allowing analysis of the spots with Image Lab 4.0 software. Calibration of the obtained spots was accomplished using standard curves of the purified catechol-G1. Kinetic parameters were calculated by non-linear regression of the Michaelis-Menten equation with SigmaPlot v12.0.

2.7. Structural characterization of purified α -D-glucosides

The structures of the purified α -D-glucosides were elucidated by a combination of 1D NMR (^1H NMR and ^{13}C NMR) and 2D NMR spectroscopy. Samples were exchanged twice in 300 μL D_2O 99.9 %_{atom} (Cambridge Isotope Laboratories, Andover, MA) with intermediate lyophilisation. Finally, samples were dissolved in 650 μL D_2O , containing acetone as internal standard ($\delta^1\text{H}$ 2.225; $\delta^{13}\text{C}$ 31.08). ^1H NMR spectra, including ^1H - ^1H and ^{13}C - ^1H correlation spectra were recorded at a probe temperature of 298K on a Varian Inova 600 spectrometer (NMR Department, University of Groningen, The Netherlands). 1D 600-MHz ^1H NMR spectra were recorded with 5000 Hz spectral width at 16k complex data points, using a WET1D pulse to suppress the HOD signal. 2D ^1H - ^1H COSY spectra were recorded in 256 increments in 4000 complex data points with a spectral width of 5000 Hz. 2D ^1H - ^1H TOCSY spectra were recorded with MLEV17 mixing sequences with 50, 90, and 150 ms spin-lock times. 2D ^{13}C - ^1H HSQC spectra were recorded with a spectral width of 5000 Hz in t_2 and 10,000 Hz in t_1 direction. 2D ^1H - ^1H ROESY spectra with a mixing time of 300 ms were recorded in 128 increments of 4000 complex data points with a spectral width of 5000 Hz. All spectra were processed using MestReNova 5.3 (Mestrelabs Research SL, Santiago de Compostela, Spain), using Whittaker Smoother baseline correction.

3. Results

Glucansucrases prefer non-carbohydrate acceptor substrates with two vicinal hydroxyl groups¹²⁰, such as catechol. The latter has a high water solubility at room temperature, rendering the addition of co-solvents unnecessary. Glycosylation of catechol with the N-terminally truncated glucansucrase of *Lactobacillus reuteri* 180 (Gtf180- ΔN)⁸² was chosen as the model reaction. Firstly, the reaction conditions were optimized towards maximal monoglycosylation and minimal α -glucan synthesis. Subsequently, the mutant library was screened, applying these optimal reaction conditions. Finally, the

optimal reaction conditions identified for catechol glycosylation were also tested for glycosylation of other acceptor substrates.

3.1. Reaction engineering of catechol glycosylation by wild-type Gtf180- Δ N

The catechol acceptor concentration was optimized towards maximal monoglycosylation and minimal α -glucan synthesis. As shown in Figure 1, formation of the monoglucoside of catechol (catechol-G1) is kinetically controlled. Incubation for 20 min was sufficient to reach maximal catechol-G1 production, coinciding with catechol depletion. Catechol-G1 was subsequently irreversibly converted into diglucoside (catechol-3`G2 and catechol-6`G2) and further (catechol-G3+). The donor substrate sucrose was not depleted yet (data not shown).

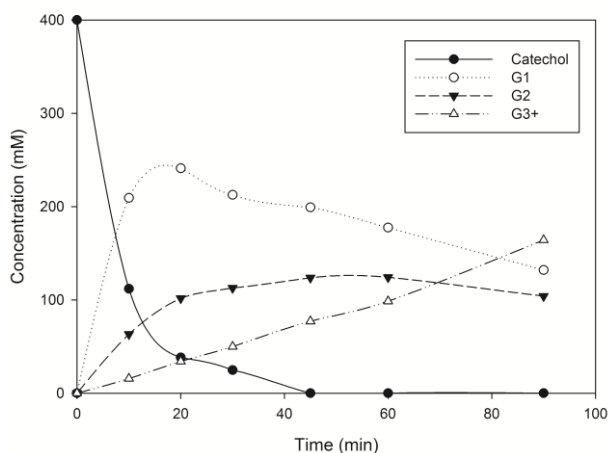


Figure 1. Time-course synthesis of α -D-glucosides of catechol by WT Gtf180- Δ N (400 mM catechol; 1000 mM sucrose; 4 U/mL Gtf180- Δ N). T = 37 °C, pH = 4.7.

Glycosylation reactions catalyzed by glucansucrases suffer from low thermodynamic favorability as pointed out by Liang et al. (2016)¹⁵¹. The production of high catechol-G1 concentrations therefore requires an excess of donor substrate sucrose to drive the reaction. We observed that the latter also had a stabilizing effect on the enzyme, allowing addition of relatively high acceptor substrate concentrations which would otherwise be detrimental for the

enzyme activity as described previously¹²⁵. Therefore, the sucrose concentration was set at 1000 mM. Kinetic analysis revealed that Gtf180- Δ N follows Michaelis-Menten kinetics at catechol acceptor substrate concentrations between 6.25 and 400 mM (Figure S1). The K_m value of Gtf180- Δ N for catechol was 103.3 mM which illustrated the need for high acceptor substrate concentrations (Table 1). Therefore, the catechol concentration was varied from 100 mM to 1000 mM while the sucrose concentration was kept constant at 1000 mM (Table 2). At catechol concentrations higher than 600 mM no glycosylated product was formed due to severe inhibition of enzyme activity by catechol. A catechol concentration of 500 mM and 600 mM only allowed partial conversion of catechol with monoglycosylation yields of 17% and 7% respectively. Reaction mixtures containing 400 mM catechol or less, displayed complete conversion of this acceptor substrate into α -D-glucoside products. Increasing the acceptor concentration from 100 to 400 mM resulted in an improvement in monoglycosylation yield from 49% to 60%, whereas the synthesis of triglycosylated products was reduced (Table 2). At higher catechol concentrations there indeed is an increased chance that the enzyme glycosylates a new acceptor substrate rather than glycosylating catechol-G1. Consequently, 400 mM catechol was chosen as the optimal acceptor concentration for the production of monoglucosides.

The K_m value of Gtf180- Δ N for the catechol-G1 acceptor substrate was 88.8 mM, which is lower than the value for catechol (103.3 mM). The k_{cat} values were 863.3 s^{-1} and 757.4 s^{-1} respectively (Table 1). Hence, under these conditions Gtf180- Δ N glycosylation of catechol-G1 into catechol-G2 and further is inevitable. In the next step we optimized monoglucoside synthesis by applying Gtf180- Δ N mutants, aiming to increase the K_m value for catechol-G1 and/or decrease the K_m value for catechol.

Table 1. Kinetic parameters of WT Gtf180- Δ N and mutants derived for catechol (6.25 - 400 mM) and catechol-G1 (6.25 - 400 mM) as acceptor substrates (with sucrose as donor substrate at 1000 mM), and α -GSP¹ of Gtf180- Δ N WT and mutants for sucrose as both donor and acceptor substrate. T = 37 °C, pH = 4.7.

Enzymes	Catechol			Catechol-G1			α -GSP
	K_m (mM)	k_{cat} (s ⁻¹)	k_{cat}/K_m (s ⁻¹ .mM ⁻¹)	K_m (mM)	k_{cat} (s ⁻¹)	k_{cat}/K_m (s ⁻¹ .mM ⁻¹)	
WT	103.3 ±	757.4 ±	7.4	88.8 ±	863.3 ±	10.2	0.556
	8.5	12.4		17.1	39.3		
L938F	85.5 ±	1872.5 ±	21.9	91.1 ±	576.2 ±	6.3	0.341
	4.0	74.7		7.3	44.0		
N1029M	58.9 ±	449.4 ±	7.7	146.9 ±	126.2 ±	0.9	0.192
	6.4	4.9		19.3	11.0		
L981A	11.0 ±	203.2 ±	18.7	177.4 ±	69.4 ±	0.4	0.049
	1.3	8.1		7.0	2.4		

¹ α -GSP is defined as the ratio of the transglycosylation activity over the total activity (measured with 1000 mM sucrose only).

Table 2. Effects of acceptor substrate concentration on the glycosylation yields and glucoside distribution¹ of WT Gtf180- Δ N for the model acceptor substrate catechol (1000 mM sucrose; 4 U/mL Gtf180- Δ N). T = 37 °C, pH = 4.7.

Catechol (mM)	Catechol glucoside (mM)				Catechol glucoside distribution (%)		
	G1	G2 _{α1-3}	G2 _{α1-6}	G3+	G1	G2	G3+
600	39.6	-	-	-	100	-	-
500	86.8	< 10.0	< 10.0	-	96	4	4
400	241.1	33.8	68.0	57.3	60	25	14
300	170.1	27.5	56.0	46.3	57	28	15
200	107.2	17.9	37.6	37.2	54	28	19
100	49.4	9.3	18.1	23.1	49	27	23

¹ All data given at maximal catechol-G1 yield (20 min incubation).

3.2. Mutational engineering of the Gtf180- Δ N enzyme

3.2.1. Selection of Gtf180- Δ N mutants

A library of 61 mutants with single amino acid residue changes (Table S1), targeting 10 amino acid residues of the Gtf180- Δ N acceptor binding sites +1 and +2, has been constructed previously^{99,100}. A quick and qualitative screening was performed to identify mutants displaying a relative increase in monoglycosylation and a decrease in α -glucan synthesis. For this purpose, 1 U/mL of every mutant was incubated for 1 h at the optimal reaction conditions (400 mM catechol, 1000 mM sucrose). The resulting reaction mixtures were subsequently spotted on TLC plates and mutually compared after staining (Figure S2).

Mutants of residues D1085, R1088 and N1089 were not affected in catechol glycosylation, since their product profiles were nearly identical to those of the WT Gtf180- Δ N. Mutants of W1065, a residue proven to be essential for both activity and acceptor binding by interacting with maltose through aromatic stacking^{83,95}, displayed a very low total activity. Although the product profiles of these mutants were improved (more catechol-G1), their low total conversion and low specific activity rendered them less useful as glycosylation biocatalyst. Mutating D1028 yielded mutants with an enhanced oligosaccharide synthesis, as suggested by the more intense α -glucan oligosaccharide tail visible on TLC (Figure S2). Since this was the opposite of what was aimed for, these mutants were not selected for further analysis. Mutants of L940 all showed a shift in diglucoside linkage type, forming almost exclusively (α 1 \rightarrow 6) bonds. Indeed, the crucial role of L940 for linkage specificity in α -glucan synthesis was demonstrated previously⁹⁸. However, no relative increase in monoglycosylation yield was detected.

Mutants of residues L938, L981 and N1029 provided the most interesting results. Every L938 mutant tested showed an increased monoglucoside synthesis and a decreased formation of di- and triglucosides; the strongest effect was observed for mutant L938F (Figure S2). Similar effects were obtained with L981 mutants, especially when the leucine residue was replaced by alanine. In case of N1029

mutations, two different effects were observed. Firstly, when replacing asparagine by either glycine or threonine, almost exclusively (α 1 \rightarrow 3) diglucosides were synthesized, as was also seen for α -glucan synthesis⁹⁹. Secondly, when asparagine was replaced by methionine and to a lesser extent by tyrosine, the formation of di- and triglucosides was significantly reduced in favor of monoglucoside synthesis (Figure S2). From each mutant group the best representative (L938F, L981A and N1029M) was selected for further characterization and subjected to detailed analysis of products formed.

3.2.2. Characterization of Gtf180- Δ N mutants: increased catechol monoglycosylation

The L938F mutant displayed a higher total activity on sucrose as both acceptor and donor substrate than Gtf180- Δ N WT (132%) at 1000 mM sucrose, whereas the L981A and N1029M mutants had reduced activity, retaining 23% and 32% of the Gtf180- Δ N WT activity respectively (data not shown). To compare the mutants with WT Gtf180- Δ N, 4 U/mL of every Gtf180- Δ N mutant enzyme was incubated at optimal reaction conditions (400 mM catechol, 1000 mM sucrose), allowing analysis of the time-course synthesis of α -D-glucosides of catechol (Figure 2). The corresponding glycosylation yields and glucoside distributions are given in Table 3.

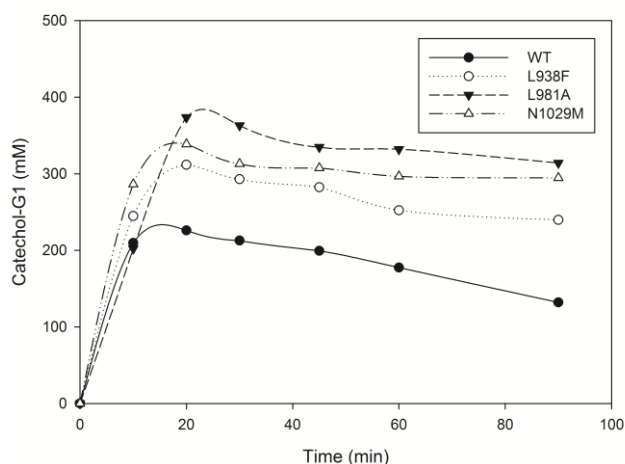


Figure 2. Time-course synthesis of α -D-Glcp-catechol by WT Gtf180- Δ N and mutants derived (400 mM catechol; 1000 mM sucrose; 4 U/mL Gtf180- Δ N). T = 37 °C, pH = 4.7.

Similarly to Gtf180- Δ N WT, all mutants completely converted catechol into α -D-glucosides. However, the glucoside distribution was altered: the mutants displayed higher monoglycosylation yields. Up to 93% catechol was converted into solely monoglycoside for the best performing mutant (L981A), compared to 60% for Gtf180- Δ N. Interestingly, each of these mutants exhibited a shift in diglycoside linkage type compared to Gtf180- Δ N, favouring the formation of α -1,3 linkages (Table 3).

Table 3. Glycosylation yields and glucoside distribution¹ of WT Gtf180- Δ N and mutants derived (400 mM catechol; 1000 mM sucrose; 4 U/mL Gtf180- Δ N). T = 37 °C, pH = 4.7.

Gtf180- Δ N	Catechol glucoside (mM)				Catechol glucoside distribution (%)		
	G1	G2 $_{\alpha-1,3}$	G2 $_{\alpha-1,6}$	G3+	G1	G2	G3
WT	241.1	33.8	68.0	57.3	60	25	15
L938F	311.3	51.8	10.0	26.9	78	15	7
N1029M	338.6	36.1	< 10.0	19.6	85	10	5
L981A	373.5	< 10.0	17.9	< 10.0	93	6	1

¹All data given at maximal catechol-G1 yield (20 min incubation).

Determination of the kinetic parameters (Table 1) revealed that two opposite but related effects form the basis for the improved monoglycosylation yields. Except for the L938F mutant, the mutants had lower k_{cat} values for the acceptor reaction with catechol and sucrose (Table 1), mainly representing a reduction in total activity with sucrose alone as shown above. However, all mutants displayed much lower K_m values for catechol than the Gtf180- Δ N WT. In particular the L981A mutant had a low K_m value of 11.0 mM for catechol, representing a 9-fold improvement compared to the Gtf180- Δ N WT. Despite the relatively low total activity of mutant L981A (23% of Gtf180- Δ N), its catalytic efficiency (k_{cat}/K_m) for the acceptor reaction with catechol (plus sucrose) was 2.5-fold higher than of Gtf180- Δ N WT. The exact opposite was observed when comparing the kinetic parameters of the mutants with Gtf180- Δ N WT for catechol-G1 as acceptor substrate: all mutants displayed higher K_m values for catechol-G1 whereas their catalytic efficiencies were substantially lower.

To elucidate the underlying molecular mechanism, the transglycosylation and total activities of the Gtf180- Δ N (mutants), incubated with sucrose only, were determined. Subsequently, the α -glucan synthesis potential (α -GSP) was calculated, defined as the ratio of the transglycosylation activity over the total activity, revealing the potential of the enzyme to use the donor substrate sucrose for α -glucan synthesis (and not for hydrolysis). As shown in Table 1, the mutants showed a decrease in α -GSP compared to the Gtf180- Δ N WT.

In conclusion, mutant L981A represents a highly efficient biocatalyst for the glycosylation of catechol, yielding roughly 100 g/L catechol-G1 (373 mM) with a yield of 93%.

3.2.3. Characterization of Gtf180- Δ N mutants: increased acceptor substrate conversion

Due to an increased affinity for catechol which resulted from an impaired α -GSP, the monoglycosylation yield of Gtf180- Δ N mutants for the glycosylation of catechol was significantly improved. Subsequently, we determined whether the

same effects could be observed when the L981A mutant was incubated with other acceptor substrates. Suppressing α -glucan synthesis by glucansucrase enzymes may provide a general strategy resulting in higher conversions of a wide range of non-carbohydrate acceptor substrates into α -D-glucosides, more specifically into monoglucosides. A diverse range of small non-carbohydrate molecules (resorcinol, hydroquinone, butanol, hexanol, octanol, pyridoxine and resveratrol) were incubated with wild type Gtf180- Δ N and the L981A mutant, plus sucrose. Indeed, compared to WT enzyme the L981A mutant displayed increased monoglycosylation yields, from 17% to 53% for resorcinol, 1% to 7% for hydroquinone, 4% to 39% for butanol, 4% to 19% for hexanol and 5% to 24% for octanol (Figure 3). To our knowledge, this is the first report of the enzymatic synthesis of hexyl- and octyl α -D-glucosides with a glucansucrase enzyme. Also in case of pyridoxine- and resveratrol glycosylation, an increase in monoglycosylation yield was observed by TLC analysis (not shown).

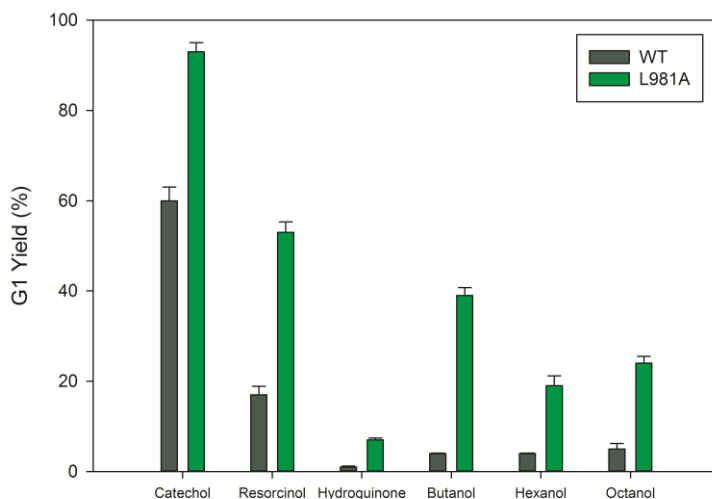


Figure 3. Monoglycosylation yields of WT Gtf180- Δ N and the L981A mutant derived (400 mM catechol/resorcinol/hydroquinone/butanol, 58 mM hexanol, 4 mM octanol; 1000 mM sucrose; 4 U/mL Gtf180- Δ N). All monoglycosylation yields represent maximum values (incubation time dependent on acceptor substrate). T = 37 °C, pH = 4.7.

As illustrated for the glycosylation of resorcinol, two effects contributed to the enhancement of the monoglycosylation yields by the L981A mutant enzyme (Figure 4). Firstly, the conversion of resorcinol acceptor substrate into α -D-glucosides was increased from 53% by WT to 87% by the mutant. Secondly, and similar to catechol glycosylation, the glycoside distribution was shifted towards mainly G1 production. With Gtf180- Δ N WT, 32% of the glycosylated resorcinol consisted of monoglucoside after 4 h of incubation, whereas the L981A mutant had converted 61% of the resorcinol into monoglucoside at $t = 4$ h. The production of monoglucoside reached its maximum long before the maximal resorcinol conversion (Figure 4). The two effects of the mutagenesis are clearly illustrated by TLC analysis of the products obtained (Figure S3): during a 4 h incubation, L981A synthesized fewer oligo- and polysaccharides than Gtf180- Δ N. Instead, more resorcinol was converted into α -D-glucosides.

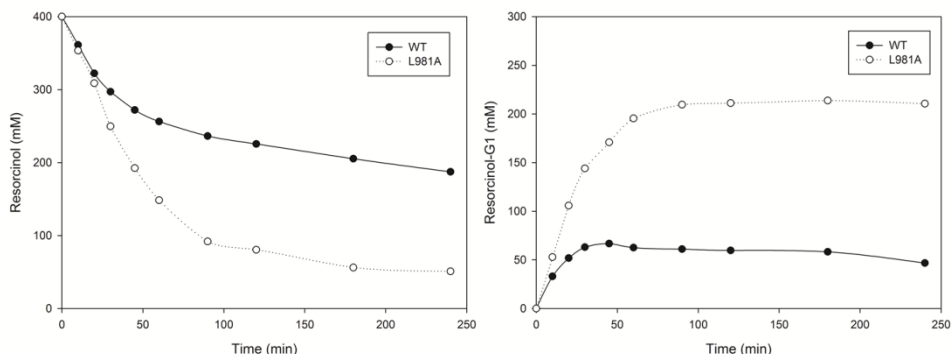


Figure 4. Conversion of the resorcinol acceptor substrate and G1 production by WT Gtf180- Δ N and the L981A mutant derived (400 mM resorcinol; 1000 mM sucrose; 4 U/mL Gtf180- Δ N (mutant)). $T = 37$ °C, $\text{pH} = 4.7$.

3.3. Structural characterization of purified α -D-glucosides

The biocatalytic synthesis of the α -D-glucosides of catechol, resorcinol, hydroquinone, butanol, hexanol and octanol was confirmed by a combination of 1D NMR (^1H NMR and ^{13}C NMR) and 2D NMR spectroscopy. Figure 5 depicts the 1D ^1H NMR spectra of the α -D-glucosides. The corresponding ^1H and ^{13}C chemical shifts are presented in the supplementary information (Tables S2 and

S3). Figures S4-S9 of the supplementary information represent the 1D ^1H NMR spectrum, and 2D ^1H - ^1H COSY, TOCSY (150 ms mixing time), ROESY (300 ms mixing time) and ^{13}C - ^1H HSQC spectra of butyl glucoside, hexyl glucoside, octyl glucoside, resorcinol-G1, hydroquinone-G1 and catechol-3`G2, respectively. The 1D ^1H NMR spectra of catechol-G1 and catechol-6`G2 matched with those found previously by te Poele et al. (2016)¹³⁸ and are presented there. For a detailed analysis of the NMR spectra, see supplementary information.

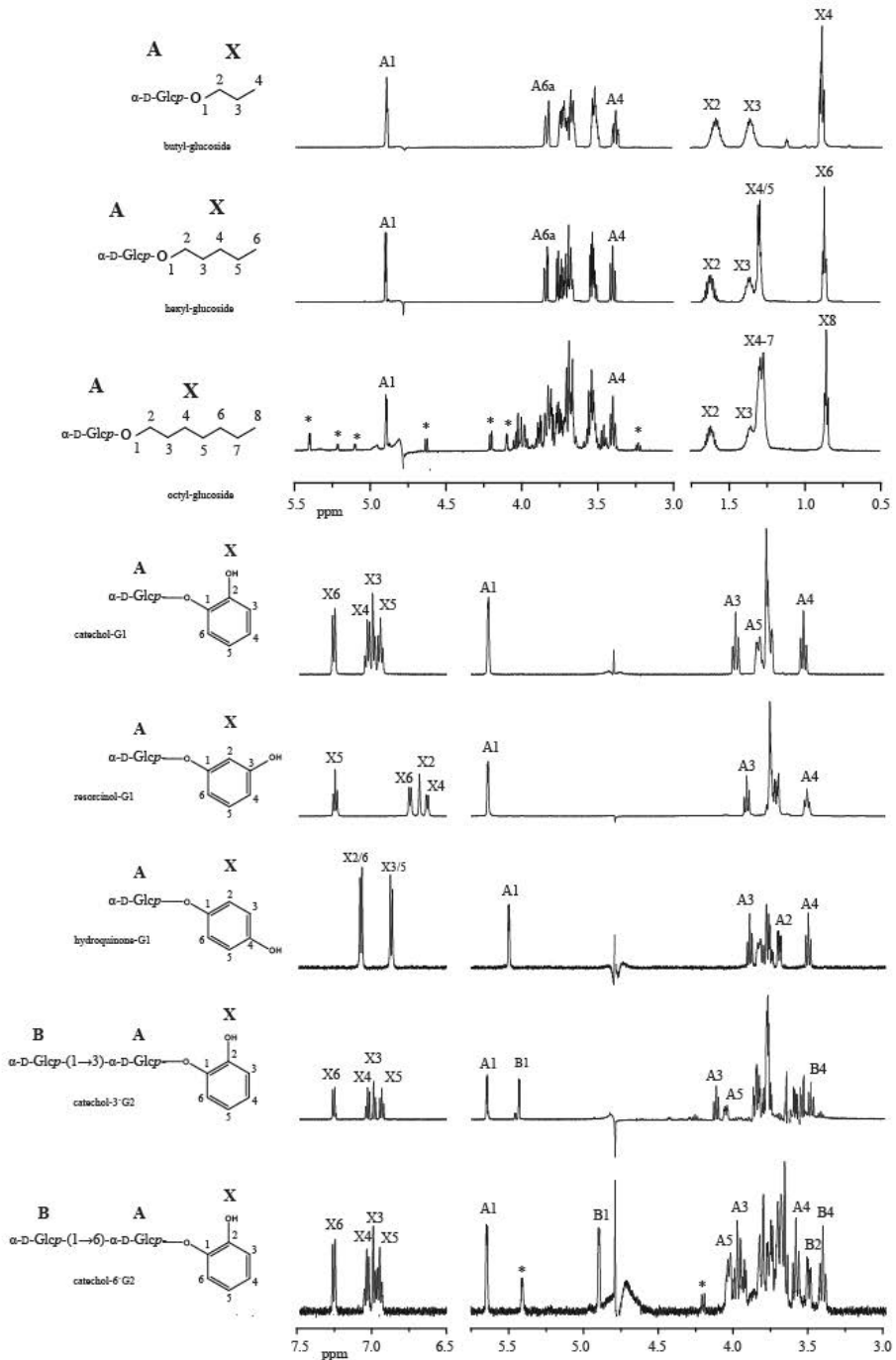


Figure 5. $1\text{D } ^1\text{H}$ NMR spectra of **A.** butyl glucoside, **B.** hexyl glucoside, **C.** octyl glucoside, **D.** catechol-G1, **E.** resorcinol-G1, **F.** hydroquinone-G1, **G.** catechol-3'G2, **H.** catechol-6'G2.

4. Discussion

In view of their broad acceptor substrate specificity, glucansucrases are considered promising glycosylation biocatalysts. However, the typical synthesis of a mixture of α -D-glucosides, oligosaccharides and α -D-glucans remains a bottleneck in their industrial application. α -Glucan synthesis is the main glucansucrase reaction but an undesired side reaction when aiming to glycosylate non-carbohydrate acceptor substrates, lowering glycosylation yields and complicating downstream processing. For example, when applying salicin and salicyl alcohol as acceptor substrates, B-1355C2 and B-1299CB-BF563 dextransucrases from *Leuconostoc mensenteroides* synthesized at least 12 and 9 different kinds of glycosides, respectively¹⁶⁹.

So far, few enzyme engineering studies with glucansucrases have focused on glycosylation of non-carbohydrate acceptor substrates. In 2014, Malbert et al. reported a significant improvement of luteolin monoglycosylation by the I228A *NpAS* mutant compared to the wild type enzyme. Docking studies attributed this enhancement to the introduction of a less hindering residue, assisting in a better positioning of luteolin in the catalytic pocket¹²⁹. In 2016, Liang et al. expanded the acceptor substrate promiscuity of GtfD from *S. mutans* by simultaneous site-saturation mutagenesis of residues Y418 and N469. The best mutant (Y418R and N469C) exhibited a significant improvement in transglycosylation activities towards several flavonoids, the major products being monoglucosylated. Docking studies were based on the crystal structure of Gtf180- Δ N and revealed three additional hydrogen bonds with the flavonoid acceptor substrate compared to the wild type, resulting in the increased catalytic efficiency of the mutant enzyme¹⁵¹. Recently, two substantial improvements were made in sucrose phosphorylase mediated glycosylation of phenolic compounds. The enhanced performance was realized by the construction of mutants with a better accessibility of the active site^{25,26}.

In the present study, the aim was to improve glycosylation yields by suppressing the competing α -glucan synthesis reaction, rather than engineering the active site to make it more suitable for non-carbohydrate acceptor substrates. As presented in Results, this resulted in a strong optimization of monoglycosylated product synthesis by the glucansucrase Gtf180- Δ N. The model acceptor substrate catechol was almost completely glycosylated into monoglycosylated product by the L981A mutant (93% compared to 60% for the wild type enzyme), substantially higher than previously reported for catechol glycosylation by GtfD from *S. mutans* (65%)¹²⁵. In comparison, the I228A *NpAS* mutant only displayed a luteolin monoglycosylation yield of 53%¹²⁹, whereas the GtfD mutant showed a catechin monoglycosylation yield of 90%¹⁵¹.

Kinetic analysis indicated that the Gtf180- Δ N mutants (partly) lost their ability to synthesize α -glucan polysaccharides, as was previously shown by Meng et al. (2015)⁹⁹. However, this positively influenced the glycosylation of catechol. Indeed, a positive correlation could be established between α -GSP and the K_m values for catechol, whereas a negative correlation was found between α -GSP and the monoglycosylation yields with catechol (Figure 6). This shows that these mutations (partly) suppressed the competing α -glucan synthesis, yielding mutants with an improved affinity for catechol as acceptor substrate. Moreover, the increased K_m values of these mutants for catechol-G1 also revealed a reduced α -GSP. Indeed, in the active site of glucansucrase enzymes, α -D-glucosides will basically behave like saccharides. Therefore, the affinities of these mutants for catechol-G1 and for saccharides are positively correlated. The combination of an improved affinity for catechol with a decreased affinity for catechol-G1 thus resulted in the higher monoglycosylation yields of these Gtf180- Δ N mutants.

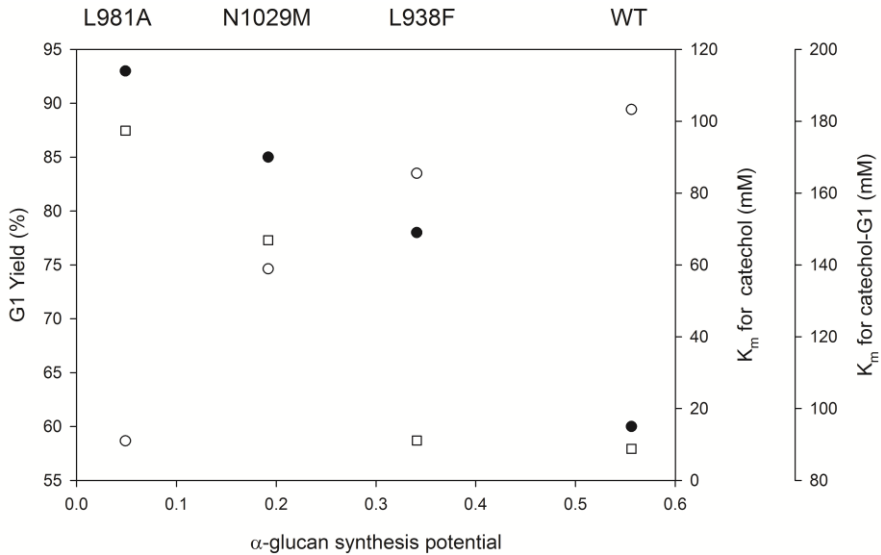


Figure 6. Correlation between α -GSP for sucrose as acceptor substrate, K_m for catechol as acceptor substrate and G1 yield of WT Gtf180- Δ N and mutants derived. Data are listed in Tables 1 and 3. ● G1 yield (%) ○ K_m for catechol (mM) □ K_m for catechol-G1 (mM)

Moreover, suppressing α -glucan synthesis by mutagenesis of Gtf180- Δ N (L981A) clearly resulted in improved monoglycosylation yields for all the phenolic and alcoholic compounds tested here. Mutagenesis of the +1 and +2 acceptor substrate binding sites thus provides a general strategy to improve the monoglycosylation yields of non-carbohydrate acceptor substrates of glucansucrase enzymes.

The architecture of the +1 acceptor substrate binding site is the main determinant of whether an acceptor substrate will bind to the active site or not, and consequently react with the covalently attached glucosyl moiety⁹⁵. The crystal structure of Gtf180- Δ N in complex with maltose, representing a typical saccharide acceptor substrate⁸³, was studied with the aim to understand how mutagenesis of the discussed residues impairs α -glucan synthesis (Figure 7). Firstly, N1029 interacts with the non-reducing end glucosyl moiety of maltose by means of direct and indirect hydrogen bonds with the C4 and C3 hydroxyl groups. Mutating the asparagine to a methionine removes this interaction,

lowering the affinity of the enzyme for maltose. Hence, α -glucan synthesis is suppressed which improves the glycosylation of non-carbohydrate acceptor substrates. In contrast, L981 and L938 do not provide maltose with hydrogen bond interactions. Due to their hydrophobic nature, they contribute by shaping the active site near subsite +1. Introducing an alanine at position 981 presumably reduces the hydrophobic interaction with the C6 of the non-reducing end glucosyl moiety of maltose. Apparently, this severely impairs α -glucan synthesis yielding a Gtf180- Δ N variant with enhanced glycosylation of non-carbohydrate acceptor substrates. On the other hand, mutating L938 to a bulky residue like phenylalanine partially blocks the +1 subsite thereby preventing maltose to efficiently interact with the other residues. This has a smaller effect on α -glucan synthesis than L981A and N1029M, resulting in a limited improvement of the glycosylation of non-carbohydrate acceptor substrates.

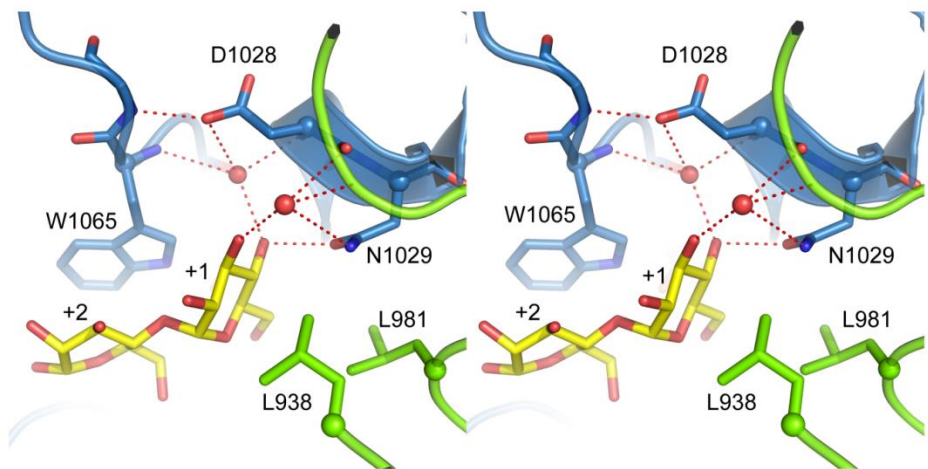


Figure 7. Stereo view of Gtf180- Δ N with the acceptor maltose (yellow carbon atoms) bound in subsites +1 and +2 (PDB: 3KLL). Residue N1029 from domain A (blue) provides direct and indirect (water-mediated) hydrogen bonds to the non-reducing end glucosyl unit bound at subsite +1. Residues L938 and L981 from domain B (green) are also near subsite +1. This figure has been adapted from Meng et al. (2015)⁹⁹.

In conclusion, by applying the optimal reaction conditions and using the best Gtf180- Δ N mutant, a wide range of non-carbohydrate acceptor substrates could

more efficiently be converted into mainly monoglycosylated products. Consequently, the glycosylation potential of the Gtf180- Δ N enzyme was strongly improved. Furthermore, the screening strategy applied in this chapter yielded mutants that can be used as templates to further engineer the Gtf180- Δ N active site for improved glycosylation of specific acceptor substrates.

Acknowledgements

The authors wish to thank the Ubbo Emmius Fund of the University of Groningen and the Special Research Fund (BOF) of Ghent University (PhD-scholarship to TD), China Scholarship Council (to XM), and EU Project NOVOSIDES FP7-KBBE-543 2010-4-265854 (to EMtP and LD), for financial support.

5. Supplementary information

5.1. Detailed analysis of the NMR spectra

5.1.1. Alkyl glucosides

The 1D ^1H NMR spectrum of the isolated product from the incubation with butanol (Figure S4) showed one anomeric signal at δ 4.901 ppm (**A** H-1; $^3J_{1,2}$ 3.91 Hz), indicative of an α -anomeric residue. The signal at δ 0.908 (**X** H-4, *t*) with an intensity corresponding with 3 protons, fits with the butanol CH_3 signal. Starting from **A** H-1 for the glucose moiety and **X** H-4 for the butanol moiety, all ^1H chemical shifts with their corresponding ^{13}C chemical shifts could be determined from 2D ^1H - ^1H and 2D ^{13}C - ^1H NMR spectra (Table S2, Figure S4). The pattern of ^1H and ^{13}C chemical shifts fits with a non-reducing terminal α -D-Glcp-residue¹⁷⁰. Due to the influence of the Glc-moiety linked to the butanol the H-1 protons are shifted to **X** H-1a (δ 3.73) and **X** H-1b (δ 3.53). The 2D ^1H - ^1H ROESY spectrum (Figure S4) showed correlations between **A** H-1 and **X** H-1a and between **A** H-1 and **X** H-2. These data confirm the successful coupling of a Glc-residue to butanol, via an α -linkage.

The 1D ^1H NMR spectrum of the isolated product of the reaction with hexanol (Figure S5) showed a pattern similar to that of α -D-Glcp-butanol, with an anomeric signal at δ 4.903 (**A** H-1; $^3J_{1,2}$ 3.87 Hz), fitting with an α -anomeric residue. The signal at δ 0.868 (**X** H-6, *t*), with an intensity corresponding with 3 protons fits with the hexanol CH_3 signal. Using 2D ^1H - ^1H and 2D ^{13}C - ^1H NMR spectroscopy all ^1H and ^{13}C chemical shifts were determined (Table S2, Figure S5). The pattern for residue **A** fits again with a non-reducing terminal α -D-Glcp-residue. The 2D ^1H - ^1H ROESY spectrum revealed correlations between **A** H-1 and **X** H-1a and between **A** H-1 and **X** H-2, confirming the coupling of an α -D-Glcp-residue to hexanol.

The 1D ^1H NMR spectrum of the isolated product of the reaction with octanol (Figure S6) showed a more complex pattern of peaks. Here the signal for **A** H-1 was observed at δ 4.898 ($^3J_{1,2}$ 3.76 Hz), similar to the butanol and hexanol products. The octanol CH_3 signal (**X** H-8) is found at δ 0.855 (t). Using 2D NMR spectroscopy all ^1H and ^{13}C chemical shifts for **A** and **X** were found (Table S2, Figure S6). The patterns for residue **A** and **X** are again comparable to those of the other alkyl glucosides. The coupling of the α -D-Glcp residue is confirmed by 2D ^1H - ^1H ROESY cross-peaks between **A** H-1 and **X** H-1a and **A** H-1 and **X** H-2.

5.1.2. Benzenediol glucosides

The 1D ^1H NMR spectra of the reaction products catechol-G1 and catechol-6`G2 from the reaction with catechol match with those found previously for α -D-Glcp-catechol and α -D-Glcp-(1 \rightarrow 6)- α -D-Glcp-catechol, respectively¹³⁸. All ^1H and ^{13}C chemical shifts are presented in Table S3.

The 1D ^1H NMR spectrum of the structure isolated from the reaction with resorcinol as acceptor (Figure S7) showed one anomeric signal at δ 5.634 (**A1**; $^3J_{1,2}$ 3.78 Hz) indicating an α -linked residue. Using 2D ^1H - ^1H and ^{13}C - ^1H NMR spectroscopy all ^1H and ^{13}C chemical shifts were assigned (Table S3, Figure S7). Compared to free Glc¹⁷⁰ the glucose H-2 signal is shifted significantly downfield (δ 3.722), probably as a result of interactions with the resorcinol aromatic ring, as observed previously for catechol glucoside¹³⁸. The pattern of ^1H and ^{13}C chemical shifts of residue **A** fit with a non-reducing terminal α -D-Glcp-residue. In the 2D ^1H - ^1H ROESY spectrum (Figure S7) interactions are observed between **A** H-1 and **X** H-2 and between **A** H-1 and **X** H-6, confirming the successful coupling of α -D-Glcp to resorcinol.

The 1D ^1H NMR spectrum of the product isolated from the reaction with hydroquinone (Figure S8) showed one α -anomeric signal at δ 5.490 (**A** H-1; $^3J_{1,2}$ 3.62 Hz) and hydroquinone signals at δ 7.078 (**X** H-2 and H-6) and at δ 6.871 (**X** H-3 and H-5). Using 2D ^1H - ^1H and ^{13}C - ^1H NMR spectroscopy all ^1H and their

corresponding ^{13}C chemical shifts were determined (Table S3, Figure S8). The pattern of ^{13}C chemical shifts of residue **A** fits with a terminal α -D-Glcp-residue. The ^1H chemical shifts of residue **A** fit best with a residue linked to an aromatic moiety, note **A** H-2 at δ 3.75, which is significantly downfield, as was observed for the catechol and resorcinol glucosides as well. The successful coupling of α -D-Glcp to hydroquinone is further supported by the 2D ^1H - ^1H ROESY correlations (Figure S8) between **A** H-1 and **X** H-2 and H-6.

The 1D ^1H NMR spectrum of the third structure isolated from the incubation with catechol (Figure S9) showed two α -anomeric signals at δ 5.635 (**A** H-1; $^3J_{1,2}$ 3.76 Hz) and δ 5.421 (**B** H-1; $^3J_{1,2}$ 3.83 Hz), fitting with two α -D-Glcp-residues. All ^1H and their corresponding ^{13}C chemical shifts were determined from 2D NMR spectra (Table S3, Figure S9). The pattern of chemical shifts for residue **A** showed significant downfield shifts of **A** H-2 (δ 3.86; $\Delta\delta$ + 0.11), **A** H-3 (δ 4.116; $\Delta\delta$ + 0.13) and **A** H-4 (δ 3.79; $\Delta\delta$ + 0.25), compared with residue **A** in α -D-Glcp-catechol (Table S3). This fits best with a 3-substitution of residue **A**¹⁷⁰. Residue **B** has a pattern of ^1H chemical shifts fitting with a terminal residue involved in an (α 1 \rightarrow 3)-linkage. The position of **B** H-5 at δ 4.050, significantly downfield compared to terminal residues involved in a (α 1 \rightarrow 4) or (α 1 \rightarrow 6)-linkage (δ 3.73-3.76)¹⁷⁰ is typical for such a residue. The 3-substitution of residue **A** is also reflected in the ^{13}C chemical shift of C-3, significantly downfield at δ 80.6¹⁷¹. Furthermore, the 2D ^1H - ^1H ROESY spectrum (Figure S9) showed correlations between **B** H-1 and **A** H-3 and between **A** H-1 and **X** H-6, confirming the structure as α -D-Glcp-(1 \rightarrow 3)- α -D-Glcp-catechol.

5.2. Tables

Table S1. List of mutants¹ of Gtf180- Δ N screened for their glycosylation potential.

1	L938A	14	A978F	27	D1028G	40	D1085Q	53	N1089D
2	L938S	15	A978S	28	D1028N	41	R1088H	54	N1089P
3	L938F	16	A978G	29	N1029Y	42	R1088K	55	W1065F
4	L938K	17	A978L	30	N1029G	43	R1088E	56	W1065K
5	L938M	18	A978P	31	N1029T	44	R1088W	57	W1065L
6	L940A	19	A978Y	32	N1029M	45	R1088T	58	W1065Q
7	L940S	20	L981A	33	N1029R	46	R1088N	59	W1065E
8	L940E	21	L981N	34	D1085Y	47	R1088G	60	W1065M
9	L940F	22	L981E	35	D1085V	48	N1089Y	61	W1065G
10	L940W	23	D1028Y	36	D1085A	49	N1089G		
11	L940G	24	D1028W	37	D1085E	50	N1089S		
12	L940M	25	D1028L	38	D1085H	51	N1089L		
13	L940C	26	D1028K	39	D1085L	52	N1089R		

¹For construction and partial characterization of these mutants, see Meng et al. (2015⁹⁹ and 2016¹⁰⁰).

Table S2. ^1H and ^{13}C chemical shifts of alkyl glucosides, relative to internal acetone ($\delta^1\text{H}$ 2.225, $\delta^{13}\text{C}$ 31.08).

	But-G1		Hex-G1		Oct-G1	
	$\delta^1\text{H}$	$\delta^{13}\text{C}$	$\delta^1\text{H}$	$\delta^{13}\text{C}$	$\delta^1\text{H}$	$\delta^{13}\text{C}$
A 1	4.901	98.8	4.903	98.8	4.898	98.7
A 2	3.52	72.0	3.540	72.0	3.54	72.0
A 3	3.69	73.9	3.694	73.8	3.70	73.8
A 4	3.398	70.2	3.402	70.3	3.401	70.1
A 5	3.68	72.4	3.68	72.4	3.68	72.5
A 6a	3.845	61.2	3.844	61.1	3.840	61.1
A 6b	3.75		3.758		3.76	
X 1a	3.73	68.8	3.73	69.1	3.72	69.0
X 1b	3.53	68.8	3.53	69.1	3.53	69.0
X 2	1.613	31.4	1.629	29.3	1.621	29.2
X 3	1.378	19.5	1.366	35.9	1.354	26.1
X 4	0.908	13.8	1.30	31.7	1.27	31.9
X 5	-	-	1.30	22.7	1.28	29.0
X 6	-	-	0.868	14.1	1.30	29.0
X 7	-	-	-	-	1.30	22.8
X 8	-	-	-	-	0.855	13.9

Table S3. ^1H and ^{13}C chemical shifts of glucosides of benzenediols, relative to internal acetone ($\delta^1\text{H}$ 2.225, $\delta^{13}\text{C}$ 31.08).

	Res-G1		HQ-G1		Cat-G1		Cat-3`G2		Cat-6`G2	
	$\delta^1\text{H}$	$\delta^{13}\text{C}$	$\delta^1\text{H}$	$\delta^{13}\text{C}$	$\delta^1\text{H}$	$\delta^{13}\text{C}$	$\delta^1\text{H}$	$\delta^{13}\text{C}$	$\delta^1\text{H}$	$\delta^{13}\text{C}$
A 1	5.634	97.8	5.490	99.2	5.626	99.0	5.635	99.1	5.648	99.1
A 2	3.722	72.1	3.701	72.0	3.75	72.2	3.86	70.8	3.78	72.3
A 3	3.916	73.8	3.898	73.9	3.986	73.9	4.116	80.6	3.984	73.9
A 4	3.518	70.4	3.510	70.3	3.536	70.2	3.79	70.6	3.596	70.1
A 5	3.76	73.4	3.839	73.2	3.84	73.5	3.85	73.1	4.043	71.9
A 6a	3.78	61.1	3.798	61.1	3.81	61.2	3.83	61.1	3.70	66.4
A 6b	3.74		3.757		3.78		3.76		3.944	
B 1	-	-	-	-	-	-	5.421	100.3	4.901	98.5
B 2	-	-	-	-	-	-	3.591	72.7	3.508	72.4
B 3	-	-	-	-	-	-	3.79	73.4	3.668	73.9
B 4	-	-	-	-	-	-	3.485	70.2	3.419	70.4
B 5	-	-	-	-	-	-	4.050	72.7	3.72	72.9
B 6a	-	-	-	-	-	-	3.86	61.1	3.827	61.5
B 6b	-		-		-		3.80		3.76	
X 2	6.689	105.2	7.078	120.0	-	-	-	-	-	-
X 3	-	-	6.871	117.1	6.995	117.8	6.992	117.8	7.015	117.8
X 4	6.737	111.1	-	-	7.041	124.8	7.040	124.8	7.056	124.9
X 5	7.258	131.7	6.871	117.1	6.951	121.9	6.944	121.6	6.974	121.7
X 6	6.754	110.0	7.078	120.0	7.266	118.2	7.268	118.1	7.274	118.3

5.3. Figures

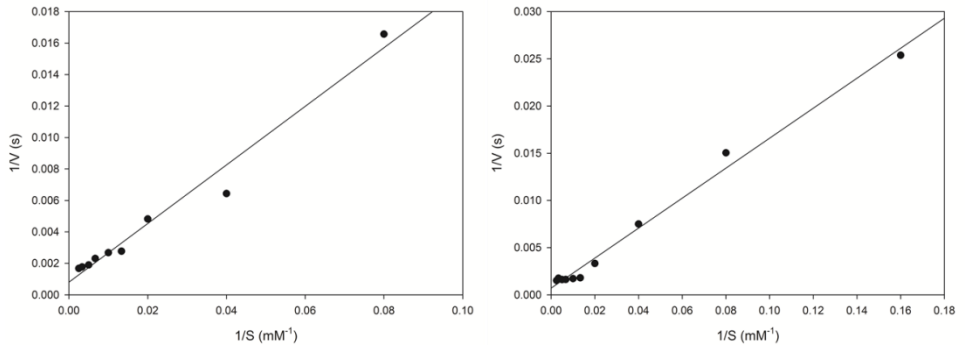
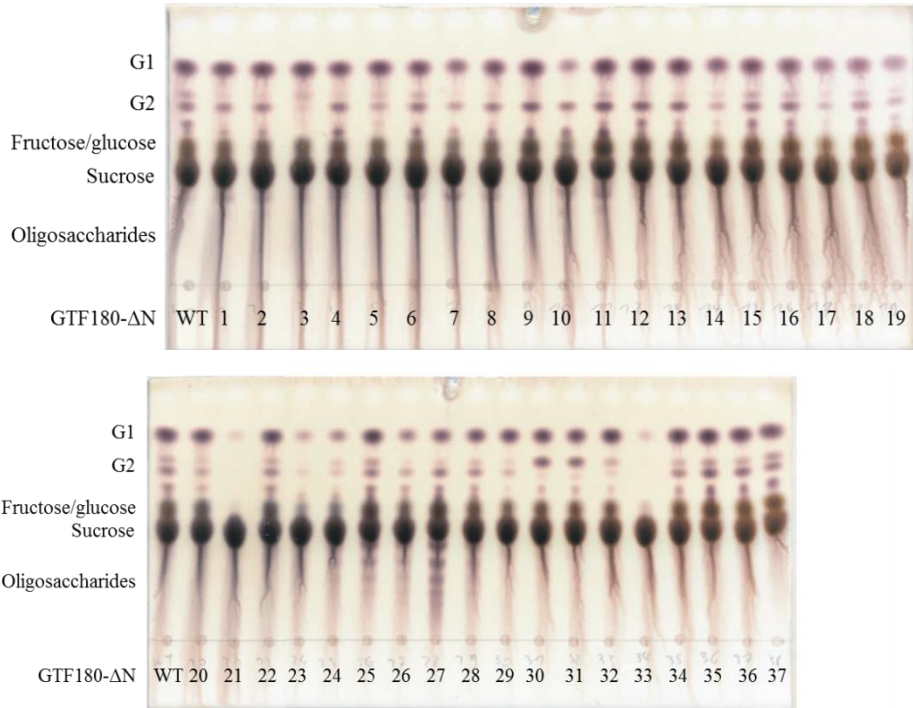


Figure S1. Lineweaver-Burk plots for the glycosylation of catechol and catechol-G1 with Gtf180- Δ N. R^2 is 0.97 and 0.99, respectively. The corresponding kinetic data are listed in Table I.



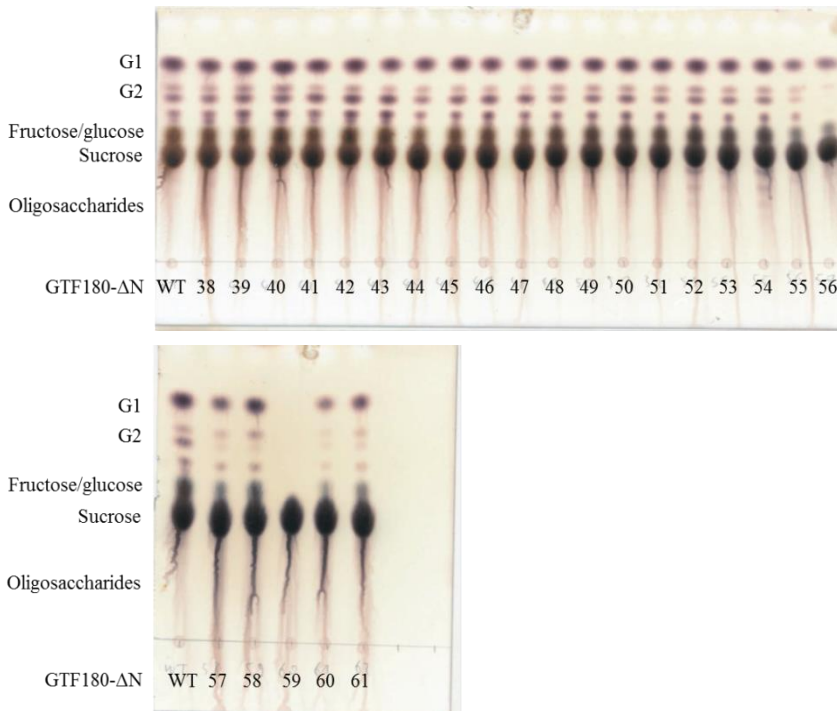


Figure S2. TLC analysis of glycosylated products synthesized by Gtf180-ΔN and mutants derived after 1 h of incubation (400 mM catechol; 1000 mM sucrose; 1 U/mL Gtf180-ΔN (mutants)). Numbers refer to mutants listed in Table I. G1 and G2 refer to the mono- and diglycosylated catechol products. Upper G2 spot: diglycosylated product with (α1→3) bond. Lower G2 spot: diglycosylated product with (α1→6) bond.

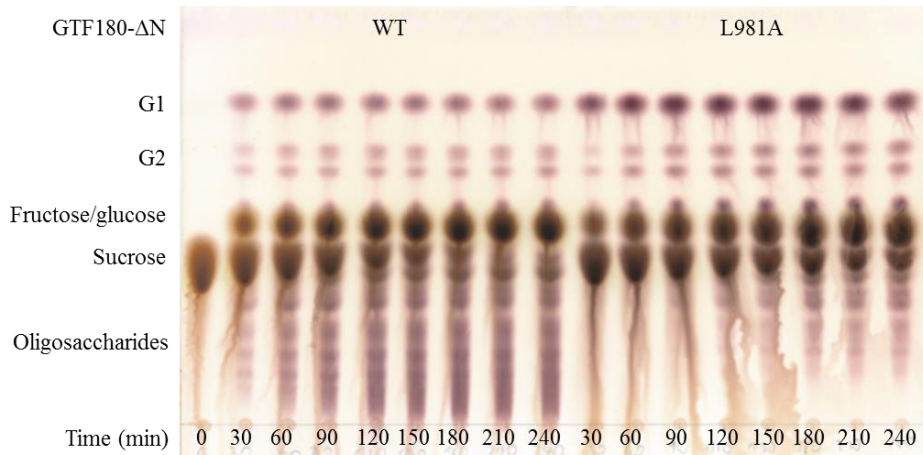


Figure S3. TLC analysis of products of resorcinol glycosylation by WT Gtf180- Δ N and the L981A mutant derived (400 mM resorcinol; 1000 mM sucrose; 4 U/mL Gtf180- Δ N (mutant)). G1 and G2 refer to the mono- and diglycosylated resorcinol products.

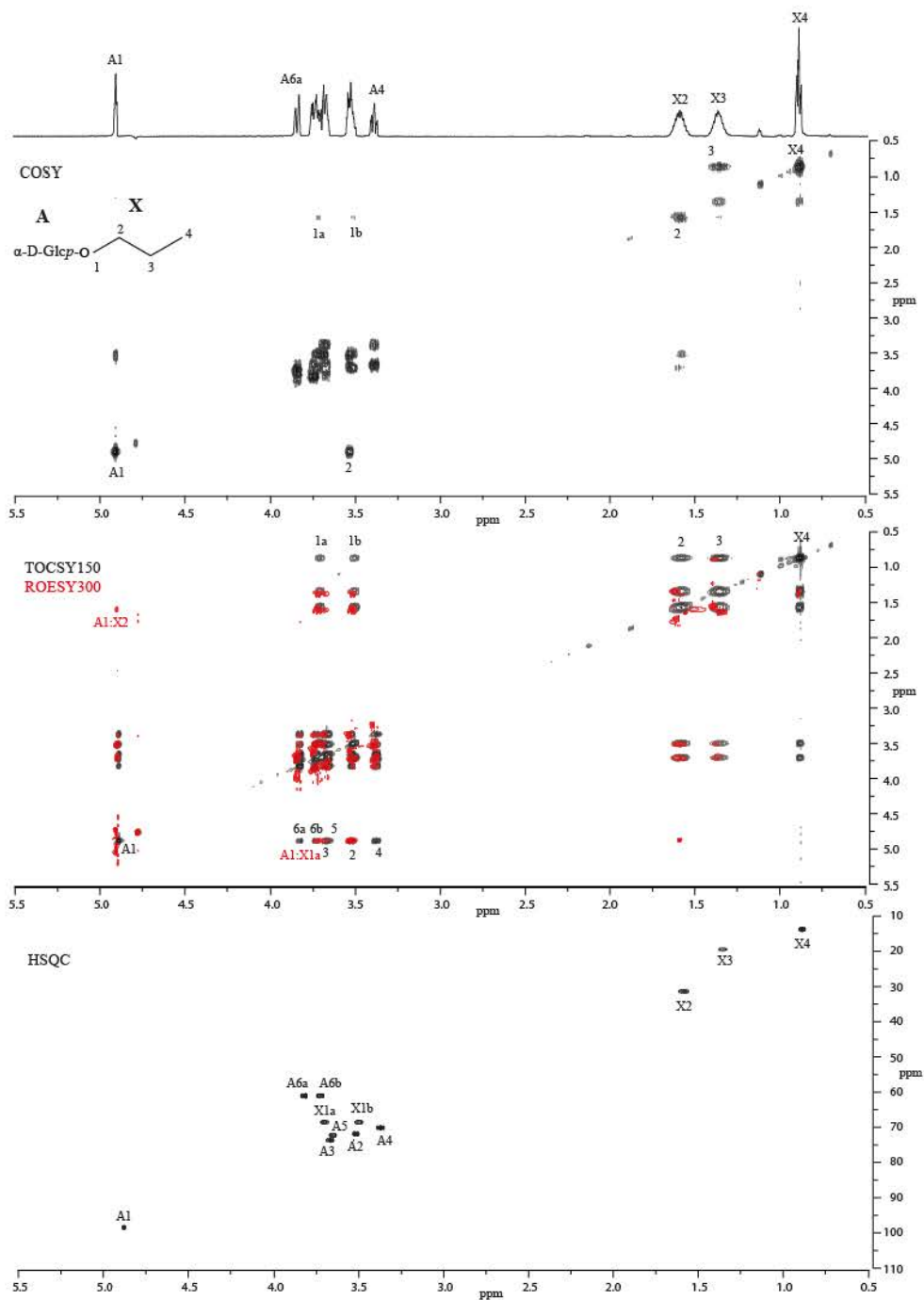


Figure S4. 1D ^1H NMR spectrum, and 2D ^1H - ^1H COSY, TOCSY (150 ms mixing time), ROESY (300 ms mixing time) and ^{13}C - ^1H HSQC spectra of butyl glucoside.

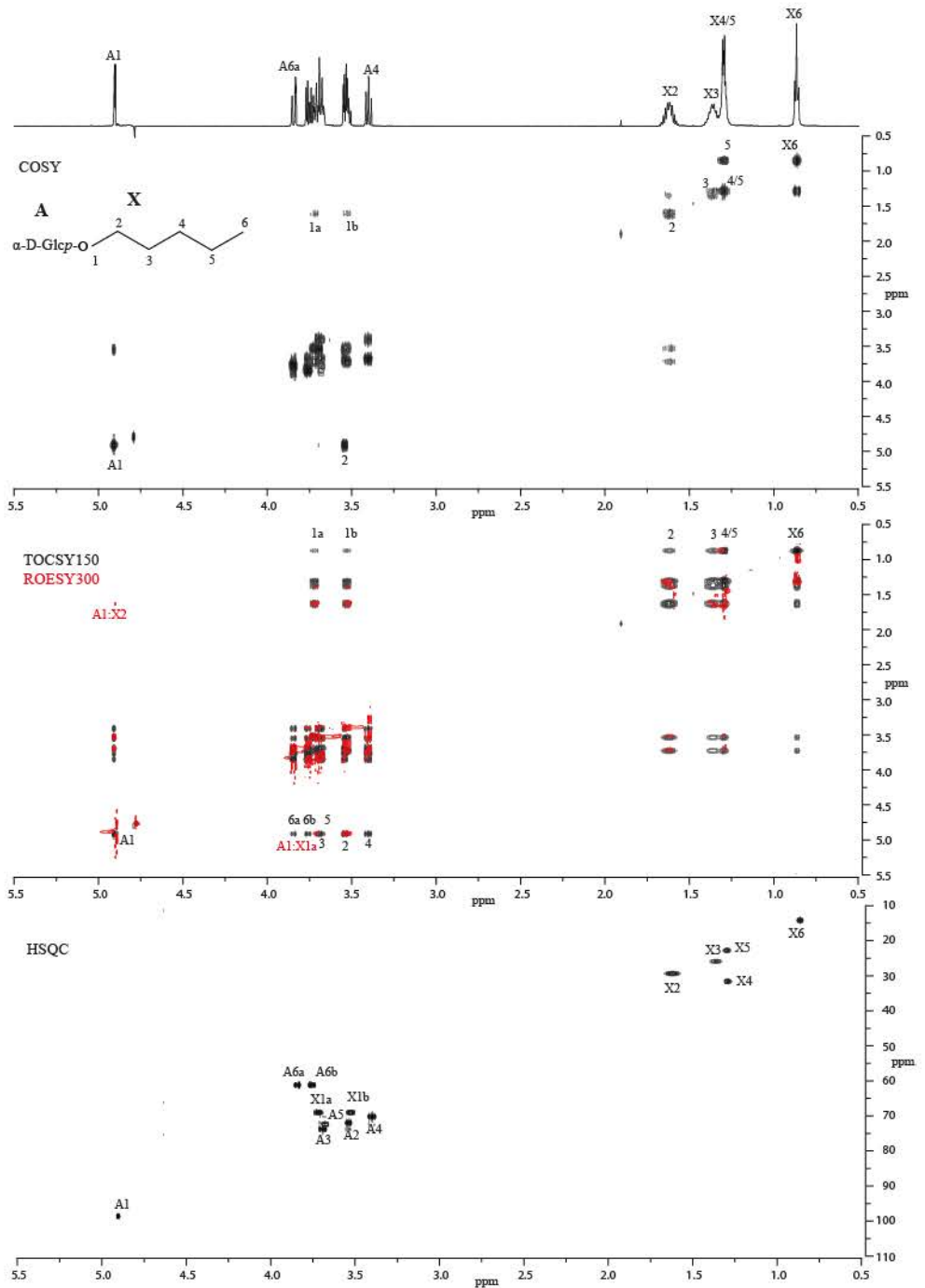


Figure S5. 1D ^1H NMR spectrum, and 2D ^1H - ^1H COSY, TOCSY (150 ms mixing time), ROESY (300 ms mixing time) and ^{13}C - ^1H HSQC spectra of hexyl glucoside.

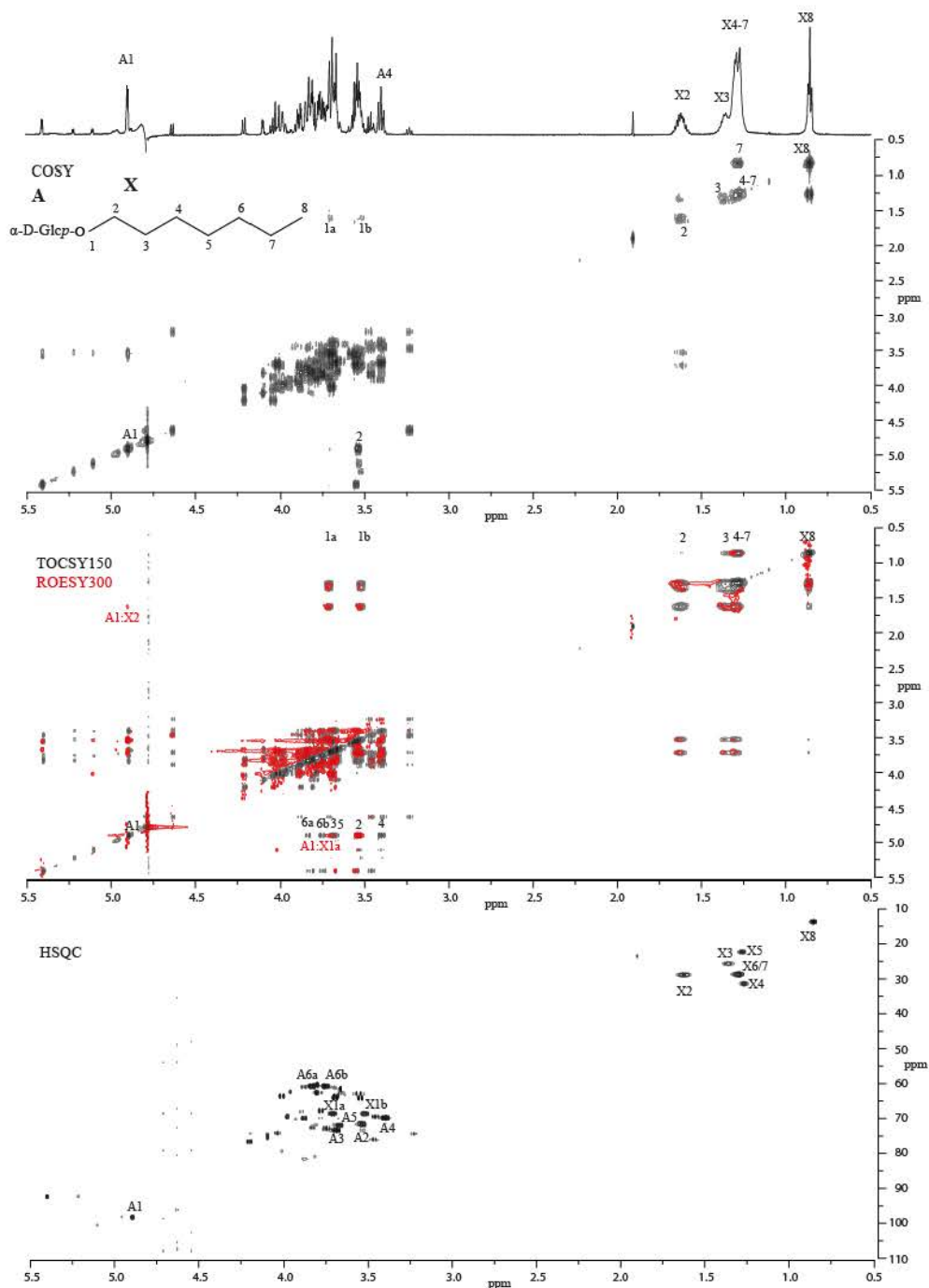


Figure S6. 1D ^1H NMR spectrum, and 2D ^1H - ^1H COSY, TOCSY (150 ms mixing time), ROESY (300 ms mixing time) and ^{13}C - ^1H HSQC spectra of octyl glucoside.

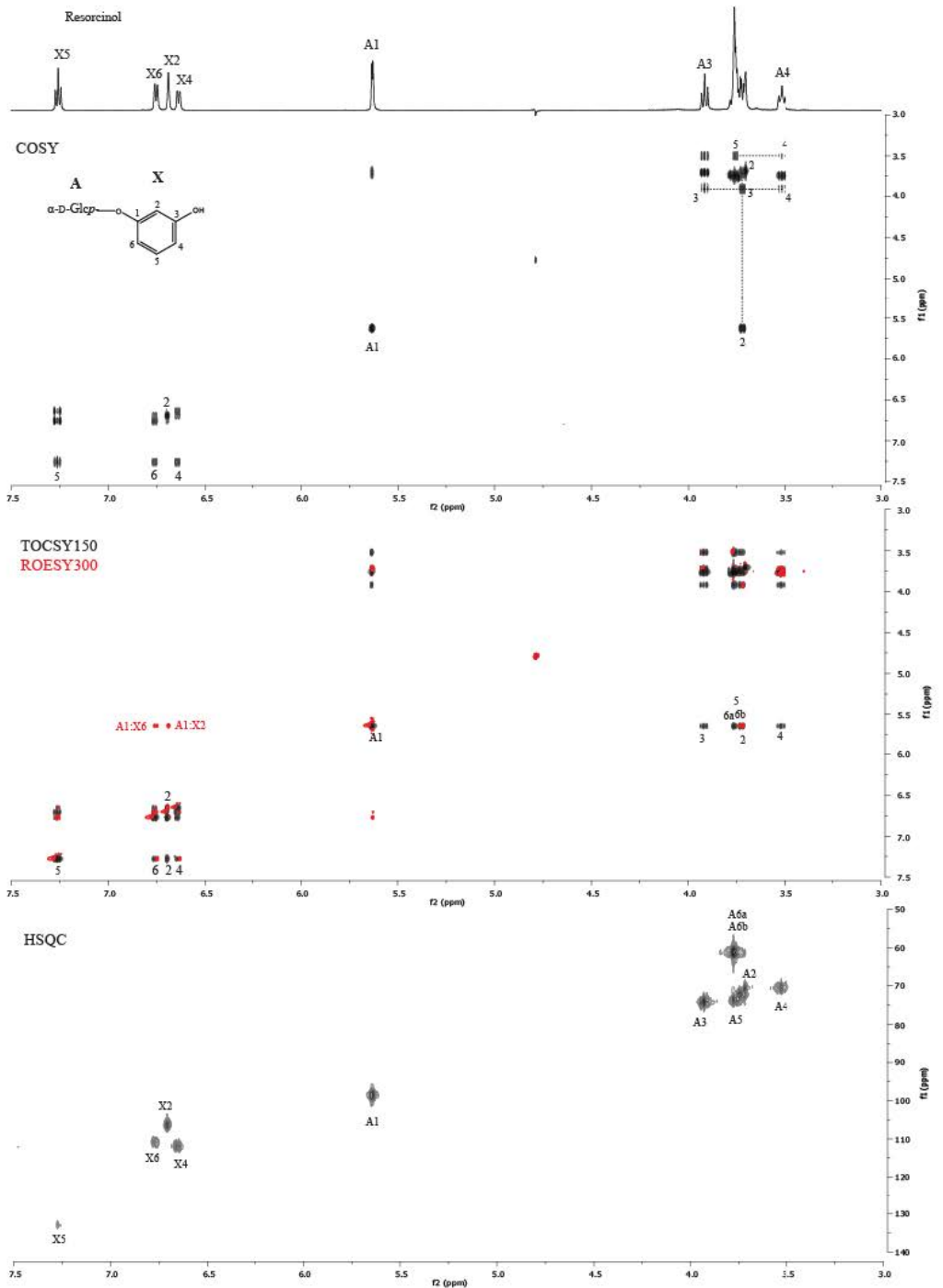


Figure S7. 1D ^1H NMR spectrum, and 2D ^1H - ^1H COSY, TOCSY (150 ms mixing time), ROESY (300 ms mixing time) and ^{13}C - ^1H HSQC spectra of resorcinol-G1.

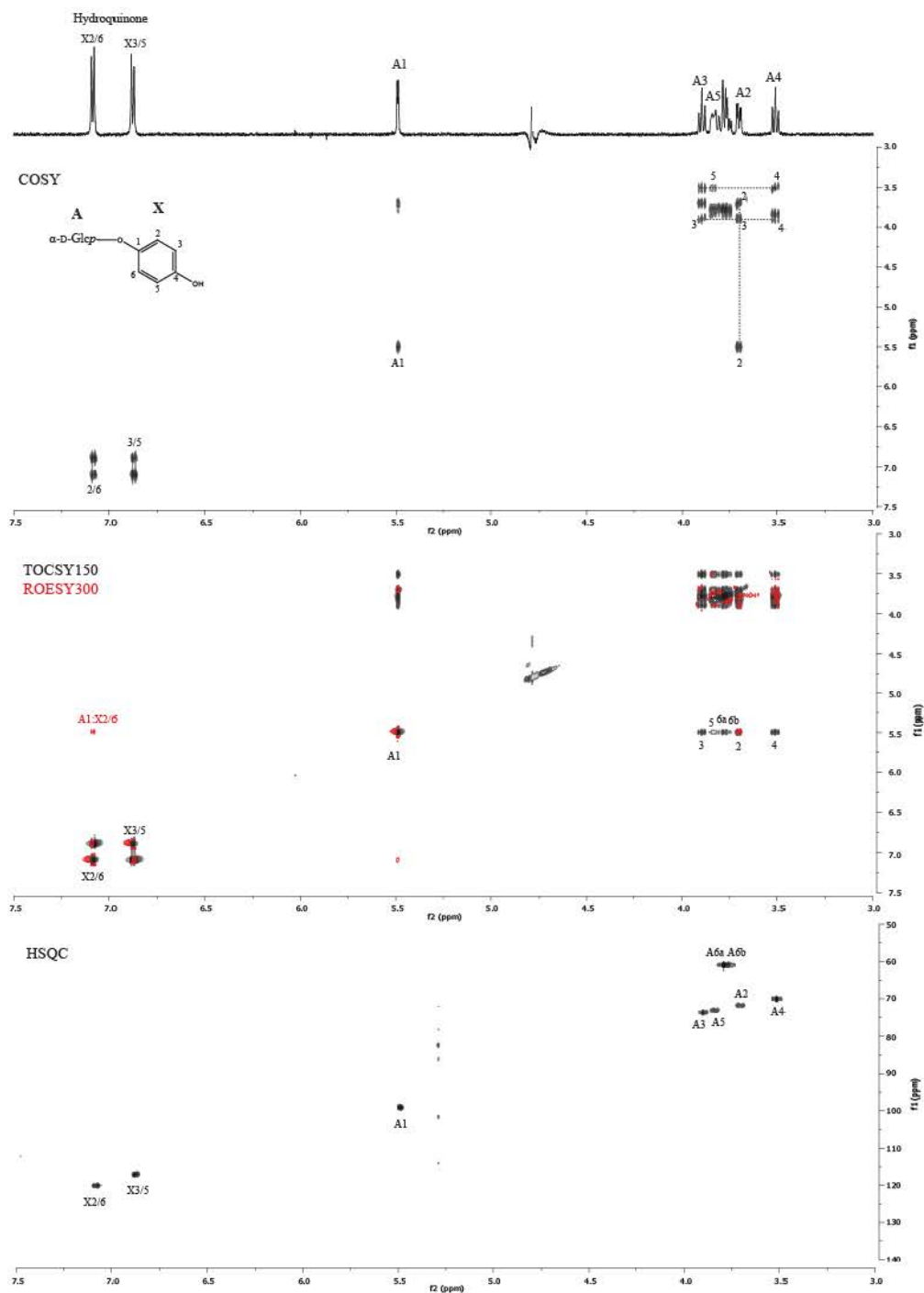


Figure S8 1D ^1H NMR spectrum, and 2D ^1H - ^1H COSY, TOCSY (150 ms mixing time), ROESY (300 ms mixing time) and ^{13}C - ^1H HSQC spectra of hydroquinone-G1.

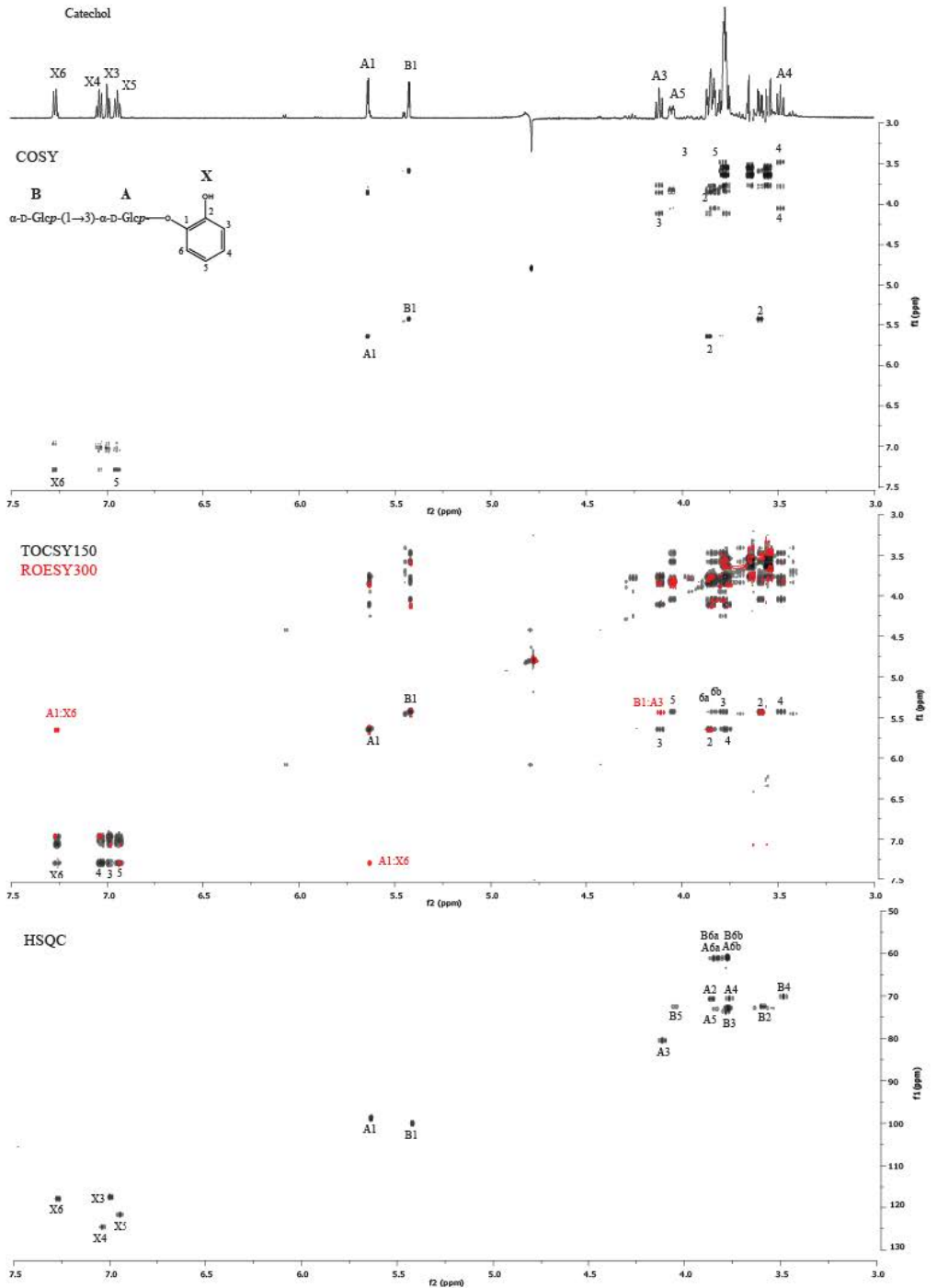


Figure S9. 1D ^1H NMR spectrum, and 2D ^1H - ^1H COSY, TOCSY (150 ms mixing time), ROESY (300 ms mixing time) and ^{13}C - ^1H HSQC spectra of catechol-3`G2.

Chapter 3

Improving the low operational stability of Gtf180- Δ N from *Lactobacillus reuteri* 180 by means of its immobilization

Tim Devlamynck^{1,2}, Wim Soetaert¹, Lubbert Dijkhuizen²
Ghent University¹, University of Groningen²

Abstract

Glucansucrases are increasingly targeted as biocatalyst for the glycosylation of non-carbohydrate acceptor substrates. A major obstacle in their industrial use remains their relatively low operational stability at high temperatures and in systems containing cosolvents and high acceptor substrate concentrations. As a consequence, glycosylation of poorly soluble compounds results in low yields and productivities as only low concentrations of these acceptor substrates can be supplied in the reaction mixture. This chapter focused on overcoming the low operational stability of Gtf180-ΔN from *Lactobacillus reuteri* 180 by cross-linking the enzyme to mesoporous silica particles, yielding an immobilized enzyme with enhanced activity at temperatures above 50 °C and in systems containing 20% DMSO, reaction conditions detrimental for the free enzyme. As a result, the glycosylation of gallic acid (GA), caffeic acid (CA) and catechin (CT) could be performed in reaction mixtures containing much higher concentrations of acceptor substrate. Their conversion was improved accordingly: from 63% to 82%, from 59% to 80%, and from 4% to 11%, for GA, CA and CT, respectively.

1. Introduction

Glucansucrases are glycoside hydrolase enzymes (GH70), catalyzing sucrose hydrolysis (minor activity) and the conversion of sucrose into α -glucan polysaccharides (major activity), linking the α -D-glucopyranosyl units by (α 1 \rightarrow 2), (α 1 \rightarrow 3), (α 1 \rightarrow 4) or (α 1 \rightarrow 6) bonds, depending on the enzyme specificity^{73,74}. In addition, they catalyze so called acceptor reactions, thereby glycosylating various (poly)phenolic and aliphatic compounds, using sucrose as donor substrate¹¹¹⁻¹¹⁴. As such, glucansucrases offer a cheap alternative for “Leloir” glycosyltransferases¹⁸, which require rare and expensive nucleotide-activated sugars as donor substrate¹³. Due to their broad acceptor substrate specificity and their use of inexpensive sucrose as donor substrate, glucansucrases have attracted considerable interest from academia and industry for their application as glycosylation biocatalyst. Glycosylation may result in an increased solubility of hydrophobic compounds³³, an improved stability of labile molecules against light and oxidation⁷, or a modified taste profile⁸.

Although several alternative acceptor substrates are indeed glycosylated by glucansucrases, very often incomplete conversions, with low to moderate yields, are obtained. Alternative acceptor substrates are per definition not the natural acceptor substrates of glucansucrases and, hence, they generally have rather high K_m values (Chapter 2)¹¹⁰. To outcompete α -glucan synthesis and hydrolysis as possible glucansucrase reactions, high concentrations of acceptor substrate are consequently required. Shifting the relative balance between the three glucansucrase reactions towards the acceptor reaction by applying high acceptor substrate concentrations was demonstrated as early as 1993 by Su and Robyt¹³². Furthermore, high space-time yields, which greatly reduce production costs, can only be achieved if the acceptor substrate concentrations are correspondingly high. It was demonstrated in Chapter 2 that suppressing α -glucan synthesis by mutational engineering enhanced the glycosylation of several phenolic and aliphatic compounds¹¹⁰. The biggest improvements were observed for small molecules such as catechol and butanol. The glycosylation of larger molecules,

such as flavonoids, was still problematic, mostly due to the low water solubility of these compounds, preventing their addition in higher concentrations. Chapter 2 also revealed that glucansucrases were inhibited by high concentrations of non-carbohydrate acceptor substrates: the glycosylation of catechol by Gtf180-ΔN from *Lactobacillus reuteri* 180 was inhibited at concentrations of catechol higher than 400 mM¹¹⁰. Similarly, catechol displayed inhibitory effects on glucansucrase GtfD from *Streptococcus mutans* GS-5 at a concentration of 200 mM¹²⁵. Finally, also the inhibition of amylosucrase (GH13) from *Neisseria polysaccharea* by several flavonoids has been reported¹²⁴.

As mentioned earlier, the limited water solubilities of many (poly)phenolic and aliphatic acceptor substrates complicate their glycosylation by glucansucrases. Increasing the solubility of acceptor substrates can be achieved by the addition of organic cosolvents such as DMSO, ethanol, acetone, etc. The main drawback of this strategy is that enzyme activity –and stability typically decrease with increasing solvent concentrations¹⁷². Determination of the initial activity of the dextransucrase from *Leuconostoc mesenteroides* NRRL B-512F in the presence of organic solvents revealed a 50% loss in activity in 20% DMSO, 15% ethanol, 15% acetone, 10% DMF and 7% acetonitrile¹³⁴. Diglyme or bis(2-methoxyethyl) ether (MEE) displayed a lower inhibitory effect on glucansucrases: the dextransucrase from *L. mesenteroides* NRRL B-512F and the alternansucrase from *L. mesenteroides* NRRL B-23192 retained more than 50% activity at an MEE concentration of 30%¹²⁰. The previous examples indicate that the combined use of high concentrations of certain acceptor substrates and high solvent concentrations may be even more detrimental for glucansucrase activity. Hence, a compromise between acceptor substrate concentration, solvent concentration and enzyme activity needed to be found.

An alternative approach comprises the application of a biphasic glycosylation system. In this way, the inhibitory effect of cosolvents can be circumvented while the solubility of the acceptor substrates is still enhanced. In a biphasic glycosylation system, the aqueous phase contains the biocatalyst and the donor substrate sucrose, whereas the organic phase contains the hydrophobic acceptor

substrates. Upon stirring, the acceptor substrates are transferred to the aqueous phase, where they are enzymatically glycosylated. Enzyme stability is correlated with solvent polarity: water miscible cosolvents distort the essential water layer that stabilizes the enzyme, whereas hydrophobic solvents will leave this layer of water molecules intact, resulting in a higher enzyme stability. Solvent polarity is expressed by the logarithm of the octanol/water partition coefficient ($\log P$). Solvents with a $\log P < 2$ will deactivate enzymes more distinctly than hydrophobic solvents with a $\log P > 4$ ¹⁷³. Furthermore, the use of a biphasic glycosylation system minimizes enzyme inhibition by acceptor substrates due to their low actual concentration in the aqueous phase; hydrophobic compounds are only slowly released from the organic phase, which acts as a substrate reservoir^{174,175}. The use of a biphasic glycosylation system was already demonstrated for the glycosylation of several phenolic and aliphatic compounds with sucrose phosphorylase from *Bifidobacterium adolescentis*, resulting in enhanced glycosylation yields²³.

Immobilization is a well-known strategy to increase the operational activity and stability of an enzyme. It may alleviate the decrease of enzyme activity and stability provoked by high solvent and acceptor substrate concentrations¹⁴⁰. An additional advantage is the possibility of recycling the immobilized biocatalyst, which can drastically lower the economic cost of the enzymatic process¹⁴¹. Glucansucrases have been described as troublesome to covalently immobilize, mainly due to inactivation of the enzyme during immobilization, e.g. by the participation of a lysine residue in the active site. Typical immobilization yields (ratio of activity of immobilized enzyme to the activity of enzyme prior immobilization) range from 3% to 22%¹⁴³⁻¹⁴⁶. In contrast, encapsulation of glucansucrases in alginate has been more successfully applied: several studies report immobilization yields up to 90%^{147,148}. However, the resulting alginate beads are not durable, since the accumulation of α -glucan polysaccharides inside the beads ultimately results in their rupture.

To our knowledge, the inhibitory effects of acceptor substrates and cosolvents on glucansucrases have never been countered by applying enzyme immobilization

nor by using a biphasic system. This chapter investigates both strategies to overcome the low operational stability of Gtf180-ΔN from *L. reuteri* 180: the application of a biphasic system with ethyl acetate as second phase, and the covalent immobilization of this enzyme on mesoporous silica particles.

2. Materials and methods

2.1. Production and purification of recombinant Gtf180-ΔN

Recombinant, N-terminally truncated Gtf180-ΔN from *Lactobacillus reuteri* 180 was produced and purified as described previously⁸⁰.

2.2. Protein determination

Protein concentration was determined using the BCATM Protein Assay kit from Pierce. The protocol as described in the kit was used. In short, 200 μL of freshly prepared assay solution was added to 25 μL of protein sample. After incubation at 37 °C for 30 min, the absorbance was measured at 562 nm. As standard series, bovine serum albumin (BSA) was used in a range from 0-2 mg/mL.

2.3. Activity assay for free and immobilized Gtf180-ΔN

Enzyme activity assays were performed at 37°C with 100 mM sucrose in 25 mM sodium acetate (pH 4.7) and 1 mM CaCl₂ unless indicated otherwise. Samples of 100 μL were taken every min over a period of 8 min and immediately inactivated with 20 μL 1 M NaOH for 30 min. The released glucose and fructose were quantified enzymatically by monitoring the reduction of NADP with the hexokinase and glucose-6-phosphate dehydrogenase/phosphoglucose isomerase assay (Roche) as described previously^{166,167}, allowing the determination of the total- (fructose release) and hydrolytic (glucose release) activities, and calculation of the transglycosylation activity.

One unit (U) of total activity corresponds to the release of 1 μ mole fructose from 100 mM sucrose in 25 mM sodium acetate (pH 4.7) and 1 mM CaCl₂ at 37 °C.

2.4. TLC analysis

TLC analysis of transglycosylation products was performed on silica gel 60 F₂₅₄ plates (Merck). The eluent consisted of *n*-butanol-acetic acid-water (2:1:1 by volume). Detection was achieved by UV absorption (254 nm) and/or staining with 10 % (v/v) H₂SO₄ containing 2 g/L orcinol.

2.5. HPLC analysis

An Agilent MetaCarb 67H column (300 mm \times 6.5 mm) was used under isocratic conditions with 2.5 mM H₂SO₄ as the mobile phase. The flow rate and temperature were set at 0.8 mL/min and 35 °C, respectively. Detection was achieved with an RID detector. Calibration of the obtained peaks was accomplished using the corresponding standard curves.

2.6. Solubility measurements

The solubility of gallic acid (GA) was determined in 250 μ L of ultrapure water, incubated in a thermoblock at 20 °C. GA was added until clear precipitation was noticeable, after which the samples were vortexed multiple times and allowed to equilibrate for 24 h. The supernatants were diluted in ethanol and subsequently subjected to HPLC analysis. Calibration was accomplished using the appropriate standard curve. The analysis was performed in duplicate.

2.7. Immobilization of Gtf180- Δ N on silanized silica particles

Before silanization (the functionalization of the silica surface with alkoxy silane molecules), the silica particles (10 g) were boiled in distilled water for 30 min. The wetted particles were then dissolved in 750 mL of a 10% solution of (3-aminopropyl)triethoxysilane (APTES) at pH 4 and subsequently heated in a water

bath at 75 °C for 4 h. The particles were washed three times with water and dried overnight at 80 °C. The silanized particles were stored at room temperature until further use.

Immobilization consisted of two steps: (1) adsorption of the enzyme on the support and (2) cross-linking of the adsorbed enzyme onto the support. In a 1.5 mL-Eppendorf tube, a suspension of 2 mg of silanized particles and 1 mL of buffered enzyme solution (containing 0.2 mg enzyme/mL) was shaken at room temperature for 1 h to ensure that adsorption equilibrium was reached. Subsequently, 10 μL of cross-linker (glutaraldehyde) was added and the suspension was shaken at room temperature for another hour. Afterwards, the supernatant was decanted using a benchtop centrifuge (10,000 g, 2 min) and the particles were washed with distilled water until no enzyme activity was detected (see 2.3.) in the wash solution.

3. Results and discussion

3.1. Solvent engineering: Applying Gtf180-ΔN in a biphasic –or cosolvent system

To improve the solubility of acceptor substrates, cosolvents such as DMSO and acetone are typically added to the glycosylation reaction mixture. The disadvantage of this strategy is that enzyme activity and stability decrease substantially. Alternatively, a biphasic glycosylation system can be implemented; hydrophobic solvents provoke less inhibition than hydrophilic ones. In 2014, De Winter et al. reported the application of a biphasic glycosylation system with sucrose phosphorylase, using ethyl acetate as second phase²³. The effect of using this system on Gtf180-ΔN catalyzed glycosylation reactions was consequently investigated. The glycosylation of ethyl gallate (EG), added to food products as antioxidant (E313) and representing a poorly soluble acceptor substrate with inhibitory effects on Gtf180-ΔN, was demonstrated previously¹³⁷ and chosen as model reaction. The enzyme was each time incubated with 1000

mM sucrose, while the concentration of EG and ethyl acetate (0 or 37.5% v/v) was varied (Figure 1).

Glycosylating 100 mM EG in the aqueous system resulted in a high conversion degree (Figure 1A), whereas the glycosylation of 100 mM EG in 37.5% ethyl acetate displayed a much lower conversion (Figure 1B). This effect can be explained by diffusion limitations between the ethyl acetate phase and the aqueous phase. The actual EG concentration near the enzyme is consequently substantially lower than 100 mM, resulting in relatively more α -glucan synthesis from sucrose at the expense of the acceptor reaction. Increasing the EG concentration to 400 mM yielded a higher product concentration, however, the EG conversion degree remained lower than in the aqueous system (Figure 1C). Conclusively, the application of a second phase to dissolve poorly soluble acceptor substrates should be avoided for glucansucrase mediated glycosylation reactions, due to the resulting decrease of acceptor substrate conversions.

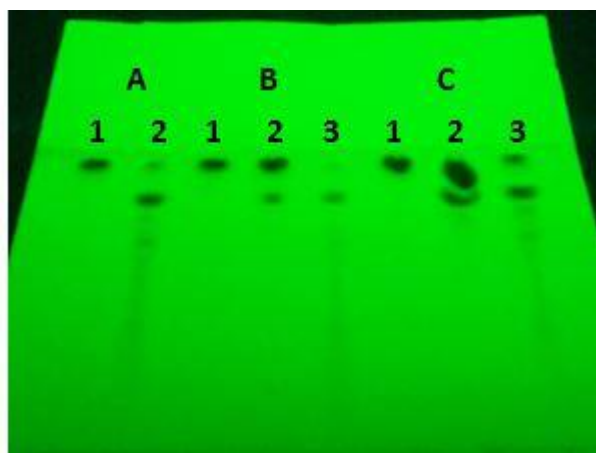


Figure 1. TLC analysis of ethyl gallate (EG) glycosylation by free Gtf180- Δ N (1000 mM sucrose, 4 U/mL enzyme), visualized by UV (254 nm). **A** 100 mM EG, 0% ethyl acetate; **B** 100 mM EG, 37.5% ethyl acetate; **C** 400 mM EG, 37.5% ethyl acetate. **A1, B1, C1** Incubation mixture without enzyme; **A2** 60 min incubation; **B2, C2** 60 min incubation (ethyl acetate phase); **B3, C3** 60 min incubation (aqueous phase).

Alternatively, the effect of using DMSO as cosolvent on Gtf180-ΔN catalyzed glycosylation reactions was investigated. The glycosylation of gallic acid (GA), a potential medicine for the treatment of Alzheimer's¹⁷⁶ and Parkinson's disease¹⁷⁷, served as case study. The solubility of GA in water at 37 °C was determined to be roughly 80 mM, which could be increased by using DMSO as cosolvent. Reactions with the free enzyme in 0%, 10% and 20% DMSO however illustrated the detrimental effect of cosolvent and acceptor substrate on Gtf180-ΔN activity (Figure 2).

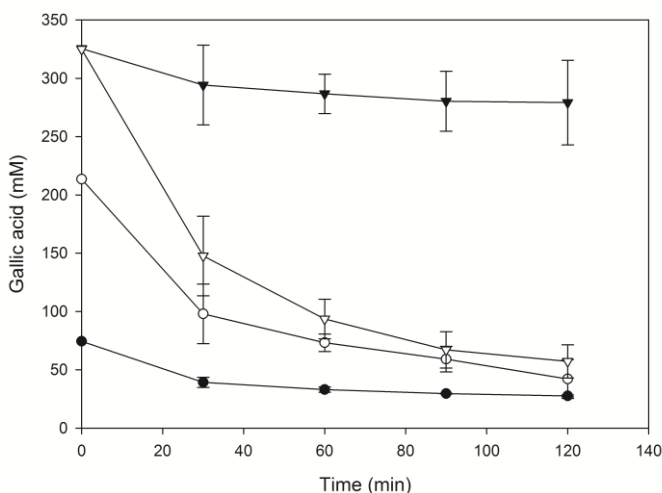


Figure 2. Depletion of gallic acid (GA) due to its glycosylation by free Gtf180-ΔN (1000 mM sucrose, 4 U/mL enzyme): ● 80 mM GA, 0% DMSO; ○ 210 mM GA, 10% DMSO; ▼ 325 mM GA, 20% DMSO; and by immobilized Gtf180-ΔN (1000 mM sucrose, 4 U/mL enzyme): ▽ 325 mM GA, 20% DMSO.

Glycosylation of GA by Gtf180-ΔN without the addition of DMSO (80 mM GA) resulted in a conversion of 63%. Interestingly, the GA conversion degree in 10% DMSO (210 mM GA) was significantly higher (80%) than in 0% DMSO (63%), indicating that the relative balance between α -glucan synthesis, sucrose hydrolysis and GA glycosylation was shifted towards the latter, due to the improved availability of the acceptor substrate GA. Glycosylation in 20% DMSO (325 mM GA) displayed a GA conversion degree of only 14%, which can be attributed to inactivation of the enzyme. Performing the glycosylation in 20%

DMSO might consequently further increase the GA conversion degree, provided that the enzyme is sufficiently stabilized.

3.2. Immobilization of Gtf180- Δ N on mesoporous silica particles

Previous paragraph was another illustration of the undesired inhibitory effects of acceptor substrates and cosolvents on Gtf180- Δ N, resulting in suboptimal glycosylation yields and conversion degrees. Immobilization of Gtf180- Δ N may alleviate this inhibition, more specifically by improving enzyme activity at high acceptor substrate –and cosolvent concentrations. Of all immobilization techniques, covalent immobilization provides the strongest interaction between enzyme and support, stabilizing the enzyme most thoroughly. Immobilization of Gtf180- Δ N on mesoporous silica particles was therefore first optimized, after which the characteristics of the immobilized enzyme were determined.

3.2.1. Optimization of Gtf180- Δ N immobilization

Several factors influence the covalent immobilization of enzymes on mesoporous silica, the most important being adsorption pH, concentration of cross-linker (mM), and enzyme loading (mg protein/g support)¹⁷⁸. Immobilizing a single layer of proteins (2-3 mg protein/m² support) may result in improved immobilization yields due to the reduction of substrate diffusion limitation and undesired conformational changes, both associated with multilayers¹⁷⁹. The specific surface area of the applied silica particles was roughly 50 m²/g. A single layer of protein was consequently formed when 100-150 mg Gtf180- Δ N/g or 4000-6000 U Gtf180- Δ N/g was adsorbed.

The pH was found to be crucial for adsorption –and cross-linking of the biocatalyst (Figure 3). An enzyme loading of 100 mg/g resulted in a nearly complete (>95%) adsorption at a pH range of 5.5-6. At a pH of 4.5 not even half of the enzyme was adsorbed, whereas 75% adsorption was achieved at a pH of 7. These results could only partly explain the sharp immobilization yield optimum: at a pH lower than 5.5, the enzyme was not efficiently cross-linked (as could be

visually observed by the absence of a red color, Figure S1), resulting in very low immobilization yields. Between a pH of 5.5 and 7, the immobilization yield decreased with increasing pH (Figure 3), suggesting that the enzyme was 'locked' in a more active conformation at slightly acidic conditions, as was demonstrated by Kondo et al. for α -amylase¹⁸⁰.

The optimal concentration of cross-linker (glutaraldehyde, GLU) generally is strongly dependent on the enzyme and carrier under consideration. For example, the immobilization of laccase using a similar protocol only required the use of 1 μ mol GLU per mg silica (~ 10 mM) to maximize the immobilization yield¹⁸¹, whereas Demarche et al. used 8 μ mol GLU per mg silica for laccase immobilization¹⁷¹. Increasing the concentration of GLU from 10 mM to 100 mM (~ 2.5 to 25 μ mol GLU per mg silica) had no effect on the immobilization yield with Gtf180- Δ N nor on its thermo-activity (data not shown). Therefore, 10 mM GLU was selected for further experimenting.

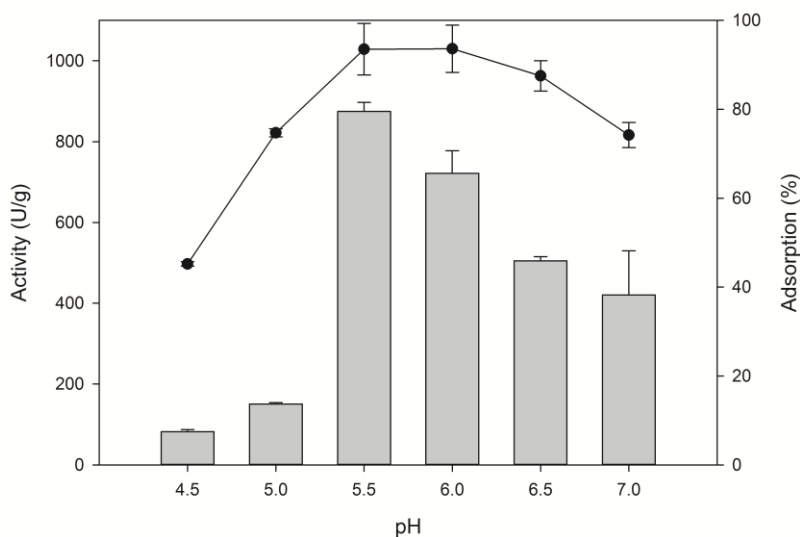


Figure 3. Effect of pH on adsorption and cross-linking of Gtf180- Δ N on mesoporous silica (4000 U/g, 10 mM GLU). **Line graph:** enzyme adsorbed (%). **Bar graph:** activity (U/g) after cross-linking.

3.2.2. Characterization of immobilized Gtf180- Δ N

Immobilized enzymes display very different characteristics compared to their soluble counterparts. Their stability and activity at high temperatures and high solvent concentrations is typically enhanced due to the 'rigidification' of the enzyme¹⁸², which may be advantageous for the glycosylation of poorly soluble acceptor substrates. The properties of glucansucrase Gtf180- Δ N immobilized on mesoporous silica were therefore compared with those of the free enzyme.

3.2.2.1. Effect of immobilization on thermo -and solvent activity

The optimal temperature for activity of the immobilized Gtf180- Δ N enzyme was found to be 55 °C, compared to 50 °C for the free enzyme. The immobilized enzyme even retained activity up to 65 °C, whereas the free enzyme lost all activity at 55 °C (Figure 4A). Improved thermo-activities are usually an indication of enhanced activities in cosolvent systems. Determination of the activity of immobilized and free enzyme in media with different concentrations of DMSO confirmed this hypothesis. The immobilized enzyme was remarkably more active in the presence of DMSO, retaining 87.3% of its solvent-free activity in 37.5% DMSO. In contrast, the free enzyme only retained 24.4% of its solvent-free activity in 25% DMSO and lost all activity at 37.5% DMSO (Figure 4B).

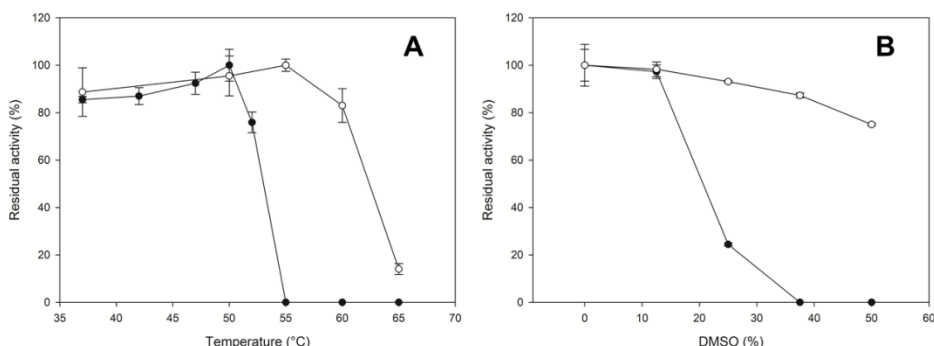


Figure 4. A. Thermo-activity of free (●) and immobilized (○) Gtf180- Δ N (100 mM sucrose, pH 4.7). **B.** Activity in solutions containing DMSO of free (●) and immobilized (○) Gtf180- Δ N (100 mM sucrose, pH 4.7, 50 °C).

3.2.2.2. Effect of immobilization on activity at high acceptor concentrations

Glucansucrases are inhibited by high concentrations of non-carbohydrate acceptor substrates, as was demonstrated for Gtf180- Δ N: the model substrate catechol could not be glycosylated at concentrations above 400 mM due to severe inhibition¹¹⁰. The immobilized enzyme was incubated with 400, 600 or 800 mM catechol and 1000 mM sucrose to determine the effect of immobilization on the glycosylation of non-carbohydrate acceptor substrates (Figure 5).

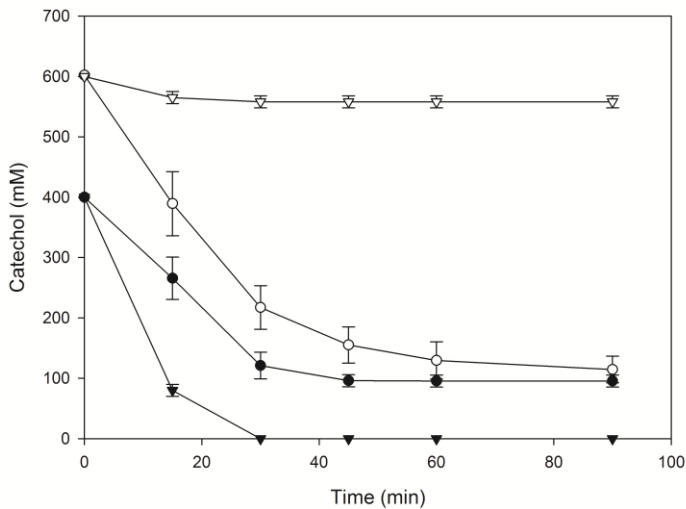


Figure 5. Depletion of catechol (CAT) due to its glycosylation by free and immobilized Gtf180- Δ N (1000 mM sucrose, 4 U/mL enzyme). ● Immobilized Gtf180- Δ N, 400 mM CAT; ○ Immobilized Gtf180- Δ N, 600 mM CAT; ▼ Free Gtf180- Δ N, 400 mM CAT; ▽ Free Gtf180- Δ N, 600 mM CAT.

Incubation of the immobilized enzyme with 400 mM catechol resulted in a 78% conversion of the latter into glycosides compared to 100% for the free enzyme. In contrast, sucrose was completely converted in both cases, indicating that the immobilized enzyme underwent undesired changes in the active site, resulting in a decreased affinity for the acceptor substrate catechol. Furthermore, 600 mM catechol was converted by the immobilized enzyme into glycosides with a conversion degree of 81%, slightly better than when incubated with 400 mM and significantly better than for the free enzyme (7%) (Figure 5). This confirms the

results of the thermo –and solvent activity experiments and demonstrates the improved operational stability of the immobilized enzyme. A concentration of 800 mM catechol resulted in deactivation of not only the free but also the immobilized enzyme (data not shown). In conclusion, the immobilized enzyme remained active at higher acceptor substrate concentrations, higher solvent concentrations and higher temperatures, compared to the free enzyme. However, its acceptor substrate affinity was altered, possibly due to participation of one or more amino acid residues in the active site during cross-linking. In fact, this is known to be one of the main disadvantages related to the use of GLU as cross-linker. Due to its small size, GLU can penetrate easily into the active site of enzymes and subsequently react with amino acid residues.

In order to prevent GLU from causing undesired changes in the active site, protecting agents, typically enzyme substrates, are used¹⁸³. Moreover, the activity of the immobilized enzyme towards the protecting agent/enzyme substrate can be improved by this ‘molecular imprinting’ of the enzyme’s active site¹⁸⁴. It is important that the substrate is not converted during immobilization to obtain the optimal protecting effect; catechol and maltose were consequently tested in different concentrations (100-400 mM) as protecting agent during Gtf180-ΔN immobilization. Unfortunately, the addition of catechol prevented cross-linking of the enzyme, whereas the addition of maltose had no effect on catechol glycosylation.

3.3. Glycosylation with immobilized Gtf180-ΔN

It was previously shown that GA glycosylation proceeds with improved conversion degrees in systems containing high GA concentrations, until DMSO and GA reach a concentration that is inhibitory to Gtf180-ΔN. In order to further improve GA glycosylation, immobilized Gtf180-ΔN was incubated in 20% DMSO, containing 325 mM GA (Figure 2).

Immobilization of Gtf180-ΔN alleviated the inhibiting effect of DMSO and GA, resulting in a GA conversion degree of 82%, which is slightly higher than the

conversion obtained after incubation of the free enzyme in 10% DMSO. In addition, the glycosylation in 20% DMSO of caffeic acid (CA), catechin (CT), and quercetin (QU) with immobilized Gtf180-ΔN was evaluated and compared with the glycosylation potential of the free enzyme in solvent-free reaction medium (Figure 6).

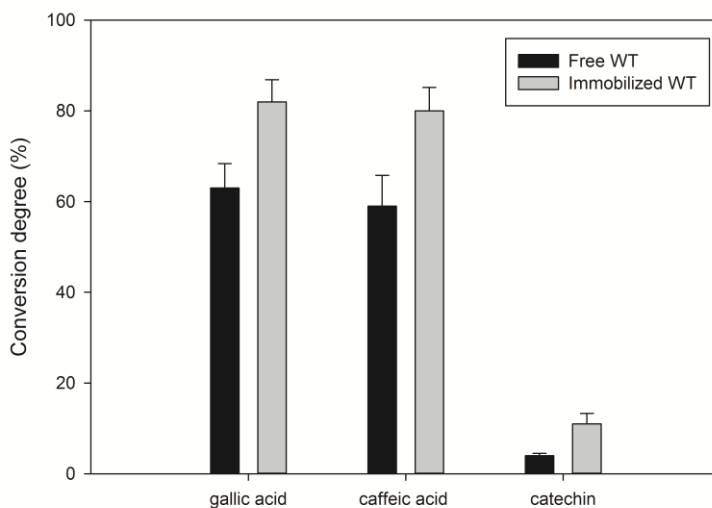


Figure 6. Conversion degrees for the glycosylation of gallic acid (GA), caffeic acid (CA) and catechin (CT) by immobilized Gtf180-ΔN in 20% DMSO and free Gtf180-ΔN in 0% DMSO (1000 mM sucrose, 4 U/mL enzyme).

CA and CT were glycosylated in 20% DMSO by the immobilized enzyme, and in 0% DMSO by the free enzyme. Similarly to GA glycosylation, higher conversions were obtained by the glycosylation systems containing 20% DMSO. QU was not glycosylated by the immobilized enzyme nor by the free enzyme, indicating that the applied strategy was ineffective in this case. The apparent very low affinity of Gtf180-ΔN for QU is clearly not sufficiently compensated by increasing its concentration in the reaction mixture. Also the suppression of α -glucan synthesis by mutational engineering (Chapter 2) did not result in improved QU conversion degrees, only causing more sucrose hydrolysis (as determined by screening of the mutant library described in Chapter 2^{99,110}). This indicates that specific

mutational engineering of Gtf180- Δ N's active site is required to enhance the glycosylation of QU and other related flavonoids.

4. Conclusions

The relatively low operational stability of Gtf180- Δ N at high temperatures and in systems containing cosolvents and high acceptor substrate concentrations ultimately results in suboptimal acceptor substrate conversion degrees. By means of its immobilization on mesoporous silica particles, the activity of Gtf180- Δ N under such conditions was substantially improved. The immobilized enzyme displayed enhanced activity at temperatures above 50 °C and in systems containing 20% DMSO, allowing the glycosylation of GA, CA and CT in systems containing much higher acceptor substrate concentrations. As a result, their conversion into glycosides was improved substantially: from 63% to 82%, from 59% to 80%, and from 4% to 11%, for GA, CA and CT, respectively. The glycosylation of QU, a compound which was very poorly glycosylated by the free enzyme, was also not successful using immobilized Gtf180- Δ N in 20% DMSO. Suppressing α -glucan synthesis by enzyme engineering (Chapter 2) nor solvent engineering (Chapter 3) were effective strategies to enhance QU's glycosylation, as this most probably requires specific mutational engineering of Gtf180- Δ N in order to increase its very low affinity for this molecule. Improving the glycosylation of related flavonoids, such as luteolin, or stilbenoids, such as resveratrol, will most probably demand the same strategy.

5. Supplementary information

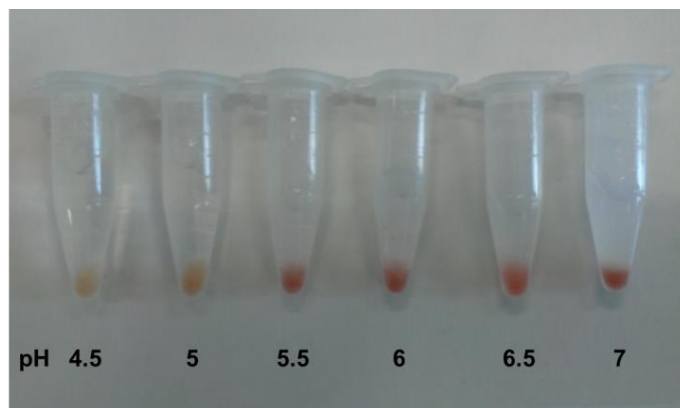


Figure S1. Successful cross-linking is indicated by the presence of a red color, caused by Rayleigh scattering.

Chapter 4

Glucansucrase (mutant) enzymes from *Lactobacillus reuteri* 180 efficiently transglucosylate *Stevia* component rebaudioside A, resulting in a superior taste

This chapter is submitted for publication as:

Evelien M. te Poele[#], Tim Devlamynck[#], Manuel Jäger, Gerrit J. Gerwig, Davy Van de Walle, Koen Dewettinck, Anna K.H. Hirsch, Johannes P. Kamerling, Wim Soetaert, Lubbert Dijkhuizen (2017) Glucansucrase (mutant) enzymes from *Lactobacillus reuteri* 180 efficiently transglucosylate *Stevia* component rebaudioside A, resulting in a superior taste. Sci Rep.

[#] these authors contributed equally to this work

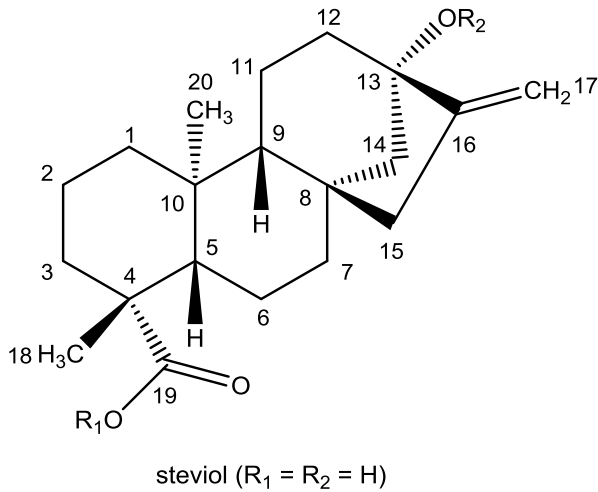
Abstract

Steviol glycosides from the leaves of the plant *Stevia rebaudiana* are high-potency natural sweeteners but suffer from a lingering bitterness. The *Lactobacillus reuteri* 180 wild-type glucansucrase Gtf180- Δ N, and in particular its Q1140E-mutant, efficiently α -glucosylated rebaudioside A (RebA), using sucrose as donor substrate. Structural analysis of the products by MALDI-TOF mass spectrometry, methylation analysis and NMR spectroscopy showed that both enzymes exclusively glucosylate the Glc(β 1 \rightarrow C-19 residue of RebA, with the initial formation of an (α 1 \rightarrow 6) linkage. Docking of RebA in the active site of the enzyme revealed that only the steviol C-19 β -D-glucosyl moiety is available for glucosylation. Response surface methodology was applied to optimize the Gtf180- Δ N-Q1140E-catalyzed α -glucosylation of RebA, resulting in a highly productive process with a RebA conversion of 95% and a production of 115 g/L α -glucosylated products within 3 h. Development of a fed-batch reaction further improved the product yield to 270 g/L by suppressing α -glucan synthesis. Sensory analysis by a trained panel revealed that glucosylated RebA products have a superior taste profile compared to RebA, showing a significant reduction in bitterness. The Gtf180- Δ N-Q1140E glucansucrase mutant enzyme thus is an efficient biocatalyst for generating α -glucosylated RebA variants with improved edulcorant/organoleptic properties.

1. Introduction

The world-wide increasing incidence of obesity, diabetes type II, cardiovascular diseases, and dental caries leads to an increased consumer demand for food products and beverages without high-calorie sugars⁴⁶. Steviol glycosides are excellent natural alternatives for sucrose and synthetic sweeteners¹⁸⁵⁻¹⁸⁹. These non-calorie compounds are extracted from the leaves of the herb plant *Stevia rebaudiana* BERTONI, a rhizomatous perennial shrub belonging to the Asteraceae [Compositae] family^{190,191}. Stevioside (~5-20% w/w of dried leaves) and rebaudioside A (RebA) (~2-5% w/w of dried leaves) are the most abundant steviol glycosides, followed in lower concentrations by rebaudioside B, C, D, E, F, M, steviolbioside, rubusoside and dulcoside A (Figure 1). Stevioside and RebA taste about 300 times sweeter than sucrose (0.4% aqueous solution). Steviol glycosides are approved as food additives in the USA since 2009 and they are on the European market (E 960, European Index) since December 2011⁴³. The main drawback for their more successful commercialization as sweeteners however, is a lingering bitter aftertaste of several steviol glycosides, experienced by about half of the human population due to a genetic basis of taste perception^{46,192}.

Structurally, steviol glycosides have *ent*-13-hydroxykaur-16-en-19-oic acid as aglycon, also called steviol (Figure 1)^{191,193}. The presence and composition of the different carbohydrate moieties at the C-19-carboxylic acid group (R₁) and at the C-13-*tert*-hydroxyl group (R₂) of steviol have a relationship with the sweetness as well as with the quality of taste of the steviol glycosides⁵². Sweetness increases and bitterness perception decreases with the total number of glycosyl residues⁴⁶. It has to be noted however, that the correlations bitterness/structure and sweetness/structure of steviol glycosides are still not fully understood, particularly in combination with the interactions with the human taste receptors^{46,192,194,195}.



Steviol glycoside	R_1 (C-19)	R_2 (C-13)
Stevioside	Glc(β 1 \rightarrow)	Glc(β 1 \rightarrow 2)Glc(β 1 \rightarrow)
Steviolbioside	H	Glc(β 1 \rightarrow 2)Glc(β 1 \rightarrow)
Rebaudioside A	Glc(β 1 \rightarrow)	Glc(β 1 \rightarrow 2)[Glc(β 1 \rightarrow 3)]Glc(β 1 \rightarrow)
Rebaudioside B	H	Glc(β 1 \rightarrow 2)[Glc(β 1 \rightarrow 3)]Glc(β 1 \rightarrow)
Rebaudioside C	Glc(β 1 \rightarrow)	Rha(α 1 \rightarrow 2)[Glc(β 1 \rightarrow 3)]Glc(β 1 \rightarrow)
Rebaudioside D	Glc(β 1 \rightarrow 2)Glc(β 1 \rightarrow)	Glc(β 1 \rightarrow 2)[Glc(β 1 \rightarrow 3)]Glc(β 1 \rightarrow)
Rebaudioside E	Glc(β 1 \rightarrow 2)Glc(β 1 \rightarrow)	Glc(β 1 \rightarrow 2)Glc(β 1 \rightarrow)
Rebaudioside F	Glc(β 1 \rightarrow)	Xyl(β 1 \rightarrow 2)[Glc(β 1 \rightarrow 3)]Glc(β 1 \rightarrow)
Rebaudioside M	Glc(β 1 \rightarrow 2)[Glc(β 1 \rightarrow 3)]Glc(β 1 \rightarrow)	Glc(β 1 \rightarrow 2)[Glc(β 1 \rightarrow 3)]Glc(β 1 \rightarrow)
Rubusoside	Glc(β 1 \rightarrow)	Glc(β 1 \rightarrow)
Dulcoside A	Glc(β 1 \rightarrow)	Rha(α 1 \rightarrow 2)Glc(β 1 \rightarrow)

Figure 1. Structures of major steviol glycosides, occurring in the leaves of *Stevia rebaudiana*. Glucose (Glc), xylose (Xyl) and rhamnose (Rha) occur in the pyranose ring form. Glc and Xyl have D configuration and Rha L configuration.

To improve the taste of steviol glycosides, especially for food applications, various (enzymatic) modifications of the carbohydrate moieties of steviol glycosides have been reported, mainly using cyclodextrin glycosyltransferase

(CGTase), α - and β -glucosidase, α - and β -galactosidase and β -fructosidase transglycosylation and β -glycosyltransferase glycosylation systems as biocatalysts⁸. In the context of our study, the reports on trans- α -glucosylation are of interest. CGTases are attractive enzymes, which catalyze coupling and disproportionation reactions, transferring glucose residues from starch or cyclodextrins to acceptor molecules, yielding Glc(α 1 \rightarrow 4) extensions. Although often high yields are obtained with steviol glycosides, CGTases have poor steviol C-13/C-19 site regioselectivity, producing mixtures of steviol glycoside derivatives with mostly (α 1 \rightarrow 4)-glucosylation at both carbohydrate moieties⁵¹. Several early studies have shown that both mono- and di-(α 1 \rightarrow 4)-glucosylation of the carbohydrate moiety at the steviol C-13 site of stevioside and rubusoside gave products with a remarkable improvement in both intensity and quality of sweetness. However, (α 1 \rightarrow 4)-glucosylation of the Glc(β 1 \rightarrow residue at the steviol C-19 site resulted in an increased bitter aftertaste and a lower sweetness intensity^{52-54,196}. α -Glucosylation of stevioside using Biozyme L (β -amylase preparation, probably contaminated with an α -glucosidase) and maltose as donor substrate resulted in a product with a decreased sweetness, but a remarkable improvement in the quality of taste [Glc(α 1 \rightarrow 6) residue attached at the Glc(β 1 \rightarrow C-19 residue), a product with a much lower sweetness [Glc(α 1 \rightarrow 6) residue attached to the terminal Glc(β 1 \rightarrow 2) residue of the β -sophorosyl-C-13 unit] and a product with a bitter taste [Glc(α 1 \rightarrow 3) residue attached to the terminal Glc(β 1 \rightarrow 2) residue of the β -sophorosyl-C-13 unit]⁶⁰.

In order to obtain steviol glycoside derivatives with improved organoleptic properties, we studied the α -glucosylation potential of mutant glucansucrase enzymes of the generally recognized as safe (GRAS) bacterium *Lactobacillus reuteri* 180 on RebA. Glucansucrases (EC 2.1.4.5; glycosyltransferases, Gtfs) are extracellular enzymes catalyzing the synthesis of α -D-glucan polymers from the donor substrate sucrose, thereby introducing different ratios of glycosidic linkages [(α 1 \rightarrow 2), (α 1 \rightarrow 3), (α 1 \rightarrow 4), (α 1 \rightarrow 6)] in their glucan products, depending on the enzyme specificities^{75,162}.

Recently, we have shown that the wild-type Gtf180- Δ N (N-terminally truncated) glucansucrase enzyme of *L. reuteri* 180 was able to glucosylate the steviol glycoside RebA, using sucrose as glucosyl donor substrate⁶⁹. About 55% of RebA was glucosylated with up to eight α -D-glucosyl units attached (RebA-G). The formed RebA derivatives only had elongations at the steviol C-19 β -D-glucosyl moiety, mainly with alternating (α 1 \rightarrow 6)- and (α 1 \rightarrow 3)-linked glucopyranose residues, starting with an (α 1 \rightarrow 6) linkage (RebA-G1). In the present study, we have screened our in-house collection of mutated Gtf180- Δ N glucansucrase enzymes for mutants with a better RebA glucosylating activity than the wild-type Gtf180- Δ N enzyme. One mutant was selected for more detailed studies and its biochemical characteristics and product profile were compared to wild-type Gtf180- Δ N. Glucosylated RebA products were isolated by flash chromatography and their structures were elucidated using MALDI-TOF mass spectrometry, methylation analysis and 1D/2D $^1\text{H}/^{13}\text{C}$ NMR spectroscopy. Furthermore, docking experiments with RebA and the available high-resolution 3D structure of Gtf180⁸³ were carried out to evaluate the experimental data. Response surface methodology was applied to optimize the reaction conditions of RebA glucosylation with the selected mutant. Finally, sensory evaluations were performed to determine the taste attributes of the novel α -glucosylated RebA derivatives.

2. Materials and methods

2.1. Glucansucrase enzymes

Gtf180- Δ N is the 117-kDa N-terminally truncated (741 residues) fragment of the wild-type Gtf180 full-length protein, derived from *L. reuteri* strain 180⁸⁰. In Gtf180- Δ N- Δ V both the N-terminal variable domain and the N-terminal domain V fragment (corresponding to the first 793 N-terminal amino acids), and the C-terminal domain V fragment (corresponding to the last 136 C-terminal amino acids) have been deleted⁸⁸. The glucansucrase Gtf180- Δ N mutant enzymes were

constructed using QuikChange site-directed mutagenesis (Stratagene, La Jolla, CA)^{80,88,97-100,102,197} (Table SI).

2.2. Standard reaction buffer

All enzymatic reactions were performed at 37 °C in 25 mM sodium acetate (pH 4.7), containing 1 mM CaCl₂.

2.3. Enzyme activity assays

Enzyme activity assays were performed at 37 °C in reaction buffer with 100 mM sucrose. Samples of 100 µL were taken every min over a period of 8 min and immediately inactivated with 20 µL 1 M NaOH. The glucose and fructose concentrations were enzymatically determined by monitoring the reduction of NADP with the hexokinase and glucose-6-phosphate dehydrogenase/phosphoglucose isomerase assays (Roche Nederland BV, Woerden, The Netherlands)¹⁶⁷. Determination of the release of glucose and fructose from sucrose allowed calculation of the total activity of the glucansucrase enzymes¹⁶⁶. One unit (U) of enzyme is defined as the amount of enzyme required for producing 1 µmol fructose per min in reaction buffer, containing 100 mM sucrose, at 37 °C.

2.4. Screening of (mutant) glucansucrases for α-glucosylation of RebA

In an initial screening, six Gtf180-ΔN-derived mutants were compared to wild-type Gtf180-ΔN by analyzing reaction products with high-performance liquid chromatography (HPLC). Then, an additional 76 Gtf180-ΔN mutants from our collection (Table SII) were screened and analyzed using thin-layer chromatography (TLC). Incubations of 3 h were performed in reaction buffer, containing ~1 mg/mL enzyme, 50 mM RebA (Sigma-Aldrich Chemie, Zwijndrecht, The Netherlands) and 1 M sucrose (for HPLC analysis) or 0.2 M sucrose (for TLC analysis). For HPLC analysis, 10 µL of the incubation mixture was diluted in 250 µL 80% methanol and centrifuged for 2 min at 15,000 × g. Then, 40 µL of the

upper phase was injected on a Luna 10 μm NH_2 column (250 \times 4.6 mm; Phenomenex, Utrecht, The Netherlands). Separation was obtained at a flow-rate of 1 mL/min under gradient elution conditions (solvent A = acetonitrile; solvent B = 0.025% acetic acid in H_2O), starting with a 2-min isocratic step of 70% solvent A followed by a linear gradient from 70 to 55% solvent A over 9 min and a final 3-min washing step of 20% solvent A. HPLC analyses were performed using an UltiMate 3000 chromatography system, equipped with a VWD-3000 UV-vis detector (ThermoFisher Scientific, Amsterdam, The Netherlands; monitoring at 210 nm). For TLC analysis, 1 μL of the enzymatic reaction mixtures was spotted on TLC sheets (Kieselgel 60 F254, 20 \times 20 cm; Merck, Darmstadt, Germany), which were developed in *n*-butanol/acetic acid/water (2:1:1, v/v/v). After drying of the sheets, the bands were visualized by orcinol/sulfuric acid staining.

2.5. Quantitative preparation of α -glucosylated RebA products

Incubations of 84 mM RebA (Tereos PureCircle Solutions, Lille, France; 97% purity, HPLC grade) were performed in 50 mL reaction buffer with 282 mM sucrose donor substrate, using 5 U/mL Gtf180- ΔN -Q1140E enzyme, during 3 h. Fractionations of RebA-G were carried out by flash chromatography using a Reveleris X2 flash chromatography system (Büchi Labortechnik AG, Flawil, Switzerland) with a Reveleris C18 cartridge (12 g, 40 μm) with water (solvent A) and acetonitrile (solvent B) as the mobile phase (30 mL/min). The following gradient elution was used: 95% solvent A (0-2 min), 95-50% solvent A (2-20 min), 50-95% solvent B (20-22 min), 95% solvent B (22-25 min). The collected fractions were evaporated *in vacuo* and subsequently freeze dried to remove the residual water.

2.6. Design of response surface methodology experiment

Response surface methodology¹⁹⁸ was applied to optimize the glucosylation of RebA. A Box-Behnken design¹⁹⁹ was generated implementing RebA concentration (mM), sucrose/RebA ratio and agitation rate (rpm) as factors. For

each of them low (-1) and high (+1) level values were assigned as follows: RebA concentration (50 mM) and (200 mM), sucrose/RebA ratio (1:1) and (4:1), agitation rate (0 rpm) and (200 rpm). The addition of 5 U/mL Gtf180- Δ N-Q1140E enzyme ensured a steady-state was reached within 3 h of incubation. The experimental design was generated and analyzed using JMP software (release 12)²⁰⁰ and consisted of 15 experiments carried out at 50 mL scale in shake flasks, continuously mixed by shaking (Table SIII). Results were analyzed with HPLC (see below). The response surface analysis module of JMP software was applied to fit the following second order polynomial equation:

$$\hat{Y} = \beta_0 + \sum_{i=1}^I \beta_i X_i + \sum_{i=1}^I \beta_{ii} X_i^2 + \sum_i \sum_j \beta_{ij} X_i X_j$$

where \hat{Y} is the predicted response, I is the number of factors (3 in this study), β_0 is the model constant, β_i is the linear coefficient associated to factor X_i , β_{ii} is the quadratic coefficient associated to factor X_i^2 and β_{ij} is the interaction coefficient between factors X_i and X_j . X_i represents the factor variable in coded form:

$$X_{c,i} = \frac{[X_i - (low + high)/2]}{(high - low)/2}$$

with $1 \leq i \leq I$, where $X_{c,i}$ is the coded variable.

For the HPLC analysis of the RebA and glucosylated RebA products, an Agilent ZORBAX Eclipse Plus C18 column (100 × 4.6 mm, 3.5 μ m) was used with water (solvent A) and acetonitrile (solvent B) as the mobile phase. The flow rate and temperature were set at 1.0 mL/min and 40 °C, respectively. The following gradient elution was used: 5-95% solvent B (0-25 min), 95% solvent B (25-27 min), 95-5% solvent B (27-30 min) and again 95% of solvent A (30-35 min). Detection was achieved with an ELS detector (evaporation temperature, 90 °C; nebulization temperature, 70 °C; gas flow rate, 1.6 SLM). Calibration of the obtained peaks for RebA and mono- α -glucosylated RebA (RebA-G1) was

accomplished using the corresponding standard curves. In this context, the concentration of multi- α -glucosylated product (RebA-G) at a specific time was calculated as the initial RebA concentration minus the RebA concentration at that time. Multi-glycosylated RebA product lacking RebA-G1 (defined as RebA-G2+) was equal to RebA-G minus RebA-G1.

2.7. Methylation analysis, mass spectrometry and NMR spectroscopy

For details of methylation analysis, gas-liquid chromatography – electron impact mass spectrometry (GLC-EIMS), matrix-assisted laser-desorption ionization time-of-flight mass spectrometry (MALDI-TOF-MS), and 1D/2D $^1\text{H}/^{13}\text{C}$ (TOCSY, ROESY, HSQC) NMR spectroscopy, see ref⁶⁹.

2.8. Molecular docking of RebA in the active site of Gtf180- ΔN and Gtf180- ΔN -Q1140E

The X-ray crystal structure of Gtf180- ΔN complexed with maltose (PDB code: 3KLL⁸³) was used for docking by using LeadIT 2.1.8 from BiosolveIT²⁰¹. The acceptor binding site was defined by manual selection and included the following amino acid residues: 935–941, 944, 964–968, 975–983, 985, 1023–1032, 1035, 1061–1069, 1082–1093, 1096, 1111, 1129–1142, 1144, 1145, 1155, 1183, 1202, 1204, 1407, 1409, 1411, 1412, 1443, 1446, 1456–1458, 1463–1466, 1504–1509, 1511, 1526, 1527, and the water molecules numbered 7, 15, 45, 83, 106, 144, 145, 172, 401, 432–436, 466, 469, 470, 527, 572, 605, 648, 666, which have at least two interactions. The crystal structure of rebaudioside A.4H₂O.1CH₃OH was taken from the literature (CSD entry: DAWCEL)²⁰², and the water and methanol were removed. The default settings were used for docking, except for the following features: the docking strategy was chosen to be driven by Entropy (Single Interaction Scan), a hard enzyme was used (maximum allowed overlap volume: 2 Å) and the maximum number of solutions per fragmentation was increased to 400. In total, 30 poses were generated with LeadIT, using the scoring function HYDE in SeeSAR²⁰³, ranked according to their estimated affinity; finally, poses with torsions flagged in red were removed. Visual inspection of the

residual poses and deletion of unreliable poses resulted in a trustable set of poses. The model of mutant Q1140E, which was used for the docking experiment, was built in PyMOL²⁰⁴ and the rotamer showing the smallest number of steric clashes was chosen.

2.9. Sensory analysis

Panellists were selected on basis of their performance on basic taste recognitions, ability to ascertain degrees of differences for specific taste stimuli at different concentrations and repeatability²⁰⁵, as verified by triangle tests and Wald sequential analysis²⁰⁶. Following the selection, the panel was trained over a 6-month period. In a first session, the panellists had to taste RebA solution at 10% (w/w) sucrose equivalent level. Their own vocabulary was used to describe taste and off-tastes as well as after tastes. In the second session, the following attributes were selected from the first session and from literature²⁰⁷⁻²⁰⁹: sweetness, liquorice, astringency and bitterness. In the following months, training sessions were alternated with discussion sessions to agree on scoring of sweetness, off-tastes, aftertastes and lingering on a 15 point hedonic scale, and evaluation protocol.

The actual Quantitative Descriptive Analysis (QDA) was performed in individual tasting booths at the UGent Sensolab (Belgium) by the trained panel (9 persons). The fixed evaluation protocol with standardized vocabulary was applied. Firstly, taste (sweetness, liquorice, astringency and bitterness) was evaluated by swirling the sample in the mouth for 5 sec after which the sample was expectorated. Secondly, aftertaste was evaluated 10 sec after swallowing the solution. Next, lingering based on the maximum taste intensity was rated 1 min later. Sucrose reference solutions (5%, 7.5% and 10% sucrose scoring 5, 7.5 and 10, respectively) were provided. Water (Spa Reine) and plain crackers were used as palate cleansers between sampling. All samples were evaluated in duplicate.

Statistical analyses were performed with SPSS 23 (SPSS Inc., Chicago, USA). All tests were done at a significance level of 0.05. One-Way ANOVA was used to

investigate any significant difference between the solutions. Testing for equal variances was executed with the Modified Levene Test. When conditions for equal variance were fulfilled, the Tukey test²¹⁰ was used to determine differences between samples. In case variances were not equal, the Games-Howell test was performed²¹¹.

Three different glucosylated products were examined: multi- α -glucosylated product, containing residual RebA (RebA-G), mono- α -glucosylated product (RebA-G1) and RebA-G lacking RebA and RebA-G1 (RebA-G2+). Note that RebA-G, as defined here, contains a very minor amount of residual RebA, in contrast to the RebA-G as quantified by HPLC analysis.

3. Results

3.1. Screening of wild-type Gtf180- Δ N and mutant glucansucrase enzymes for α -glucosylation of RebA

The RebA glucosylation activity of 82 mutant enzymes of Gtf180- Δ N (Tables SI and SII) was compared to that of the Gtf180- Δ N wild-type enzyme. To this end, 50 mM RebA was incubated for 3 h with ~1 mg/mL of each enzyme in reaction buffer, containing either 0.2 M sucrose (for TLC product analysis) or 1 M sucrose (for HPLC product analysis). It has to be noted that the *in vivo* and most important activity of glucansucrases is the synthesis of α -D-glucan polymers and oligosaccharides from the donor substrate sucrose⁷⁵. During the transglucosylation reaction with acceptor substrates such as steviol glycosides, the formation of α -gluco-oligo/polysaccharides is observed as a side-reaction, occurring to a varying extent depending on the specific (mutant) glucansucrase. The TLC (Figure S1) and HPLC (Figure S2) profiles obtained after the different enzyme incubations with RebA and sucrose clearly showed that most of the Gtf180- Δ N mutants could α -glucosylate RebA in similar amounts (based on spot intensity) as the wild-type Gtf180- Δ N enzyme (TLC lane 77). Mutant A978P (TLC lane 64) and mutants Q1140E and S1137Y (Figure S2), however, converted

more RebA than the wild-type enzyme, as can be seen by a smaller amount of residual RebA after the 3 h incubation. Some mutants, i.e. L981A (TLC lane 31), W1065L (TLC lane 71) and W1065Q (TLC lane 72), converted comparable amounts of RebA as the wild-type enzyme, but showed almost no polymerization activity, as indicated by the absence of the α -gluco-oligo/polysaccharide tails on TLC. However, previously it has been shown that the mutations L981A, W1065L and W1065Q had a dramatic effect on the overall enzyme activity, resulting in a 93, 87 and 93% decrease at 100 mM sucrose, respectively^{99,102}. Of all mutants tested, Q1140E showed the highest RebA conversion (Figure S2), and was therefore chosen for further studies, and compared to the wild-type Gtf180- Δ N enzyme. Mutant Gtf180- Δ N-Q1140E contains a single amino acid substitution (from a glutamine to a glutamate) close to the transition-state-stabilizing residue D1136⁹⁷.

3.2. Analytical details of α -glucosylated RebA products prepared with Gtf180- Δ N-Q1140E

For structural analysis purposes, a large-scale preparation of α -glucosylated RebA products was performed using 84 mM RebA, 282 mM sucrose and 5 U/mL Gtf180- Δ N-Q1140E enzyme (pH 4.7, 3 h, 37 °C). The applied incubation conditions, shown to be optimal, were taken from the Box-Behnken experimental design study, as described in the section “Optimization of the synthesis of α -glucosylated RebA” (see below). The used commercial RebA substrate is of high purity, as indicated by its ¹H NMR spectrum (Figure S3; for the assignment of the resonances, see ref⁶⁹), MALDI-TOF mass spectrum (Figure S4) and methylation analysis (Table SIV). Contamination with other steviol glycosides was not detected, which is also of importance for the sensory analysis.

MALDI-TOF-MS analysis of the total RebA-incubation mixture (RebA-G) showed a series of quasi-molecular ions $[M+Na]^+$, revealing remaining RebA (m/z 989.7) and extensions of RebA with one (major peak, m/z 1152.9) up to eight glucose residues (m/z 2287.9) (Figure S4). The ¹H NMR spectrum of RebA-G (Figure 2A) showed the typical steviol core signal pattern as seen for RebA (Figure S3).

Besides the four β -anomeric ^1H signals related to RebA (for structure, see Figure 3; Glc1, δ 5.425; Glc2, δ 4.700; Glc3, δ 4.801; Glc4, δ 4.700), one additional α -anomeric ^1H signal of similar intensity at δ 4.870 (Glc5) stemming from mono- α -glucosylated RebA was observed, together with very minor α -anomeric signals (marked with * in Figure 2A) at δ 5.42 and δ 5.27, and a H-5 signal at δ 4.10, reflecting the presence of higher α -glucosylated RebA products (<10%).

Flash chromatography fractionations were carried out to separate mono- α -glucosylated RebA (major fraction RebA-G1; MALDI-TOF-MS analysis: $[\text{M}+\text{Na}]^+$, m/z 1152.9; Figure S4) from higher α -glucosylated RebA products (pooled very minor fractions RebA-G2+) and residual RebA. The ^1H NMR spectrum of RebA-G1 (Figure 2B) is identical to that reported recently for RebA-G1, prepared with the wild-type Gtf180- ΔN enzyme⁶⁹. The very minor pool of higher α -glucosylated RebA fractions, RebA-G2+, was not used for further structural analysis. In summary, it can be concluded that the mutant Gtf180- ΔN -Q1140E enzyme synthesizes as dominant product (77.7% in RebA-G) the same mono- α -glucosylated RebA derivative RebA-G1 as shown for the wild-type Gtf180- ΔN enzyme, i.e. a product with a specific elongation of the steviol C-19 β -D-Glcp moiety of RebA with an α -D-Glcp-(1 \rightarrow 6) residue (Figure 3). Taking into account the structural data of the α -glucosylated RebA products isolated in the wild-type Gtf180- ΔN /RebA/sucrose incubation study⁶⁹, combined with the above-mentioned extra minor signals in the ^1H NMR spectrum of RebA-G (Figure 2A), it can be concluded that also in the case of the Gtf180- ΔN -Q1140E/RebA/sucrose incubation, RebA-G1 is further extended at the C-19 site with mainly alternating (α 1 \rightarrow 3)- and (α 1 \rightarrow 6)-linked D-Glcp residues. The methylation analysis data of RebA-G and RebA-G1, presented in Table SIV, support the NMR data.

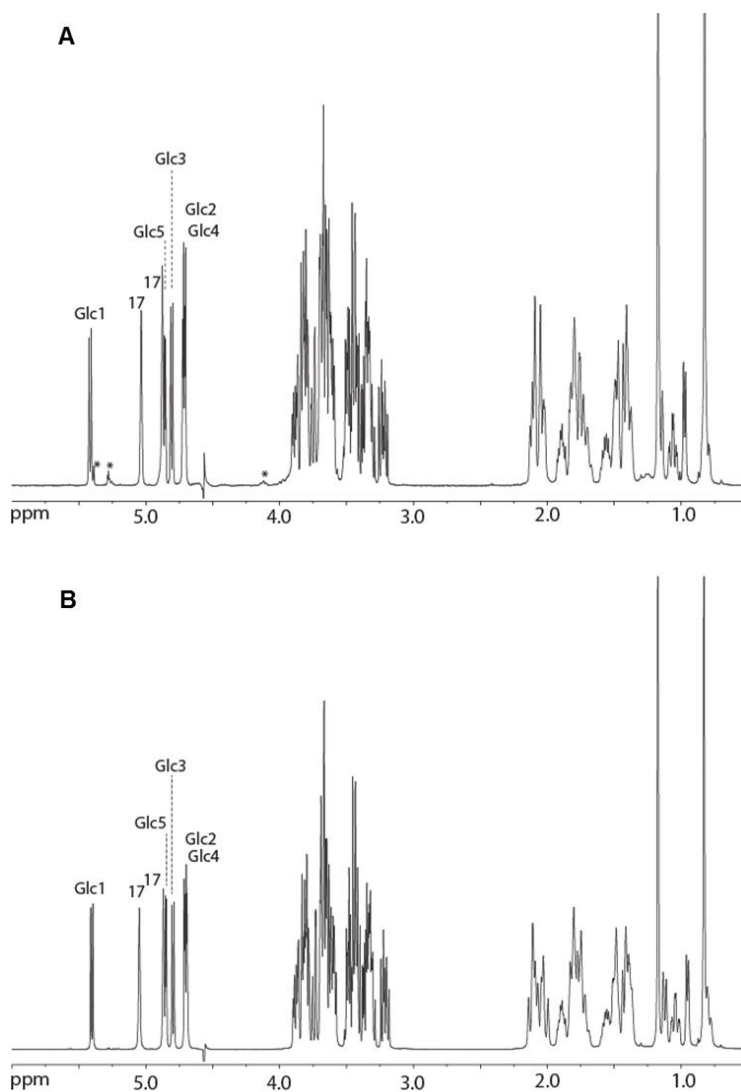


Figure 2. 500-MHz ^1H NMR spectra of (A) RebA-G and (B) RebA-G1, recorded in D_2O at 310 K. The positions of the anomeric protons of the glucose residues (see Figure 3) are indicated, as well as the steviol C-17 protons in the anomeric region. Products were synthesized using the mutant Gtf180- ΔN -Q1140E enzyme. Spectrum B is identical to that of RebA-G1, prepared with the wild-type Gtf180- ΔN enzyme, and recently published with a complete assignment of resonances⁶⁹. * signals stemming from higher α -glucosylated RebA products. Chemical shifts (δ) are expressed in ppm by reference to internal acetone (δ 2.225).

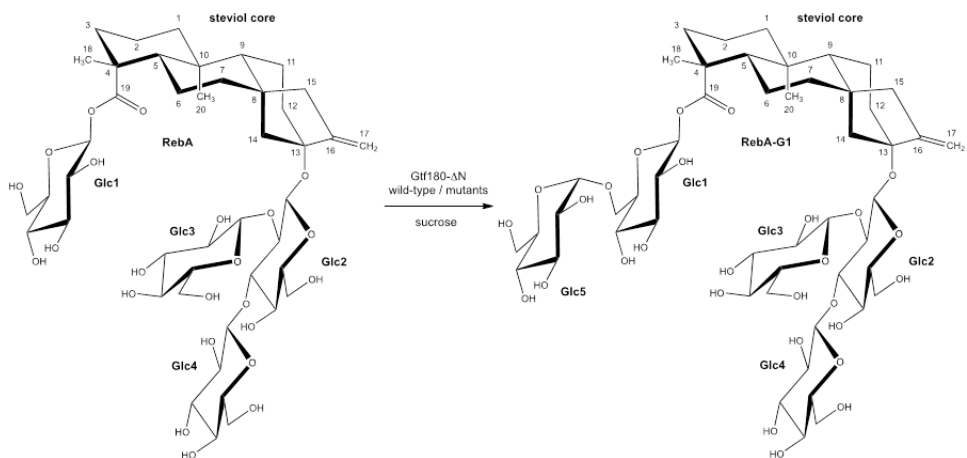


Figure 3. Major reaction product RebA-G1, obtained from the incubation of RebA with wild-type Gtf180- Δ N and mutant Gtf180- Δ N-Q1140E enzymes, in the presence of sucrose.

3.3. Optimization of the synthesis of α -glucosylated RebA

Batch reaction. RebA is only sparingly soluble in water (< 10 mM) at room temperature, however, it readily forms supersaturated solutions in water on simple stirring²¹². It was observed that up to 200 mM RebA could be dissolved at 37 °C before it started precipitating at 90 min. Hence, an efficient conversion of 200 mM RebA into glucosylated products has to be achieved within 90 min in order to prevent a suboptimal glucosylation yield caused by precipitation of RebA. Important factors for an optimal conversion of RebA into α -glucosylated RebA (RebA-G) are the RebA concentration, the ratio of donor substrate sucrose over acceptor substrate RebA (D/A ratio) and the agitation speed.

A response surface methodology (RSM) using a Box-Behnken experimental design was performed considering three factors: X_1 , RebA concentration (mM); X_2 , D/A ratio; X_3 , agitation speed (rpm). The addition of 5 U/mL Gtf180- Δ N-Q1140E enzyme ensured that a steady state in RebA conversion was obtained well before precipitation could occur for the highest RebA concentration (90 min). The results of the Box-Behnken experimental design are summarized in Table SIII. The analysis of variance (ANOVA) showed R^2 values of 98.8%, 78.0% and

99.3% for RebA conversion degrees (%), RebA-G1/RebA-G ratio (%) and amount of RebA-G synthesized (mM), respectively. The effects of the factors were analyzed applying the response surface contour plots (Figure 4).

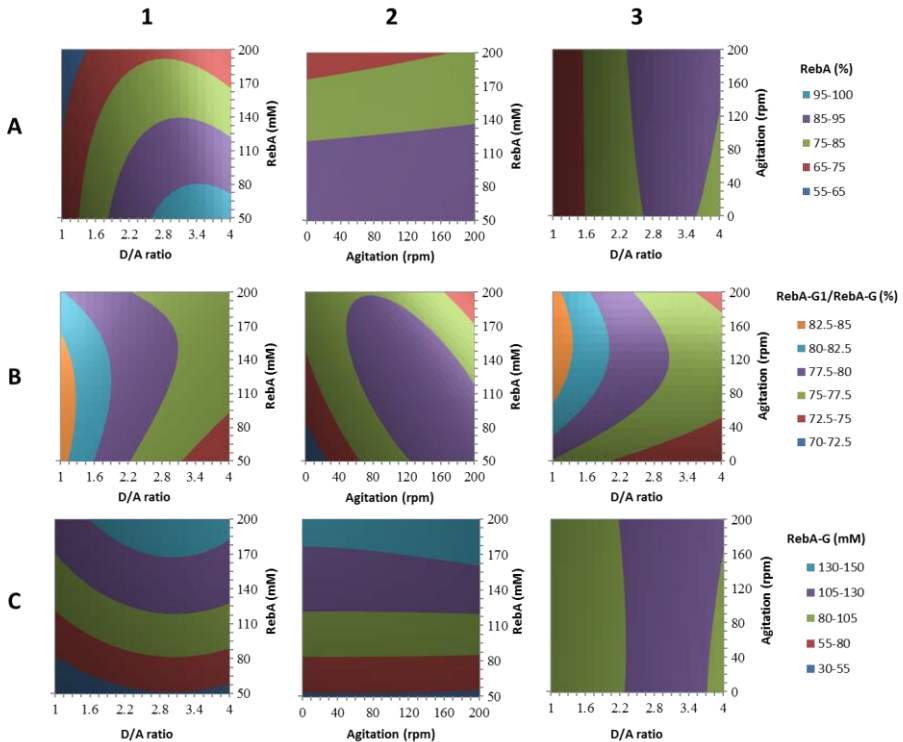


Figure 4. Response surface methodology contour plots of RebA glucosylation by Gtf180- Δ N-Q1140E, showing the effects of RebA concentration (mM), D/A ratio (ratio of donor substrate sucrose over acceptor substrate RebA) and agitation (rpm) on (A) RebA conversion degree (%); (B) RebA-G1/RebA-G ratio (%); (C) RebA-G synthesized (mM).

In summary, RebA conversion degrees decreased with increasing RebA concentrations, independent of the sucrose concentration (Figure 4A1). The RebA conversion degrees displayed an optimum at a D/A ratio of 2.5-3.5, depending on the RebA concentration (Figures 4A1-A3). Increasing the D/A ratio initially resulted in improved RebA conversion degrees, reflecting that more sucrose was available to drive the reaction. A further increase of the D/A ratio resulted in less RebA glucosylation in favor of more α -glucan synthesis. Agitation

had only a slight effect on RebA conversion degrees and amount of RebA-G synthesized (Figures 4A2-C2). Agitation influenced the RebA-G1/RebA-G ratio more strongly: the highest ratios were observed at an agitation speed of approximately 185 rpm (Figures 4B2-B3). Furthermore, low D/A ratios favored high RebA-G1/RebA-G ratios, since less donor substrate sucrose was available to glucosylate RebA-G1 into multi-glucosylated products (Figure 4B1).

The resulting Box-Behnken model (Table SIII) was subsequently used for the optimization of the reaction conditions. An efficient conversion of RebA into RebA-G yielding a maximal amount of RebA-G (at least 95%) was aimed for. The model predicted the synthesis of 80 mM RebA-G in case the following conditions were applied: 5 U/mL Gtf180- Δ N-Q1140E, 84 mM RebA, 282 mM sucrose and 185 rpm. The validation test resulted in the synthesis of 79 mM (or 115 g/L) RebA-G with a RebA-G1/RebA-G ratio of 77.7% (Figure 5A), which was in very good agreement with the prediction. Applying identical conditions for the glucosylation of RebA with wild-type Gtf180- Δ N resulted only in the conversion of 49.7% RebA, yielding 42 mM RebA-G with a RebA-G1/RebA-G ratio of 54.4% (Figure 5B). Hence, the Q1140E-mutant not only converted more RebA into RebA-G than wild-type Gtf180- Δ N (94.5% vs. 49.7%), its RebA-G consisted mostly of mono- α -glucosylated product RebA-G1 (77.7% vs. 54.4%). Compared to wild-type (45.6%), Q1140E produced less RebA-G2+ (22.3%), which is the minor fraction of the RebA glucosides with 2 and more glucose units.

Fed-batch reaction. The main remaining bottleneck for RebA glucosylation with Gtf180- Δ N-Q1140E is the synthesis of α -glucans at high sucrose concentrations, preventing complete RebA glucosylation at high RebA concentrations (Figure 4A1). This issue was addressed by performing a fed-batch reaction, in which sucrose was added to the reaction in fixed intervals of 20 min in order to keep the sucrose concentration low and hence suppress α -glucan formation as much as possible. The addition of 50 U/mL enzyme ensured complete usage of sucrose within 20 min and complete conversion of RebA within 3 h. Figure 5C represents RebA glucosylation at 200 mM RebA and an average sucrose concentration of 50 mM (fluctuating between 0-100 mM). In comparison to the batch reaction (200

mM RebA, 570 mM sucrose; Figure 5D), the RebA fed-batch conversion (Figure 5C) increased from 76.4% to 94.1%, attributed to a further suppressed α -glucan synthesis. The product yield consequently increased to 188 mM (or 270 g/L) RebA-G (Figure 5C).

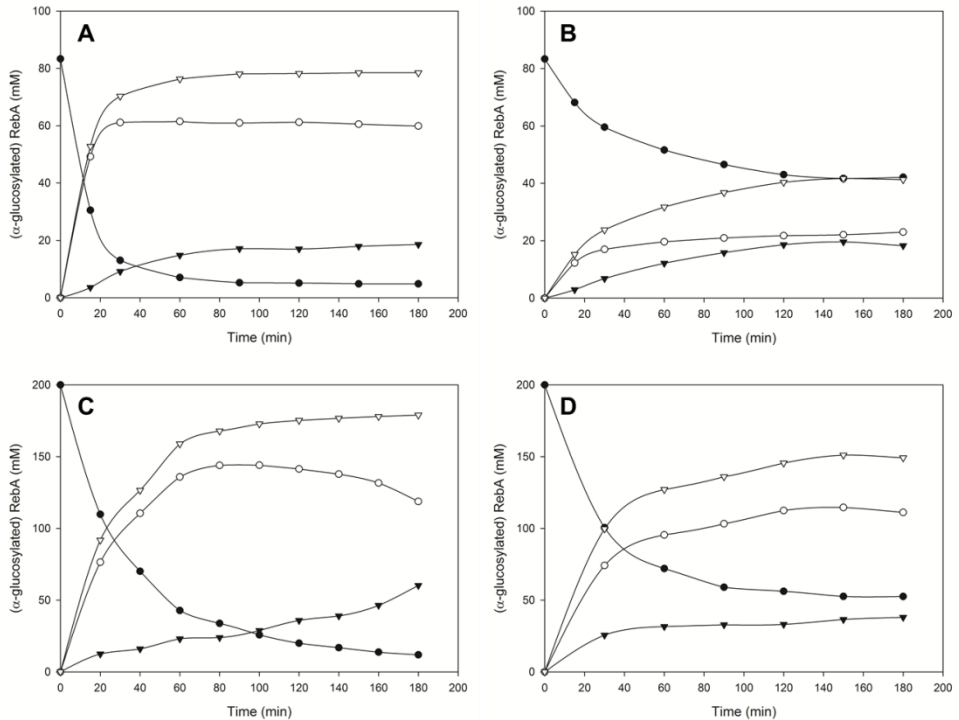


Figure 5. Time course of RebA glucosylation by (A) Gtf180- Δ N-Q1140E at optimal batch conditions (84 mM RebA; 282 mM sucrose; 5 U/mL), (B) Gtf180- Δ N at optimal batch conditions (84 mM RebA; 282 mM sucrose; 5 U/mL), (C) Gtf180- Δ N-Q1140E at optimal fed-batch conditions (200 mM RebA; 50 mM sucrose; 50 U/mL) and (D) Gtf180- Δ N-Q1140E at batch conditions (200 mM RebA; 570 mM sucrose; 5 U/mL). ● RebA, ○ RebA-G1, ▼ RebA-G2+, ▽ RebA-G. For the definition of these products, see Methods “Design of response surface methodology experiment”.

3.4. Docking of RebA in the active site of wild-type Gtf180- Δ N and mutant Q1140E

To gain further insight into the α -glucosylation of RebA by the Gtf180- Δ N wild-type enzyme and its mutant Gtf180- Δ N-Q1140E, *in silico* docking studies²⁰¹ were performed. To this end, the crystal structure of RebA as reported by ref²⁰² was used. Docking of RebA into the wild-type Gtf180- Δ N active site (X-ray crystal structure of a complex of Gtf180- Δ N with maltose; PDB code: 3KLL⁸³) afforded the pose as depicted in Figure 6A, showing that only the steviol C-19 β -D-glucosyl moiety (Glc1 in Figure 3) of RebA is available for glucosylation, especially at the HO-6 group, due to its orientation. Hydrogen bonding of Glc1 HO-6 with the catalytic residue D1136 possibly supports deprotonation in the glycosylation step (Figure 6C). A π - π -stacking interaction with W1065 as well as hydrogen bonding of Glc1 HO-4 and HO-3 to the backbone of D1136 was observed and appears to hold the Glc1 residue in place.

Docking of RebA into the active site of the mutant Gtf180- Δ N-Q1140E afforded the pose as depicted in Figure 6B. The binding of the steviol C-19 β -D-glucosyl moiety (Glc1 in Figure 3) is identical to the wild-type enzyme, but fewer hydrogen bonds of the steviol C-13 trisaccharide moiety (Glc2, Glc3 and Glc4 in Figure 3) were observed (Figure 6D). The modified binding pocket, resulting from the mutation, does not influence the binding of the steviol C-19 β -D-glucosyl unit, given that the mutation is not in direct proximity of the monosaccharide. The experimental observation that mutant Q1140E leads to more efficient α -glucosylation could be explained by the possibility that deprotonation of Glc1 HO-6 is aided by a water-mediated hydrogen bond between Glc1 HO-6 and E1140 as depicted in Figure 6B. The finding that the Q1140E mutant shows mostly mono-glucosylation instead of oligo-glucosylation is currently difficult to explain on the basis of these docking results.

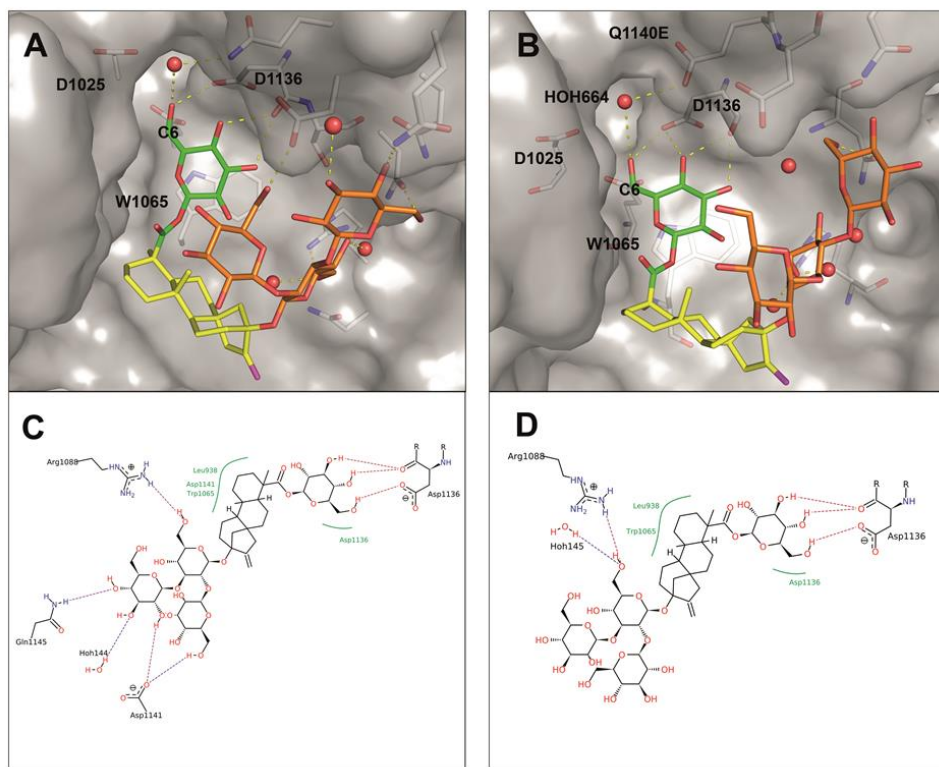


Figure 6. Docking poses of RebA into wild-type Gtf180- Δ N (PDB: 3KLL; **A** and **C**) and mutant Q1140E (**B** and **D**). The steviol part is indicated in yellow, the Glc1(β 1 \rightarrow residue at the steviol C-19 site in green and the Glc3(β 1 \rightarrow 2)[Glc4(β 1 \rightarrow 3)]Glc2(β 1 \rightarrow trisaccharide at the steviol C-13 site in orange. For monosaccharide coding system, see Figure 3.

3.5. Sensory analysis of glucosylated RebA products

A sensory analysis of aqueous solutions sweetened with RebA and glucosylated RebA products, prepared with the mutant Gtf180- Δ N-Q1140E enzyme, was performed by a trained panel, evaluating 9 different taste attributes. Three different glucosylated products were examined: multi- α -glucosylated product, containing residual RebA (RebA-G), mono- α -glucosylated product (RebA-G1) and RebA-G lacking RebA and RebA-G1 (RebA-G2+). The mean scores of the attributes of the sweetened water solutions are shown in Figure 7.

The glucosylated RebA products were all significantly less bitter than RebA, displaying almost no bitterness at all. Equally important, RebA-G and RebA-G1 retained the very high sweetness inherent to RebA. In contrast, RebA-G2+ was significantly less liquorice, astringent and lingering than RebA but also significantly less sweet, retaining only half of the RebA sweetness. The sensory analysis also revealed that RebA-G and RebA-G1 have very similar taste profiles, both combining a very high sweetness with a very low bitterness and other off-flavors. So, the small amounts of RebA and RebA-G2+ in RebA-G apparently do not influence the taste profile, when compared with RebA-G1. Therefore, RebA-G is the preferred product for commercialization, since it can be produced more economically, not requiring further purification and separation steps.

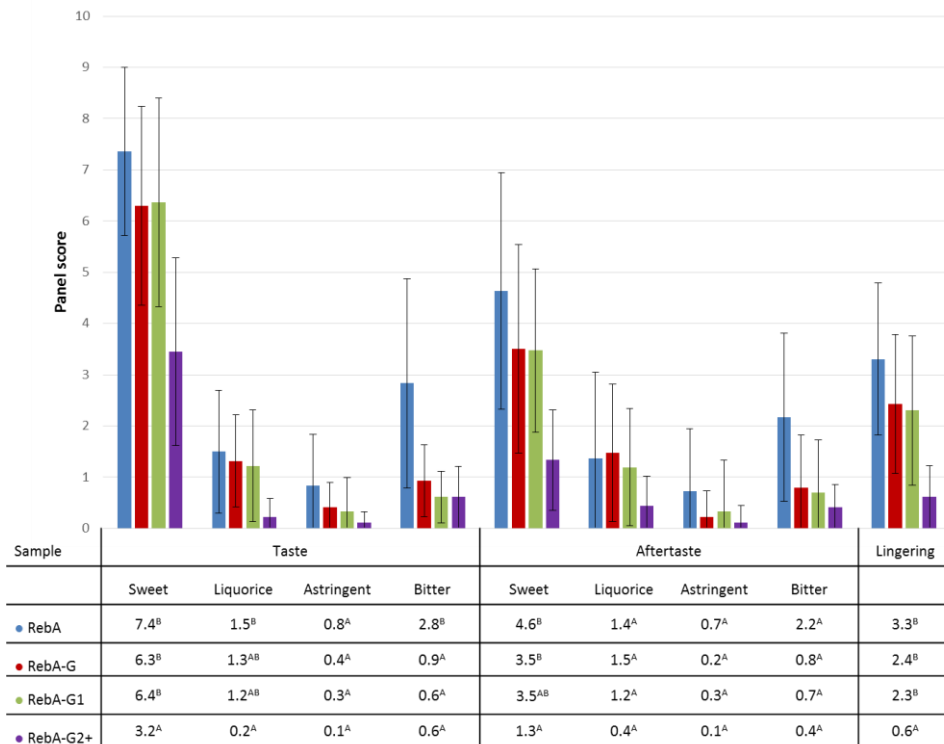


Figure 7. Sensory analysis of RebA, RebA-G, RebA-G1 and RebA-G2+. ^{A,B}: different letters indicate significant differences ($p < 0.05$) between solutions following one-way ANOVA and post-hoc test.

4. Discussion

The *Stevia rebaudiana* plant is a major source of high-potency natural sweeteners (steviol glycosides) for the growing natural food market of the future¹⁸⁶, however, due to their slight bitterness and unpleasant and lingering aftertaste, large-scale application of steviol glycosides is still hampered. In the past, several attempts have been made to improve the quality and sweet taste of steviol glycosides by modifying the carbohydrate moieties at the C-13 *tert*-hydroxyl and the C-19 carboxylic acid functions of steviol via transglycosylation reactions⁸.

In the present study, we have successfully used the glucansucrase mutant enzyme Gtf180- Δ N-Q1140E from *Lactobacillus reuteri* 180 (with sucrose as donor substrate) to glucosylate the steviol glycoside RebA, an important *Stevia* component. In a screening of 82 mutant enzymes of Gtf180- Δ N, mutant Q1140E was selected for further studies and compared to the wild-type Gtf180- Δ N enzyme. At optimal conditions, mutant Q1140E achieved ~95% RebA conversion into mainly mono- α -glucosylated RebA product RebA-G1 (Figure 3), compared to only 55% conversion by the wild-type enzyme. Under batch conditions, a high product yield of 115 g/L RebA-G (79 mM) was obtained within 3 h (from 84 mM RebA), applying only 5 U/mL of the Q1140E mutant enzyme. The product yield could even be enhanced to 270 g/L RebA-G (188 mM; from 200 mM RebA) by adopting a fed-batch reaction with stepwise addition of sucrose. This reduced availability of sucrose effectively suppressed the formation of α -gluco-oligo/polysaccharides. Instead, sucrose was mainly used as donor substrate for RebA glycosylation by the Q1140E enzyme, yielding more RebA α -glucosides.

The Gtf180- Δ N-Q1140E mutant glucosylated RebA specifically at the steviol C-19 position, introducing a Glc(α 1 \rightarrow 6) residue at the ester-linked Glc(β 1 \rightarrow residue. This finding is in line with the present knowledge about the wild-type Gtf180- Δ N enzyme, which also specifically elongates the C-19 glucose residue with mainly alternating (α 1 \rightarrow 6)- and (α 1 \rightarrow 3)-linked glucose units⁶⁹. In contrast to

the modified steviol glycosides prepared by incubation with CGTases, thereby introducing only (α 1 \rightarrow 4)-linked glucose residues, the (α 1 \rightarrow 3) and (α 1 \rightarrow 6) linkages are resistant to hydrolysis by the human amylolytic enzymes in saliva, which may prolong the sweet taste in the mouth.

Molecular docking studies were performed to gain insight into the glucosylation mechanism of RebA at the molecular level and to elucidate how a single amino acid change in Gtf180- Δ N, namely Q1140E, significantly improved RebA conversion. Docking of RebA into the active site of the Gtf180- Δ N wild-type enzyme indicated that only its steviol C-19-ester-linked Glc(β 1 \rightarrow residue is available for glycosylation. The Q1140E mutation is predicted not to affect the orientation and position of RebA in the active site, supporting the experimental observation that both enzymes specifically α -glucosylate RebA at the Glc1(β 1 \rightarrow C-19 residue, and not at the Glc3(β 1 \rightarrow 2)[Glc4(β 1 \rightarrow 3)]Glc2(β 1 \rightarrow C-13 trisaccharide (Figure 3). Furthermore, the docking results showed that Glc1 HO-6 and not Glc1 HO-3 of the Glc1(β 1 \rightarrow C-19 residue of RebA is prominently available for glucosylation. This is in agreement with the experimental results that both wild-type and mutant Gtf180- Δ N enzymes attach the first Glc residue (Glc5) exclusively via an (α 1 \rightarrow 6)-linkage. A faster and more efficient glucosylation of RebA was obtained by replacement of glutamine with the more negatively charged glutamate at position 1140 (mutant Q1140E). Conceivably, deprotonation of Glc1 HO-6 is aided by a water-mediated hydrogen bond between Glc1 HO-6 and glutamate, which is absent with glutamine at position 1140 (Figure 6). The finding that Q1140E shows mostly mono-glucosylation is currently difficult to explain on basis of the docking results. Elucidation of the Q1140E mutant protein 3D structure, followed by a comparison of the Gtf180- Δ N wild-type and mutant Q1140E structures, ideally in complex with RebA, may shed more light on the observed differences in RebA glucosylation.

An important finding in our study was that the multi-glucosylated RebA product (RebA-G) had a significantly reduced bitterness compared to RebA. This improved steviol glycoside product mixture thus displays appealing sensory properties and is likely to find application as a functional food ingredient. This

study also shows that Gtf180- Δ N-Q1140E is a very efficient catalyst for α -glucosylation of steviol glycosides.

5. Supplementary information

Table SI. Survey of wild-type glucansucrase Gtf180- Δ N of *L. reuteri* 180, and mutants derived, evaluated in this study. The 3-letter code DHT represents mutating amino acid residues D1085, R1088, and N1089 to D, H, and T, respectively. The same is valid for the other mutants shown with their 3-letter codes.

Mutation	Feature	Ref
Gtf180- Δ N	wild-type; N-terminally truncated	80
Gtf180- Δ N- Δ V	domain V deletion mutant	88
PNS (V1027P:S1137N:A1139S)	triple mutant	197
Q1140E/A/H, S1137Y	near transition state stabilizing residue D1136	97
L940G/M/C/A/S/E/F/W	near acceptor subsite +1	98
L938A/S/F/K/M, A978F/S/G/L/P/Y, L981A/N/K, D1028Y/W/L/K/G/N, N1029Y/R/G/P/T/M	near acceptor subsite +1	99
DHT, NRL, VKG, YTS, ETL, AAA, MYM, FFF, DED, LLL, D1085Y/V/A/E/H/L/Q, R1088E/W/T/N/G/H/K, N1089Y/G/S/L/R/D/P	near acceptor subsite +2	100
W1065F/K/L/Q/G/T/E/F	near acceptor subsite +1 and +2	102
Δ V L938N	L938 mutation in Gtf180- Δ N- Δ V	unpublished
Δ V L940E/F	L940 mutations in Gtf180- Δ N- Δ V	88

Table SII. Gtf180- Δ N mutants, screened for their RebA α -glucosylation potential with sucrose as donor substrate. Numbers shown here correspond to the TLC profiles (Figure S1). The 3-letter code DHT represents mutating amino acid residues D1085, R1088, and N1089 to D, H, and T, respectively. The same is valid for the other mutants shown with their 3-letter codes.

1.	DHT	21.	N1089D	41.	D1085A	61.	A978S
2.	NRL	22.	N1089P	42.	D1085E	62.	A978G
3.	VKG	23.	L940G	43.	D1085H	63.	A978L
4.	YTS	24.	L940M	44.	D1085L	64.	A978P
5.	ETL	25.	L940C	45.	D1085Q	65.	A978Y
6.	AAA	26.	L940A	46.	R1088H	66.	Δ V L938N
7.	MYM	27.	L940S	47.	R1088K	67.	Δ V L940E
8.	FFF	28.	L940E	48.	D1028Y	68.	Δ V L940F
9.	DED	29.	L940F	49.	D1028W	69.	W1065F
10.	LLL	30.	L940W	50.	D1028L	70.	W1065K
11.	R1088E	31.	L981A	51.	D1028K	71.	W1065L
12.	R1088W	32.	L981N	52.	D1028G	72.	W1065Q
13.	R1088T	33.	L981K	53.	D1028N	73.	W1065G
14.	R1088N	34.	L938A	54.	N1029Y	74.	W1065T
15.	R1088G	35.	L938S	55.	N1029R	75.	W1065E
16.	N1089Y	36.	L938F	56.	N1029G	76.	W1065F
17.	N1089G	37.	L938K	57.	N1029P	77.	Gtf180- Δ N
18.	N1089S	38.	L938M	58.	N1029T	-	no enzyme
19.	N1089L	39.	D1085Y	59.	N1029M		
20.	N1089R	40.	D1085V	60.	A978F		

Table SIII. Box-Behnken experimental design and results for the variables studied. Second-degree polynomial equation with coefficients of each factor is given for RebA conversion (%), RebA-G1/RebA-G (%) and amount of RebA-G synthesized (mM). X_1 , RebA concentration (mM); X_2 , D/A ratio; X_3 , agitation speed (rpm).

Pattern	X_1	X_2	X_3	RebA conversion (%)	RebA-G1/RebA-G (%)	RebA-G (mM)	
1	+0+	200	2.5	200	73.8	76.3	147.6
2	0-+	125	1	200	64.3	83.4	80.6
3	-0+	50	2.5	200	94.1	77.2	47.1
4	0--	125	1	0	63.4	80	79.3
5	0	200	4	100	66.6	74.8	133.2
6	-0-	50	2.5	0	97	67.7	48.6
7	--0	50	4	100	96.5	75.8	48.3
8	0+-	125	4	0	82.7	72.6	103.4
9	--0	50	1	100	67.4	85	33.8
10	0	125	2.5	100	85.5	78.9	106.9
11	+--0	200	1	100	60.7	75.6	121.4
12	0	125	2.5	100	85.4	78	106.8
13	0	125	2.5	100	85.4	78.5	106.8
14	0++	125	4	200	88	72.2	110
15	+0-	200	2.5	0	69.1	77	138.2

$$\text{RebA conversion} = 85.4333 - 10.6000X_1 + 9.7500X_2 + 1.000X_3 - 5.8000X_1X_2 + 1.9000X_1X_3 + 1.1000X_2X_3 - 1.8667X_1^2 - 10.7667X_2^2 - 0.0667X_3^2.$$

$$\text{RebA-G1/RebA-G} = 78.4333 - 0.2375X_1 - 3.5375X_2 + 1.5250X_3 + 2.1250X_1X_2 - 2.5500X_1X_3 - 0.8500X_2X_3 - 1.6292X_1^2 + 0.9708X_2^2 - 2.2542X_3^2.$$

$$\text{RebA-G} = 106.8333 + 45.3250X_1 + 9.9750X_2 + 1.9750X_3 - 0.6750X_1X_2 + 2.7250X_1X_3 + 1.3250X_2X_3 - 10.3042X_1^2 - 12.3542X_2^2 - 1.1542X_3^2.$$

Table SIV. Methylation analysis of the carbohydrate moieties in RebA and α -glucosylated RebA products RebA-G and RebA-G1.

Alditol acetate	R_t^a	Structural feature	Peak area (%)		
			RebA	RebA-G	RebA-G1
2,3,4,6-Hex ^b	1.00	Glc p (1→	74	58	61
2,4,6-Hex	1.16	→3)Glc p (1→	-	3	-
3,4,6-Hex	1.18	→4)Glc p (1→	-	tr ^c	tr ^c
2,3,4-Hex	1.22	→6)Glc p (1→	-	17	18
4,6-Hex	1.32	→2,3)Glc p (1→	26	20	21
2,4-Hex	1.39	→3,6)Glc p (1→	-	2	-

^a R_t , retention time relative to 1,5-di-*O*-acetyl-2,3,4,6-tetra-*O*-methylglucitol (1.00) on GLC.

^b 2,3,4,6-Hex = 1,5-di-*O*-acetyl-2,3,4,6-tetra-*O*-methylglucitol-1-*d*. etc.

^c tr = trace (<2%).

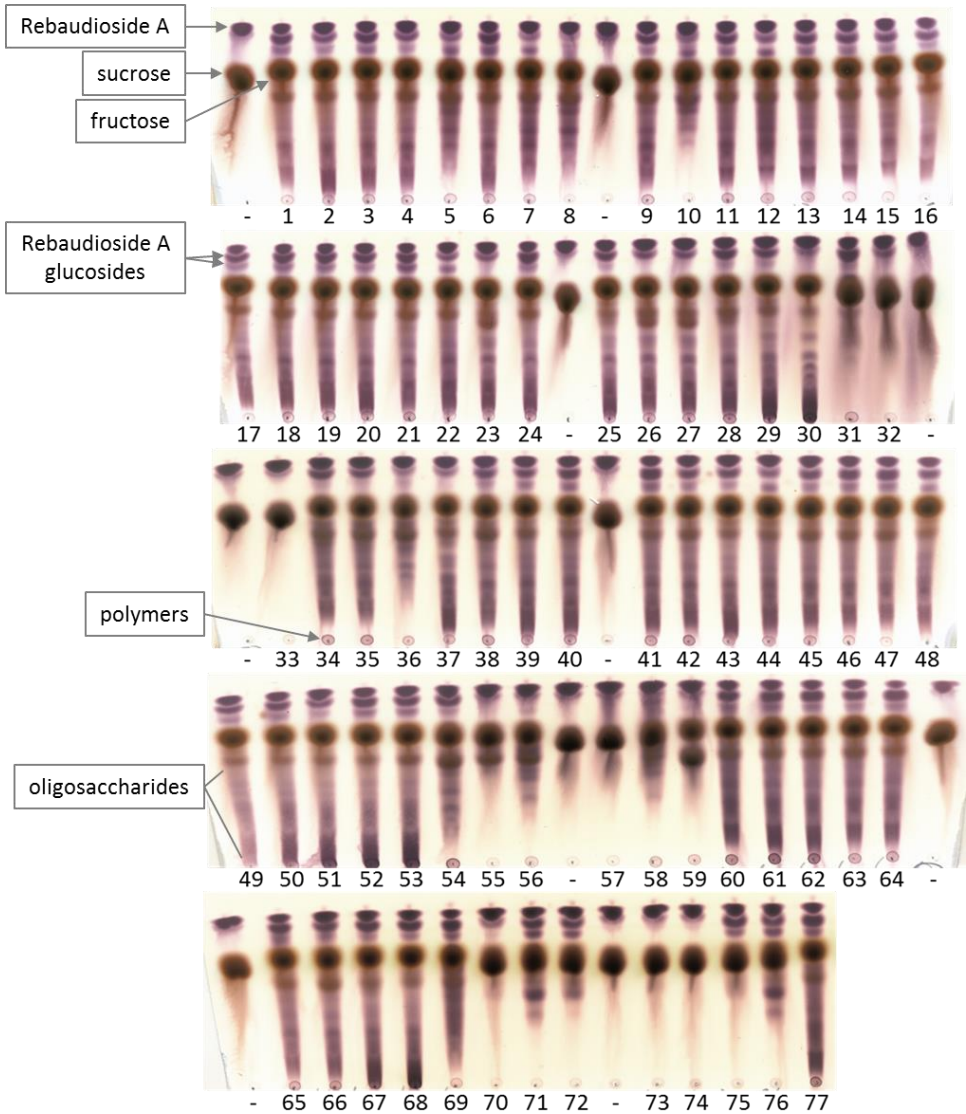


Figure S1. TLC substrate/product profiles after a 3 h incubation at 37 °C of a buffer solution (pH 4.7) containing 50 mM RebA, 0.2 M sucrose and ~1 mg/mL wild-type Gtf180- Δ N (lane 77) or Gtf180- Δ N mutant enzymes.

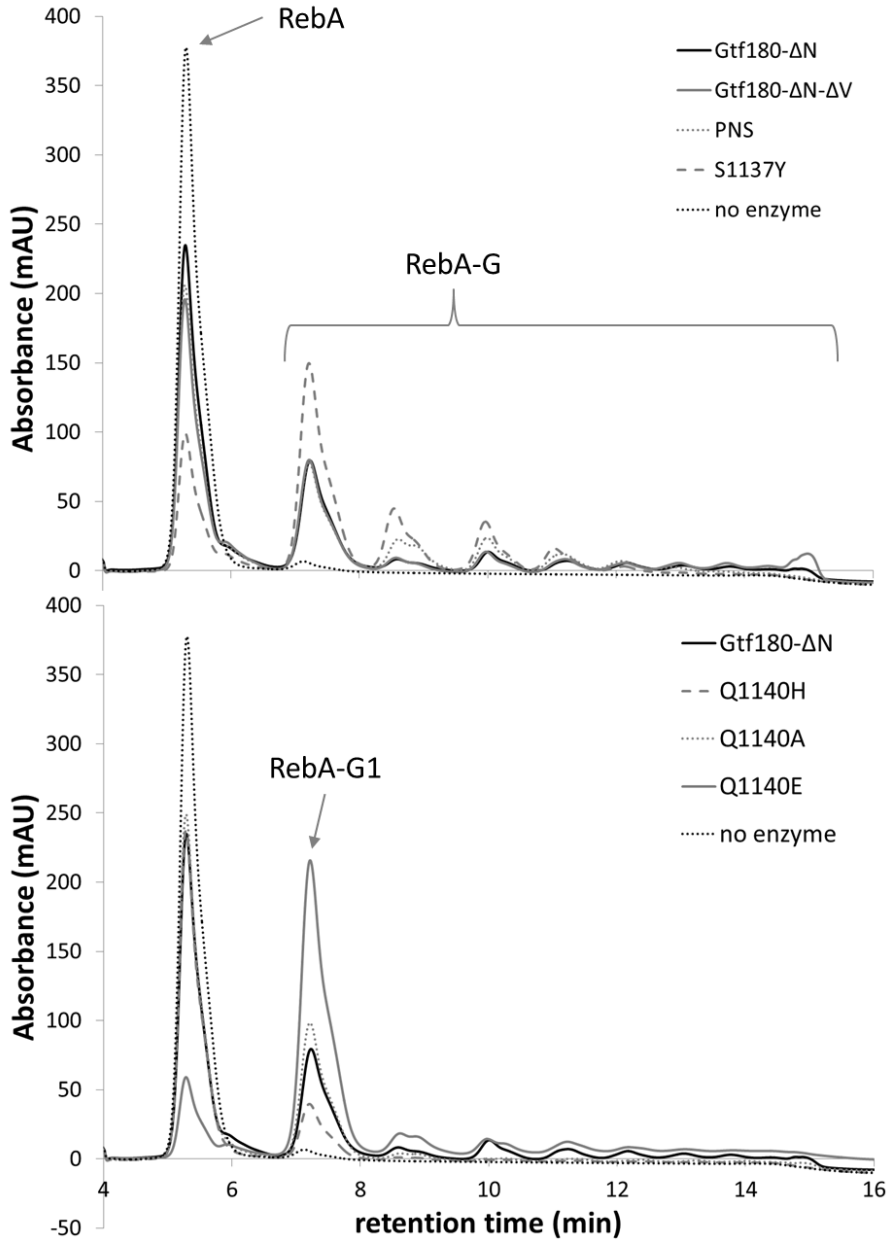


Figure S2. HPLC substrate/product profiles after a 3 h incubation at 37 °C of a buffer solution (pH 4.7) containing 50 mM RebA, 1 M sucrose and ~1 mg/mL wild-type Gtf180- Δ N, wild-type Gtf180- Δ N- Δ V or Gtf180- Δ N mutant enzymes. RebA-G: total amount of α -glucosylated RebA product. RebA-G1: mono- α -glucosylated RebA.

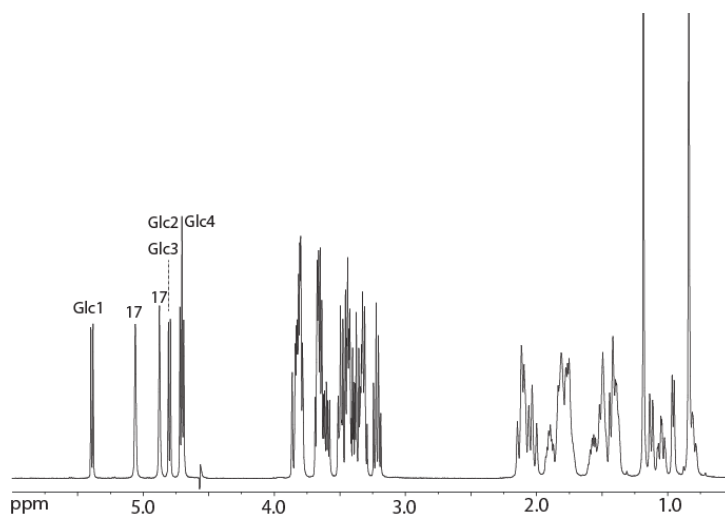


Figure S3. 500-MHz ^1H NMR spectrum of commercial RebA, supplied by Tereos PureCircle, recorded in D_2O at 310 K. The positions of the anomeric protons of the glucose residues (Figure 3) are indicated, as well as the steviol C-17 protons in the anomeric region. The spectrum is identical to that of commercial RebA, supplied by Aldrich-Sigma Chemie, and recently published with a complete assignment of resonances⁶⁹.

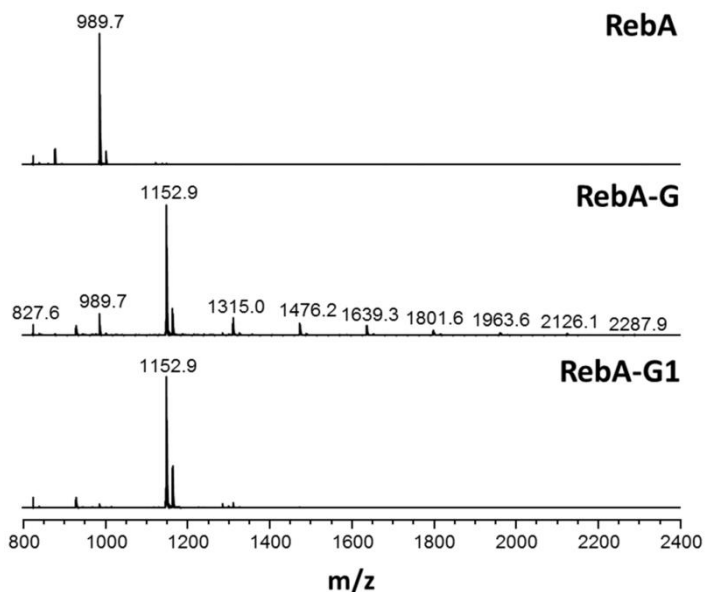


Figure S4. MALDI-TOF mass spectra of RebA, RebA-G and RebA-G1.

Chapter 5

Glucosylation of stevioside by Gtf180- Δ N-Q1140E improves its taste profile

Tim Devlamynck¹, Koen Quataert¹, Evelien M. te Poele², Gerrit J. Gerwig³,
Johannis P. Kamerling³, Wim Soetaert¹, Lubbert Dijkhuizen²

¹Ghent University, ²University of Groningen, ³University of Utrecht

Abstract

The adverse health effects of sucrose overconsumption, typical for diets in developed countries, necessitate the use of low-calorie sweeteners. Since their approval by the European Commission in 2011, steviol glycosides have increasingly been used as high-intensity sweetener in food products. The most prevalent steviol glycoside in the leaves of *Stevia rebaudiana* is stevioside. Due to its lingering bitterness and off-flavors, it has found limited applications in food products, as the better tasting rebaudioside A (RebA) is preferred. Enzymatic glucosylation of stevioside is a well-known strategy to reduce this bitterness. Up to date, many glucosylation reactions of stevioside or RebA suffer from low productivities. In this chapter, the optimized α -glucosylation of stevioside with glucansucrase Gtf180- Δ N-Q1140E, previously shown to efficiently glucosylate RebA as well, is reported. The structures of the novel steviol glycosides were elucidated by NMR spectroscopy, mass spectrometry, and methylation analysis, revealing that stevioside was mainly glucosylated at the C-19 glucosyl moiety. In contrast to RebA glucosylation, minor products were also glucosylated at the C-13 site. Sensory analysis of the glucosylated stevioside products by a trained panel revealed significant reductions in bitterness and off-flavors compared to stevioside, while the typical intensive sweetness of steviol glycosides was retained.

1. Introduction

Over the past decade, Western society has increasingly been confronted with lifestyle diseases such as type 2 diabetes, ischaemic heart attacks and various cardiovascular diseases. The cost for society in Europe is estimated to be 2% to 4% of the total healthcare cost²¹³. The risk to suffer from lifestyle diseases increases significantly when the BMI is higher than 25 kg/m²^{214,215}. A study from Calle et al.²¹⁶ even revealed that 14% to 20% of all cancer deaths may also be related to overweight or obesity. Important causes of overweight are a decrease of physical activity and inappropriate dietary patterns. Moreover, an excessive sugar intake appears to be directly associated with an increase in body weight²¹⁷. A wider array of sweet food products with less or even no sugar content is consequently a necessity in order to reduce the prevalence of lifestyle diseases.

Consumers are more and more aware of the relationship between diet-related diseases and healthy foods but are nevertheless not so eager to decrease their intake of sweet food products²¹⁸. In addition, the 'natural' character of the applied sweeteners is increasingly perceived by consumers to be equally important as their taste²¹⁹. The implementation into the market of natural, high-intensity sweeteners is thus driven by a strong consumer demand. Up to this date, several candidates have been proposed to take up this role: sweet-tasting proteins such as monatin and thaumatin²²⁰, and other plant extracts like glycyrrhizin from the root of *Glycyrrhiza glabra*²²¹, mogrosides from monk fruit (*Siraitia grosvenorii*)²²², and steviol glycosides (SG) from the leaves of *Stevia rebaudiana*¹⁸⁶. Since the European Commission authorized the use of high purity SG ($\geq 95\%$), such as rebaudioside A (RebA) and stevioside (Stev), in foods and beverages, stevia-based products have rapidly expanded across the European market. Recently, it was shown that SG, by means of their steviol group, potentiate Ca²⁺-dependent activity of TRPM5, a cation channel protein essential for taste transduction of sweet, bitter, and umami in chemosensory cells²²³. As a result, the sweetness of SG is intensified, whereas their bitterness lingers on. Interestingly, TRPM5 also facilitates insulin release by the pancreas, preventing high blood glucose

concentrations and consequently the development of type 2 diabetes²²⁴. A study on mice revealed that TRPM5 potentiation by SG protected them against the development of high-fat diet-induced hyperglycaemia, prompting the authors to propose SG as cost-effective antidiabetic drugs²²⁵.

Unfortunately, roughly half of the human population attributes an unpleasant lingering bitterness to RebA and Stev, as reflected by the considerable sequence variation in the genes encoding for the bitter receptors hTAS2R4 and hTAS2R14⁴⁶. One strategy to solve this issue consists in the addition of masking agents such as several sugar alcohols²²⁶. In order to circumvent the use of masking agents, enzymatic glucosylation of RebA and Stev has been proposed as a means to (partially) remove their bitterness⁸. Several enzymes, typically UDP-glucosyltransferases (UGTases)⁵⁷⁻⁵⁹ and cyclodextrin glucanotransferases (CGTases)⁵⁰⁻⁵⁶, have already been applied for this purpose. However, UGTases require expensive nucleotide-activated sugars as donor substrate¹³, whereas CGTases possess poor C-13/C-19 regioselectivity, producing mixtures of α -glucosylated SG⁵¹.

Alternatively, glucansucrases (GS) can be applied for the glucosylation of SG. GS (EC 2.1.4.-) are enzymes found only in lactic acid bacteria, of which most members, including *Lactobacillus reuteri*, have the generally-recognized-as-safe (GRAS) status. They use the donor substrate sucrose to catalyze the synthesis of α -glucan polysaccharides, thereby introducing different ratios of glycosidic linkages, depending on the enzyme specificity⁷⁵. It was demonstrated that suppressing this α -glucan synthesis by mutational engineering improved the glucosylation of non-natural acceptor substrates such as catechol¹¹⁰. In chapter 4, the glucosylation of RebA with the Q1140E mutant of glucansucrase enzyme Gtf180- Δ N from *Lactobacillus reuteri* 180 was reported⁶⁸⁻⁷⁰. RebA was only glucosylated at the C-19 glucosyl moiety, producing mainly mono- α -glucosylated product with an (α 1 \rightarrow 6)-linkage, but also α -glucosides with two or more glucosyl units attached. The glucosylation of Stev, the most abundant steviol glycoside, was not addressed. Here, we report a careful optimization of the enzymatic glucosylation of Stev by the same enzyme. The structures of the two main α -

glucosylated Stev products were characterized by NMR spectroscopy, mass spectrometry, and methylation analysis. Sensory analysis by a trained panel revealed a substantial decrease in bitterness and off-flavors of the glucosylated products compared to Stev and RebA.

2. Materials and methods

2.1. Stevioside

Stevioside (>85 % purity, HPLC) was obtained from TCI Europe.

2.2. Production and purification of recombinant Gtf180-ΔN-Q1140E

Recombinant, N-terminally truncated Gtf180-ΔN from *Lactobacillus reuteri* 180 and derived Q1140E mutant were produced and purified as described previously^{70,80,99}.

2.3. Gtf180-ΔN-Q1140E activity assays

One unit (U) of enzyme activity corresponds to the conversion of 1 μmole sucrose (used for hydrolysis and transglycosylation) in a solution containing 100 mM sucrose, 25 mM sodium acetate (pH 4.7) and 1 mM CaCl₂, at 37 °C.

Enzyme activity assays were performed at 37 °C with 100 mM sucrose in 25 mM sodium acetate (pH 4.7) and 1 mM CaCl₂. Samples of 150 μL were taken every min over a period of 8 min and immediately inactivated with 30 μL 1 M NaOH. The sucrose concentrations of the samples were subsequently quantified by means of HPLC analysis (see HPLC analysis), allowing the calculation of the enzyme activity as defined above.

2.4. HPLC analysis

Two HPLC analyses were performed. For the analysis of glucose, fructose and sucrose, an Agilent MetaCarb 67H column (300 x 6.5 mm) was used under isocratic conditions with 2.5 mM H₂SO₄ as the mobile phase. The flow rate and temperature were set at 0.8 mL/min and 35 °C, respectively. Detection was achieved with an RI detector. Calibration of the obtained peaks was accomplished using the corresponding standard curves.

For the analysis of the steviol glycosides, an Agilent ZORBAX Eclipse Plus C18 column (100 x 4.6 mm, 3.5 µm) was used with water (solvent A) and acetonitrile (solvent B) as the mobile phase. The flow rate and temperature were set at 1.0 mL/min and 40 °C, respectively. Following gradient elution was used: 5-95% solvent B (0-25 min), 95% solvent B (25-27 min), 95-5% solvent B (27-30 min) and again 95% of solvent A (30-35 min). Detection was achieved with an ELS detector (evaporation temperature: 90 °C, nebulization temperature: 70 °C, gas flow rate: 1.6 SLM). Calibration of the obtained peaks was accomplished using the corresponding standard curves.

2.5. Design of response surface methodology experiment

Response surface methodology¹⁹⁸ was applied to optimize the Gtf180-ΔN-Q1140E catalyzed glucosylation of stevioside (acceptor substrate) with sucrose as donor substrate, while minimizing the synthesis of α-glucan oligosaccharides. All experiments were performed in 25 mM sodium acetate (pH 4.7), supplemented with 1 mM CaCl₂, at 37 °C. The addition of 10 U/mL enzyme ensured a steady-state was reached within 3 h of incubation. A Box-Behnken design¹⁹⁹ was generated implementing stevioside concentration (mM), sucrose/stevioside ratio (D/A ratio) and agitation rate (rpm) as factors. For each of them low (-1) and high (+1) level values were assigned as follows: stevioside concentration (25 mM) and (100 mM), D/A ratio (1) and (20), agitation rate (0 rpm) and (200 rpm). The experimental design was generated and analyzed using JMP software (release 12)²⁰⁰ and consisted of 15 experiments carried out at 5

mL scale (Table SI). The response surface analysis module of JMP software was applied to fit the following second order polynomial equation:

$$\hat{Y} = \beta_0 + \sum_{i=1}^I \beta_i X_i + \sum_{i=1}^I \beta_{ii} X_i^2 + \sum_i \sum_j \beta_{ij} X_i X_j$$

where \hat{Y} is the predicted response, I is the number of factors (3 in this study), β_0 is the model constant, β_i is the linear coefficient associated to factor X_i , β_{ii} is the quadratic coefficient associated to factor X_i^2 and β_{ij} is the interaction coefficient between factors X_i and X_j . X_i represents the factor variable in coded form:

$$X_{c,i} = \frac{[X_i - (low + high)/2]}{(high - low)/2}$$

with $1 \leq i \leq I$, where $X_{c,i}$ is the coded variable.

2.6. Production and purification of α -glucosylated stevioside

The production of α -glucosylated stevioside was performed at 50 mL scale in a shake flask, by incubating 31 mM stevioside and 524 mM sucrose with 10 U/mL Gtf180- Δ N-Q1140E at 37 °C in 25 mM sodium acetate (pH 4.7) and 1 mM CaCl₂ for 3 h. The α -glucosylated stevioside products were purified from the incubation mixture by flash chromatography using a Reveleris X2 flash chromatography system with a Reveleris C18 cartridge (12 g, 40 μ m) with water (solvent A) and acetonitrile (solvent B) as the mobile phase (30 mL/min). Following gradient elution was used: 95% solvent A (0-2 min), 95-50% solvent A (2-20 min), 50-95% solvent B (20-22 min), 95% solvent B (22-25 min). Detection was achieved with UV (210 nm). The collected fractions were evaporated *in vacuo* and subsequently freeze dried to remove the residual water.

2.7. Alkaline hydrolysis of α -glucosylated stevioside and TLC analysis

To release the carbohydrate moiety linked to the C-19 carboxyl group, a 1 h stevioside incubation with Gtf180- Δ N-Q1140E (50 mM stevioside, 100 mM sucrose in 25 mM sodium acetate (pH 4.7) and 1 mM CaCl₂, 37 °C) was subjected to alkaline hydrolysis. Briefly, the stevioside incubation mixture was transferred into 1.0 M NaOH and heated at 80 °C for 2.5 h, then cooled down, and neutralized with 6 M HCl. Samples were spotted in lines of 1 cm on a TLC sheet (Merck Kieselgel 60 F254, 20x20 cm), which was developed in *n*-butanol:acetic acid:water = 2:1:1. Bands were visualized by orcinol/sulfuric acid staining and compared with a simultaneous run of standard compounds.

2.8. Methylation analysis

Steviol glycoside samples were permethylated using CH₃I and solid NaOH in (CH₃)₂SO, as described previously²²⁷, then hydrolyzed with 2 M trifluoroacetic acid (2 h, 120 °C) to give a mixture of partially methylated monosaccharides. After evaporation to dryness, the mixture was dissolved in H₂O and reduced with NaBD₄ (2 h, room temperature). Subsequently, the solution was neutralized with 4 M acetic acid and boric acid was removed by repeated co-evaporation with methanol. The obtained partially methylated alditol samples were acetylated with 1:1 acetic anhydride-pyridine (30 min, 120 °C). After evaporation to dryness, the mixtures of partially methylated alditol acetates (PMAAs) were dissolved in dichloromethane and analyzed by GLC-EI-MS on an EC-1 column (30 m x 0.25 mm; Alltech), using a GCMS-QP2010 Plus instrument (Shimadzu Kratos Inc., Manchester, UK) and a temperature gradient (140-250 °C at 8 °C/min)²²⁸.

2.9. Mass spectrometry

Matrix-assisted laser desorption ionization time-of-flight mass spectrometry (MALDI-TOF-MS) was performed on an AximaTM mass spectrometer (Shimadzu Kratos Inc.), equipped with a nitrogen laser (337 nm, 3 ns pulse width). Positive-ion mode spectra were recorded using the reflector mode at a resolution of 5000

FWHM and delayed extraction (450 ns). Accelerating voltage was 19 kV with a grid voltage of 75.2%. The mirror voltage ratio was 1.12 and the acquisition mass range was 200-6000 Da. Samples were prepared by mixing on the target 1 μ L sample solutions with 1 μ L aqueous 10% 2,5-dihydroxybenzoic acid in 70% acetonitrile as matrix solution.

2.10. NMR spectroscopic analysis

Resolution-enhanced 1D/2D 500-MHz $^1\text{H}/^{13}\text{C}$ NMR spectra were recorded in D_2O on a Bruker DRX-500 spectrometer (Bijvoet Center, Department of NMR Spectroscopy, Utrecht University). To avoid overlap of anomeric signals with the HOD signal, the 1D and 2D spectra were run at 310 K. Data acquisition was done with Bruker Topspin 2.1. Before analysis, samples were exchanged twice in D_2O (99.9 atom% D, Cambridge Isotope Laboratories, Inc., Andover, MA) with intermediate lyophilisation, and then dissolved in 0.6 mL D_2O . Fresh solutions of ~ 4 mg/mL were used for all NMR measurements. Suppression of the HOD signal was achieved by applying a WEFT (water eliminated Fourier transform) pulse sequence for 1D NMR experiments and by a pre-saturation of 1 s during the relaxation delay in 2D experiments. The 2D TOCSY spectra were recorded using an MLEV-17 (composite pulse devised by Levitt et al.²²⁹) mixing sequence with spin-lock times of 20, 50, 100 and 200 ms. The 2D ^1H - ^1H ROESY spectra were recorded using standard Bruker XWINNMR software with a mixing time of 200 ms. The carrier frequency was set at the downfield edge of the spectrum in order to minimize TOCSY transfer during spin-locking. Natural abundance 2D ^{13}C - ^1H HSQC experiments (^1H frequency 500.0821 MHz, ^{13}C frequency 125.7552 MHz) were recorded without decoupling during acquisition of the ^1H FID. The NMR data were processed using the MestReNova 9 program (Mestrelab Research SL, Santiago de Compostella, Spain). Chemical shifts (δ) are expressed in ppm by reference to internal acetone (δ_{H} 2.225 for ^1H and δ_{C} 31.07 for ^{13}C).

2.10 Sensory analysis

Sensory analysis was performed in individual tasting booths at the UGent Sensolab (Belgium) by a trained panel (7 persons), as described previously in chapter 4⁷⁰. In short, taste (sweetness, liquorice, astringency and bitterness) was evaluated by swirling the sample in the mouth for 5 sec after which the sample was expectorated. Aftertaste was evaluated 10 sec after swallowing the solution. Lingering based on the maximum taste intensity was rated 1 min later. Sucrose reference solutions (5%, 7.5% and 10% sucrose, scoring 5, 7.5 and 10, respectively) were provided. Water (Spa Reine) and plain crackers were used as palate cleansers between sampling. All samples were evaluated in duplicate.

Statistical analyses were performed with SPSS 23 (SPSS Inc., Chicago, USA). All tests were done at a significance level of 0.05. One-Way ANOVA was used to investigate any significant difference between the solutions. Testing for equal variances was executed with the Modified Levene Test. When conditions for equal variance were fulfilled, the Tukey test²¹⁰ was used to determine differences between samples. In case variances were not equal, Games-Howell was performed²¹¹.

Three different solutions sweetened with Stev products were examined: 588 mg/L mono- α -glucosylated product (Stev-G1), 588 mg/L multi- α -glucosylated product, containing residual Stev, Stev-G1 and higher α -glucosides (Stev-G) and 1176 mg/L multi- α -glucosylated product (Stev-G').

3. Results

3.1. Synthesis of α -glucosylated stevioside with Gtf180- Δ N-Q1140E

Gtf180- Δ N and the derived Gtf180- Δ N-Q1140E mutant also readily glucosylated stevioside. Optimization of the reaction conditions for rebaudioside A (RebA) glucosylation with Gtf180- Δ N-Q1140E revealed the importance of selecting

adequate concentrations of donor substrate sucrose and acceptor substrate RebA. The addition of too much sucrose resulted in suboptimal yields due to increased α -glucan synthesis⁷⁰. The glucosylation of stevioside (Stev) was therefore also optimized by response surface methodology (RSM), using a Box-Behnken experimental design. Following factors were considered: X_1 Stev concentration (mM); X_2 the ratio of donor substrate sucrose over acceptor substrate Stev (D/A ratio); X_3 agitation speed (rpm). The addition of 10 U/mL enzyme ensured that a steady state in Stev conversion was obtained within 3 h. The results of the Box-Behnken experimental design are summarized in Table SI. The analysis of variance (ANOVA) showed R^2 values of 98.75% and 98.72% for Stev conversion degree (%) and amount of α -glucosylated Stev (Stev-G) synthesized (mM), respectively. The effects of the factors were analyzed applying the response surface contour plots (Figure 1).

Higher Stev conversion degrees were obtained at decreasing Stev concentrations, independent on the concentration of donor substrate sucrose. The effect of the D/A ratio on Stev conversion degrees displayed a distinct optimum, similarly to RebA glucosylation with Gtf180- Δ N-Q1140E⁷⁰. An increase of D/A ratio initially resulted in improved Stev conversion degrees, indicating that sucrose drives the reaction. However, as sucrose also acts as primer for α -glucan synthesis, a further increase of D/A ratio resulted in less Stev glucosylation in favor of more α -glucan synthesis. This confirmed that the concentrations of sucrose and Stev need to be carefully optimized. In contrast, the effect of agitation on Stev conversion degrees and amount of Stev-G synthesized was negligible.

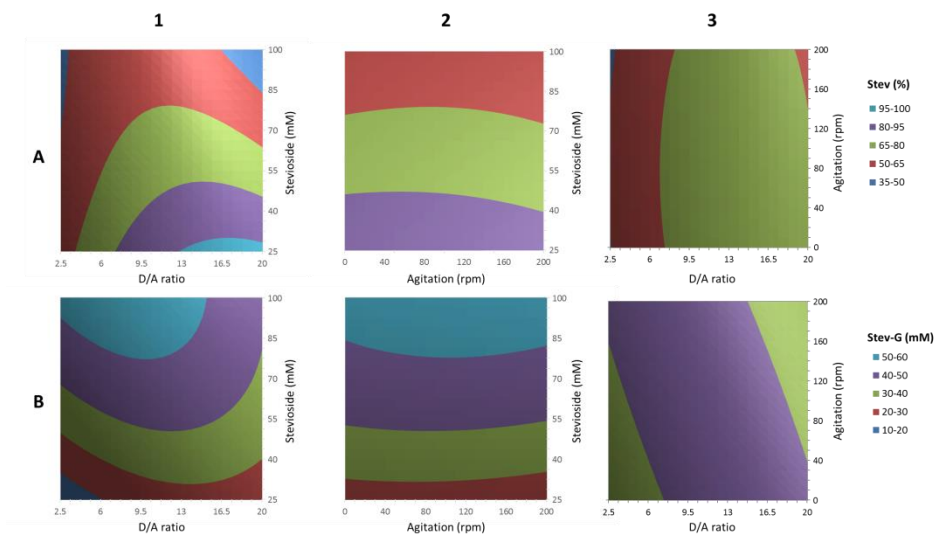


Figure 1. Response surface methodology contour plots of stevioside glucosylation by Gtf180- Δ N-Q1140E, showing the effects of: Stev concentration (mM); D/A ratio (ratio of donor substrate sucrose over acceptor substrate Stev); agitation (rpm) on: (A) Stev conversion degree (%); (B) Stev-G synthesized (mM).

The resulting model was consequently used for the optimization of the reaction conditions. An efficient conversion of Stev into Stev-G (at least 95%), yielding a maximal amount of Stev-G, was targeted. The model predicted the synthesis of 29 mM Stev-G in case following conditions were applied: 31 mM Stev, 524 mM sucrose (D/A ratio of 16.9) and 0 rpm. The validation test resulted in the synthesis of 28 mM Stev-G (Figure 2A), which was in good agreement with the prediction. Compared to RebA glucosylation with Gtf180- Δ N-Q1140E⁷⁰, much more donor substrate sucrose was needed to completely convert Stev (D/A ratio of 16.9 compared to 3.4), whereas less glycosylated product could be obtained (28 mM compared to 80 mM), indicating that the enzyme has a lower affinity for Stev than for RebA. Equally remarkable was that while RebA was mainly converted into mono- α -glucosylated product (RebA-G1, 77.7%), Stev was only for 32.5% converted into mono- α -glucosylated product (Stev-G1). Applying the optimal conditions for the glucosylation of Stev with wild type Gtf180- Δ N resulted only in the conversion of 60.9% Stev with a Stev-G1/Stev-G ratio of 23.7% (Figure 2B).

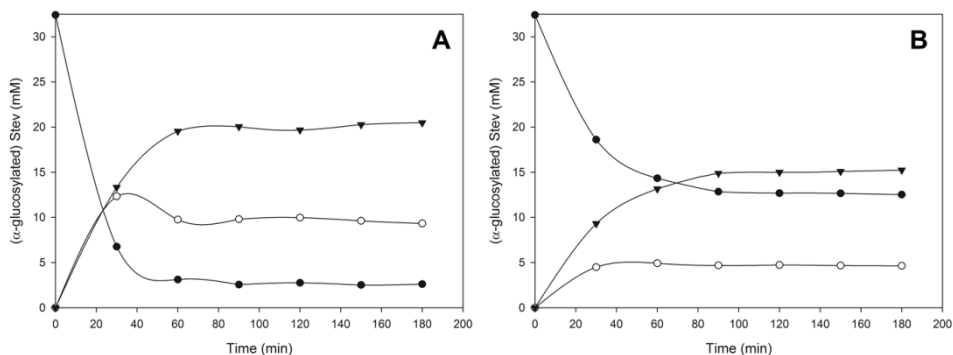


Figure 2. Time course of stevioside glucosylation by Gtf180-ΔN-Q1140E (**A**) and Gtf180-ΔN (**B**) at optimal batch conditions (31 mM Stev; 524 mM sucrose; 10 U/mL enzyme). ● Stev ○ Stev-G1 ▼ Stev-G2+.

3.2. Structural characterization of α-glucosylated stevioside products

Incubation of 31 mM Stev and 524 mM sucrose with Gtf180-ΔN-Q1140E resulted in the synthesis of several α-glucosylated stevioside products (Figure 3). The 2 main products (Stev-G1 and Stev-G2) were analyzed by a combination of 1D and 2D NMR spectroscopy, methylation analysis and mass spectrometry. Detailed structural analysis of novel steviol glycosides is of great value, since the sensory properties are known to depend on the number, location and configuration of the introduced glycosyl moieties⁸. Figure 4 depicts the 1D ¹H NMR spectra while Figure 5 shows the corresponding chemical structures. The ¹H and ¹³C chemical shifts are presented in Tables SII and SIII.

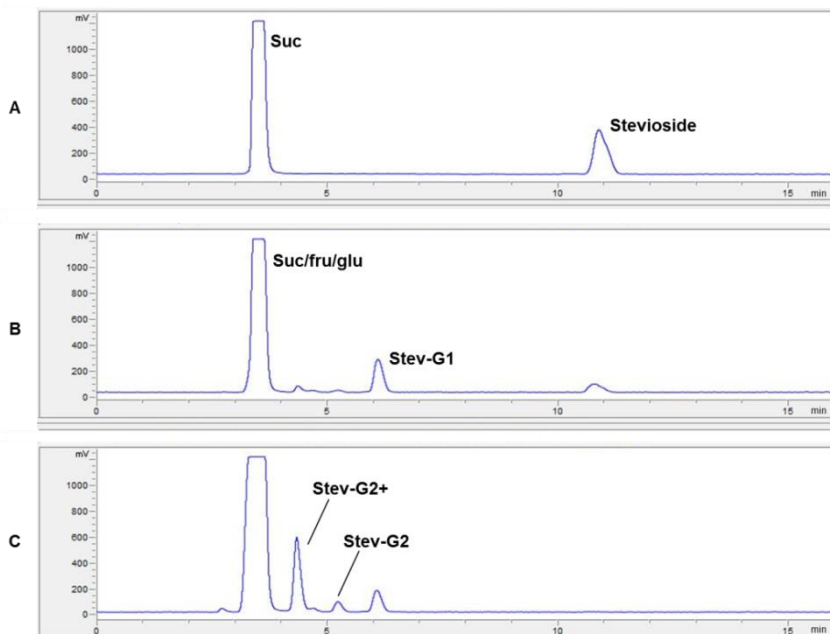


Figure 3. HPLC separation profiles of a 3 h incubation of 31 mM Stev and 524 mM sucrose with 10 U/mL Gtf180- Δ N-Q1140E. **A** 0 min, **B** 30 min, **C** 180 min of incubation at 37 °C. **Suc** sucrose, **fru** fructose, **glu** glucose.

3.2.1. Stev-G1

Methylation analysis (Table SIV) of Stev-G1 (Stev+1Glc, according to MALDI-TOF-MS: m/z 989.7 $[M+Na]^+$ (Figure 6B)) showed terminal Glcp, 2-substituted Glcp and 6-substituted Glcp (molar ratio 2:1:1), indicating that transglucosylation had resulted in elongation but not in branching. The ^1H NMR spectrum of Stev-G1 (Figure 4B) showed resonances of one main α -glucosylated Stev product, however, with five small (anomeric) signals (indicated with *: δ_{H} 5.35, 4.45, 4.14, 3.98, 3.16 in Figure 4B) of extra compounds (<10%). The spectrum between 0.8 and 2.2 ppm represented the typical steviol core signal pattern as seen for Stev (Figure 4A). Besides the three β -anomeric ^1H signals related to Stev (Glc1, δ_{H} 5.415; Glc2, δ_{H} 4.725; Glc3, δ_{H} 4.675), one extra anomeric ^1H resonance (δ_{H} 4.862; $J_{1,2}$ 3.7 Hz), partially overlapping with one steviol C-17 proton, was

observed, stemming from a new α -linked Glc residue (Glc4). The latter ^1H signal correlated with a ^{13}C resonance at δ_{C} 99.3 in the HSQC spectrum (Figure S1).

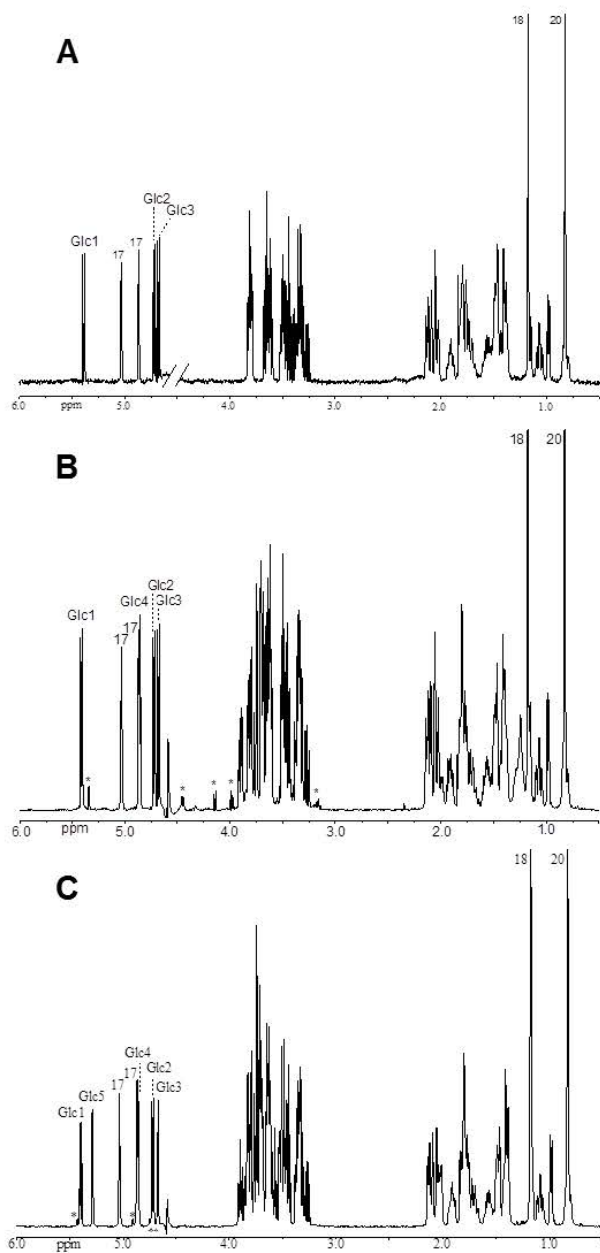


Figure 4. 500-MHz ^1H NMR spectrum of Stev (A), Stev-G1 (B), and Stev-G2 (C), recorded in D_2O at 310 K. * Resonances stemming from additional product(s).

Applying 2D NMR spectroscopy (TOCSY with different mixing times, ROESY and HSQC), the $^1\text{H}/^{13}\text{C}$ chemical shifts of the steviol core (Table SII) and the four Glc residues (Table SIII) of Stev-G1 were assigned (Figure S1). The ^1H and ^{13}C chemical shift sets of Glc2 and Glc3 correspond to those of Stev, suggesting that no modifications had occurred in the carbohydrate moiety at the steviol C-13 site. The TOCSY Glc4 H-1 track (δ_{H} 4.862) showed the complete scalar coupling network H-1,2,3,4,5,6a,6b, and combined with the Glc4 C-1–C-6 set of chemical shifts (HSQC), a terminal Glc(α 1 \rightarrow 6) unit is indicated. Based on the inter-residual ROESY cross-peaks between Glc4 H-1 (δ_{H} 4.862) and Glc1 H-6a/b (δ_{H} 3.89/3.70), combined with the ^{13}C downfield shift of 4.5 ppm for Glc1 C-6 (δ_{C} 66.7; Stev Glc1 C-6: δ_{C} 62.2) (HSQC spectrum, Figure S1), a Glc4(α 1 \rightarrow 6)Glc1 disaccharide element could be established⁶⁹.

The conclusive structure of the main compound in Stev-G1 was consequently determined as Stev elongated with a Glc p (α 1 \rightarrow 6) residue at the Glc1(β 1 \rightarrow) on the C-19 site of the steviol core (Figure 5B).

3.2.2. Stev-G2

Methylation analysis (Table SIV) of Stev-G2 (Stev+2Glc, according to MALDI-TOF-MS: m/z 1152.0 $[\text{M}+\text{Na}]^+$ (Figure 6C)) showed terminal Glc p and 2-substituted Glc p , 4-substituted Glc p , and 6-substituted Glc p (molar ratio 2:1:1:1), together with a trace amount (<2%) of 2,6-substituted Glc p . The ^1H NMR spectrum of Stev-G2 (Figure 4C) exhibited the typical steviol core signal pattern as seen for Stev (Figure 4A). Besides the three β -anomeric ^1H carbohydrate signals related to Stev (Glc1, δ_{H} 5.415; Glc2, δ_{H} 4.727; Glc3, δ_{H} 4.674), two α -anomeric ^1H resonances of equal intensity (δ_{H} 4.863; $J_{1,2}$ 3.9 Hz and δ_{H} 5.292; $J_{1,2}$ 3.7 Hz) were observed, stemming from two new α -linked Glc residues (Glc4 and Glc5). The ^1H NMR spectrum indicated the presence of one main di- α -glucosylated Stev product, together with very minor products (<10%) represented by four small anomeric signals (indicated with *: δ_{H} 5.43, 4.91, 4.75, 4.71 in Figure 4C).

Using 2D NMR spectroscopy (TOCSY with different mixing times, ROESY and HSQC), the $^1\text{H}/^{13}\text{C}$ chemical shifts of the steviol core (Table SII) and the five Glc residues (Table SIII) of Stev-G2 (main compound) were assigned (Figure S2)⁶⁹. The ^1H and ^{13}C chemical shift sets of Glc2 and Glc3 correspond closely with those of Stev and Stev-G1, suggesting that no modifications had occurred in the carbohydrate moiety at the steviol C-13 site.

However, the TOCSY Glc4 H-1 track (δ_{H} 4.863) showed a scalar coupling network H-1,2,3,4,5,6a,6b, different from that of Glc4 in Stev-G1, in particular H-3 (δ_{H} 3.90) and H-4 (δ_{H} 3.58), and together with the ^{13}C chemical shift of Glc4 C-4 (δ_{C} 77.9, 44, $\Delta\delta_{\text{C}}$ 6.6 ppm), a 4-substituted Glc4 residue is indicated (in accordance with the methylation analysis). The HSQC spectrum (Figure S2) showed a Glc1 C-6 (16a-16b) downfield shift ($\Delta\delta_{\text{C}}$ 5.2 ppm) as earlier observed for Glc1 in Stev-G1 ($\Delta\delta_{\text{C}}$ 4.5 ppm), indicating the presence of the Glc4(α 1 \rightarrow 6)Glc1 disaccharide element, leading to the establishment of a Glc5(α 1 \rightarrow 4)Glc4(α 1 \rightarrow 6)Glc1 trisaccharide linked to the C-19 of the steviol core. The inter-residual ROESY cross-peaks (spectrum not shown) between Glc4 H-1 (δ_{H} 4.863) and Glc1 H-6a/b (δ_{H} 3.85/3.74) and between Glc5 H-1 (δ_{H} 5.292) and Glc4 H-4 (δ_{H} 3.58) confirmed the glycosidic linkages between the three Glc residues. Furthermore, the 4-substitution of Glc4 was supported by the typical $^1\text{H}/^{13}\text{C}$ chemical shifts of its H-3/C-3 (43, δ_{H} 3.90 / δ_{C} 74.8) in the HSQC spectrum (Figure S2).

The conclusive structure of the main compound in Stev-G2 is consequently Stev elongated with a Glc p (α 1 \rightarrow 4)Glc p (α 1 \rightarrow 6) element at the Glc1(β 1 \rightarrow) residue on the C-19 site of the steviol core (Figure 5C).

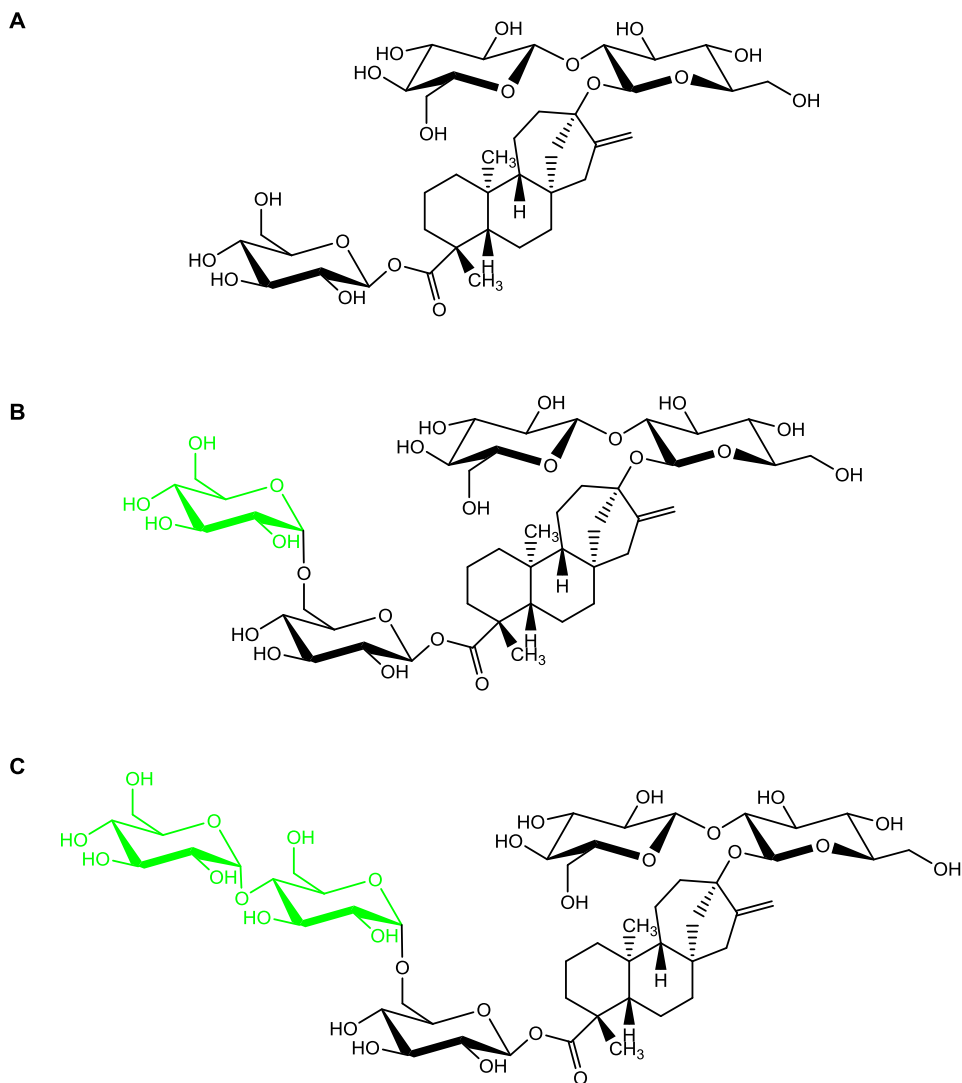


Figure 5. Chemical structures of Stev (A), Stev-G1 (B), and Stev-G2 (C).

3.2.3 Stev-G

Besides Stev-G1 and Stev-G2, Stev-G was composed of a wide array of α -glucosylated Stev products (Stev-G2+), as demonstrated by MALDI-TOF mass spectrometry, showing the m/z $[M+Na]^+$ peaks of Stev+1Glc up to Stev+9Glc (Figure 6D). It has to be noted that each peak may contain more than one compound, as different glycosidic linkage types may be present. Indeed,

methylation analysis (data not shown) showed six partially methylated alditol acetates, indicating the complexity of the Stev-G2+ mixture.

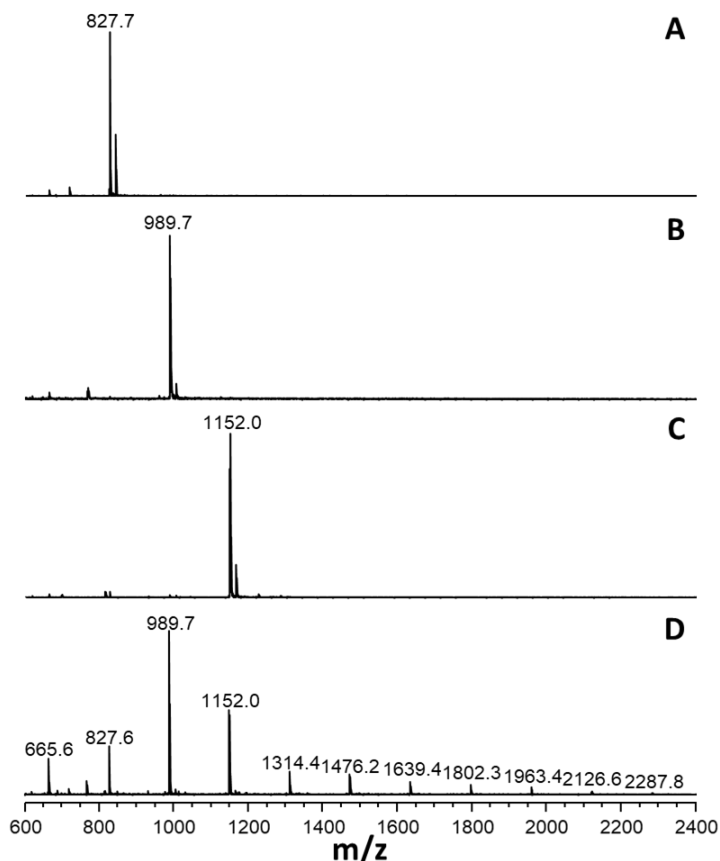


Figure 6. MALDI-TOF mass spectra of (A) Stev, (B) Stev+1Glc, (C) Stev+2Glc, (D) Stev-G. The α -glycosylated Stev products were obtained after incubation with Gtf180- Δ N-Q1140E and removal of residual carbohydrates. Mass peaks could be assigned to m/z $[M+Na]^+$ values of Stev+1Glc (989.7), Stev+2Glc (1152.0), up to Stev+9Glc (2287.8).

Alkaline hydrolysis of the Stev-G mixture suggested that Stev was not specifically glucosylated at the C-19 site but also at the C-13 site (Figure 7). Indeed, treatment of Stev with NaOH resulted in hydrolysis of the C-19-ester group, yielding steviolbioside. Therefore, the appearance of a product spot representing the same size as Stev after alkaline hydrolysis of Gtf180- Δ N-Q1140E-glycosylated Stev might suggest the formation of steviolbioside with one extra

glucose at the C-13 site. In other words, Stev-G2+ contains products glucosylated at the C-13 site, in contrast to RebA-G2+ which is completely composed of RebA products glucosylated at the C-19 site. Further structural analysis by means of NMR spectroscopy is nevertheless needed to confirm these results.

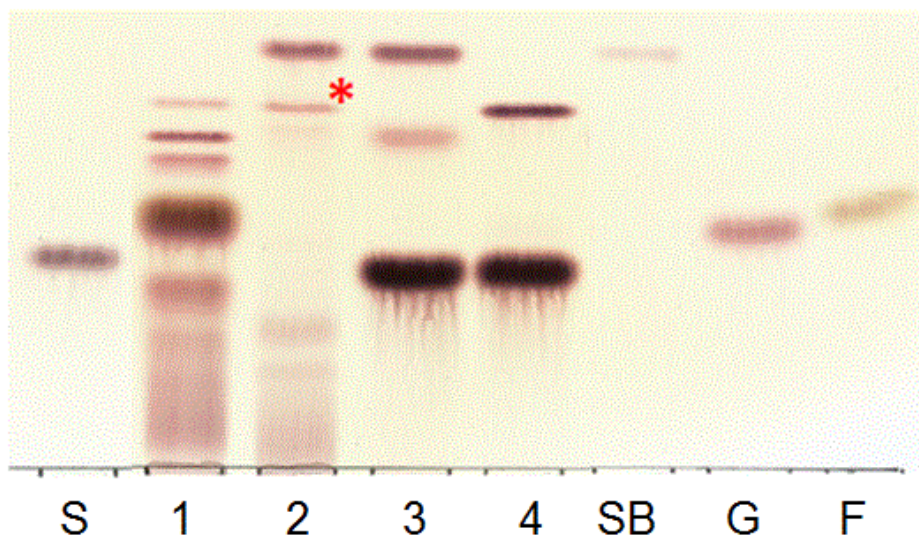


Figure 7. Alkaline hydrolysis of α -glucosylated stevioside (Stev-G) produced by Gtf180- Δ N-Q1140E. **S** sucrose, **1** Stev incubation (1 h), **2** Stev incubation (1 h) + NaOH, **3** Stev incubation (0 h) + NaOH, **4** Stev incubation (0 h), **SB** steviolbioside, **G** glucose, **F** fructose. * might suggest the formation of a product with the same size as stevioside, i.e. steviolbioside with one extra glucose at the C-13 site.

3.3. Sensory analysis of glucosylated stevioside products

The (α 1 \rightarrow 6)-glucosylation of Stev at the C-19 site is reported to improve its taste quality, mostly by alleviating its bitterness and off-flavors⁶⁶. A sensory analysis of aqueous solutions sweetened with Stev and several glucosylated Stev products was performed by a trained panel, evaluating 9 different taste attributes. Three different product solutions were examined: 588 mg/L mono- α -glucosylated product (Stev-G1), 588 mg/L multi- α -glucosylated product, containing residual

Stev, Stev-G1 and higher α -glucosides (Stev-G) and 1176 mg/L multi- α -glucosylated product (Stev-G'). The mean scores of the taste attributes of the sweetened solutions are shown in Figure 8.

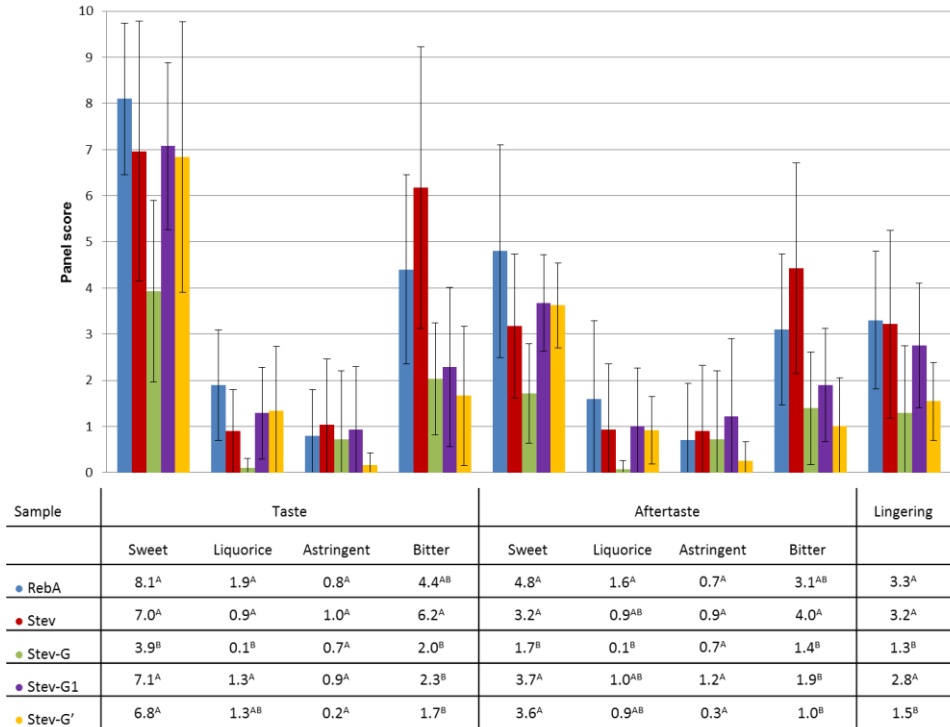


Figure 8. Sensory analysis of stevioside (Stev), Stev-G, Stev-G1 and Stev-G'. ^{A,B}: different letters indicate significant differences ($p < 0.05$) between solutions following one-way ANOVA and post-hoc test.

All α -glucosylated stevioside products were significantly less bitter than stevioside. Stev-G1 retained the very high sweetness typical for steviol glycosides such as stevioside. In contrast, Stev-G was significantly less sweet than stevioside, which can be explained by the relatively large proportion of multi- α -glucosylated products. Multi- α -glucosylation resulted not only in a further decrease of bitterness, but simultaneously decreased sweetness as well. In addition, Stev-G was also significantly less liquorice and lingering than stevioside (Figure 8). Doubling the concentration of Stev-G from 588 mg/L to 1176 mg/L

roughly resulted in a duplication of the sweetness, equaling the sweetness level of stevioside, whereas bitterness and off-flavors were still equally suppressed. Glucosylation of stevioside with Gtf180- Δ N-Q1140E is thus a very adequate method to improve its sensory properties, i.e. by reducing the typical bitterness to a very low level.

4. Discussion

Even though Stev is the most abundant of all steviol glycosides extracted from the leaves of the *Stevia* plant, its lingering bitterness prevents applications in low-calorie foods and beverages. All current *Stevia* food products are based on RebA, perceived as less bitter than Stev, implying that the latter is discarded as a “side product”. This chapter demonstrated that the α -glucosylation of Stev with Gtf180- Δ N-Q1140E offers a viable method to significantly reduce its bitterness. A very high Stev conversion of 95%, yielding 50 g/L Stev-G within 3 h, while using only 10 U/mL enzyme, was obtained after optimization of the reaction conditions by RSM. Structural analysis revealed that Stev was mostly glucosylated at the C-19 site, initially through an (α 1 \rightarrow 6)-linkage, after which the synthesized Stev-G1 was glucosylated through an (α 1 \rightarrow 4)-linkage, yielding Stev-G2 (Figure 5). MALDI-TOF and MS analysis indicated that a complex mixture of many other multi-glucosylated products (> 50% of Stev-G) was formed by the enzyme, as opposed to RebA α -glucosylation by Gtf180- Δ N-Q1140E, resulting in the synthesis of mostly mono- α -glycosylated product (77%)⁷⁰. As a consequence, Stev-G was perceived half as sweet as Stev, an undesired effect which could be compensated by doubling the dose of Stev-G. Remarkably, this did not affect the significantly reduced perception of bitterness nor of other off-flavors.

A previous study already reported the application of a dextransucrase from *Leuconostoc citreum* KM20⁶⁶ for the glucosylation of Stev: a high conversion degree (94%) was obtained, however, much more enzyme (4500 U/mL vs. 10 U/mL) and a longer incubation time (5 days vs. 3 h) was needed. The volumetric productivity per U enzyme of the mutant Gtf180- Δ N-Q1140E enzyme reaction is

consequently more than 2,000 times higher. Transglucosylation of stevioside, using sucrose as donor substrate, was also achieved with an alternansucrase (EC 2.4.1.140) from *L. citreum* SK24.002, an enzyme that also makes ($\alpha 1 \rightarrow 6$) and ($\alpha 1 \rightarrow 3$) linkages^{67,230,231}. Under optimized reaction conditions, a maximum conversion degree of only 44% was achieved. Stevioside was elongated at the terminal Glc($\beta 1 \rightarrow 2$) residue of the β -sophorosyl unit at the steviol C-13 site with an ($\alpha 1 \rightarrow 6$) linkage. Also a tri-glucosyl-stevioside was structurally characterized and was shown to be a ($\alpha 1 \rightarrow 3$)-($\alpha 1 \rightarrow 6$)-($\alpha 1 \rightarrow 3$) extension at the terminal Glc($\beta 1 \rightarrow 2$) residue at C-13. A taste comparison of the products was not reported. In addition, a mono-glucosylated stevioside product, containing a Glc($\alpha 1 \rightarrow 6$) residue at the steviol C-19-ester-linked Glc($\beta 1 \rightarrow$ residue (comparable with Stev-G1), has been synthesized with β -amylase Biozyme L and maltose as glucose donor. This also led to an improvement in quality of taste⁶⁰, just like shown here for the Gtf180- Δ N-Q1140E products. However, also products elongated at the C-13 site were synthesized, resulting in a decreased quality of taste.

These examples illustrate the three main requirements for any enzymatic Stev glucosylation process: an adequate product specificity, a complete Stev conversion and a high space-time yield. The here described process is clearly superior to the other glucansucrase-catalyzed Stev glucosylation reactions, adequately meeting all three requirements.

5. Supplementary information

Table SI. Box-Behnken experimental design and results for the variables studied. Second-degree polynomial equation with coefficients of each factor is given for amount of Stev-G synthesized (mM) and stevioside conversion degree (%). X_1 stevioside (mM), X_2 D/A ratio, X_3 agitation (rpm).

	Pattern	X_1	X_2	X_3	Stev-G (mM) ¹	Stev conversion (%) ²
1	+0+	100	11.25	200	55.5	55.5
2	0-+	62.5	2.5	200	28.3	45.3
3	-0+	25	11.25	200	22.5	90.0
4	0--	62.5	2.5	0	30.3	48.5
5	++0	100	20	100	38.1	38.1
6	-0-	25	11.25	0	23.2	92.9
7	--0	50	20	20	23.7	94.8
8	0+-	62.5	20	0	42.9	68.6
9	--0	25	2.5	100	14.8	59.3
10	000	62.5	11.25	100	44.9	71.8
11	+-0	100	2.5	100	51.6	51.6
12	000	62.5	11.25	100	45.2	72.4
13	000	62.5	11.25	100	45.6	72.9
14	0++	62.5	20	200	39.8	63.6
15	+0-	100	11.25	0	53.2	53.2

$$^1 \text{ Stev-G} = 45.0500 + 14.2725X_1 - 0.1875X_2 - 0.1900X_3 - 5.6000X_1X_2 + 0.7550X_1X_3 - 5.5250X_2X_3 - 5.1100X_1^2 - 7.8900X_2^2 - 1.3350X_3^2$$

$$^2 \text{ Stev conversion} = 72.1000 - 17.3225X_1 + 7.5500X_2 - 1.0975X_3 - 12.2500X_1X_2 + 1.2950X_1X_3 - 0.4500X_2X_3 - 2.6225X_1^2 - 13.7725X_2^2 - 1.8275X_3^2$$

Table SII. ^1H and ^{13}C chemical shifts (δ)^a for the steviol part of Stev, Stev-G1, and Stev-G2, recorded in D_2O at 310 K. For chemical structures, see Figure 5.

Carbon ^b number	Stev		Stev-G1		Stev-G2	
	δ ^1H	δ ^{13}C	δ ^1H	δ ^{13}C	δ ^1H	δ ^{13}C
1	0.82	41.4	0.82	41.3	0.83	41.3
	1.82		1.82		1.82	
2	1.31	20.3	1.30	20.3	1.30	20.3
	1.60		1.60		1.51	
3	1.07	38.5	1.07	38.5	1.09	38.6
	2.05		2.04		2.04	
5	1.16	57.7	1.16	57.7	1.17	57.7
6	1.66	22.1	1.68	22.8	1.82	22.9
	1.81		1.80		2.04	
7	1.40	42.0	1.43	42.1	1.42	42.1
	1.49		1.47		1.49	
9	0.98	54.4	0.98	54.2	0.98	54.4
11	1.68	22.7	1.70	22.9	1.66	22.9
	1.83		1.83		1.80	
12	1.48	37.5	1.48	37.6	1.48	37.5
	1.90		1.90		1.90	
14	1.39	45.6	1.40	45.5	1.41	45.5
	2.13		2.12		2.13	
15	2.06	48.2	2.06	48.1	2.05	48.1
	2.10		2.09		2.08	
17	4.87	105.4	4.87	105.4	4.87	105.4
	5.04		5.04		5.04	
18	1.18	29.2	1.18	29.3	1.18	29.2
20	0.83	16.4	0.83	16.5	0.83	16.4

^a In ppm relative to internal acetone (δ 2.225 for ^1H and δ 31.07 for ^{13}C).

^b As ^{13}C data have been deduced from HSQC measurements, ^{13}C chemical shifts in D_2O are missing for C-4, C-8, C-10, C-13, C-16 and C-19.

Table SIII. ^1H and ^{13}C chemical shifts (δ)^a for the Glcp residues of Stev, Stev-G1, and Stev-G2, recorded in D₂O at 310 K. For chemical structures, see Figure 5.

Residue	Stev		Stev-G1		Stev-G2	
	δ ^1H	δ ^{13}C	δ ^1H	δ ^{13}C	δ ^1H	δ ^{13}C
Glc1 ($\beta 1 \rightarrow \text{C}-19$)						
H-1	5.40	95.4	5.41	95.5	5.41	95.4
H-2	3.46	73.6	3.46	73.0	3.45	73.4
H-3	3.50	78.0	3.50	77.8	3.50	77.9
H-4	3.40	70.7	3.45	70.6	3.45	70.6
H-5	3.50	77.7	3.70	77.0	3.70	76.9
H-6a	3.82	62.2	3.89	66.7	3.85	67.4
H-6b	3.67		3.70		3.74	
Glc2 ($\beta 1 \rightarrow \text{C}-13$)						
H-1	4.73	97.2	4.72	97.3	4.73	97.2
H-2	3.49	82.2	3.49	82.2	3.49	82.1
H-3	3.62	77.6	3.62	77.7	3.62	77.6
H-4	3.34	71.2	3.34	71.1	3.35	71.0
H-5	3.33	77.2	3.34	77.4	3.34	77.2
H-6a	3.80	62.2	3.80	62.2	3.80	62.2
H-6b	3.63		3.63		3.65	
Glc3 ($\beta 1 \rightarrow 2$)						
H-1	4.67	104.3	4.67	104.5	4.67	104.4
H-2	3.26	75.7	3.27	75.8	3.27	75.8
H-3	3.45	77.0	3.45	77.3	3.45	77.0
H-4	3.32	71.2	3.34	71.1	3.33	71.2
H-5	3.35	77.4	3.34	77.4	3.35	77.2
H-6a	3.82	62.2	3.82	62.2	3.82	62.2
H-6b	3.64		3.64		3.64	
Glc4			($\alpha 1 \rightarrow 6$)Glc1		($\alpha 1 \rightarrow 6$)Glc1	
H-1			4.86	99.3	4.86	99.2
H-2			3.48	73.0	3.53	72.9
H-3			3.65	74.4	3.90	74.8
H-4			3.36	71.3	3.58	77.9
H-5			3.62	73.5	3.70	71.7
H-6a			3.75	62.0	3.75	61.8
H-6b			3.68		3.70	
Glc5					($\alpha 1 \rightarrow 4$)Glc4	
H-1					5.29	101.6
H-2					3.52	73.1

H-3	3.63	74.3
H-4	3.37	71.0
H-5	3.64	74.3
H-6a	3.78	61.8
H-6b	3.70	

^a In ppm relative to the signal of internal acetone (δ 2.225 for ¹H and δ 31.07 for ¹³C).

^b Substituted carbon positions are indicated in *italics*.

Table SIV. Methylation analysis of the carbohydrate moieties in Stev, Stev-G1, and Stev-G2.

PMAA	<i>R_t</i> ^a	Structural feature	Peak area (%) ^b		
			Stev	Stev-G1	Stev-G2
2,3,4,6-Hex ^c	1.00	Glc <i>p</i> (1→	66	52	42
3,4,6-Hex	1.15	→2)Glc <i>p</i> (1→	34	25	21
2,3,6-Hex	1.18	→4)Glc <i>p</i> (1→	-	-	19
2,3,4-Hex	1.22	→6)Glc <i>p</i> (1→	-	23	18
3,4-Hex	1.39	→2,6)Glc <i>p</i> (1→	-	-	tr ^d

^a *R_t*, retention time relative to 1,5-di-*O*-acetyl-2,3,4,6-tetra-*O*-methylglucitol (1.00) on GLC.

^b Average values from triplo determination (not corrected by response factors).

^c 2,3,4,6-Hex = 1,5-di-*O*-acetyl-2,3,4,6-tetra-*O*-methylhexitol-1-*d*, etc.

^d tr = trace (<2%).

Figure S1. HSQC, TOCSY and ROESY spectrum of the carbohydrate part of Stev-G1, recorded in D₂O at 310 K. In HSQC, 22 means cross-peak H-2/C-2 of residue Glc2, etc. 16a-16b means cross-peaks H-6's/C-6 of residue Glc1, shifted downfield ($\Delta\delta_C$ 4.5 ppm) due to substitution Glc4(α 1 \rightarrow 6)Glc1. Significant cross-peaks, concerning glycosidic linkages, are indicated in red.

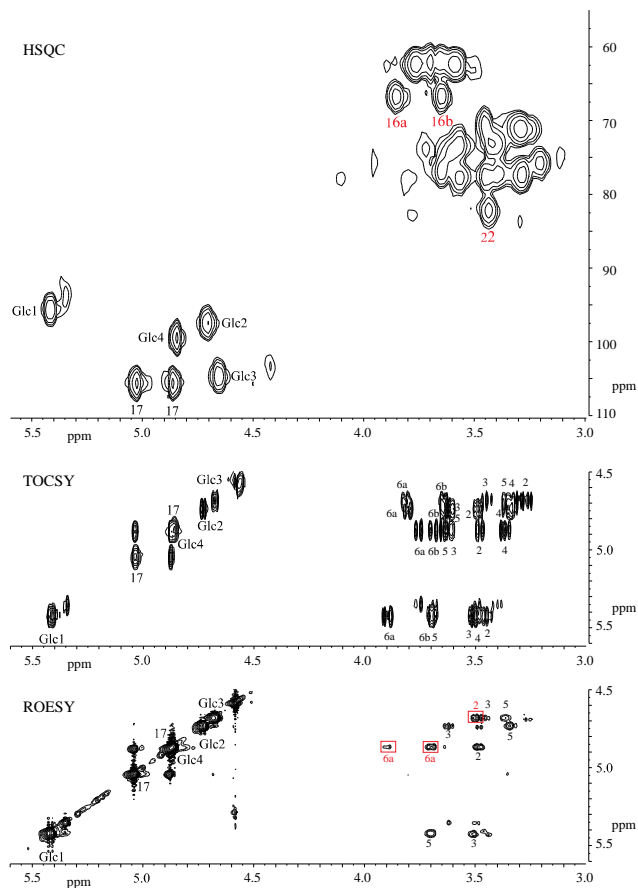
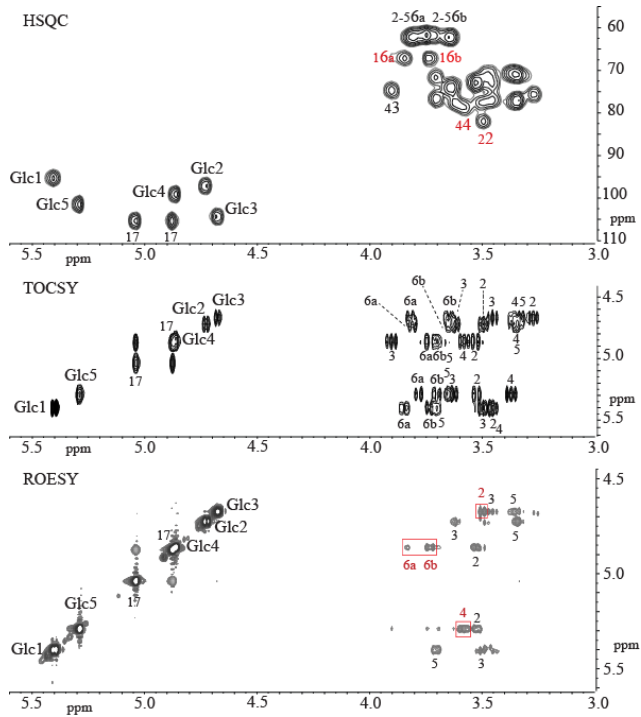


Figure S2. HSQC, TOCSY and ROESY spectra of the carbohydrate part of Stev-G2, recorded in D₂O at 310 K. In the HSQC spectrum, 22 means cross-peak H-2/C-2 of residue Glc2, etc. Assignments in red reflect the substituted positions of the residues. In the ROESY spectrum, the inter-residual cross-peaks confirming the Glc3(β 1 \rightarrow 2)Glc2 and Glc5(α 1 \rightarrow 4)Glc4(α 1 \rightarrow 6)Glc1 linkages are indicated with red boxes.



Chapter 6

Biocatalytic production of novel steviol glycosides with improved taste: scale-up, downstream processing and cost analysis

Tim Devlamynck^{1,2}, Evelien M. te Poele², Wim Soetaert¹, Lubbert Dijkhuizen²
Ghent University¹, University of Groningen²

Abstract

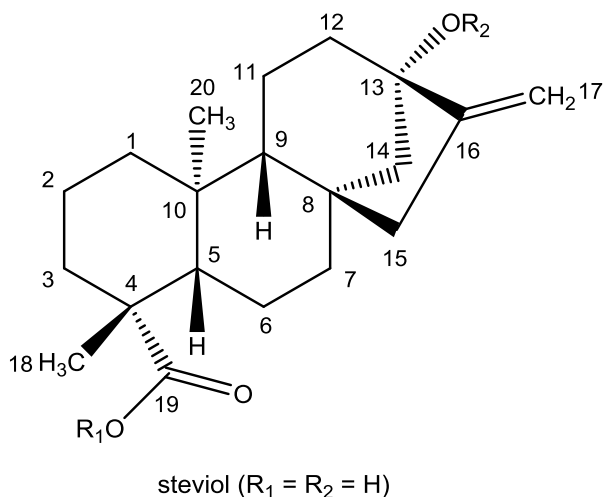
Previously we reported the efficient laboratory scale glucosylation of the *Stevia* components rebaudioside A (RebA) and stevioside with the Q1140E mutant of glucansucrase Gtf180- Δ N from *Lactobacillus reuteri* 180. Sensory analysis by a trained panel revealed that the glucosylated products possess a superior taste profile, displaying a significant reduction in bitterness compared to RebA and stevioside. As the developed technology holds excellent commercial potential, this chapter focused on the scale-up of the Gtf180- Δ N- Δ V-Q1140E catalyzed glucosylation of RebA and stevioside. An eco-friendly and efficient downstream processing of the glucosylated products was developed and demonstrated at 7.5 L scale, allowing the production of 250 g glucosylated RebA product. Estimates of the production costs indicated the economic feasibility of the overall process. The major factor in the total production cost was the acceptor substrate, i.e. RebA or stevioside; in contrast, the biocatalyst cost represented only a minor part. In an attempt to lower the overall production cost even further, the glucosylation of low-grade stevia extract (roughly a 50:50 mixture of stevioside and RebA) was demonstrated. The sensory properties of the resulting product mixture were perceived as excellent by a trained panel, mainly due to a significant reduction in bitterness.

1. Introduction

The steviol glycosides extracted from the plant *Stevia rebaudiana* (Figure 1), native in Paraguay and Brazil, were approved for use as high-intensity sweetener (HIS) in food products by the USA in 2009 and by the European Commission in 2011⁴³. The share of HIS in the global sweetener market, estimated at \$68 billion in 2014, is currently not significant⁴⁴, however, the world-wide increasing incidence of obesity and other diet-related diseases is expected to increase the consumer demand for low-calorie food products and beverages⁴⁶. The HIS market is consequently predicted to grow at a fast compound annual growth rate (CAGR) of more than 5%. The natural character of stevia HIS gives it a competitive edge over synthetic HIS such as aspartame and saccharin, suffering from a bad reputation among consumers. As a result, stevia is currently the fastest growing HIS on the market, displaying a CAGR of roughly 8.5%⁴⁴. The World Health Organization even projects that stevia will eventually replace 20% of the sugar segment, equaling a \$10 billion industry⁴⁵, which is significantly greater than current stevia sales, estimated at \$347.0 million in 2014⁴⁴.

The main impediment to accomplish these projections is the lingering bitterness displayed by most steviol glycosides, including stevioside (5-10% of leaf dry weight) and rebaudioside A (2-4% of leaf dry weight, RebA), the only steviol glycosides which can be economically extracted from the *Stevia* plant¹⁹⁰⁻¹⁹². Not surprisingly, several companies have launched next-generation stevia products with improved taste. For example, USA-based MycoTechnology produces mushroom-derived enzymes (MycoZyme) which can be added to stevia products to remove their bitterness (<http://www.mycotechcorp.com>). In addition, a joint venture of Cargill and Evolva aims to develop a process for the fermentative production of rebaudioside D and M, two steviol glycosides perceived as less bitter than RebA, but difficult to extract from the *Stevia* leaves, in 2018 (<http://www.evolva.com>)^{39,58,71}. However, the relatively high production costs, caused by inadequate strain characteristics and associated fermentation and downstream processing costs, have forced this joint venture to set back the

launching date several times since 2013. Dutch multinational DSM is developing a similar technology, applying a recombinant yeast (*Yarrowia lipolytica*) to produce steviol glycosides (<http://www.dsm.com>)²³². However, no new announcements have followed the initial 2014 press release.



Steviol glycoside	R ₁ (C-19)	R ₂ (C-13)
Stevioside	Glc(β1→	Glc(β1→2)Glc(β1→
Steviolbioside	H	Glc(β1→2)Glc(β1→
Rebaudioside A	Glc(β1→	Glc(β1→2)[Glc(β1→3)]Glc(β1→
Rebaudioside B	H	Glc(β1→2)[Glc(β1→3)]Glc(β1→
Rebaudioside C	Glc(β1→	Rha(α1→2)[Glc(β1→3)]Glc(β1→
Rebaudioside D	Glc(β1→2)Glc(β1→	Glc(β1→2)[Glc(β1→3)]Glc(β1→
Rebaudioside E	Glc(β1→2)Glc(β1→	Glc(β1→2)Glc(β1→
Rebaudioside F	Glc(β1→	Xyl(β1→2)[Glc(β1→3)]Glc(β1→
Rebaudioside M	Glc(β1→2)[Glc(β1→3)]Glc(β1→	Glc(β1→2)[Glc(β1→3)]Glc(β1→
Rubusoside	Glc(β1→	Glc(β1→
Dulcoside A	Glc(β1→	Rha(α1→2)Glc(β1→

Figure 1. Chemical structures of the most prevalent steviol glycosides found in the leaves of *Stevia rebaudiana*. Glucose (Glc), xylose (Xyl) and rhamnose (Rha) occur in the pyranose ring form. Glc and Xyl have the D configuration and Rha the L configuration.

Alternatively, enzymatic glucosylation has been proposed as a bitterness-eliminating process⁸. The main challenges faced here are to obtain an adequate product specificity, a complete RebA and stevioside conversion and a high space-time yield. The majority of described processes fail in fulfilling at least one of these three requirements. Glucosylations catalyzed by cyclodextrin glucanotransferases, α -amylases and β -amylases, are characterized by relatively high product yields, however, their lack of C-13/C-19-regiospecificity (Figure 1) renders them less useful as industrial biocatalyst: products with enhanced and reduced bitterness are obtained^{50-56,60-62}. For example, (α 1 \rightarrow 4)-glucosylation of stevioside at the C-13 steviol position yielded products with improved intensity and quality of sweetness, whereas (α 1 \rightarrow 4)-glucosylation at the C-19 position resulted in an increased bitterness^{52-54,196}. In contrast, the *in vitro* use of UDP-glycosyltransferases, catalyzing the conversion of RebA into rebaudioside D and M, yielded glycosides with improved sensory properties but suffered from very low productivities⁵⁷⁻⁵⁹. The application of β -glucosidases, introducing the naturally occurring β -linkages, resulted not only in the glucosylation of the steviol glycosides substrates but also in their hydrolysis, yielding products with an inferior taste profile⁶³⁻⁶⁵.

As illustrated in chapters 4 and 5, the α -glucosylation of RebA and stevioside with the glucansucrase Gtf180- Δ N-Q1140E from *Lactobacillus reuteri* 180, using sucrose as donor substrate, offers a viable method for the production of next-generation stevia products⁶⁸⁻⁷⁰. The Q1140E mutation improved the conversion from roughly 50% to 95%, yielding 115 g/L and 50 g/L α -glucosylated product, for RebA and stevioside glucosylation, respectively. Structural analysis and sensory analysis by a trained panel revealed that introducing a single (α 1 \rightarrow 6) linked glucosyl moiety at their Glc(β 1 \rightarrow C-19) residues yielded monoglucosylated products with a superior taste profile compared to their respective substrates. The multiglucosylated products displayed even better taste profiles (reduced bitterness and off-flavors), however, this was accompanied with an undesirable decrease in sweetness. Altogether, the mixtures of mono –and multiglucosylated RebA and Stev products showed most potential: an intensive sweetness combined with a very limited bitterness (see 3.4. Sensory analysis).

The RebA and stevioside glucosylation reactions were demonstrated only at laboratory scale, whereas chromatography was applied as purification method, a technology which is better avoided as it is too costly for industrial use. This chapter therefore aimed to develop this laboratory scale process with commercial potential into a cheap and straightforward pilot-plant process, allowing the synthesis of product samples for food safety analysis and for testing and tasting in several food products, such as chocolate, candy, etc. Furthermore, an accelerated shelf life study was performed to determine the stability of the introduced (α 1 \rightarrow 6) linkage in buffer solutions mimicking the acidic conditions in soft drinks. Finally, cost analysis of the glucosylation processes provided guidelines for future research and development activities in order to decrease the production costs.

2. Materials and methods

2.1. Stevioside, rebaudioside A and low-grade stevia extract

Stevioside was obtained from TCI Europe (> 85% pure, HPLC), rebaudioside A (RebA) from Tereos PureCircle Solutions (97% pure, HPLC). Low-grade stevia extract (Steviasol, 95% steviol glycosides) was mainly composed of RebA and stevioside (~ 50:50 mixture, as determined with HPLC).

2.2. Production and purification of recombinant Gtf180- Δ N- Δ V-Q1140E

Initial experiments with *Escherichia coli* BL21 (DE3) strains (Invitrogen, Carlsbad, USA), expressing either the N-terminally truncated Gtf180- Δ N-Q1140E^{70,80,97} or the N- and V-terminally truncated⁸⁸ Gtf180- Δ N- Δ V-Q1140E^{70,97} from *Lactobacillus reuteri* 180, were performed in shake flasks at 1 L scale, after which the biocatalyst production was performed at 7.5 L scale in a Labfors 5 bioreactor. The inoculum was routinely grown at 37 °C in shake flasks (200 rpm) containing LB medium (10 g/L tryptone, 5 g/L yeast extract, 5 g/L NaCl, pH 7.0) supplemented with 100 mg/L ampicillin. After overnight growth, 200 mL inoculum

was added to 5 L of LB medium supplemented with 30 g/L glucose and 100 mg/L ampicillin. The temperature, agitation rate and aeration rate were set at 37 °C, 350 rpm and 1 vvm, respectively. The dissolved oxygen concentration was maintained above 30% by gradually and automatically increasing the agitation rate to 1200 rpm. The pH was maintained at 7.0 by automatic addition of 25 % NH₄OH and 1 M H₂SO₄. Anti-foam was added occasionally to prevent foaming. Optical density measurements were performed in a spectrophotometer at 600 nm (OD₆₀₀). At an OD₆₀₀ of 5 the culture was induced with IPTG (final concentration of 0.1 mM). After 9 h of fermentation the glucose was depleted and the cells harvested by centrifugation (3000 g, 10 min). The cells were resuspended in lysis buffer and subsequently homogenized (800 bar, 3 cycles). Cell debris was removed by centrifugation (3000 g, 10 min) followed by microfiltration (0.5 µm). The crude enzyme was stable at 4 °C for several months and used accordingly for the production of glucosylated RebA (RebA-G).

2.3. Glucansucrase activity assay

One unit (U) of enzyme activity corresponds to the conversion of 1 µmole sucrose (used for hydrolysis and transglycosylation) in a solution of 100 mM sucrose, 25 mM sodium acetate (pH 4.7) and 1 mM CaCl₂ at 37 °C.

Enzyme activity assays, using approximately 50 mg/mL enzyme, were performed at 37°C with 100 mM sucrose in 25 mM sodium acetate (pH 4.7) and 1 mM CaCl₂. Samples of 150 µl were taken every min over a period of 8 min and immediately inactivated with 30 µl 1 M NaOH. The sucrose concentrations of the samples were subsequently quantified by means of HPLC analysis (see 2.4. HPLC analysis), allowing the calculation of the enzyme activity as defined above.

2.4. HPLC analysis

Two different types of HPLC analyses were performed. For the analysis of glucose, fructose and sucrose, an Agilent MetaCarb 67H column (300 mm x 6.5 mm) was used under isocratic conditions with 2.5 mM H₂SO₄ as the mobile

phase. The flow rate and temperature were set at 0.8 mL/min and 35°C, respectively. Detection was achieved with an RID detector. Calibration of the obtained peaks was accomplished using the corresponding standard curves.

For the analysis of the steviol glycosides an Agilent ZORBAX Eclipse Plus C18 column (100 mm × 4.6 mm, 3.5 μm) was used with water (solvent A) and acetonitrile (solvent B) as the mobile phase. The flow rate and temperature were set at 1.0 mL/min and 40 °C, respectively. The following gradient elution was used: 5-95% solvent B (0-25 min), 95% solvent B (25-27 min), 95-5% solvent B (27-30 min) and again 95% of solvent A (30-35 min). Detection was achieved with an evaporative light scattering detector (ELSD) (evaporation temperature: 90 °C, nebulization temperature: 70 °C, gas flow rate: 1.6 standard liter per min, SLM). Calibration of the obtained peaks was accomplished using the corresponding standard curves, obtained from previously purified glucosylated RebA (RebA-G) and stevioside (Chapters 4 and 5).

2.5. Yeast fermentation

RebA glucosylation reaction mixture (50 mM RebA, 125 mM sucrose) was incubated with 5, 10, 20 and 30 g/L (wet cell weight) fresh baker's yeast (*Saccharomyces cerevisiae*, AB Mauri) to remove sucrose, glucose, and fructose. Samples were taken at 0, 2, 4, 6 and 8 h, and subjected to HPLC analysis to determine the removal rate of both saccharides and RebA glucosides. The experiments were performed in duplicate.

2.6. Determination of adsorption and desorption characteristics

Adsorption experiments were carried out by adding a fixed amount of adsorbent (Lewatit® VP OC 1064 MD PH from LANXESS, 1 g) to six 50 ml Falcon tubes containing 10 mL dilutions of the RebA glucosylation mixture (with RebA-G concentrations ranging from 10 g/L to 60 g/L). The Falcon tubes were subsequently placed in a shaker at a temperature of 30 °C, 35 °C and 40 °C and

an agitation rate of 200 rpm for 60 min. The adsorption capacity q_e (g RebA-G/kg resin) and adsorption efficiency A (%) were calculated as follows:

$$q_e = \frac{(C_0 - C_e)V}{W}$$
$$A = \frac{C_0 - C_e}{C_0}$$

where C_0 is the initial RebA-G concentration (g/L), C_e is the RebA-G concentration at equilibrium (g/L), V is the volume of the solution (10 mL) and W is the mass of the adsorbent (1 g).

The obtained adsorption isotherms were analyzed using the Langmuir adsorption isotherm, which is represented by the following equation:

$$q_e = \frac{q_{\max}KC_e}{1 + KC_e}$$

where q_{\max} is the maximum adsorption capacity (g RebA-G/kg resin) and K is the Langmuir adsorption constant (L/g).

For the desorption experiments 10 mL of solvent was added to 4 g of adsorbent (equivalent to 1.5 bed volumes) loaded with a known amount of RebA-G. The 50 mL Falcon tubes were subsequently placed in a shaker at a room temperature and an agitation rate of 200 rpm for 60 min. The desorption capacity q_d (g RebA-G/kg resin) was calculated as follows:

$$q_d = \frac{C_dV}{W}$$

where C_d is the RebA-G concentration at equilibrium (g/L), V is the volume of the solution (10 mL) and W is the mass of the adsorbent (4 g). The experiments were performed in duplicate.

C_0 , C_e and C_d were determined applying HPLC analysis as described before.

2.7. Continuous adsorption of glucosylated rebaudioside A

After optimization of the static adsorption of RebA-G onto Lewatit® VP OC 1064 MD PH resin, its continuous adsorption was evaluated at laboratory scale (120 g of resin, bed volume (BV) of 200 mL), and finally at pilot-plant scale (2 kg of resin, BV of 3.34 L). After supplying the RebA glucosylation reaction mixture, 3 BV of water were immediately supplied to remove any residual sugars and α -glucans. Subsequently, six BV of 70% isopropanol were added to elute the adsorbed RebA-G. Several flow rates (3, 4.5 and 6 BV/h) and adsorbate loadings (50-100 g RebA-G/kg resin) were tested at laboratory scale, after which the optimal continuous adsorption was performed at pilot-plant scale (see also 2.8.).

2.8. Production and purification of glucosylated rebaudioside A

The production of glucosylated RebA (RebA-G) was performed at 7.5 L scale in a Labfors 5 bioreactor. The temperature and agitation rate were set at 37 °C and 185 rpm, respectively. The pH was maintained at 4.7 by automatic addition of 1 M NH₄OH and 1 M H₂SO₄. No buffer agent was added. The medium contained the optimal substrate- and enzyme concentrations as determined in chapter 4 (84 mM RebA, 282 mM sucrose, 5 U/mL Gtf180- Δ N- Δ V-Q1140E) supplemented with 1 mM CaCl₂. RebA (97% purity, HPLC grade) was obtained from Tereos PureCircle Solutions.

After completion of the reaction, the protein was removed by briefly (10 min) incubating the reaction mixture at 95 °C, after which the precipitated protein was removed by filtration. RebA-G was isolated from the reaction mixture by adsorption onto Lewatit® VP OC 1064 MD PH macroporous resin. Washing thoroughly with water removed any residual sugars and α -glucans. RebA-G was desorbed with 70% isopropanol. The resulting mixture was concentrated by evaporation *in vacuo* and ultimately freeze-dried, yielding pure RebA-G.

2.9. Cost analysis

The base case used for the cost analysis was RebA-G production in batch mode. The production costs were estimated by using the process mass balances as obtained in chapter 4 (RebA glucosylation)⁷⁰ and the current chapter (enzyme production (see also 2.1.) and downstream processing (DSP) of RebA-G (see also 2.6. and 2.7.). Guidelines as presented by Tufvesson et al.²³³ were followed for the cost estimation. Several assumptions were made in order to simplify the economic model (see supplementary information for detailed information). In short: The production scale of the enzyme fermentation and the enzymatic glucosylation were both fixed at 10 m³ (75% working volume). To run the fermentation, including set-up, harvesting and cleaning, 96 man-hours were allocated. The cost to obtain crude enzyme (homogenization, centrifugation to remove cell debris, and finally microfiltration) was assigned a value of €200/kg enzyme²³³. For the execution of the enzymatic glucosylation, including product recovery, 120 man-hours was considered. The cost of direct labor was assigned a value of €30/h, based on data from Eurostat (<http://ec.europa.eu/eurostat>). Supervision costs and indirect operating costs such as quality control corresponded to 100% of the direct labor costs.

Tables SI and SII summarize the various raw materials needed to run one production cycle (for definition, see supplementary information). The prices of the raw materials were obtained from the respective suppliers. Tables SIII-VII summarize the equipment related costs, utilities costs, and finally labor costs.

2.10. Sensory analysis

The sensory analysis was performed in individual tasting booths at the UGent Sensolab (Belgium) by a trained panel (9 persons), as described in chapter 4⁷⁰. In short, all solutions contained 588 mg/L of sweetener. Their taste (sweetness, liquorice, astringency and bitterness) was evaluated by swirling the sample in the mouth for 5 sec after which the sample was expectorated. Aftertaste was evaluated 10 sec after swallowing the solution. Lingering based on the maximum

taste intensity was rated 1 min later. Sucrose reference solutions (5%, 7.5% and 10% sucrose scoring 5, 7.5 and 10, respectively) were provided. Water (Spa Reine) and plain crackers were used as palate cleansers between sampling. All samples were evaluated in duplicate.

Statistical analyses were performed with SPSS 23 (SPSS Inc., Chicago, USA). All tests were done at a significance level of 0.05. One-Way ANOVA was used to investigate any significant difference between the solutions. Testing for equal variances was executed with the Modified Levene Test. When conditions for equal variance were fulfilled, the Tukey test was used to determine differences between samples²¹⁰. In case variances were not equal, a Games-Howell post-hoc test was performed²¹¹.

2.11. Stability analysis

The stability of RebA and RebA-G was determined by conducting an accelerated shelf life study at 80 °C in acidic buffer solutions (50 mM citric acid (pH 2.8 and 3.8) and 50 mM phosphate (pH 2.8 and 3.8)). Five mg of product was added to 10 ml buffer. All sample solutions were transferred to 1.5 mL Eppendorf tubes and incubated for 72 h in a thermoblock at 80 °C. Samples were taken at 0, 24, 48 and 72 h, and subjected to HPLC analysis.

3. Results and discussion

3.1. Biocatalyst production

The biocatalyst production generally forms an important factor of the total cost of a biocatalytic process at industrial scale²³³. A productive enzyme fermentation, yielding a highly active biocatalyst, are thus two essential features of any cost-effective enzymatic process.

The N-terminally truncated Gtf180- Δ N-Q1140E (117 kDa) and the N- and V-terminally truncated Gtf180- Δ N- Δ V-Q1140E (95 kDa) were both produced by fermenting the respective recombinant *Escherichia coli* strains in 1 L shake flasks, resulting in the production of 1306 U/mL and 1646 U/mL of enzyme, respectively. Incubation of 5 U/mL of the single enzymes in the optimal RebA glucosylation reaction mixture, as determined in chapter 4 (84 mM RebA, 282 mM sucrose)⁷⁰, resulted in identical RebA-G synthesis. Indeed, domain V is known to be crucial only for glucansucrase processivity; its deletion impairs polysaccharide synthesis, however, the acceptor reaction is not affected⁸⁸. Nevertheless, deletion of domains N plus V resulted in a higher enzyme yield, which may reflect its lower molecular mass compared to the N-terminally truncated variant. In addition, the induction temperature is known to influence Gtf180 enzyme expression. Lower temperatures typically result in higher enzyme yields, due to improved enzyme folding and decreased aggregation of the protein into inclusion bodies. This was previously shown for the expression of GtfB²³⁴ and Gtf180- Δ N⁹⁹ and was confirmed by studying the effect of the induction temperature on Gtf180- Δ N- Δ V-Q1140E expression (data not shown). However, as it was technically very complicated to lower the temperature below 37 °C at 7.5 L scale and, hence, at industrial scale, the fermentation was performed at 37 °C.

The production of Gtf180- Δ N- Δ V-Q1140E at 7.5 L scale yielded 38,320 U of enzyme or 815 mg of protein per L fermentation medium, which was obtained from roughly 45 g/L wet biomass (Figure S1). From the results obtained in chapter 4, it was calculated that 43,480 U of enzyme are needed to produce 1 kg RebA-G in batch mode. Consequently, the achieved enzyme production represented a theoretical production of 880 g RebA-G per L fermentation medium or about 1080 kg RebA-G per kg Gtf180- Δ N- Δ V-Q1140E. According to Tufvesson et al., a productivity of 670-1700 kg product/kg enzyme is required for the biocatalytic production of fine chemicals with a typical cost between €15-100/kg product^{233,235,236}. The obtained productivity clearly meets this requirement. The effect of the Gtf180- Δ N- Δ V-Q1140E production cost on the RebA-G

production cost is discussed in more detail later in this chapter (3.3. Cost analysis).

3.2. Downstream processing of glucosylated RebA

Glucosylated RebA (RebA-G) was selected as model product for the development of the downstream processing (DSP). Glucosylated stevioside (Stev-G) was purified following the same principle as applied for RebA-G purification. The two products are consequently interchangeable in the context of DSP.

3.2.1. Yeast fermentation

In addition to the synthesis of RebA-G, two types of by-products are produced by the enzyme: fermentable sugars such as fructose and glucose (and some remaining sucrose substrate), and α -glucan oligo- and polysaccharides. A common strategy to remove fermentable sugars is *Saccharomyces cerevisiae* fermentation²³⁷, a very cheap and sustainable DSP option, provided that the desired product (RebA-G) is not metabolized. As illustrated in Figure 2, *S. cerevisiae* was indeed able to ferment sucrose, fructose and glucose, while no loss of RebA-G was observed. Besides CO₂, ethanol and glycerol were produced by the yeast as side-products. A yellow color was observed after fermentation, suggesting the formation of other side-products.

3.2.2. Selective precipitation

As the α -glucans were not metabolized by the yeast, their removal required an additional step. In theory, the differences in solubility between α -glucans and RebA-G in organic solvents may result in their selective precipitation. The precipitate can then be easily separated from the supernatant. A patent of Cargill, describing the use of antisolvent crystallization (precipitation) to separate steviol glycosides, offered a useful protocol²³⁸. In short, the yeast-treated reaction mixture was evaporated until a sugar content of 30 °Bx (degrees Brix, the sugar

content of an aqueous solution, equaling 30% weight sugar), after which 3 volumes of ethanol, methanol or isopropanol were gradually added to provoke crystallization. Unfortunately, the majority of α -glucans precipitated simultaneously with RebA-G, preventing their complete separation. Hence, it was decided to change strategy and attempt separation by selective adsorption.

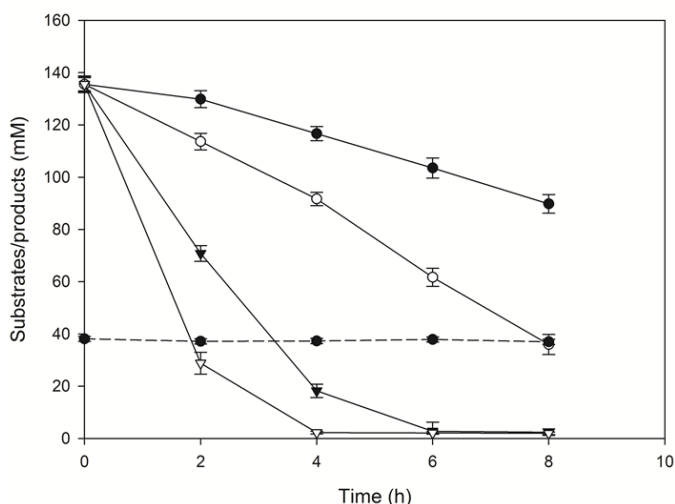


Figure 2. HPLC analysis of the utilization of fermentable sugars, present in RebA glucosylation reaction mixture (50 mM RebA, 125 mM sucrose), by *Saccharomyces cerevisiae* (● 5, ○ 10, ▼ 20, ▽ 30 g/L fresh yeast). RebA-G (dashed line) was not metabolized under all circumstances tested.

3.2.3. Selective adsorption

Selective adsorption of RebA-G onto several hydrophobic macroporous resins was evaluated. From the evaluated resins, Lewatit® VP OC 1064 MD PH displayed most potential and was consequently selected for further experimenting. The adsorption isotherms of RebA-G on this resin were determined at 30 °C, 35 °C and 40 °C and were described by the Langmuir model with good fit (R^2 of 0.92, 0.89 and 0.98 respectively, Figure 3). The highest adsorption capacity q_e was observed at 40 °C, suggesting an endothermic adsorption process, as previously described for the adsorption of RebA and stevioside onto mixed-mode macroporous resin²³⁹. Even at the lowest

temperature tested (30 °C), a sufficiently high adsorption efficiency (A) was obtained: as much as 92.0 g RebA-G could be adsorbed per kg resin with an A of 94%.

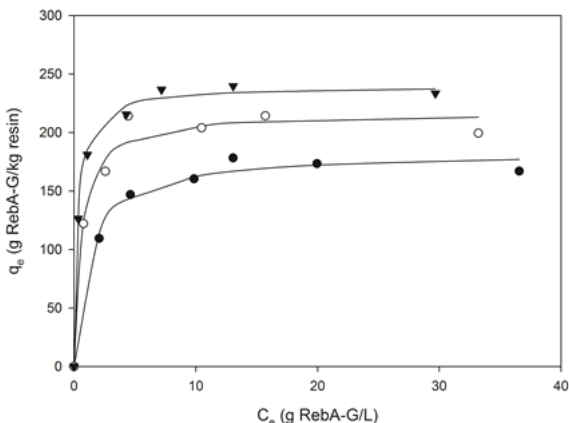


Figure 3. Adsorption isotherms of RebA-G on Lewatit VP OC 1064 MD PH resin at 30 °C (●), 35 °C (○) and 40 °C (▼). The obtained results were described by the Langmuir model with good fit (R^2 of 0.92, 0.89 and 0.98 respectively). q_{max} of 183, 217 and 240 g RebA-G/kg resin, respectively. K of 0.80, 1.73 and 3.1 L/g, respectively.

A compatible desorbing solvent was selected by evaluating the respective desorption capacities (q_d) at room temperature (Figure 4). Isopropanol (70 vol%) displayed most potential with a q_d of 91.3 g RebA-G/kg resin and was consequently selected as eluent for the production process.

Based on the previous results, an efficient continuous adsorption process was developed at room temperature, targeting complete adsorption with the highest dynamic adsorption capacity (DAC) possible. An important factor in the optimization of a continuous adsorption process is the flow rate. In general, low flow rates favor high adsorption efficiencies since the adsorbate has more time to interact with the adsorbent, preventing its breakthrough. The effect of the flow rate on the continuous adsorption of RebA-G onto Lewatit VP OC 1064 MD PH resin was therefore studied (Figure 5).

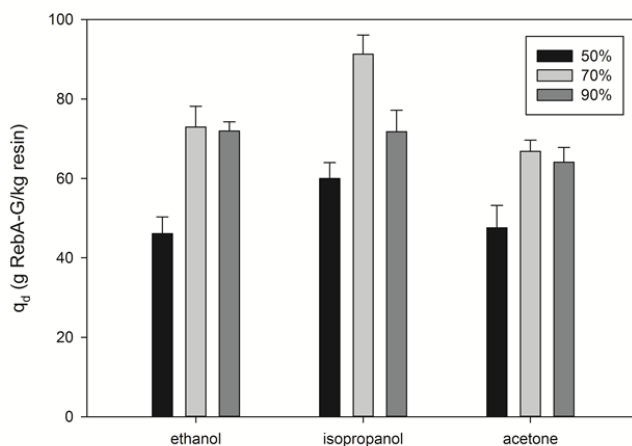


Figure 4. Desorption of RebA-G from Lewatit VP OC 1064 MD PH resin at room temperature, applying different percentages by volume of ethanol, isopropanol and acetone. Desorption capacities (q_d , defined in 2.5.) are given.

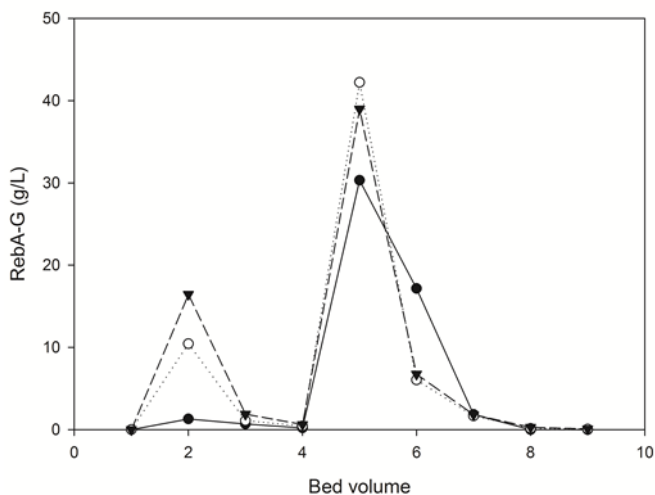


Figure 5. Continuous adsorption of the RebA glucosylation reaction mixture (at zero time: 84 mM RebA, 282 mM sucrose, 5 U/mL enzyme) onto Lewatit VP OC 1064 MD PH resin at a flow rate of 3 (●), 4.5 (○), and 6 (▼) BV/h. The amount of RebA-G (g/L) eluting from the resin is given.

Applying flow rates of 4.5 and 6 bed volumes per h (BV/h) caused considerable breakthrough of RebA-G, which resulted in suboptimal adsorption efficiencies of

79% and 68%, respectively. The application of a flow rate of 3 BV/h resulted in a near complete adsorption (96%) and a DAC of 95.7 g RebA-G/kg resin, similar to the optimal static adsorption capacity (92.0 g RebA-G/kg resin). Only 3 bed volumes of 70% isopropanol were subsequently needed for a near complete recovery of the product. The successful separation of RebA-G from the fermentable sugars and α -glucans is clearly shown by TLC analysis (Figure S2). The developed continuous adsorption was consequently used to treat 4 L RebA glucosylation reaction mixture (containing 60 g/L RebA-G), yielding 250 g of amorphous RebA-G, composed of (by mass) 4% RebA, 60% monoglucosylated RebA (RebA-G1) and 36% multiglucosylated RebA (RebA-G2+) (Figure S3). As the applied desorbing solvent (70% isopropanol) can be reused after evaporation, the developed DSP is not only efficient (almost no loss of RebA-G) but also eco-friendly.

3.3. Cost analysis of stevia glucosylation

3.3.1. Base case: RebA glucosylation

Any new production process must meet a number of criteria to be successfully implemented at industrial scale. Besides analyzing safety matters and environmental and legal issues, the process economics need to be evaluated²⁴⁰. Assessing the economic feasibility of a process is achieved by performing a production cost estimation, a powerful tool to guide research and development activities in order to turn lab-scale processes into commercially viable ones. Production costs can be divided into two categories: capital investment (CapEx) and operation costs (OpEx), both considered for the cost estimation of the base case (for detailed information, see supplementary information). A production scale of 10 m³ for both the enzyme fermentation and the enzymatic glucosylation was assumed. It should be noted that production volume has a major impact on the production costs: increasing the volume from 1 m³ to multiple cubic meters is accompanied by a cost reduction of several orders of magnitude²³³. The assignment of an adequate production scale is typically based on the expected sales, however, that was outside the scope of this chapter.

Tables I and II summarize the results obtained for the base case analysis. For the detailed results, see supplementary information (Tables SI-VII). Figure 6 illustrates the cost contribution of the different resources on the enzyme production (A) and RebA-G production, including DSP (B).

Table I. Cost analysis of Gtf180- Δ N- Δ V-Q1140E production in batch mode.

Resources	Cost (€/kg enzyme)	Relative cost (%)
Fermentation	2106	91
Raw materials	114	5
Utilities	34	1
Labor	950	41
Equipment	1008	44
Enzyme recovery	200	9
Total	2306	100

Table II. Cost analysis of RebA-G production and glucosylated steviol glycosides (GSG) production in batch mode, using RebA and low-grade stevia extract (steviol glycosides, SG) as acceptor substrate, respectively.

Resources	Cost (€/kg RebA-G)	Relative cost (%)	Cost (€/kg GSG)	Relative cost (%)
Biocatalysis	70.7	79	41.3	66
Enzyme	2.1	2	3.5	6
Sucrose	0.6	1	1.8	3
RebA/SG	56.5	63	17.1	27
Utilities	< 1	< 1	< 1	< 1
Labor	4.2	5	6.9	11
Equipment	7.1	8	11.6	19
DSP	18.5	21	21.3	34
Resin	12.7	14	12.7	20
IPA	1.1	1	1.1	2
Utilities	< 1	1	< 1	1
Labor	4.2	5	6.9	11
Total	89.2	100	62.6	100

A common drawback to implement an enzymatic process at industrial scale is the relatively high cost of the biocatalyst²³³. Although the enzyme production cost for the base case in itself is relatively high (€2306/kg enzyme), cost analysis revealed that the biocatalyst cost (€2.1/kg RebA-G) represents only 2% of the total RebA-G production cost. As rule of thumb, €1.5/kg product is an allowable cost contribution of the biocatalyst to the total production cost of fine chemicals, i.e. products with a typical cost between €15-100/kg product^{233,235,236}. The estimated biocatalyst cost for the base case is roughly of the same order and consequently fulfills this requirement. The enzyme production consists mostly of labor- and equipment costs, which is typical for fermentation processes at 10 m³ scale or lower (Figure 6).

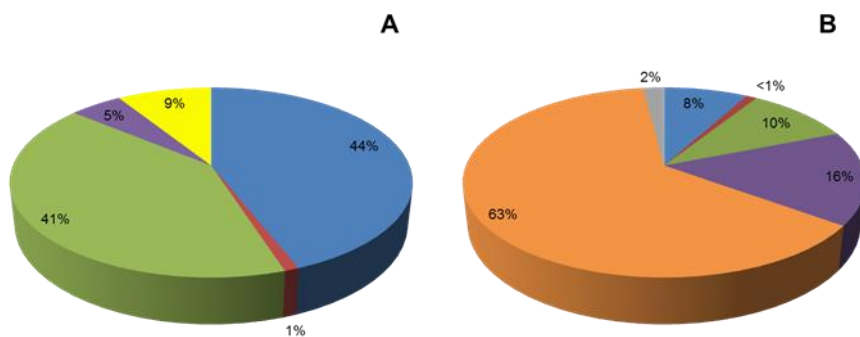


Figure 6. Cost contribution of various resources to the enzyme production cost (A) and the RebA-G production cost (B): ● Labor, ● Equipment, ● Raw materials, ● Utilities, ● Enzyme recovery, ● RebA, ● Enzyme (Gtf180-ΔN-ΔV-Q1140E).

The low cost contribution of Gtf180-ΔN-ΔV-Q1140E to the RebA-G production cost is explained by the high biocatalyst activity (k_{cat} for sucrose as donor substrate is 300/s)⁹⁸, allowing the addition of a relatively low amount of enzyme (5 U/mL) to the glucosylation reaction medium. As discussed previously, this results in a theoretical production of 880 g RebA-G per L fermentation medium. Nevertheless, there is still margin to reduce the fermentation cost. By performing the fermentation in fed-batch mode much higher cell densities (up to OD₆₀₀ of 100) and consequently higher enzyme titers (up to 10 g/L) may be obtained²³³. As a result, labor- and equipment costs would decrease substantially.

The total RebA-G production cost equals €89.2/kg RebA-G, representing an extra cost of 12% compared to high-purity RebA, sold at €80/kg (Tereos PureCircle Solutions). Since the price of sucrose is roughly €0.70/kg and RebA-G is around 150 times sweeter than sucrose, a selling price of €105/kg RebA-G can still be considered as competitive. If RebA-G is sold at this price, a profit of €15/kg RebA-G is obtained.

As demonstrated in chapter 4, glucosylating RebA in fed-batch mode resulted in higher production yield compared to the batch production (270 vs 115 g/L RebA-G). However, the much lower productivity per kg enzyme (1080 vs 253 kg RebA-G/kg enzyme), due to the addition of 10 times more enzyme, was translated into an undesirable production cost increase of €11.1/kg RebA-G. From an economic perspective, the batch reaction is thus preferred. It has to be noted that further optimization of the fed-batch reaction, thereby decreasing the applied enzyme activity (U/mL), may allow further reduction of the production cost.

3.3.2. Alternative case: glucosylation of low-grade stevia extract

Remarkably, the base case analysis shows that RebA-G production cost is dominated by the cost of the acceptor substrate RebA (63%). A major cost reduction consequently may be achieved by changing the acceptor substrate: instead of high-purity RebA, low-grade stevia extract could be used as substrate, which is commonly marketed for roughly €40/kg (Tereos PureCircle Solutions, or half of the price for high-purity RebA (€80/kg, Tereos PureCircle Solutions). Moreover, glucosylating mixtures of steviol glycosides also offers the possibility to valorize stevioside, whose glucosylation by Gtf180- Δ N-Q1140E was already demonstrated in chapter 5. The glucosylation of different self-made stevioside/RebA mixtures and of low-grade stevia extract (Steviasol), basing the experimental design on the optimal reaction conditions for stevioside glucosylation, as determined in chapter 5 (31 mM steviol glycosides, 524 mM sucrose), was also successful (data not shown), yielding roughly 50 g/L glucosylated steviol glycosides (GSG). The economic model of the base case was changed accordingly, resulting in a production cost of €62.7/kg GSG, a

substantial reduction of almost 30% compared to RebA-G production (Table II). The glucosylation of a mixture of steviol glycosides consequently provides a substantial economic advantage over the glucosylation of high-purity RebA.

3.4. Sensory analysis of glucosylated stevioside/RebA mixture

The previous paragraph demonstrated the economic advantage of glucosylating a mixture of steviol glycosides. However, the sensory properties of the obtained product must at least be similar to those of RebA-G to justify this change of acceptor substrate. As proof of concept, a sensory analysis of a glucosylated mixture (obtained from glucosylating low-grade stevia extract), containing 50% Stev-G and 50% RebA-G (RebA-G/Stev-G), was performed by a trained panel, evaluating 9 different taste attributes. The mean scores of the attributes of the sweetened water solutions are shown in Figure 7 and were compared with the sensory properties of RebA-G and Stev-G.

The sensory properties of the RebA-G/Stev-G mixture, compared to RebA and stevioside, were clearly improved, mainly due to a significant reduction in bitterness. Interestingly, the relatively low sweetness of Stev-G was compensated by the high sweetness of RebA-G, yielding a product with excellent edulcorant properties. RebA-G was identified as the most promising high-intensity sweetener, combining a high sweetness with a very low off-flavor intensity. If taste has the highest priority, the glucosylation of high-purity RebA is thus preferred, as the presence of stevioside deteriorated the sensory properties of the RebA-G/Stev-G.

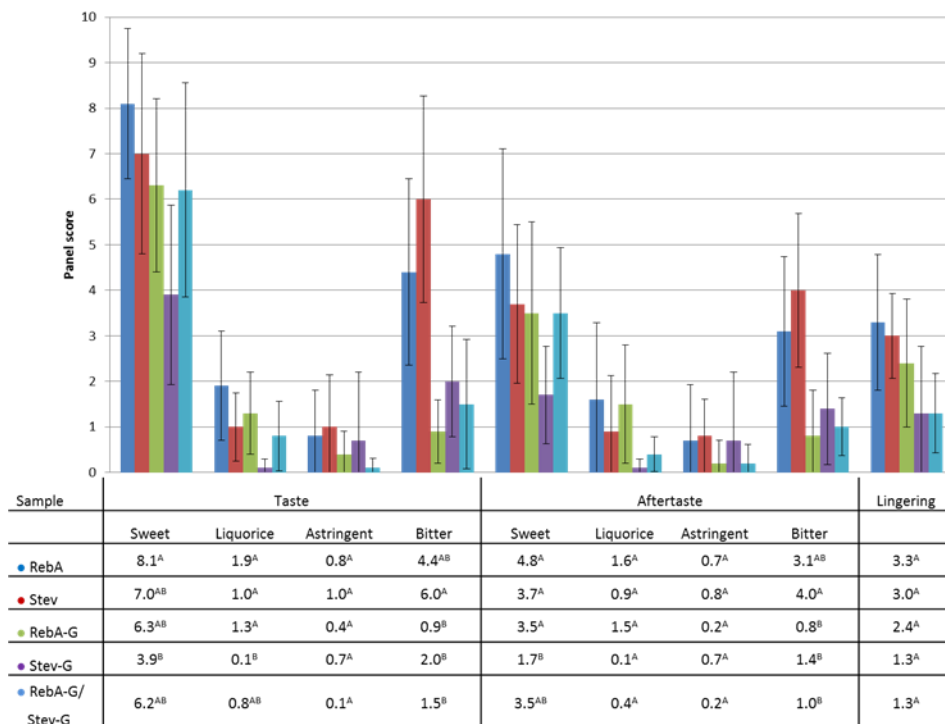


Figure 7. Sensory analysis of solutions containing 588 mg/L RebA, stevioside (Stev), RebA-G, Stev-G and a 50:50 RebA-G/Stev-G mixture. Sweetness, bitterness and off-flavors were rated on a scale of 10. Mean values are given in the table. ^{A,B}: different letters indicate significant differences ($p < 0.05$) between solutions following one-way ANOVA and post-hoc test.

3.5. Stability analysis of glycosylated stevia products

In order to be used in beverages as high-intensity sweetener, the glycosylated stevia products need to be stable during storage over prolonged periods of time. Commercial soft drinks such as cola and lemonade typically have a low pH in the range of 2.8-3.8²⁴¹. Several studies have indicated that the rate and extent of degradation of RebA and stevioside are dependent on pH, buffer type, buffer concentration and temperature²⁴¹⁻²⁴³. Degradation typically involves the hydrolysis of the glycosidic linkages of the steviol glycosides, deteriorating their flavor. In case of RebA-G, it is particularly important that the enzymatically introduced ($\alpha 1 \rightarrow 6$) linkage is stable so that the improved taste is maintained. The

stability of RebA and RebA-G was determined by conducting an accelerated shelf life study at 80 °C and pH 2.8 and 3.8 (50 mM citric acid and 50 mM phosphate), as shown in Figure 8.

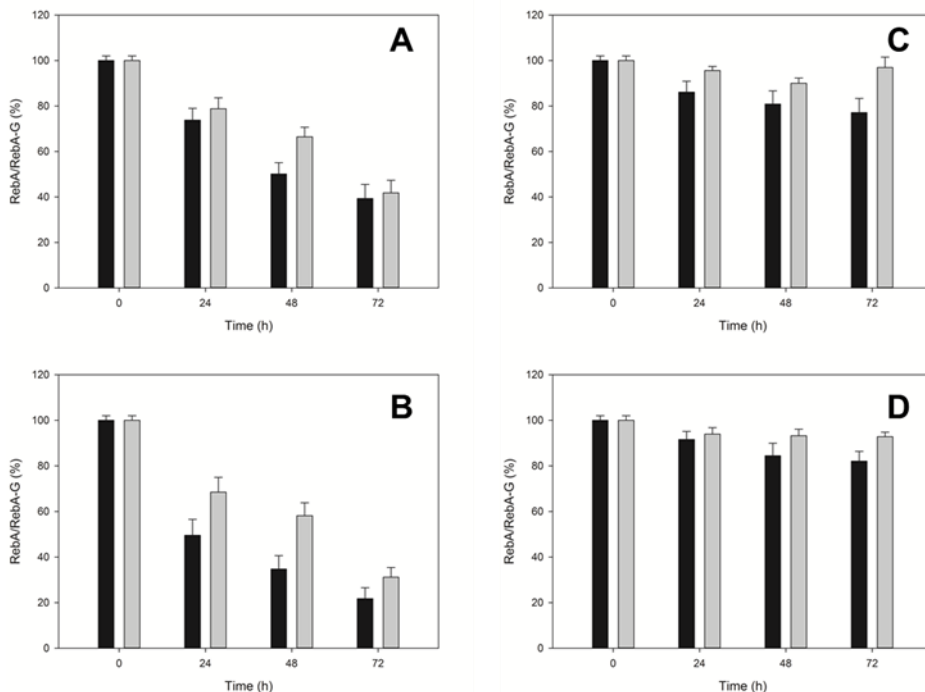


Figure 8. Stability of 500 mg/L RebA (*black*) and RebA-G (*grey*) in different acidic solutions. **A** 50 mM phosphate, pH 2.8; **B** 50 mM citric acid, pH 2.8; **C** 50 mM phosphate, pH 3.8; **D** 50 mM citric acid, pH 3.8.

RebA-G appears to be sufficiently stable to be applied in low pH soft drinks, it actually displayed a higher stability than RebA in all buffers tested. Buffer type and pH strongly influenced the degradation rate. In general, HPLC analysis revealed that incubations in citric acid buffer resulted in more degradation than in phosphate buffer. At pH 2.8 the half-life ($t_{1/2}$) of RebA-G in phosphate and citric acid buffer, was 63.9 and 52.0 h, respectively. In contrast, RebA-G was only slightly degraded at pH 3.8, even after 72 h ($t_{1/2}$ of 779.8 and 520.6 h, in phosphate and citric acid buffer, respectively). HPLC analysis suggested that RebA-G was degraded into RebA and subsequently into stevioside. Other degradation products could not be detected.

4. Conclusions

This chapter demonstrates the technical and economic feasibility of glucosylating steviol glycosides with the Gtf180- Δ N- Δ V-Q1140E enzyme. The strength of the technology lies in the high activity of this biocatalyst, suppressing the associated costs, as revealed by the cost analysis. Furthermore, selective adsorption of the glucosylated products onto macroporous resin offers a straightforward and efficient method for their purification. Based on the cost analysis, it was suggested to glucosylate mixtures of steviol glycosides rather than high-purity RebA or stevioside, as this results in a 30% cost reduction. From a taste quality perspective, the glucosylation of high-purity RebA is nevertheless preferred. Finally, the glucosylation reaction was successfully scaled up to 7.5 L scale, allowing the production of samples for food safety analysis and testing in several food products, such as chocolate, candy, etc. In future work demonstration of the complete process at pilot-plant scale will be an essential requirement to survive the so-called valley of death, which is faced by many novel technologies.

5. Supplementary information

5.1. Cost analysis: Assumptions and economic model

The base case used for the cost analysis is the glucosylation of high-purity RebA in batch mode at optimal reaction conditions (84 mM RebA, 282 mM sucrose, 5 U/mL Gtf180- Δ N- Δ V-Q1140E)⁷⁰.

General assumptions

- Plant is located in Western Europe.
- The facilities are part of a multi-purpose plant with shared utilities, services, offices, quality control, etc.
- Capital investment included equipment, instrumentation and piping needed for RebA-G production, excluding DSP.
- Scale: One bioreactor and one blending tank of 10 m³ with 75% working volume, shared for fermentation and biocatalysis.
- Costs are given in €.

Production is as follows:

- One optimal fermentation at 10 m³ yields enzyme to perform 8 enzymatic glucosylations at 10 m³. As a result, 1 week of fermentation is followed by 8 weeks of biocatalysis, defined as 1 production cycle.
- Equipment is used to perform 5 production cycles per year, yielding 34.5 metric tons of RebA-G.
- The volume consumption of stevia is expected to reach 8,507 metric tons per year by the end of 2020⁴⁴. The assumed production would consequently represent 0.4% of the total stevia market.

Raw materials

Table SI. Raw materials needed to run one fermentation batch at 10 m³.

Raw materials	Quantity (kg)	Price (€/kg)
Glucose	225	0.5
Tryptone	75	3.0
Yeast extract	37.5	4.0
NaCl	37.5	2.1
Ampicillin	0.75	38.0
IPTG	0.18	154.0
H ₂ O	7125	0.01
Total cost		694 €/batch

It was assumed that the adsorption resin was reused during one year of production (40 times) and that the eluent (70% isopropanol) was recovered after evaporation and consequently reused during one year of production.

Table SII. Raw materials needed to run one enzymatic glycosylation reaction, including DSP, at 10 m³.

Raw materials	Quantity (kg)	Price (€/kg)
Enzyme	0.8	2,306
Sucrose	723	0.7
RebA	609	80
CaCl ₂ ·2H ₂ O	1	122
H ₂ O	6200	0.01
Resin	9,400	46.7
Isopropanol	25,875	1.5
H ₂ O	14,110	0.01

Calculation of the capital investment

To calculate the total installed cost (TIC), the total purchase cost was multiplied by the Lang factor $K = 5^{244}$.

To calculate the capital investment cost per production cycle, the total investment cost, equal to TIC, was converted into an equivalent annual cost by multiplying TIC with the annuity factor k :

$$k = \frac{i}{1 - (1 + i)^{-t}}$$

with the interest rate $i = 0.07$ and the equipment lifetime $t = 15$ yrs.

As one production cycle consists of 1 fermentation batch and 8 enzymatic glucosylations, the equipment cost per production cycle was allocated as follows: 11% to the fermentation, 89% to the glucosylation.

Table SIII. Equipment related costs.

Equipment	Specifications	Price (€)
Blending tank	10 m ³	51,500
Pump, gear	5 m ³ /h	33,000
Heat exchanger	10 MW	50,000
Air compressor	10 m ³ /min	54,000
Fermenter	10 m ³	175,000
Total purchase cost		€363,500
Total installed cost (TIC)		€1,817,500
Annuity ($k = 0.14$)		€199,500/year
Maintenance		€26,000/year
Other		€49,000/year
Annual cost		€275,000/year
Cost per production cycle		€55,000
Cost per fermentation batch		€6110
Cost per enzymatic glucosylation		€6110

Utilities

The price of electricity was fixed at €0.1/kWh.

Table SIV. Utilities needed to run one fermentation batch at 10 m³.

Utilities	Specifications	kWh
Sterilization (20-140 °C)	4,187 J/kg.K	1047
Aeration (1 vvm)	5 kW/m ³	400
Agitation (500 rpm)	5 kW/m ³	400
Waste treatment	€2/m ³	
Total utilities cost		€207/batch

Table SV. Utilities needed to run one enzymatic glucosylation at 10 m³.

Utilities	Specifications	kWh
Agitation (185 rpm)	1.9 kW/m ³	57
Heating (37 °C)	4,187 J/kg.K	148
Waste treatment	€2/m ³	
Total utilities cost		€26/batch

At kg scale, the last step of RebA-G production consisted of freeze-drying to remove the residual water. As freeze-drying is technically and economically not feasible at ton scale, spray drying was considered as last purification step for the cost analysis. Firstly, the mixture obtained after elution (2% solids) was evaporated until a solid content of 50% by means of a mechanical vapor recompression (MVR). Energy consumption of MVR and spray drying were based on Fox et al.²⁴⁵.

Table SVI. Utilities needed to perform DSP of RebA-G.

Utilities	kWh
Evaporation	476
Spray drying	1917
Total utilities cost	€249/batch

Labor

Table SVII. Labor cost.

Utilities	Man-hours
Fermentation	96
Biocatalysis + DSP	120

5.2. Figures

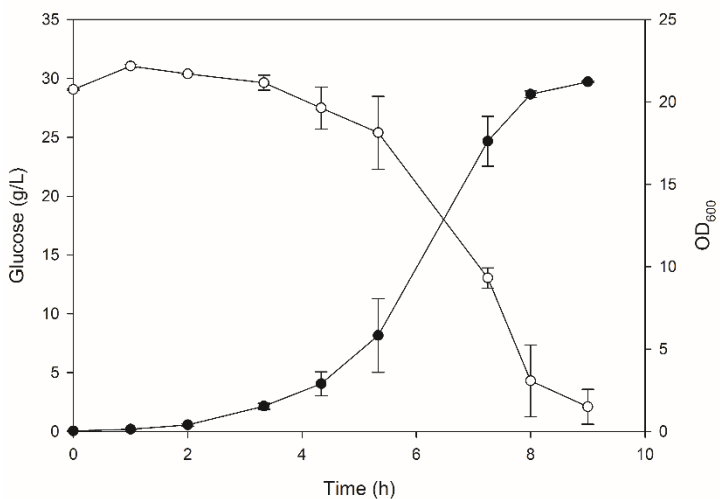


Figure S1. Biocatalyst production: growth of the recombinant *Escherichia coli* BL21 (DE3) strain, expressing Gtf180- Δ N- Δ V-Q1140E, in LB medium supplemented with 30 g/L glucose. Induction with IPTG after 4 h of incubation. ● OD₆₀₀, ○ glucose.

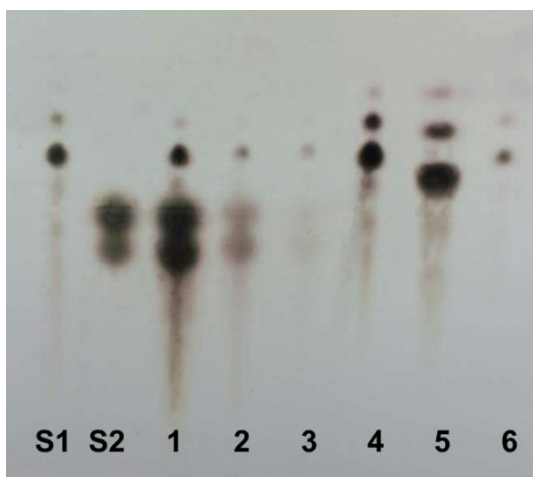


Figure S2. Continuous adsorption of RebA glycosylation reaction mixture (84 mM RebA, 282 mM sucrose, 5 U/mL enzyme) onto Lewatit VP OC 1064 MD PH resin at a flow rate of 4.5 BV/h. **S1** RebA-G; **S2** glucose, fructose and sucrose; **1-3** wash fractions; **4-6** elution fractions.

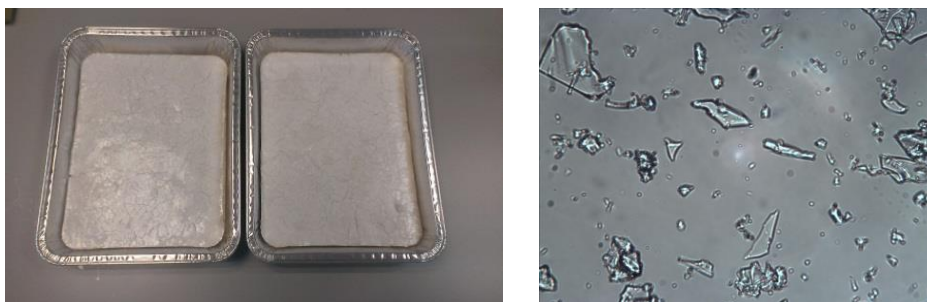


Figure S3. Glucosylated RebA (RebA-G), obtained after selective adsorption on macroporous resin, evaporation *in vacuo* and ultimately freeze-drying.

Chapter 7

Enzymatic transglucosylation of neohesperidin dihydrochalcone: glucansucrase Gtf180- Δ N-Q1140E as biocatalyst for the glycodiversification of sweet glycosides

Tim Devlamynck^{1,2}, Gerrit Gerwig³, Wim Soetaert¹, Lubbert Dijkhuizen²
University of Ghent¹, University of Groningen², University of Utrecht³

Abstract

Increasing rates of obesity and diabetes type 2 lead to a rapidly growing number of health-conscious consumers, fueling the demand for low-calorie food products. Natural high-intensity sweeteners (HIS), of which steviol glycosides [e.g. rebaudioside A (RebA)] extracted from the leaves of *Stevia rebaudiana* are best known, have a competitive edge over synthetic HIS such as aspartame and acesulfame K, suffering from a bad reputation among consumers. Over the years, several other natural compounds have been proposed as possible products for the HIS market of the future. An interesting target is the flavor enhancer neohesperidin dihydrochalcone (NHDC). The main disadvantages of NHDC are its low water solubility at room temperature, resulting in a relatively low bioavailability, and an unpleasant lingering aftertaste. This chapter reports the α -glucosylation of NHDC with glucansucrase Gtf180- Δ N-Q1140E from *Lactobacillus reuteri* 180, using sucrose as donor substrate, in an attempt to improve its sensory and physicochemical properties. Structure elucidation of the novel glucosylated products revealed that NHDC was glucosylated at the β -D-glucosyl unit and the α -L-rhamnosyl unit, through an (α 1 \rightarrow 6) and (α 1 \rightarrow 4) linkage, respectively. The obtained conversion degree of 65% offers a good starting point for future improvements by reaction engineering. The α -glucosylated NHDC products displayed much higher water solubilities than NHDC and retained strong anti-oxidant capacities, enabling their use as nutraceuticals. Sensory analysis by a trained panel revealed limited bitterness suppressing effects of NHDC and its α -glucosylated products on RebA, in contradiction to previous reports.

1. Introduction

Previously we demonstrated the potential of the glucansucrase enzyme Gtf180- Δ N and in particular its Q1140E mutant⁹⁷ to trans- α -glucosylate rebaudioside A (RebA) and stevioside as a means to improve their sensory properties⁶⁸⁻⁷⁰. In addition to these steviol glycosides from *Stevia rebaudiana*, also neohesperidin dihydrochalcone (NHDC, Figure 1) has attracted considerable attention from the food industry, due to its intensive sweetness. Later on, NHDC's remarkable properties as flavor enhancer, as such contributing to the mouth feel of several food products and/or suppressing the bitterness displayed by other compounds, expanded the interest in this versatile molecule²⁴⁶⁻²⁴⁸.

First discovered in 1963 by Horowitz and Gentili²⁴⁶, NHDC is industrially produced by hydrogenation of neohesperidin (hesperetin 7-O-neohesperidoside), a flavanone glycoside isolated from citrus fruits such as mandarin, orange and grapefruit²⁴⁹. Recently, NHDC was found to naturally occur as a minor constituent in the plant *Oxytropis myriophylla*²⁵⁰ and in the bark of the tree *Eysenhardtia polystachya*²⁵¹. Classified as a semisynthetic sweetener, NHDC is roughly 340 times sweeter than sucrose and was approved as sweetener by the European Union in 1994. Similarly to other highly sweet glycosides such as glycyrrhizin (*Glycyrrhiza glabra*, liquorice) and most steviol glycosides, NHDC displays a lingering liquorice aftertaste limiting its application as the sole sweetener in foods and beverages²⁵². NHDC is best applied in sweetener blends: it displays strong synergistic effects when combined with other sweeteners such as saccharin, aspartame, and RebA²⁵³. The total sweetness intensity of such mixtures is greater than the theoretical sum of the intensities of the individual components²⁵⁴. The use of NHDC thus provides a substantial economic benefit, as much less of the other sweetener needs to be supplied.

In addition, NHDC finds many applications as a flavor enhancer in a wide range of food –and pharmaceutical products, as such identified by the E number E959²⁵⁵⁻²⁵⁷. A typical example concerns the enhancement of the creaminess of

dairy products such as yogurt and ice cream. Moreover, NHDC is particularly effective in masking the bitterness displayed by several other compounds, such as limonin and naringin from citrus fruits. A patent application from 2012 even claims that the bitterness and astringency exhibited by RebA and monk fruit extract are very effectively suppressed by the addition of 10 ppm NHDC²⁵⁸. Also the pharmaceutical industry makes good use of this remarkable NHDC characteristic to reduce the bitterness of several drugs in tablet form, such as the antipyretic paracetamol²⁵⁹. More recently, several studies have attributed strong antioxidant²⁶⁰⁻²⁶², hepatoprotective (preventing damage to the liver)²⁶³ and prebiotic²⁶⁴ properties to NHDC. In the context of all these possible applications, the main disadvantage of NHDC is its low water solubility at room temperature (0.4 g/L), resulting in a relatively low bioavailability and limiting its application as sweetener in water based dispersions, such as syrups and jams²⁶⁵.

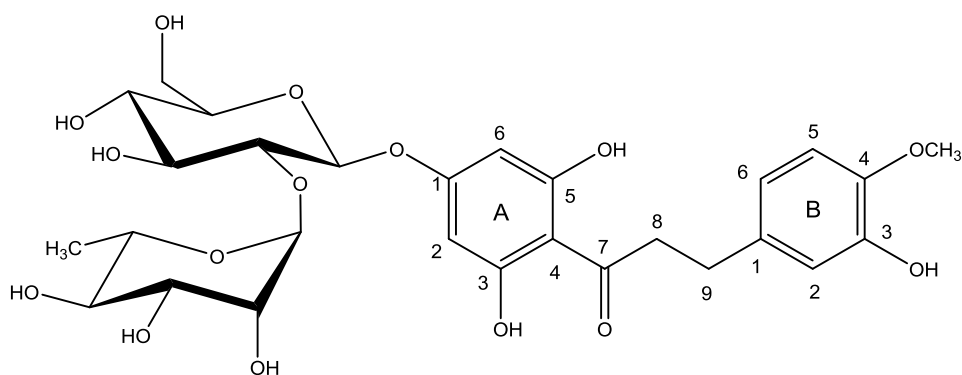


Figure 1. Chemical structure of neohesperidin dihydrochalcone (NHDC) with carbon atom numbering as applied in the structure elucidation. The numbering used is arbitrary (similar to Caccia et al. 1998²⁶⁶) as there is no consensus in literature.

NHDC contains 9 hydroxy groups (Figure 1): 3 of rhamnose, 3 of glucose and 3 of the aglycon (2 on the A-ring and 1 on the B-ring). In theory, all these hydroxy groups can be enzymatically glycosylated, depending on the biocatalyst and its substrate specificity and regioselectivity. To our knowledge, NHDC glycosylation has been reported only once: by applying maltogenic amylase from *Bacillus stearothermophilus*, NHDC was maltosylated at the β -D-glucosyl unit through an

(α 1 \rightarrow 6) linkage, resulting in a 700-fold increase of solubility and a 7-fold decrease of sweetness²⁶⁷. Previously, we reported the trans- α -glucosylation of a wide variety of compounds, ranging from catechol to more complex molecules such as steviol glycosides, with Gtf180- Δ N from *Lactobacillus reuteri* 180 and derived mutants, highlighting the broad acceptor substrate specificity of this enzyme^{68-70,110}. This chapter reports the transglucosylation of NHDC with Gtf180- Δ N-Q1140E, yielding three new-to-nature α -glucosylated NHDC derivatives. A detailed structural analysis is provided, a necessity for the evaluation of the quality and safety of novel food products. In addition, the sensory properties, anti-oxidant capacities and solubilities of the α -glucosylated NHDC products were compared to NHDC.

2. Materials and methods

2.1. Production and purification of glucosylated NHDC

The production of glucosylated NHDC (Ingrizo) was performed at 50 mL scale in a shake flask, in duplicate. Samples were analyzed by HPLC. The temperature and agitation rate were set at 37 °C and 150 rpm, respectively. Gtf180- Δ N-Q1140E⁹⁷ (5 U/mL), produced as described previously⁷⁰, was incubated in a 20% ethanol solution containing 20 g/L NHDC and 125 mM sucrose supplemented with 25 mM sodium acetate (pH 4.7) and 1 mM CaCl₂. One unit (U) of enzyme activity corresponds to the conversion of 1 μ mole sucrose (used for hydrolysis and transglucosylation) in a solution of 100 mM sucrose, 25 mM sodium acetate (pH 4.7) and 1 mM CaCl₂ at 37 °C.

After completion of the reaction (i.e. when a steady state was reached), glucosylated NHDC was isolated from the reaction mixture by adsorption onto Lewatit VP OC 1064 MD PH macroporous resin. A washing step with water removed the residual sugars and α -glucan oligosaccharides. Desorption of glucosylated NHDC was achieved with 70% isopropanol. The resulting mixture was evaporated *in vacuo* and subsequently applied onto a Reveleris X2 flash

chromatography system, applying a Reveleris amino cartridge (40 μm) with water (solvent A) and acetonitrile (solvent B) as the mobile phase. Following gradient elution was used: 99% solvent B (0-2 min), 99-35% solvent B (2-20 min), 35% solvent B (20-25 min). The collected fractions were evaporated *in vacuo* and subsequently freeze dried to remove the residual water.

2.2. MALDI-TOF-mass spectrometry

Matrix-assisted laser desorption ionization time-of-flight mass spectrometry (MALDI-TOF-MS) was performed on an AximaTM mass spectrometer (Shimadzu Kratos Inc., Manchester, UK), equipped with a Nitrogen laser (337 nm, 3 ns pulse width). Positive-ion mode spectra were recorded using the reflector mode at a resolution of 5000 FWHM and delayed extraction (450 ns). Accelerating voltage was 19 kV with a grid voltage of 75.2%. The mirror voltage ratio was 1.12 and the acquisition mass range was 200-2000 Da. Samples were prepared by mixing on the target 1 μL sample solutions with 1 μL aqueous 10% 2,5-dihydroxybenzoic acid in 40% acetonitrile as matrix solution, containing 0.1% TFA.

2.3. Methylation analysis

Samples were permethylated using CH_3I and solid NaOH in DMSO, as described by Ciucanu and Kerek (1984)²²⁷, then hydrolyzed with 2 M TFA (2 h, 120 °C) to give the mixture of partially methylated monosaccharides. After evaporation to dryness and redissolving in H_2O , reduction was performed with NaBD_4 (2 h, room temperature). After neutralization with 4 M acetic acid and removal of boric acid by co-evaporation with methanol, the samples were acetylated with acetic anhydride/pyridine (1:1, 30 min, 120 °C). After evaporation to dryness and redissolving in dichloromethane, the mixtures of partially methylated alditol acetates (PMAAs) were analyzed by gas-liquid chromatography – electron ionization – mass spectrometry (GLC-EI-MS) on an EC-1 column (30 m x 0.25 mm, Alltech), using a gas chromatograph mass spectrometer (GCMS-QP2010 Plus from Shimadzu Kratos Inc.) and a temperature gradient (140-250 °C at 8 °C/min)²²⁸.

2.4. NMR spectroscopy

Resolution-enhanced 1D/2D 500-MHz $^1\text{H}/^{13}\text{C}$ NMR spectra were recorded in D_2O on a Bruker DRX-500 spectrometer (Bijvoet Center, Department of NMR Spectroscopy, Utrecht University) at a probe temperature of 310 K. Data acquisition was done with Bruker Topspin 2.1. Before analysis, samples were exchanged twice in D_2O (99.9 atom% D, Cambridge Isotope Laboratories, Inc., Andover, MA) with intermediate lyophilization, and then dissolved in 0.6 mL D_2O . Suppression of the deuterated water signal (HOD) was achieved by applying a WEFT (water eliminated Fourier transform) pulse sequence for 1D NMR experiments and by a selective pre-saturation pulse of 1 s during the relaxation delay in 2D experiments. The 2D TOCSY spectra were recorded using an MLEV-17 (composite pulse devised by Levitt et al., 1982) mixing sequence with spin-lock times of 20, 50, 100 and 200 ms. The 2D ^1H - ^1H ROESY spectra were recorded using standard Bruker XWINNMR software with a mixing time of 200 ms. The carrier frequency was set at the downfield edge of the spectrum in order to minimize TOCSY transfer during spin-locking. Natural abundance 2D ^{13}C - ^1H HSQC experiments (^1H frequency 500.0821 MHz, ^{13}C frequency 125.7552 MHz) were recorded without decoupling during acquisition of the ^1H FID. The NMR data were processed using the MestReNova 9 program (Mestrelab Research SL, Santiago de Compostella, Spain). Chemical shifts (δ) are expressed in ppm by reference to internal acetone (δH 2.225 for ^1H and δC 31.07 for ^{13}C).

2.5. Solubility measurements

The solubilities of NHDC and α -glucosylated NHDC products were determined in 250 μL of ultrapure water, incubated in a thermoblock at 25 $^\circ\text{C}$. Products were added until clear precipitation was noticeable, after which the samples were vortexed multiple times and allowed to equilibrate for 24 h. The supernatants were diluted in ethanol and subsequently subjected to HPLC analysis. Calibration was accomplished using the appropriate standard curves, obtained after purification of the glycosylated products as described in 2.1. All analyses were performed in duplicate.

2.6. Determination of 2,2-diphenyl-1-picrylhydrazyl (DPPH) radical-scavenging activity

The 2,2-diphenyl-1-picrylhydrazyl (DPPH) assay is widely used to determine the anti-oxidant potential of various compounds. DPPH possesses an unpaired valence electron susceptible to scavenging by molecules displaying anti-oxidant activity, a chemical reaction which can be followed spectrophotometrically²⁶⁸.

The DPPH radical-scavenging activity was evaluated by adding 100 μL of methanol, containing various concentrations of NHDC and α -glucosylated NHDC products (10-1000 μM), to 200 μL of methanol supplemented with 200 μM DPPH. The samples were incubated at room temperature during 15 min in complete darkness, after which their absorbance was measured at 517 nm. The (glucosylated) NHDC concentration required to reduce the absorbance by 50% (EC_{50}) was calculated by linear regression (of the linear part) of the absorption curves. Analyses were performed in duplicate. Butylated hydroxytoluene (BHT) was included in the experiments to serve as comparison.

2.7. Sensory analysis

The sensory analysis was performed in individual tasting booths at the UGent Sensolab (Belgium) by a trained panel (9 persons). In short, taste (sweetness, liquorice, astringency and bitterness) was evaluated by swirling the sample in the mouth for 5 sec after which the sample was expectorated. Aftertaste was evaluated 10 sec after swallowing the solution. Lingering based on the maximum taste intensity was rated 1 min later. Sucrose reference solutions (5%, 7.5% and 10% sucrose, scoring 5, 7.5 and 10, respectively) were provided. Water (Spa Reine) and plain crackers were used as palate cleansers between sampling. Following sweetened solutions were tasted: 588 mg/L rebaudioside A (RebA, Tereos PureCircle Solutions), 588 mg/L RebA + 10 ppm NHDC, 588 mg/L RebA + 10 ppm monoglucosylated NHDC (NHDC-G1), and 588 mg/L RebA + 10 ppm diglucosylated NHDC (NHDC-G2). All samples were evaluated in duplicate.

Statistical analyses were performed with SPSS 23 (SPSS Inc., Chicago, USA). All tests were done at a significance level of 0.05. One-Way ANOVA was used to investigate any significant difference between the solutions. Testing for equal variances was executed with the Modified Levene Test. When conditions for equal variance were fulfilled, the Tukey test was used to determine differences between samples²¹⁰. In case variances were not equal, a Games-Howell post-hoc test was performed²¹¹.

3. Results and discussion

3.1. Production of glucosylated NHDC

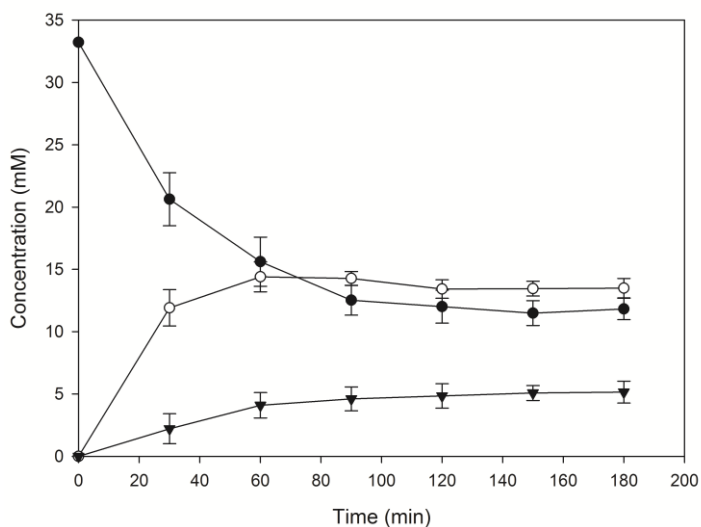


Figure 2. HPLC analysis of the synthesis of α -D-glucosides of NHDC by Gtf180- Δ N-Q1140E in time (33 mM NHDC; 125 mM sucrose; 20% v/v EtOH; 5 U/mL enzyme). ● NHDC, ○ NHDC-G1, ▼ NHDC-G2. Sucrose was depleted after 180 min.

As NHDC is only sparingly soluble in water (0.4 g/L), a cosolvent had to be supplied to the glycosylation reaction mixture in order to avoid suboptimal yields and conversion degrees. Indeed, as demonstrated in chapter 3, higher concentrations of acceptor substrate generally result in higher conversion degrees. Gtf180- Δ N-Q1140E retained its activity in solutions with up to 20% v/v

EtOH (Figure S1). The reaction mixture was consequently composed of 20% v/v EtOH, containing 33 mM NHDC (maximal amount that could be dissolved), and 125 mM sucrose, enough donor substrate to drive the reaction to completion. The incubation of 5 U/mL Gtf180- Δ N-Q1140E in this reaction mixture resulted in a NHDC conversion degree of 64.4% (Figure 2). HPLC analysis also revealed that at least two major products were synthesized, 62% NHDC-G1 and 38% NHDC-G2.

3.2. Structural characterization of glucosylated NHDC products

NHDC was enzymatically transglycosylated by Gtf180- Δ N-Q1140E, at first sight resulting in the formation of 2 major products (Figure 2). However, purifying the reaction mixture with flash chromatography resulted in the isolation of three major glucosylated products (P1, P2, P3), of which P1 and P2 were formed in equal amounts. MALDI-TOF mass spectrometric analysis revealed the same quasi-molecular mass peaks m/z 796.5 $[M+Na]^+$ and m/z 812.5 $[M+K]^+$ for P1 and P2, indicating NHDC+1Glc (MW = 774 Da), as compared to NHDC (MW = 612 Da) showing m/z 634.5 $[M+Na]^+$ and m/z 650.6 $[M+K]^+$. P3 showed m/z 958.6 $[M+Na]^+$ and m/z 974.6 $[M+K]^+$, indicating NHDC+2Glc (MW = 936 Da). In other words, NHDC-G1 consists of products P1 and P2, whereas NHDC-G2 was equal to P3.

In order to obtain information about the linkage pattern of the carbohydrate moieties of the products, methylation analysis was performed (Table SI). For NHDC, the expected terminal Rhamnose and 2-substituted Glucose in molar ratio 1:1 was found. Additionally, in P1 and P2, the presence of 4-substituted Rhamnose and 2,6-disubstituted Glucose was observed, respectively. P3 showed both of the latter residues. The minor amounts of \rightarrow 6)Glc p (1 \rightarrow and \rightarrow 2)Glc p (1 \rightarrow found by methylation analysis indicate that the products were not 100% pure.

Different NMR spectroscopic techniques (1 H- and 13 C-NMR, TOCSY, ROESY and HSQC) were used to investigate the structures of the transglucosylated

NHDC derivatives. Firstly, NMR spectroscopy was performed with the acceptor substrate NHDC in D_2O to obtain reference data (Figure 3). In spite of the reported low solubility of NHDC in water, D_2O samples were easily obtained. It has to be noted that the 1H chemical shifts are strongly affected by temperature and sample concentrations (probably due to self-association of NHDC in D_2O).

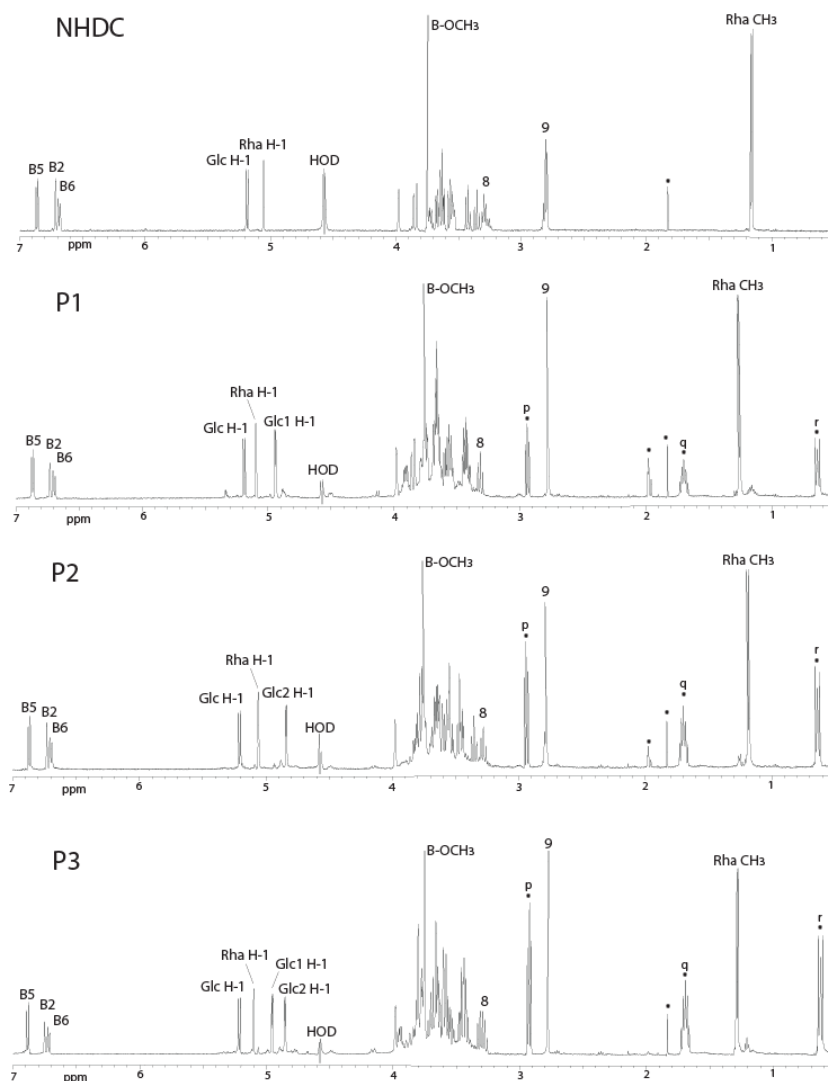


Figure 3. 1D 500-MHz 1H NMR spectra of NHDC, P1, P2 and P3, recorded in D_2O at 310 K. * resonance signals stemming from contamination(s).

The 500-MHz ^1H NMR spectrum (Figure 3) of NHDC showed the signals of the aromatic protons at δ 6.87 [d, $J=8.2$ Hz, B5], at δ 6.72 [s, $J=2.0$ Hz, B2], and at δ 6.70 [d, $J=8.2$ Hz, B6], together with two methylene groups [δ 3.29 (C8) and δ 2.81 (C9)] and a methoxy group [δ 3.75 (B-OCH₃)], typical for the dihydrochalcone skeleton²⁶⁶. The aromatic proton signals of A2 and A6 (see NHDC structure, Figure 1), initially found at δ 5.99, had disappeared due to exchange with deuterium from the solvent (D₂O) after prolonged time at 310 K²⁶⁹. Also, the C8 proton, in α position to the carbonyl group (C7), is susceptible to deuterium exchange via the keto-enol route, consequently, ^{13}C correlations in HSQC experiments will not be observed. Concerning the carbohydrate moiety, the ^1H NMR spectrum exhibited signals due to one β -D-glucopyranosyl unit [δ 5.185 (d, $J=7.6$ Hz, Glc H-1)] and one α -L-rhamnopyranosyl unit [δ 5.059 (br s, $J < 2$ Hz, Rha H-1) and δ 1.168 (d, $J=6.1$ Hz, Rha CH₃)]. The assignment of the signals (Table SII) was made through 2D NMR TOCSY experiments, using different mixing times, and in combination with ROESY and HSQC (Figures S2 and S3). Indeed, the obtained NMR data of NHDC (Table SII) were in agreement with She et al. (2011)²⁵⁰ and Caccia et al. (1998)²⁶⁶.

The 500-MHz ^1H NMR spectrum (Figure 3) of fractions P1 and P2 showed an extra α -anomeric proton at δ 4.936 ($J=3.7$ Hz) and at δ 4.845 ($J=3.7$ Hz), respectively, stemming from two differently attached glucose units, denoted as Glc1 and Glc2. Compared to NHDC, the NMR spectrum of fraction P3 showed signals stemming from both Glc1 and Glc2 (δ 4.955: $J=3.7$ Hz and δ 4.855: $J=3.7$ Hz). The resonance signals indicated with * in Figure 3 (e.g. p, q and r, having mutual TOCSY connections) are stemming from contamination(s). The total assignment of NMR signals (Table SII) was made through 2D NMR TOCSY, HSQC and ROESY experiments in a similar way as for NHDC (Figures S4-9), revealing that Glc1 and Glc2 were attached to NHDC at the α -L-rhamnopyranosyl unit through an ($\alpha 1 \rightarrow 4$) linkage and at the β -D-glucopyranosyl unit through an ($\alpha 1 \rightarrow 6$) linkage, respectively (Figure 4). In other words, P3 contained both the newly formed ($\alpha 1 \rightarrow 4$) linkage present in P1 and the ($\alpha 1 \rightarrow 6$) linkage introduced in P2. The results are in agreement with the methylation analyses (Table ...). To

our knowledge, these α -glucosylated NHDC derivatives have not been described before and can thus be considered new-to-nature.

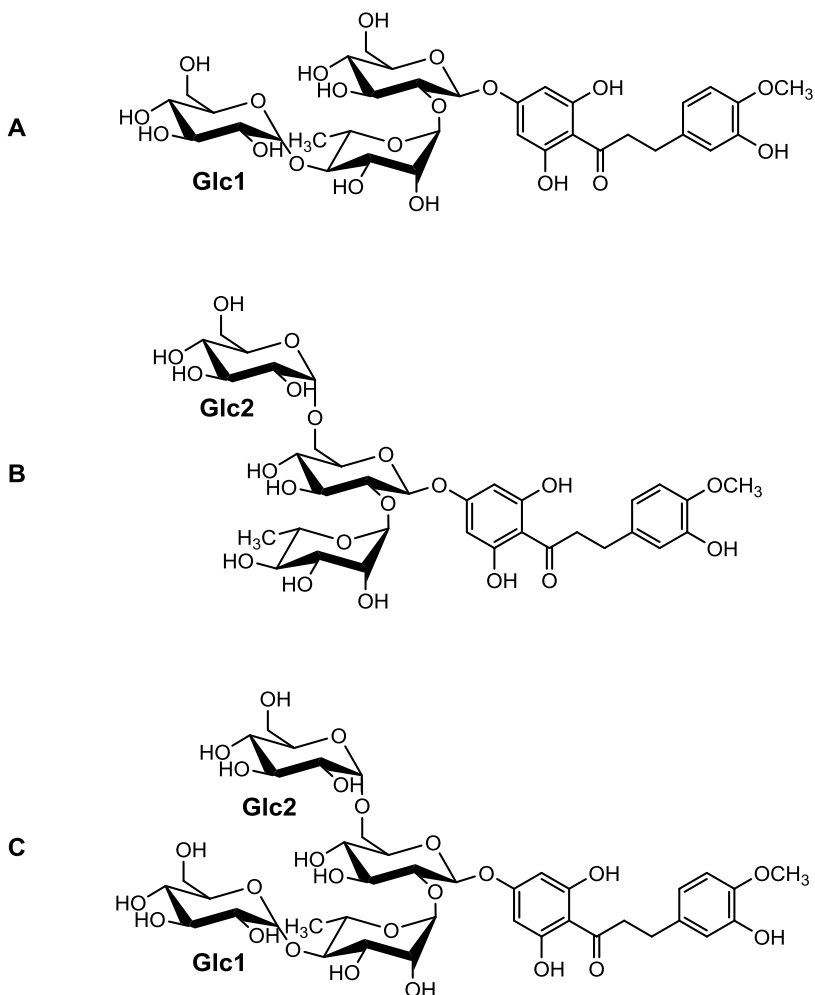


Figure 4. Chemical structures of α -glucosylated NHDC products: **A** NHDC-P1, **B** NHDC-P2 and **C** NHDC-P3.

3.3. Sensory analysis of glucosylated NHDC products

NHDC is not only a high-intensity sweetener (340 times sweeter than sucrose), it is reported to suppress the bitterness displayed by other sweeteners such as RebA. A sensory analysis of aqueous solutions sweetened with RebA and 10

ppm NHDC, NHDC-G1, and NHDC-G2 was performed by a trained panel, evaluating 9 different taste attributes (Figure 5).

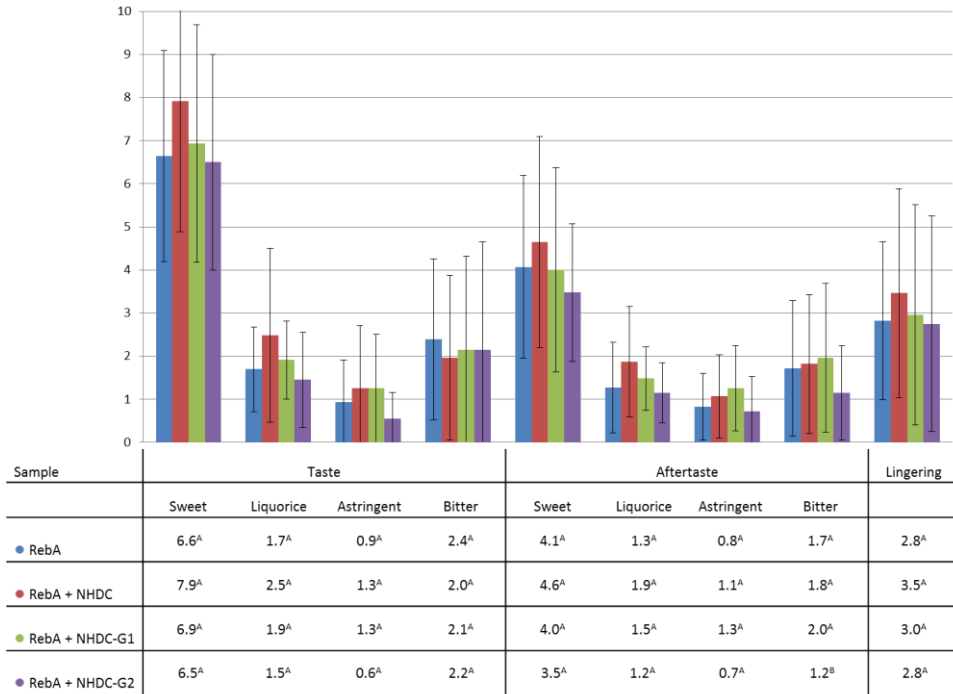


Figure 5. Sensory analysis of RebA, RebA + 10 ppm NHDC, RebA + 10 ppm NHDC-G1 and RebA + 10 ppm NHDC-G2. Sweetness, bitterness and off-flavors were rated on a scale of 15. Mean values are given in the table. ^{A,B}: different letters indicate significant differences ($p < 0.05$) between solutions following one-way ANOVA and post-hoc test.

In general, the trained panel perceived only slight differences between the various solutions. The claimed bitterness suppressing effect of NHDC was detected by the trained panel, however, the difference with the NHDC-less RebA solution was not significant. Only the addition of 10 ppm NHDC-G2 resulted in a significant reduction of RebA's bitter aftertaste. A possible explanation is the addition of too little NHDC, although Sun et al.²⁵⁸ recommended a similar dose of 10 ppm. Nevertheless, the solution containing RebA + 10 ppm NHDC was perceived as sweeter than the NHDC-less RebA solution, confirming NHDC's synergistic effect. Slight increases in astringency, liquorice taste, and lingering

were also observed, typical consequences of adding NHDC. Interestingly, the addition of NHDC-G1 and NHDC-G2 instead of NHDC reduced these undesired side-effects. However, as the trained panel was not able to perceive significant differences between the various solutions, investigation of the appropriate dose is required to obtain conclusive results. The limited availability of the trained panel prevented further experimenting. In any case, it appears that α -glucosylation of RebA by Gtf180- Δ N-Q1140E⁶⁸⁻⁷⁰ is a much more effective strategy to decrease its bitterness than the addition of (glucosylated) NHDC. In this context, analysis of the sensory properties of a solution containing (glucosylated) NHDC and glucosylated RebA (RebA-G) is also an interesting option.

3.4. Solubility of glucosylated NHDC products

The low solubility of NHDC prevents possible applications as nutraceutical, to exploit its strong anti-oxidant properties. Determination of the solubilities in water of NHDC and its α -glucosylated products revealed an impressive 800-fold increase of solubility for NHDC-G1, whereas NHDC-G2 was even more soluble (Table I). Previously, maltosylation of NHDC at the β -D-glucosyl unit, introduced through an (α 1 \rightarrow 6) linkage, resulted in a 700-fold increase of solubility²⁶⁷. An alternative approach consisted of the cosolubilization of NHDC with sodium saccharin, resulting in a 200-fold increase of solubility, significantly lower than the improvement obtained after glycosylation²⁶⁵.

3.5. Anti-oxidant properties of glucosylated NHDC products

In general, glycosylation of anti-oxidants increases their solubility in water, however, the antioxidant capacity typically decreases¹³⁹. The ability of NHDC and α -glucosylated NHDC products to scavenge DPPH was consequently evaluated (Table I). Although glucosylating NHDC clearly reduced the scavenging activity (EC_{50}), NHDC-G1 and NHDC-G2 still showed excellent anti-oxidant capacities, displaying EC_{50} 's similar to the established anti-oxidant butylated hydroxytoluene (BHT) which possessed an EC_{50} of 35.2 μ M (determined experimentally).

Considering the substantially improved water solubility of α -glucosylated NHDC (NHDC-G, composed of NHDC-G1 and NHDC-G2) compared to NHDC, NHDC-G can be considered a more promising and useful anti-oxidant.

Table I. Solubility in water and DPPH radical-scavenging activity (EC_{50}) of NHDC and α -glucosylated NHDC products. EC_{50} is the (glucosylated) NHDC concentration required to reduce the absorbance of a solution with 200 μ M DPPH at 517 nm by 50%.

Compound	Solubility (mM)	EC_{50} (μ M)
NHDC	0.6 \pm 0.1	27.3 \pm 4.0
NHDC-G1	490.9 \pm 45.2	34.3 \pm 1.7
NHDC-G2	> 600.0	48.7 \pm 1.5

4. Conclusions

NHDC finds many applications as flavor enhancer (E959) in the food- and pharmaceutical industry due to its ability to suppress bitterness and astringency, for example in the antipyretic paracetamol²⁵⁵⁻²⁵⁹. The strong anti-oxidant capacity displayed by NHDC has further increased the interest in this versatile molecule²⁶⁰⁻²⁶². NHDC's main drawback is its low solubility in water, which reduces its bioavailability but also its applicability as a high-intensity sweetener²⁶⁵. Gtf180- Δ N-Q1140E catalyzed glycosylation of NHDC, using sucrose as donor substrate, yielded three new-to-nature α -glucosylated NHDC products displaying improved solubilities and retained anti-oxidant capacities. Sensory analysis of the flavor enhancing effects of (α -glucosylated) NHDC on RebA by a trained panel revealed a slight decrease of bitterness and an increased sweetness. In future work different concentrations of (α -glucosylated) NHDC and RebA will be evaluated. This may provide valuable information about the appropriate doses that should be applied to obtain the optimal bitterness suppressing effect. Although the obtained conversion degree of roughly 65% was not of the same order as for RebA and stevioside glycosylation (95%)⁶⁸⁻⁷⁰, it forms a good starting point for a profound optimization of the reaction conditions. Additionally, the screening of the available Gtf180- Δ N mutant library⁹⁹ may reveal variants with improved NHDC glycosylation potential.

5. Supplementary information

Table SI. Linkage analysis of the glycosyl moieties in NHDC and in α -glucosylated NHDC products.

PMAA	R_t^a	Structural feature	Peak area (%) ^b			
			NHDC	P1	P2	P3
1,5-di-O-acetyl-2,3,4-tri-O-methyl-5-CH ₃ pentitol	0.76	Rhap(1→	49	tr	28	tr
1,4,5-tri-O-acetyl-2,3-di-O-methyl-5-CH ₃ pentitol	0.93	→4)Rhap(1→	-	25	tr	21
1,5-di-O-acetyl-2,3,4,6-tetra-O-methylhexitol	1.00	Glc(1→	-	36	33	52
1,2,5-tri-O-acetyl-3,4,6-tri-O-methylhexitol	1.16	→2)Glc(1→	51	32	4	3
1,5,6-tri-O-acetyl-2,3,4-tri-O-methylhexitol	1.22	→6)Glc(1→	-	4	3	2
1,2,5,6-tetra-O-acetyl-3,4-di-O-methylhexitol	1.39	→2,6)Glc(1→	-	3	32	22

^a R_t , retention time relative to 1,5-di-O-acetyl-2,3,4,6-tetra-O-methylglucitol (1.00) on GLC.

^b average values (no molar response/correction factors used).

Table SII. ^1H and ^{13}C chemical shift values (δ , ppm)^a of NHDC and glycosylated derivatives P1, P2 and P3 in D_2O at 310 K. Substituted carbon positions are indicated in grey.

	NHDC		P1		P2		P3	
	δ ^1H	δ ^{13}C	δ ^1H	δ ^{13}C	δ ^1H	δ ^{13}C	δ ^1H	δ ^{13}C
B2	6.72	115.3	6.73	115.5	6.74	115.6	6.75	115.5
B5	6.87	112.7	6.87	112.7	6.88	112.9	6.88	112.8
B6	6.70	119.6	6.70	120.2	6.71	120.5	6.72	120.1
B-OCH ₃	3.75	55.9	3.76	55.9	3.75	56.2	3.76	56.0
8	3.29	42.2	3.30	41.8	3.30	41.9	3.28	42.0
9	2.81	29.8	2.78	30.0	2.79	30.1	2.79	30.0
Glc $\beta\text{H-1}$	5.185	97.0	5.184	97.0	5.215	97.0	5.215	97.0
H-2	3.58	78.7	3.58	78.6	3.58	79.0	3.58	78.4
H-3	3.64	75.7	3.65	76.0	3.65	76.0	3.67	76.2
H-4	3.43	68.7	3.43	68.9	3.47	71.9	3.47	71.6
H-5	3.57	75.6	3.56	75.8	3.76	74.7	3.76	74.2
H-6a	3.85	60.3	3.85	60.4	3.80	66.3	3.81	66.3
H-6b	3.67		3.66		3.78		3.77	
Rha $\alpha\text{H-1}$	5.059	101.0	5.085	100.4	5.065	101.3	5.103	100.5
H-2	3.98	69.9	3.97	70.3	3.98	70.4	3.98	70.2
H-3	3.64	69.7	3.74	68.5	3.65	70.6	3.77	68.2
H-4	3.36	71.6	3.42	81.0	3.36	71.8	3.43	81.0
H-5	3.74	68.7	3.91	67.5	3.76	68.5	3.95	67.6
CH ₃	1.17	16.6	1.26	16.9	1.19	16.9	1.29	16.6
			Glc($\alpha\text{1}\rightarrow\text{4}$)Rha$\alpha$				Glc($\alpha\text{1}\rightarrow\text{4}$)Rha$\alpha$	
Glc1 $\alpha\text{H-1}$	-	-	4.940	99.0	-	-	4.955	98.9
H-2	-	-	3.43	71.4	-	-	3.44	71.5
H-3	-	-	3.55	76.0	-	-	3.59	75.0
H-4	-	-	3.31	69.2	-	-	3.32	69.3
H-5	-	-	3.78	71.7	-	-	3.78	72.0
H-6a	-	-	3.77	60.1	-	-	3.78	60.2
H-6b	-	-	3.68		-	-	3.66	
					Glc($\alpha\text{1}\rightarrow\text{6}$)Glc$\beta$		Glc($\alpha\text{1}\rightarrow\text{6}$)Glc$\beta$	
Glc2 $\alpha\text{H-1}$	-	-	-	-	4.845	98.1	4.855	97.8
H-2	-	-	-	-	3.46	70.5	3.46	71.0
H-3	-	-	-	-	3.68	72.9	3.71	73.0
H-4	-	-	-	-	3.29	69.5	3.28	69.3
H-5	-	-	-	-	3.56	71.9	3.57	72.0
H-6a	-	-	-	-	3.69	60.3	3.68	60.2
H-6b	-	-	-	-	3.62		3.62	

^a In ppm relative to internal acetone (δ 2.225 for ^1H and δ 31.07 for ^{13}C).

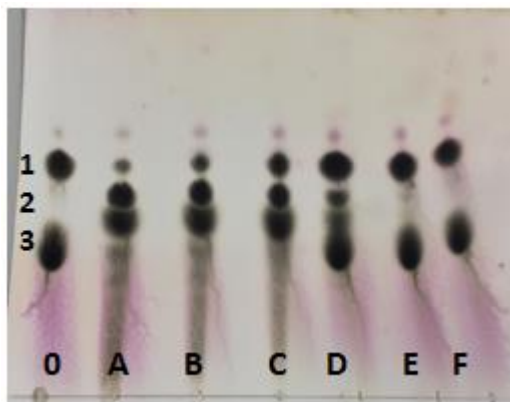


Figure S1. Transglycosylation activity of Gtf180- Δ N-Q1140E after a 1 h incubation in RebA glycosylation mixtures (84 mM RebA, 282 mM sucrose) containing **A** 0%, **B** 10%, **C** 20%, **D** 30%, **E** 40%, and **F** 50% EtOH. **1** RebA, **2** Monoglucosylated RebA (RebA-G1), **3** Sucrose.

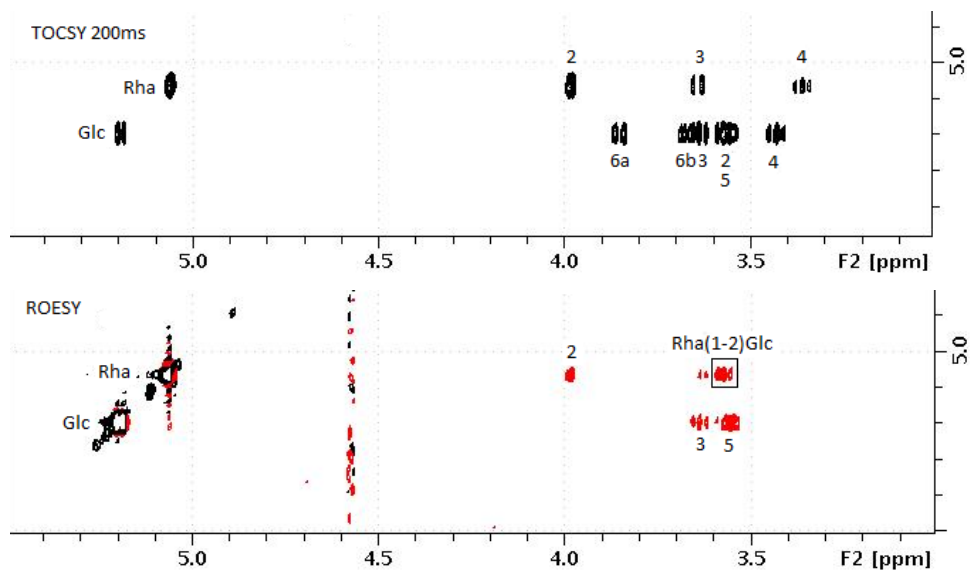


Figure S2. TOCSY (200 ms) and ROESY spectrum of the carbohydrate part of NHDC, recorded in D_2O at 310 K.

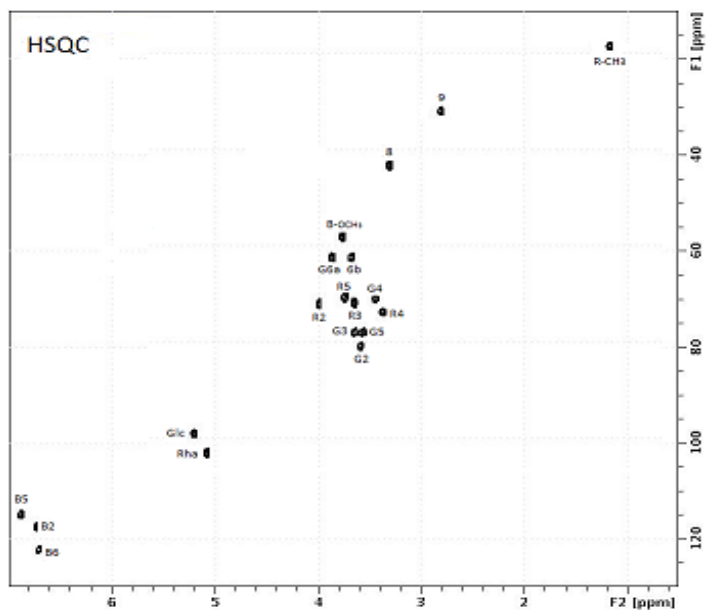


Figure S3. HSQC spectrum of NHDC, recorded in D_2O at 310 K.

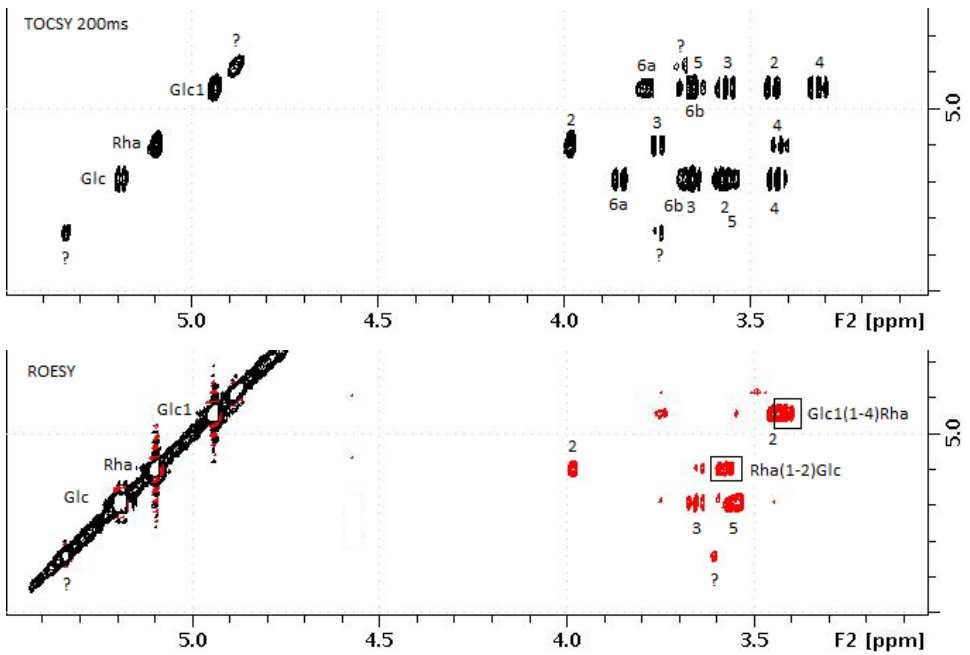


Figure S4. TOCSY and ROESY spectrum of the carbohydrate part of P1, recorded in D₂O at 310 K.

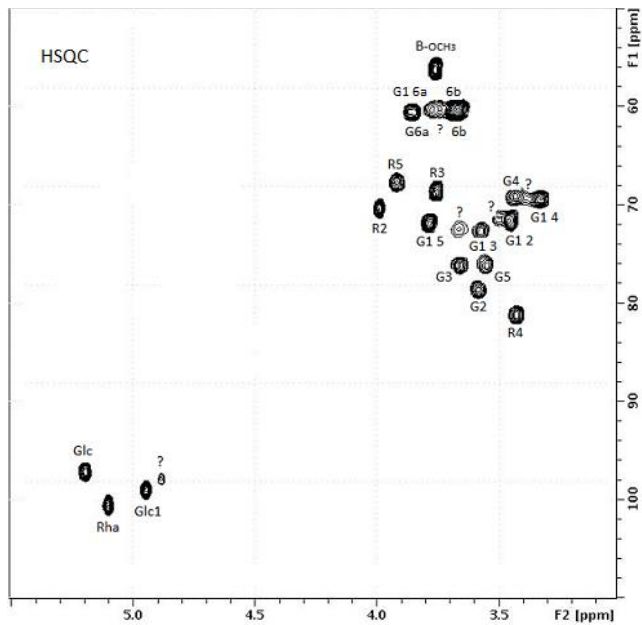


Figure S5. HSQC spectrum of the carbohydrate part of P1, recorded in D₂O at 310 K. ?, signals stemming from contamination(s).

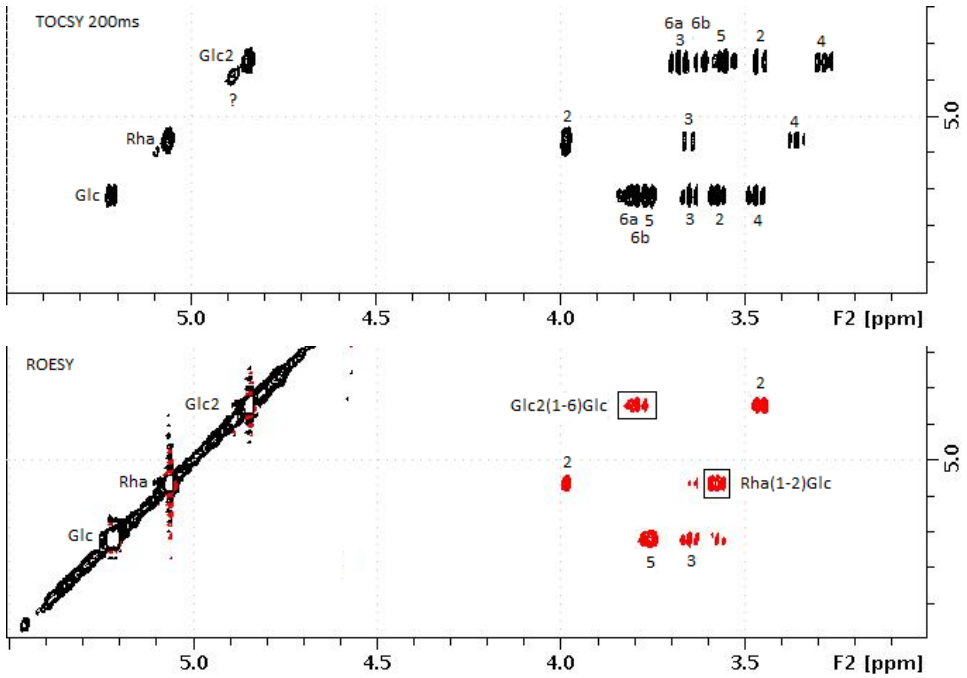


Figure S6. TOCSY and ROESY spectrum of the carbohydrate part of P2, recorded in D₂O at 310 K.

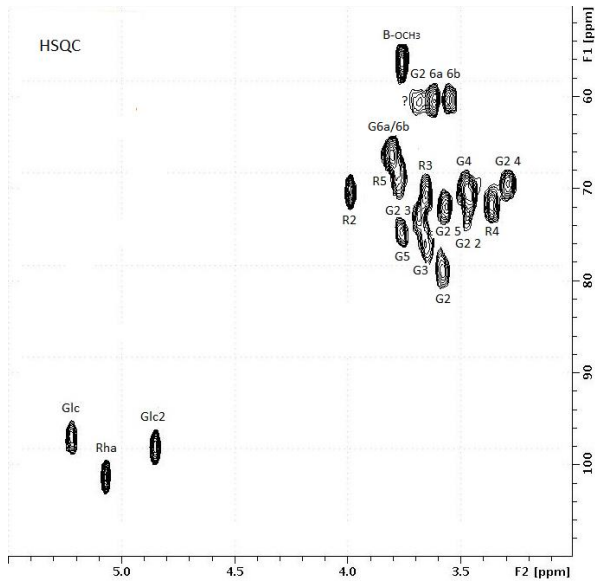


Figure S7. HSQC spectrum of the carbohydrate part of P2, recorded in D₂O at 310 K.

?, signals stemming from contamination(s).

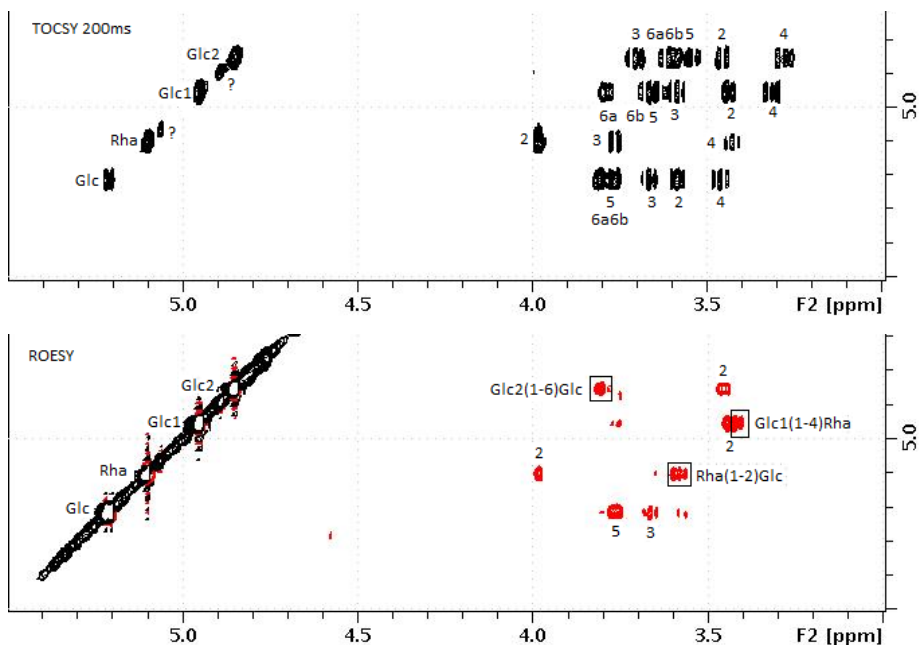


Figure S8. TOCSY and ROESY spectrum of the carbohydrate part of P3, recorded in D_2O at 310 K.

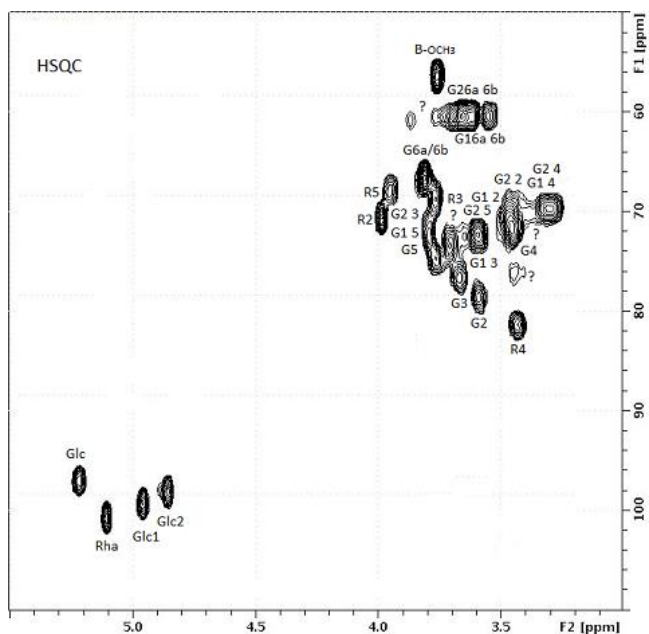


Figure S9. HSQC spectrum of the carbohydrate part of P3, recorded in D_2O at 310 K. ?, signals stemming from contamination(s).

Chapter 8

Summary and future prospects

Part 1: Dealing with the limitations of glucansucrases

The introduction of a glycosyl moiety can influence the physicochemical and biological properties of organic molecules such as anti-oxidants, antibiotics, and flavors⁶. The chemical synthesis of glycosides is characterized by multistep routes generating lots of waste. One-step enzymatic glycosylation, thereby taking advantage of the high specificity of enzymes, is preferred as 5-fold less waste is produced compared to chemical glycosylation¹⁷. Among all carbohydrate-active enzymes that can be applied as glycosylation biocatalyst, glucansucrases have received a considerable part of the attention due to their broad acceptor substrate specificity and use of inexpensive sucrose as donor substrate.

Glucansucrases are glycoside hydrolase enzymes (GH70) originating from Gram-positive lactic acid bacteria. They catalyze the conversion of sucrose into α -glucan polysaccharides, linking the α -D-glucopyranosyl units by (α 1 \rightarrow 2), (α 1 \rightarrow 3), (α 1 \rightarrow 4), or (α 1 \rightarrow 6) bonds, depending on the enzyme specificity^{73,74}. In addition, they are able to transfer glucosyl groups to a wide array of carbohydrate and non-carbohydrate acceptor molecules, catalyzing the so-called acceptor reaction⁷⁵. To this date, most research on the acceptor reaction of glucansucrases has focused on the discovery of new acceptor substrate specificities^{111-113,120-131}. Less progress has been made on the detailed structural characterization of products obtained, or the improvement of glucansucrases as industrial glycosylation biocatalyst, neither by reaction –nor enzyme engineering strategies.

Glucansucrases display a number of drawbacks, in particular if the acceptor reaction is targeted. First of all, the main glucansucrase catalyzed reaction is the synthesis of α -glucan polysaccharides from sucrose. It strongly impedes the efficient glycosylation of alternative acceptor substrates and complicates downstream processing of the glycosylated products. **Chapter 2** explored the potential of the N-terminally truncated glucansucrase Gtf180 from *Lactobacillus reuteri* 180 (Gtf180- Δ N)⁸⁰ and derived mutants^{99,100} as glycosylation

biocatalysts¹¹⁰. Three Gtf180-ΔN mutants (L938F, L981A and N1029M) were selected from a mutant library on the basis of their impaired α-glucan synthesis. Analysis of the glycosylation of the model acceptor substrate catechol by these mutants revealed that this apparent imperfection resulted in a substantial increase in monoglycosylation yield. Also several other phenolic and alcoholic compounds were more efficiently converted into glycosylated products by the selected mutants. For example, the resorcinol conversion degree of the L981A variant tripled compared to the WT enzyme, reaching a substantial 53%. Further analysis showed that these mutants possess a higher affinity for the model acceptor substrate catechol but a lower affinity for its mono-α-D-glucoside product, explaining the improved monoglycosylation yields. An explanation of how mutagenesis of residues L938, L981 and N1029 impaired α-glucan synthesis was provided by analyzing the available high resolution 3D crystal structure of the Gtf180-ΔN protein. On the downside, the k_{cat} of the best performing mutant (L981A) displayed a 4-fold decrease compared to the WT enzyme. In addition, the glycosylation of larger non-carbohydrate acceptor substrates such as resveratrol or quercetin remained problematic, partly due to the low water solubility of these compounds. The L981A mutant could nevertheless serve as template for further mutational engineering of the Gtf180-ΔN enzyme, targeting the improved glycosylation of specific acceptor substrates.

A second drawback related to the use of glucansucrases is their relatively low operational stability at high temperatures and in systems containing high acceptor substrate concentrations and cosolvents^{110,120,125}. Immobilization of Gtf180-ΔN on mesoporous silica particles enhanced its activity at temperatures above 50 °C and high concentrations of DMSO, conditions detrimental for the free enzyme (**Chapter 3**). Covalent cross-linking of Gtf180-ΔN with glutaraldehyde resulted in an undesired side-effect: less catechol was converted by the immobilized enzyme compared to the free enzyme, in favor of sucrose hydrolysis. Stabilizing Gtf180-ΔN by the developed immobilization protocol nevertheless allowed its incubation in 20% DMSO systems containing several poorly soluble acceptor substrates such as gallic acid and (+)-catechin, resulting in their improved glycosylation.

Part 2: Glycosylation of steviol glycosides

The steviol glycosides extracted from the leaves of the plant *Stevia rebaudiana* were approved for use as high-intensity sweetener (HIS) in food products by the European Commission in 2011⁴³. Stevia extract consists mainly of the steviol glycosides stevioside and rebaudioside A (RebA), however, they display a bitter (after)taste which prevents the creation of zero-calorie stevia soft drinks and a complete sugar substitution in other food products⁴⁶. Solving this taste issue could therefore greatly expand stevia sales and enforce its position on the HIS market. The correlation between the structure of steviol glycosides and their taste quality is still not fully understood, however, it is clear that the latter depends on the number, location and configuration of the glycosyl moieties⁸. Hence, the enzymatic glycosylation of steviol glycosides has been proposed as effective tool to improve their sensory properties⁵⁰⁻⁷⁰.

Screening of our in-house collection of glucansucrases revealed that only Gtf180-ΔN from *L. reuteri* 180 is able to glycosylate RebA, displaying a RebA conversion of roughly 50% (**Chapter 4**). As this is insufficient for industrial applications, the ability of several Gtf180-ΔN mutants to glycosylate RebA was explored, revealing that the Q1140E mutant is the most promising variant. Structural analysis of the products showed that both enzymes exclusively glycosylate RebA at the Glc(β1→C-19 residue, with the formation of an (α1→6) linkage. Docking of RebA in the enzyme's active site provided an explanation for these results: only the steviol C-19 β-D-glucosyl moiety is available for glycosylation. Several previous studies already demonstrated the importance of an adequate C-13/C-19-regiospecificity for the taste quality of the glycosylated products. For example, (α1→4)-glycosylation of stevioside and rubusoside at the C-13 steviol position yielded products with improved intensity and quality of sweetness, whereas (α1→4)-glycosylation at the C-19 position resulted in an increased bitterness⁵²⁻⁵⁴. Alternatively, (α1→6)-glycosylation at the C-19 site of stevioside improved its taste profile⁶⁰.

Optimizing the reaction conditions of the Gtf180- Δ N-Q1140E-catalyzed glycosylation of RebA by response surface methodology (RSM) yet again identified the (low) remaining α -glucan synthesis as an important impediment to obtain high conversion degrees and high product concentrations. Nevertheless, a highly productive process with a RebA conversion of 95% and a production of 115 g/L glycosylated product (RebA-G) within 3 h was achieved at optimal reaction conditions. Development of a fed-batch reaction with continuous addition of relatively low sucrose levels further improved the product yield to 270 g/L by adequately further suppressing α -glucan synthesis. Sucrose acts as primer for α -glucan synthesis^{103,104,135}; a constant excess of RebA relative to sucrose therefore favored the glycosylation of RebA. The continuous addition of sucrose ensured that enough donor substrate was available to drive the reaction. On the downside, 10 times more enzyme had to be supplied to the reaction mixture in order to obtain a 95% conversion within 3 h, which substantially adds to the production costs. Additionally, performing the fed-batch reaction required the addition of 34% more sucrose compared to performing the glycosylation in batch mode. Altogether, the batch reaction is thus preferred over the fed-batch reaction as performed in this work.

Sensory analysis of RebA and the glycosylated RebA products by a trained panel showed that RebA-G has a superior taste profile, displaying a significant reduction in bitterness compared to RebA. Glycosylation of RebA at the Glc(β 1 \rightarrow C-19 residue with the introduction of an (α 1 \rightarrow 6) linkage is thus a very appropriate method to improve its sensory properties. Whether the off-flavors are sufficiently reduced to allow the production of zero-calorie soft drinks, jams, yoghurts, etc. is currently unknown. Answering this question requires the analysis of the sensory properties of the end product, including for example the bulking agent. In addition, the physicochemical properties of the ingredients, such as viscosity, density, etc. play an important role for the taste quality of the end product.

Stevioside is the most prevalent steviol glycoside (5-10% of leaf dry weight) and is perceived by consumers as more bitter than RebA (2-4% of leaf dry weight).

This explains why all commercial stevia products are high-purity variants of RebA, while stevioside is considered as an undesired side-product. Improvement of the sensory properties of stevioside by means of its glycosylation consequently offers an opportunity to valorize this “waste” stream. Incubation of stevioside with Gtf180- Δ N-Q1140E indeed resulted in its glycosylation, although at a lower efficiency than RebA glycosylation (as determined by RSM): 50 g/L glycosylated stevioside product (Stev-G) was produced with a 95% conversion, using 5 times more sucrose than needed for RebA glycosylation (**Chapter 5**). Elucidation of the glycosylated stevioside product structures revealed that, in contrast to RebA glycosylation, stevioside was not exclusively glycosylated at the C-19 site; minor products were also glycosylated at the C-13 site. Similarly to RebA glycosylation, the main product was glycosylated at the C-19 site, with the introduction of an (α 1 \rightarrow 6) linkage (Stev-G1). Remarkably, the most prevalent diglycosylated product contained an (α 1 \rightarrow 4) linkage and not the expected (α 1 \rightarrow 3) –or (α 1 \rightarrow 6) linkages, reflecting the regular linkage specificity of Gtf180⁸².

Sensory analysis of the glycosylated stevioside products showed a significant reduction in bitterness compared to stevioside. The trained panel perceived Stev-G1 as sweet as stevioside but also as significantly less bitter. The large proportion of multiglycosylated products in Stev-G (67.5%) was translated into a significantly reduced sweetness, in contrast to RebA-G (22.3% multiglycosylated products) which maintained the sweetness of RebA. Interestingly, a double dose of Stev-G displayed a sweetness level similar to that of stevioside whereas bitterness remained equally suppressed. Comparison of the sensory properties of RebA-G and Stev-G identified the former as the superior product.

As the glycosylation of RebA and stevioside with Gtf180- Δ N-Q1140E showed great potential at laboratory scale, an efficient overall process at kg scale, including downstream processing, was developed (**Chapter 6**). Ultimately, adsorption of the glycosylated product with removal of sucrose, fructose, glucose and α -glucan oligo –and polysaccharides was applied as main purification step. An estimation of the production costs demonstrated the main strength of the process: the biocatalyst represents a minor part of the total cost, which is mostly

determined by the cost of the acceptor substrate, i.e. RebA or stevioside. A major cost reduction of 30% can consequently be achieved by using low-grade stevia extract as acceptor substrate instead of the more costly high-purity steviol glycosides. An additional advantage is that the side-product stevioside is valorized, representing an extra economic profit. If taste quality is priority, RebA is preferred as acceptor substrate as it displays a superior taste profile.

Gtf180- Δ N-Q1140E also displayed activity towards neohesperidin dihydrochalcone (NHDC), even though a lower conversion degree (64%) was obtained (**Chapter 7**). Use of 5-10 ppm NHDC with RebA is known to result in a decreased bitterness perception. Unfortunately, this is accompanied by an unpleasant lingering sensation, caused by NHDC²⁴⁷. Its glycosylation by Gtf180- Δ N-Q1140E resulted in a decreased perception of the off-flavors by the trained panel. In general, the bitterness suppressing effect of (glycosylated) NHDC on RebA was limited; RebA glycosylation reduced its bitterness much more effectively. Very recently, NHDC was attributed with potent anti-oxidant, hepatoprotective and prebiotic properties²⁶⁰⁻²⁶⁴. NHDC's low water solubility²⁶⁵, restricting its application as nutraceutical, was overcome by its glycosylation, while its anti-oxidant potential remained very high.

Conclusions

This thesis explored the potential of Gtf180- Δ N from *L. reuteri* 180 and derived mutants to glycosylate a wide range of alternative acceptor substrates. It was shown that the Q1140E mutant is particularly suited to glycosylate steviol glycosides. High conversion degrees and product yields were obtained, and the glycosylated products displayed a superior taste profile compared to RebA and stevioside. The developed processes consequently hold excellent potential to be implemented at industrial scale.

The Q1140E mutant was also able to glycosylate other glycosides, such as NHDC, although at a lower efficiency than the glycosylation of steviol glycosides.

This is another illustration of the broad carbohydrate acceptor substrate specificity of Gtf180- Δ N and derived mutants. The high water solubility of carbohydrates forms an additional advantage for their Gtf180- Δ N catalyzed glycosylation, thus avoiding the use of inhibitory cosolvents in the reaction mixture.

The glycosylation of non-carbohydrate acceptor substrates was achieved with more difficulty, partly due to their low water solubility and their inhibition of Gtf180- Δ N. α -Glucan synthesis was identified as important impediment for the glycosylation of these compounds, however, its suppression by mutational engineering only partially solved the problem. In other words, specific mutants will need to be constructed to further improve the Gtf180- Δ N glycosylation potential, similarly to the approach followed for the glycosylation of steviol glycosides by the Q1140E mutant of Gtf180- Δ N.

In conclusion, the glucansucrase enzyme Gtf180- Δ N holds considerable potential as glycosylation biocatalyst, in particular for the glycosylation of carbohydrate acceptor substrates. The development of industrial processes will first and foremost depend on the construction of adequate mutants displaying high conversion degrees, and secondly, on the optimization of the reaction conditions, thereby suppressing α -glucan synthesis from sucrose as much as possible.

Samenvatting en conclusies

Deel 1: Omgaan met de limitaties van glucansucrases

De introductie van een glycosylgroep kan zowel de fysicochemische als biologische eigenschappen van organische moleculen, zoals antioxidanten, antibiotica en smaakstoffen, beïnvloeden⁶. De chemische synthese van glycosiden is een meerstapsproces dat gekenmerkt wordt door de productie van een grote hoeveelheid afvalproducten. Enzymatische glycosylatie geniet de voorkeur; de hoge specificiteit van enzymen leidt immers tot de productie van 5 keer minder afval¹⁷. Van alle koolhydraat-actieve enzymen die gebruikt kunnen worden als biokatalysator voor de glycosylatie van moleculen zijn glucansucrases meerdere keren naar voren geschoven als uitstekend alternatief. Deze enzymen bezitten een brede acceptorsubstraatspecificiteit en gebruiken sucrose als donorsubstraat, een goedkope en gemakkelijk te verkrijgen grondstof.

Glucansucrases behoren tot de glycoside hydrolase GH70-familie. Ze katalyseren de conversie van sucrose in α -glucan polysachariden, en daarbij verbinden ze de α -D-glucopyranosyl eenheden met (α 1 \rightarrow 2), (α 1 \rightarrow 3), (α 1 \rightarrow 4), of (α 1 \rightarrow 6) bindingen, afhankelijk van de enzymspecificiteit^{73,74}. Daarnaast zijn glucansucrases ook in staat om glucosylgroepen te transfereren van sucrose naar een brede waaier van koolhydraat en niet-koolhydraat acceptormoleculen, de zogenaamde acceptorreactie⁷⁵. Tot op vandaag heeft het meeste onderzoek naar de acceptorreactie van glucansucrases zich toegespitst op de ontdekking van nieuwe acceptorsubstraatspecificiteiten^{111-113,120-131}. Er is echter minder vooruitgang geboekt op het vlak van de gedetailleerde structuurbepaling van de geglycosyleerde producten, of wat betreft het verbeteren van deze enzymen als industriële biokatalysator, noch door reactie noch door enzym-engineering strategieën.

Het toepassen van de acceptorreactie van glucansucrases voor de glycosylatie van organische moleculen wordt getypeerd door een aantal nadelen. Glucansucrases katalyseren in principe de synthese van α -glucan

polysachariden vanuit sucrose, in dit geval zowel het donor als acceptorsubstraat. Dit verhindert uiteraard de efficiënte glycosylatie van alternatieve acceptorsubstraten en compliceert de opzuivering van de geglycosyleerde producten. **Hoofdstuk 2** verkende het potentieel van het N-terminaal getrunceerde glucansucrase Gtf180 van *Lactobacillus reuteri* 180 (Gtf180- Δ N)⁸⁰ en afgeleide mutanten^{99,100} als glycosylatiebiokatalysator¹¹⁰. Drie Gtf180- Δ N mutanten (L938F, L981A and N1029M) werden geselecteerd uit een mutantenbibliotheek op basis van hun verzwakte α -glucansynthese. Analyse van de glycosylatie van het acceptorsubstraat catechol door deze mutanten onthulde dat deze ogenschijnlijke imperfectie resulteerde in een substantiële verbetering van de monoglycosylatie-opbrengst. Ook verscheidene andere fenolische en alcoholische verbindingen werden efficiënter geglycosyleerd door de geselecteerde mutanten. In vergelijking met het WT-enzym was de omzetting van bijvoorbeeld resorcinol in geglycosyleerde producten door de L981A-variant verdrievoudigd van 17% tot 53%. Deze resultaten werden andermaal bevestigd door de kinetische analyse van de mutanten; ze hadden een hogere affiniteit voor het acceptorsubstraat catechol maar een lagere affiniteit voor het monogeglycosyleerde catecholproduct. Analyse van de beschikbare 3D-structuur van het Gtf180- Δ N-proteïne verklaarde hoe mutagenese van residuen L938, L981 en N1029 de α -glucansynthese verzwakte in het voordeel van de acceptorreactie. Toch bleef de glycosylatie van grotere (niet-koolhydraat) acceptorsubstraten, zoals resveratrol en quercetine, problematisch, deels door de lage oplosbaarheid in water van deze moleculen. De L981A-mutant vormt desalniettemin een goed vertrekpunt voor verdere mutationale engineering om de glycosylatie van vooraf gedefinieerde acceptorsubstraten te verbeteren.

Een tweede nadeel inherent aan het gebruik van glucansucrases is hun relatief lage operationele stabiliteit bij hoge temperaturen en in systemen met hoge acceptorsubstraatconcentraties en cosolventen^{110,120,125}. Immobilisatie van Gtf180- Δ N op mesoporeuze silicapartikels verbeterde de enzymactiviteit bij temperaturen hoger dan 50 °C en in systemen met hoge DMSO-concentraties, condities die normalerwijs zeer schadelijk zijn voor het enzym (**Hoofdstuk 3**). Het cross-linken van Gtf180- Δ N met glutaraaldehyde resulteerde echter in een

ongewenst neveneffect: minder catechol werd geconverteerd door het geïmmobiliseerde enzym in vergelijking met het vrije enzym, ten gunste van meer sucrosehydrolyse. Incubatie van geïmmobiliseerd Gtf180- Δ N in systemen met 20% DMSO leidde desalniettemin tot de verbeterde glycosylatie van een aantal slecht oplosbare verbindingen, zoals catechine en galloorzuur.

Deel 2: Glycosylatie van steviolglycosiden

Het gebruik van steviolglycosiden, verbindingen die geëxtraheerd worden uit de bladeren van de plant *Stevia rebaudiana*, als intensieve zoetstof is in 2011 goedgekeurd door de Europese Commissie⁴³. Steviaextract bestaat voornamelijk uit de steviolglycosiden stevioside en rebaudioside A (RebA), wiens bittere (na)smaak de creatie van calorieloze frisdrank en een volledige suikervervanging in andere voedingsproducten in de weg staat⁴⁶. Het oplossen van deze smaakkwestie zou de populariteit en bijgevolg het verkoopsucces van stevia substantieel kunnen verhogen en daarmee een sterke positie voor stevia op de zoetstofmarkt vrijwaren. Hoe de chemische structuur van steviolglycosiden hun smaakkwiteit beïnvloedt is nog steeds niet helemaal duidelijk. Het staat echter vast dat deze laatste afhangt van het aantal, de locatie en configuratie van de glycosylgroepen⁸. Het spreekt dus voor zich dat de enzymatische glycosylatie van steviolglycosiden een veelbelovend middel is om diens smaakeigenschappen te verbeteren⁵⁰⁻⁷⁰.

Screening van onze in-house glucansucrasecollectie onthulde dat alleen Gtf180- Δ N van *L. reuteri* 180 in staat is om RebA te glycosyleren en daarbij een 50% conversie bereikt (**Hoofdstuk 4**). Omdat deze omzetting vanuit industrieel perspectief te laag is, werd een mutantenbibliotheek gescreend op basis van een verbeterde RebA-conversie, wat leidde tot de ontdekking van de Q1140E-mutant. Structurele analyse van de geglycosyleerde producten toonde aan dat beide enzymen RebA exclusief glycosyleren op het Glc(β 1 \rightarrow C-19) residu, met de introductie van een (α 1 \rightarrow 6)-binding. Docking van RebA in het actieve centrum van het enzym gaf een visuele interpretatie voor deze resultaten: enkel de steviol

C-19 β -D-glucosylgroep is beschikbaar voor glycosylatie. Voorgaande studies hadden het belang van de C-13/C-19-regiospecificiteit op de smaakqualiteit van de geglycosyleerde producten al aangetoond. Bijvoorbeeld, (α 1 \rightarrow 4)-glycosylatie van stevioside en rubusoside op de C-13-steviolpositie resulteerde in producten met een betere en intensievere zoete smaak. De introductie van dezelfde (α 1 \rightarrow 4)-binding op de C-19-positie leidde dan weer tot meer bitterheid⁵²⁻⁵⁴. Hiermee in tegenstelling: (α 1 \rightarrow 6)-glycosylatie op de C-19-positie van stevioside verbeterde diens smaakprofiel⁶⁰.

Optimalisatie van de reactiecondities d.m.v. response surface methodology (RSM) duidde eens te meer de lage maar nog steeds aanwezige α -glucansynthese aan als belangrijkste belemmering in het behalen van hoge omzettingen en productconcentraties. Toch kon er een zeer productief proces ontwikkeld worden: het toepassen van de optimale condities stond de productie toe van 115 g/L geglycosyleerd product (RebA-G) binnen 3 uur, met een hoge RebA-conversie van 95%. Het aannemen van een fed-batchsysteem, waarbij de concentratie van donorsubstraat sucrose constant op een laag niveau wordt gehouden door middel van diens continue toevoeging, leidde tot een verdere verbetering van de productconcentratie tot 270 g/L. Omdat sucrose de primer is voor α -glucansynthese^{103,104,135}, creëert de constante overmaat van RebA t.o.v. sucrose immers condities ten gunste van RebA-glycosylatie. Tegelijkertijd zorgt de continue toevoeging van sucrose ervoor dat er voldoende donorsubstraat aanwezig is om de reactie voort te drijven.

Smaakanalyse van RebA en de geglycosyleerde RebA-producten door een getraind panel liet zien dat RebA-G beschikt over een superieur smaakprofiel, met een significant gereduceerde bitterheid, in vergelijking tot RebA. Glycosylatie van RebA op het Glc(β 1 \rightarrow C-19-residu, met de introductie van een (α 1 \rightarrow 6)-binding, is dus een zeer geschikte methode om diens smaakeigenschappen te verbeteren. Of het smaakprofiel al dan niet voldoende verbeterd is voor de productie van calorieuze frisdrank, confituur, yoghurt, e.d. vereist uiteraard de smaakanalyse van het respectievelijke eindproduct.

Stevioside is het meest voorkomende steviolglycoside (5-10% van het droge bladgewicht) maar wordt door consumenten als bitterder bevonden dan RebA (2-4% van het droge bladgewicht). Dit verklaart waarom alle commerciële steviaproducten zeer zuivere varianten zijn van RebA, terwijl stevioside wordt beschouwd als een ongewenst nevenproduct. Het verbeteren van stevioside's smaakeigenschappen d.m.v. glycosylatie biedt dus een opportuniteit om ook dit nevenproduct te valoriseren. Hoewel incubatie van stevioside met Gtf180- Δ N-Q1140E inderdaad resulteerde in diens glycosylatie, verliep de reactie minder efficiënt dan RebA-glycosylatie (bepaald door RSM): om 50 g/L geglycosyleerd product (Stev-G) te produceren binnen 3 uur, met een conversie van 95%, was er 5 keer meer sucrose en 2 keer meer enzym nodig (**Hoofdstuk 5**). Structurele analyse van de geglycosyleerde producten onthulde dat, in tegenstelling tot RebA-glycosylatie, stevioside niet exclusief geglycosyleerd werd op de C-19-positie; een kleine hoeveelheid producten bleek geglycosyleerd op de C-13-positie. Net als bij RebA-glycosylatie was het belangrijkste product geglycosyleerd op de C-19-positie, met de introductie van een (α 1 \rightarrow 6)-binding (Stev-G1). Het meest voorkomende digeglycosyleerde product bevatte een (α 1 \rightarrow 4)-binding en niet een verwachte (α 1 \rightarrow 3) –of (α 1 \rightarrow 6)-binding (specifiek voor de Gtf180- Δ N-producten met sucrose alleen⁸²).

Smaakanalyse van de geglycosyleerde producten toonde een significante bitterheidsreductie aan ten opzichte van stevioside. Het getrainde panel oordeelde dat Stev-G1 net zo zoet was als stevioside maar ook significant minder bitter. Het grote aandeel aan multigeglycosyleerde producten in Stev-G (67.5%) vertaalde zich in een significant gereduceerde zoetheid, in tegenstelling tot RebA-G (22.3% multigeglycosyleerde producten) dat RebA's zoetheid behield. Dit probleem kon echter opgelost worden door het verdubbelen van de Stev-G dosis want daardoor werd een gelijkwaardige zoetheid als bij stevioside bereikt maar was er nog steeds sprake van een significante bitterheidsreductie. In vergelijking met Stev-G was RebA-G duidelijk het superieure product.

Omdat de glycosylatie van RebA en stevioside met Gtf180- Δ N-Q1140E veel potentieel toonde op laboratoriumschaal, werd een efficiënt proces, inclusief

productopzuivering, ontwikkeld op kg-schaal (**Hoofdstuk 6**). Uiteindelijk werd gekozen voor specifieke adsorptie van het geglycosyleerde product om sucrose, fructose en de α -glucanoligo –en polysachariden te verwijderen. Analyse van de productiekosten onthulde de grote kracht van het proces: het enzym vertegenwoordigt slechts een klein deel van de totale kosten, die vooral worden bepaald door de kosten van het acceptorsubstraat, RebA of stevioside. Een substantiële kostenreductie van 30% kan dus bewerkstelligd worden door stevia-extract van lagere kwaliteit te gebruiken als acceptorsubstraat i.p.v. de duurdere steviolglycosiden van hoge zuiverheid. Een bijkomend voordeel is dat het nevenproduct stevioside gevaloriseerd wordt, een extra economische winst. Als smaakwaliteit de prioriteit is, dan vormt RebA-glycosylatie de beste keuze aangezien RebA-G een superieure smaak heeft.

Daarnaast kon Gtf180- Δ N-Q1140E ook neohesperidine dihydrochalcon (NHDC) glycosyleren, ook al werd een relatief lage omzetting (64%) bereikt (**Hoofdstuk 7**). Het is bekend dat het gebruik van 5-10 ppm NHDC in een RebA-oplossing een vermindering van de bitterheid tot gevolg heeft. Jammer genoeg gaat dit gepaard met een onprettige en slepende nasmaak, veroorzaakt door NHDC²⁴⁷. Diens glycosylatie door Gtf180- Δ N-Q1140E resulteerde in een geringe verbetering van de ongewenste nasmaak. In het algemeen was het bitterheidsonderdrukkende effect van (geglycosyleerd) NHDC op RebA vrij miniem; RebA-glycosylatie bleef overeind als meest effectieve manier om diens smaak te verbeteren. Recent onderzoek kende ook krachtige antioxidant –en prebiotische eigenschappen toe aan NHDC²⁶⁰⁻²⁶⁴. De lage wateroplosbaarheid van NHDC²⁶⁵, wat diens toepassing als nutraceutical in de weg staat, werd verbeterd d.m.v. glycosylatie met Gtf180- Δ N-Q1140E, terwijl de sterke antioxidanteigenschappen door glycosylatie behouden bleven.

Conclusies

Deze thesis verkende het potentieel van *L. reuteri* 180 Gtf180- Δ N en afgeleide mutanten om een brede waaier aan alternatieve acceptorsubstraten te glycosyleren. Hierbij werd aangetoond dat de Q1140E-mutant bijzonder geschikt is om steviolglycosiden te glycosyleren. Niet alleen werden hoge conversies en productconcentraties bekomen, de geglycosyleerde producten beschikten over een superieur smaakprofiel in vergelijking met RebA en stevioside. De ontwikkelde processen hebben dus een uitstekend potentieel om geïmplementeerd te worden op een industriële schaal.

De Q1140E-mutant was daarnaast ook in staat om andere glycosiden, in het bijzonder NHDC, te glycosyleren, hoewel deze reactie minder efficiënt was dan de glycosylatie van steviolglycosiden. Toch is dit nogmaals een illustratie van de brede acceptorsubstraatspecificiteit van Gtf180- Δ N en afgeleide mutanten wat betreft de glycosylatie van koolhydraten. De uitstekende wateroplosbaarheid van koolhydraten is hiervoor uiteraard een extra voordeel aangezien de additie van inhiberende cosolventen niet nodig is.

De glycosylatie van niet-koolhydraten verliep met meer moeite, mede door hun lage wateroplosbaarheid en hun inhibitie van Gtf180- Δ N. α -Glucansynthese werd aangeduid als belangrijkste struikelblok voor de efficiënte glycosylatie van deze verbindingen. Onderdrukking van de α -glucansynthese door mutationale engineering zorgde voor een beperkt verbeterde omzetting. Er zullen dus specifieke mutanten geconstrueerd moeten worden om Gtf180- Δ N's glycosylatiepotentieel verder uit te bouwen en te verbeteren. Een gelijkwaardige benadering zoals gevolgd voor de glycosylatie van steviolglycosiden zou het meest succesvol moeten zijn.

Als finale conclusie kan dus gesteld worden dat glucansucrase Gtf180- Δ N zeker een toekomst heeft als glycosylatiebiokatalysator, in het bijzonder voor de glycosylatie van koolhydraten. Het succes van industriële processen zal eerst en

vooral afhangen van de constructie van gepaste mutanten, leidend tot hoge omzettingen, en ten tweede, de nauwkeurige optimalisatie van de reactiecondities, daarbij α -glucansynthese zoveel mogelijk onderdrukkend.

References

References

1. Li S, Yang X, Yang S, Zhu M, Wang X (2012) Technology prospecting on enzymes: application, marketing and engineering. *Comput Struct Biotechnol J* 2:1-11.
2. Choi JM, Han SS, Kim HS (2015) Industrial applications of enzyme biocatalysis: current status and future aspects. *Biotechnol Adv* 33:1443-1454.
3. Liu L, Yang H, Shin HD, Chen RR, Li J, Du G, Chen J (2013) How to achieve high-level expression of microbial enzymes: strategies and perspectives. *Bioengineered* 4:212-223.
4. Damborsky J, Brezovsky J (2014) Computational tools for designing and engineering enzymes. *Curr Opin Chem Biol* 19:8-16.
5. Singh R, Kumar M, Mittal A, Mehta PK (2016) Microbial enzymes: industrial progress in 21st century. *3 Biotech* 6:174.
6. Křen V, Martínková L (2001) Glycosides in medicine: The role of glycosidic residue in biological activity. *Curr Med Chem* 8:1303-1328.
7. Yamamoto I, Muto N, Nagata E, Nakamura T, Suzuki Y (1990) Formation of a stable L-ascorbic acid α -glucoside by mammalian α -glucosidase-catalyzed transglucosylation. *Biochim Biophys Acta* 1035:44-50.
8. Gerwig GJ, te Poele EM, Dijkhuizen L, Kamerling JP (2016) *Stevia* glycosides: Chemical and enzymatic modifications of their carbohydrate moieties to improve the sweet-tasting quality. *Adv Carbohydr Chem Biochem* 73:1-72.
9. Wong A, Toth I (2001) Lipid, sugar and liposaccharide based delivery systems. *Curr Med Chem* 8:1123-1136.
10. Křen V, Řezanka T (2008) Sweet antibiotics – the role of glycosidic residues in antibiotic and antitumor activity and their randomization. *FEMS Microbiol Rev* 32:858-889.
11. Schwarz M, Hillebrand S, Habben S, Degenhardt A, Winterhalter P (2003) Application of high-speed countercurrent chromatography to the large-scale isolation of anthocyanins. *Biochem Eng J* 14:179-189.
12. Bai XL, Yue TL, Yuan YH, Zhang HW (2010) Optimization of microwave-assisted extraction of polyphenols from apple pomace using response surface methodology and HPLC analysis. *J Sep Sci* 33:3751-3758.
13. Desmet T, Soetaert W, Bojarova P, Kren V, Dijkhuizen L, Eastwick-Field V, Schiller A (2012) Enzymatic glycosylation of small molecules: Challenging substrates require tailored catalysts. *Chem Eur J* 18:10786-10801.
14. Demchenko AV (2008) Handbook of chemical glycosylation: Advances in stereoselectivity and therapeutic relevance. Wiley-VCH.
15. Zhu X, Schmidt RR (2009) New principles for glycoside-bond formation. *Angew Chem Int Ed* 48:1900-1934.
16. Guo J, Ye X (2010) Protecting groups in carbohydrate chemistry: influence on stereoselectivity of glycosylations. *Molecules* 15:7235-7265.
17. de Roode BM, Franssen MCR, van der Padt A, Boom RM (2003) Perspectives for the industrial enzymatic production of glycosides. *Biotechnol Prog* 19:1391-1402.
18. Lairson LL, Henrissat B, Davies GJ, Withers SG (2008) Glycosyltransferases: structures, functions, and mechanisms. *Annu Rev Biochem* 77:521-555.

19. Masada S, Kawase Y, Nagatoshi M, Oguchi Y, Terasaka K, Mizukami H (2007) An efficient chemoenzymatic production of small molecule glucosides with in situ UDP-glucose recycling. *FEBS Lett* 581:2562-2566.
20. Terasaka K, Mizutani Y, Nagatsu A, Mizukami H (2012) *In situ* UDP-glucose regeneration unravels diverse functions of plant secondary product glycosyltransferases. *FEBS Lett* 586:4344-4350.
21. Schmölzer K, Gutmann A, Diricks M, Desmet T, Nidetzky B (2016) Sucrose synthase: A unique glycosyltransferase for biocatalytic glycosylation process development. *Biotechnol Adv* 34:88-111.
22. Aerts D, Verhaeghe TF, Roman BI, Stevens CV, Desmet T, Soetaert W (2011) Transglucosylation potential of six sucrose phosphorylases toward different classes of acceptors. *Carbohydr Res* 346:1860-1867.
23. De Winter K, Desmet T, Devlamyntck T, Van Renterghem L, Verhaeghe T, Pelantová H, Křen V, Soetaert W (2014) Biphasic catalysis with disaccharide phosphorylases: chemoenzymatic synthesis of α -D-glucosides using sucrose phosphorylase. *Org Process Res Dev* 18:781-787.
24. Luley-Goedl C, Nidetzky B (2010) Carbohydrate synthesis by disaccharide phosphorylases: Reactions, catalytic mechanisms and application in the glycosciences. *Biotechnol J* 5:1324-1338.
25. Dirks-Hofmeister ME, Verhaeghe T, De Winter K, Desmet T (2015) Creating space for large acceptors: Rational biocatalyst design for resveratrol glycosylation in an aqueous system. *Angew Chem Int Ed Engl* 54:9289-9292.
26. Kraus M, Grimm C, Seibel J (2016) Redesign of the active site of sucrose phosphorylase through a clash-induced cascade of loop shifts. *Chembiochem* 17:33-36.
27. Balogh T, Baross L, Kosáry J (2004) Novel reaction systems for the synthesis of O-glucosides by enzymatic reverse hydrolysis. *Tetrahedron* 60:679-682.
28. van Rantwijk F, Woudenberg-van Oosterom M, Sheldon RA (1999) Glycosidase-catalysed synthesis of alkyl glycosides. *J Mol Catal* 6:511-532.
29. Vic G, Crout DHG (1995) Synthesis of allyl and benzyl β -D-glucopyranosides, and allyl β -D-galactopyranoside from D-glucose or D-galactose and the corresponding alcohol using almond β -D-glucosidase. *Carbohydr Res* 279:315-319.
30. Wang LX, Huang W (2009) Enzymatic transglycosylation for glycoconjugate synthesis. *Curr Opin Chem Biol* 13:592-600.
31. Yang M, Davies GJ, Davis BG (2007) A glycosynthase catalyst for the synthesis of flavonoid glycosides. *Angew Chem Int Ed* 46:3885-3888.
32. Desmet T, Soetaert W (2011) Enzymatic glycosyl transfer: mechanisms and applications. *Biotransform* 29:1-18.
33. Torres P, Poveda A, Jimenez-Barbero J, Parra JL, Comelles F, Ballesteros A, Plou F (2011) Enzymatic synthesis of α -glucosides of resveratrol with surfactant activity. *Adv Synth Catal* 353:1077-1086.
34. De Bruyn F, Maertens J, Beauprez J, Soetaert W, De Mey M (2015) Biotechnological advances in UDP-sugar based glycosylation of small molecules. *Biotechnol Adv* 33:288-302.

References

35. Endo T, Koizumi S, Tabata K, Kakita S, Ozaki A (1999) Large-scale production of N-acetyllactosamine through bacterial coupling. *Carbohydr Res* 316:179-183.
36. Koizumi S, Endo T, Tabata K, Ozaki A (1998) Large-scale production of UDP-galactose and globotriose by coupling metabolically engineered bacteria. *Nat Biotechnol* 16:847-850.
37. Brochado AR, Matos C, Moller BL, Hansen J, Mortensen UH, Patil KR (2010) Improved vanillin production in baker's yeast through in silico design. *Microb Cell Fact* 9:84.
38. Choi O, Lee JK, Kang SY, Pandey RP, Sohng JK, Ahn JS, Hong YS (2014) Construction of artificial biosynthetic pathways for resveratrol glucoside derivatives. *J Microbiol Biotechnol* 24:614-618.
39. Kishore GM, Motion M, Hicks PM, Hansen J, Houghton-Larsen J, Hansen EH, Mikkelsen MD, Tavares S, Blom C (2011) Production of steviol glycosides in microorganisms. WO2011153378.
40. Kim BG, Kim HJ, Ahn JH (2012) Production of bioactive flavonol rhamnosides by expression of plant genes in *Escherichia coli*. *J Agric Food Chem* 60:11143-11148.
41. Pandey RP, Parajuli P, Koirala N, Lee JH, Park YI, Sohng JK (2014) Glucosylation of isoflavonoids in engineered *Escherichia coli*. *Mol Cells* 37:172-177.
42. De Bruyn F, De Paepe B, Maertens J, Beauprez J, De Cocker P, Mincke S, Stevens C, De Mey M (2015) Development of an in vivo glucosylation platform by coupling production to growth: Production of phenolic glucosides by a glycosyltransferase of *Vitis vinifera*. *Biotech Bioeng* 112:1594-1603.
43. Commission Regulation (EU) No 1131/2011. Official Journal of the European Union (2011).
44. Future Market Insights (2014) Stevia market: Global industry analysis and opportunity assessment 2014 – 2020. <http://www.futuremarketinsights.com>
45. World Health Organization (2016) Evaluation of certain food additives. <http://www.who.int>
46. Hellfritsch C, Brockhoff A, Stähler F, Meyerhof W, Hofmann T (2012) Human psychometric and taste receptor responses to steviol glycosides. *J Agric Food Chem* 60:6782-6793.
47. Shi J, Feng Y, Zhao C, Wang H (2010) Process for rebaudioside D. WO 2010146463.
48. Chen P, Li Y, Peng S (2014) Novel process for the preparation of rebaudioside D and other related naturally occurring sweeteners. US20140296499.
49. Prakash I, Markosyan A, Bunders C (2014) Development of next generation stevia sweetener: Rebaudioside M. *Foods* 3:162-175.
50. Li S, Li W, Xiao Q, Xia Y (2013) Transglycosylation of stevioside to improve the edulcorant quality by lower substitution using cornstarch hydrolyzate and CGTase. *Food Chem* 138:2064-2069.
51. Abelyan V, Balayan A, Ghochikyan V, Markosyan A (2004) Transglycosylation of stevioside by cyclodextrin glucanotransferases of various groups of microorganisms. *Appl Biochem Microbiol* 40:129-134.
52. Darise M, Mizutani K, Kasai R, Tanaka O (1984) Enzymic transglucosylation of rubusoside and the structure- sweetness relationship of steviol- bisglycosides. *Agric Biol Chem* 102483-2488.

53. Fukunaga Y, Miyata T, Nakayasu N, Mizutani K, Kasai R, Tanaka O (1989) Enzymatic transglucosylation products of stevioside – separation and sweetness-evaluation. *Agric Biol Chem* 53:1603-1607.
54. Ohtani K, Aikawa Y, Ishikawa H, Kasai R, Kitahata S, Mizutani K, Doi S, Nakaura M, Tanaka O (1991) Further study on the 1,4- α -transglucosylation of rubusoside, a sweet steviol-bisglucoside from *Rubus suavissimus*. *Agric Biol Chem* 55:449-453.
55. Jaitak V, Kaul VK, Bandna, Kumar N, Singh B, Savergave LS, Jogdand VV, Nene S (2009) Simple and efficient enzymatic transglycosylation of stevioside by β -cyclodextrin glucanotransferase from *Bacillus firmus*. *Biotechnol Lett* 31:1415-1420.
56. Yu X, Yang J, Li B, Yuan H (2015) High efficiency transformation of stevioside into a single mono-glycosylated product using a cyclodextrin glucanotransferase from *Paenibacillus* sp. CGMCC 5316. *World J Microbiol Biotechnol* 31:1983-1991.
57. Markosyan A, Prakash I, Chaturvedula VSP (2013) High purity steviol glycosides. WO2013176738.
58. Mikkelsen MD, Hansen J, Simon E, Brianza F, Semmler A, Olsson K, Carlsen S, Düring L, Ouspenski A, Hicks P (2014) Methods for improved production of rebaudioside D and rebaudioside M. WO2014122227.
59. Wang Y, Chen L, Li Y, Li Y, Yan M, Chen K, Hao N, Xu L (2015) Efficient enzymatic production of rebaudioside A from stevioside. *Biosci Biotechnol Biochem* 80:67-73.
60. Lobov SV, Kasai R, Ohtani K, Yamasaki K (1991) Enzymic production of sweet stevioside derivatives: Transglucosylation by glucosidases. *Agric Biol Chem* 55:2959-2965.
61. Ye F, Yang R, Hua X, Shen Q, Zhao W, Zhang W (2013) Modification of stevioside using transglucosylation activity of *Bacillus amyloliquefaciens* α -amylase to reduce its bitter aftertaste. *LWT – Food Sci Technol* 51:524-530.
62. Ye F, Yang R, Hua X, Shen Q, Zhao W, Zhang W (2014) Modification of steviol glycosides using α -amylase. *LWT – Food Sci Technol* 57:400-405.
63. Kusama S, Kusakabe I, Nakamura Y, Eda S, Murakami K (1986) Transglucosylation into stevioside by the enzyme system from *Streptomyces* sp. *Agric Biol Chem* 50:2445-2451.
64. Kusakabe I, Watanabe S, Morita R, Terahara M, Murakami K (1992) Formation of a transfer product from stevioside by the cultures of *Actinomycete*. *Biosci Biotechnol Biochem* 56:233-237.
65. De Oliveira BH, Packer JF, Chimelli M, de Jesus DA (2007) Enzymatic modification of stevioside by cell-free extract of *Gibberella fujikuroi*. *J Biotechnol* 131:92-96.
66. Ko JA, Nam SH, Park JY, Wee Y, Kim D, Lee WS, Ryu YB, Kim YM (2016) Synthesis and characterization of glucosyl stevioside using *Leuconostoc* dextranase. *Food Chem* 211:577-582.
67. Musa A, Miao M, Zhang T, Jiang B (2014) Biotransformation of stevioside by *Leuconostoc citreum* SK24.002 alternansucrase acceptor reaction. *Food Chem* 146:23-29.
68. te Poele EM, Dijkhuizen L, Gerwig GJ, Kamerling JP (2016) Methods for the enzymatic modification of steviol glycosides, modified steviol glycosides obtainable thereby, and the use thereof as sweeteners. WO 2016144175.

References

69. Gerwig GJ, te Poele EM, Dijkhuizen L, Kamerling JP (2017) Structural analysis of rebaudioside A derivatives obtained by *Lactobacillus reuteri* 180 glucansucrase-catalyzed trans- α -glucosylation. *Carbohydr Res* 440-441:51-62.
70. te Poele EM, Devlamynck T, Jäger M, Gerwig GJ, Van de Walle D, Dewettinck K, Hirsch AKH, Kamerling JP, Soetaert W, Dijkhuizen L (2017) Glucansucrase (mutant) enzymes from *Lactobacillus reuteri* 180 efficiently transglucosylate *Stevia* component rebaudioside A, resulting in a superior taste. *Sci Reports*. Submitted for publication.
71. Olsson K, Carlsen S, Semmler A, Simon E, Mikkelsen MD, Møller BL (2016) Microbial production of next-generation stevia sweeteners. *Microb Cell Fact* 15, DOI: 10.1186/s12934-016-0609-1.
72. Costa-Font M, Gil JM, Traill WB (2008) Consumer acceptance, valuation of and attitudes towards genetically modified food: Review and implications for food policy. *Food Policy* 33:99-111.
73. Monchois V, Willemot RM, Monsan P (1999) Glucansucrases: mechanism of action and structure-function relationships. *FEMS Microbiol Rev* 23: 131-151.
74. van Hijum SAFT, Kralj S, Ozimek LK, Dijkhuizen L, van Geel-Schutten IGH (2006) Structure-function relationships of glucansucrase and fructansucrase enzymes from lactic acid bacteria. *Microbiol Mol Biol Rev* 70:157-176.
75. Leemhuis H, Pijning T, Dobruchowska JM, van Leeuwen SS, Kralj S, Dijkstra BW, Dijkhuizen L (2013) Glucansucrases: three-dimensional structures, reactions, mechanism, α -glucan analysis and their implications in biotechnology and food applications. *J Biotechnol* 163:250-272.
76. Kumari A, Catanzaro R, Marotta F (2011) Clinical importance of lactic acid bacteria: a short review. *Acta Biomed* 82:177-180.
77. Bounaix MS, Gabriel V, Morel S, Robert H, Rabier P, Remaud-Siméon M, Gabriel B, Fontagné-Faucher C (2009) Biodiversity of exopolysaccharides produced from sucrose by sourdough lactic acid bacteria. *J Agric Food Chem* 57:10889-10897.
78. Passerini D, Vuillemin M, Ufarte L, Morel S, Loux V, Fontagné-Faucher C, Remaud-Siméon M, Moulis C (2015) Inventory of the GH70 enzymes encoded by *Leuconostoc citreum* NRRL B-1299 – identification of three novel α -transglucosylases. *FEBS J* 282:2115-2130.
79. Ooshima T, Matsumura M, Hoshino T, Kawabata S, Sobue S, Fujiwara T (2001) Contributions of three glucosyltransferases to sucrose-dependent adherence of *Streptococcus mutans*. *J Dent Res* 80:1672-1677.
80. Kralj S, van Geel-Schutten IGH, Dondorff MMG, Kirsanovs S, van der Maarel MJEC, Dijkhuizen L (2004) Glucan synthesis in the genus *Lactobacillus*: isolation and characterization of glucansucrase genes, enzymes and glucan products from six different strains. *Microbiology* 150:3681-3690.
81. Monchois V, Willemot RM, Remaud-Simeon M, Croux C, Monsan P (1996) Cloning and sequencing of a gene coding for a novel dextransucrase from *Leuconostoc mesenteroides* NRRL B-1299 synthesizing only alpha (1-6) and alpha (1-3) linkages. *Gene* 182:23-32.

82. Pijning T, Vujicic-Zagar A, Kralj S, Eeuwema W, Dijkhuizen L, Dijkstra BW (2008) Biochemical and crystallographic characterization of a glucansucrase from *Lactobacillus reuteri* 180. *Biocat Biotrans* 26:12-17.
83. Vujicic-Zagar A, Pijning T, Kralj S, Lopez CA, Eeuwema W, Dijkhuizen L, Dijkstra BW (2010) Crystal structure of a 117 kDa glucansucrase fragment provides insight into evolution and product specificity of GH70 enzymes. *Proc Natl Acad Sci USA* 107:21406-21411.
84. Pijning T, Vujičić-Zagar A, Kralj S, Dijkhuizen L, Dijkstra BW (2012) Structure of the alpha-1,6/alpha-1,4-specific glucansucrase GtfA from *Lactobacillus reuteri* 121. *Acta Crystallogr Sect F Struct Biol Cryst Commun* 68:1448-1454.
85. Ito K, Ito S, Shimamura T, Weyand S, Kawarasaki Y, Misaka T, Abe K, Kobayashi T, Cameron AD, Iwata S (2011) Crystal structure of glucansucrase from the dental caries pathogen *Streptococcus mutans*. *J Mol Biol* 408:177-186.
86. Brison Y, Pijning T, Malbert Y, Fabre É, Mourey L, Morel S, Potocki-Véronèse G, Monsan P, Tranier S, Remaud-Siméon M, Dijkstra BW (2012) Functional and structural characterization of α -(1 \rightarrow 2) branching sucrose derived from DSR-E glucansucrase. *J Biol Chem* 287:7915-7924.
87. Pijning T, Vujicic-Zagar A, Kralj S, Dijkhuizen L, Dijkstra BW (2014) Flexibility of truncated and full-length glucansucrase Gtf180 enzymes from *Lactobacillus reuteri* 180. *FEBS J* 281:2159-2171.
88. Meng X, Dobruchowska JM, Pijning T, Gerwig GJ, Kamerling JP, Dijkhuizen L (2015) Truncation of domain V of the multidomain glucansucrase Gtf180 of *Lactobacillus reuteri* 180 heavily impairs its polysaccharide-synthesizing ability. *Appl Microbiol Biotechnol* 99:5885-5894.
89. MacGregor EA, Jespersen HM, Svensson B (1996) A circularly permuted alpha-amylase-type alpha/beta-barrel structure in glucan-synthesizing glycosyltransferases. *FEBS Lett* 378:263-266.
90. Lombard V, Golaconda Ramulu H, Drula E, Coutinho PM, Henrissat B (2014) The Carbohydrate-active enzymes database (CAZy) in 2013. *Nucleic Acids Res* 42:490-495.
91. Henrissat B, Davies G (1997) Structural and sequence-based classification of glycoside hydrolases. *Curr Opin Struct Biol* 7:637-644.
92. Uitdehaag JC, Mosi R, Kalk KH, van der Veen BA, Dijkhuizen L, Withers SG, Dijkstra BW (1999) X-ray structures along the reaction pathway of cyclodextrin glycosyltransferase elucidate catalysis in the alpha-amylase family. *Nat Struct Biol* 6:432-436.
93. van Leeuwen SS, Kralj S, van Geel-Schutten IH, Gerwig GJ, Dijkhuizen L, Kamerling JP (2008) Structural analysis of the alpha-D-glucan (EPS180) produced by the *Lactobacillus reuteri* strain 180 glucansucrase GTF180 enzyme. *Carbohydr Res* 343:1237-1250.
94. van Leeuwen SS, Kralj S, van Geel-Schutten IH, Gerwig GJ, Dijkhuizen L, Kamerling JP (2008) Structural analysis of the alpha-D-glucan (EPS35-5) produced by the *Lactobacillus reuteri* strain 35-5 glucansucrase GTFa enzyme. *Carbohydr Res* 343:1251-1265.

References

95. Leemhuis H, Pijning T, Dobruchowska JM, Dijkstra BW, Dijkhuizen L (2012) Glycosidic bond specificity of glucansucrases: on the role of acceptor substrate binding residues. *Bioat Biotrans* 30:366-376.
96. Kralj S, van Geel-Schutten IGH, Faber EJ, van der Maarel MJEC, Dijkhuizen L (2005) Rational transformation of a *Lactobacillus reuteri* 121 reuteransucrase into a dextransucrase. *Biochemistry* 44:9206-9216.
97. van Leeuwen SS, Kralj S, Eeuwema W, Gerwig GJ, Dijkhuizen L, Kamerling JP (2009) Structural characterization of bioengineered alpha-D-glucans produced by mutant glucansucrase GTF180 enzymes of *Lactobacillus reuteri* strain 180. *Biomacromolecules* 10:580-588.
98. Meng X, Dobruchowska JM, Pijning T, Lopez CA, Kamerling JP, Dijkhuizen L (2014) Residue Leu940 has a crucial role in the linkage and reaction specificity of the glucansucrase GTF180 of the probiotic bacterium *Lactobacillus reuteri* 180. *J Biol Chem* 289:32773-32782.
99. Meng X, Pijning T, Dobruchowska JM, Gerwig GJ, Dijkhuizen L (2015) Characterization of the functional roles of amino acid residues in acceptor binding subsite +1 in the active site of the glucansucrase GTF180 enzyme of *Lactobacillus reuteri* 180. *J Biol Chem* 290:30131-30141.
100. Meng X, Dobruchowska JM, Pijning T, Gerwig GJ, Dijkhuizen L (2016) Synthesis of new hyper-branched α -glucans from sucrose by *Lactobacillus reuteri* 180 glucansucrase mutants. *J Agr Food Chem* 64:433-442.
101. Meng X, Pijning T, Dobruchowska JM, Yin H, Gerwig GJ, Dijkhuizen L (2016) Structural determinants of alternating (α 1 \rightarrow 4) and (α 1 \rightarrow 6) linkage specificity in reuteransucrase of *Lactobacillus reuteri*. *Sci Rep* 6:35261.
102. Meng X, Pijning T, Tietema M, Dobruchowska JM, Yin H, Gerwig GJ, Kralj S, Dijkhuizen L (2017) The essential role of W1065 in the glucansucrase GTF180 of *Lactobacillus reuteri* 180 for activity, polysaccharide synthesis and linkage specificity. *Food Chem* 217:81-90.
103. Dobruchowska JM, Meng X, Leemhuis H, Gerwig GJ, Dijkhuizen L, Kamerling JP (2013) Gluco-oligomers initially formed by the reuteransucrase enzyme of *Lactobacillus reuteri* 121 incubated with sucrose and malto-oligosaccharides. *Glycobiology* 23:1084-1096.
104. Cheetham NWH, Slodki ME, Walker GJ (1991) Structure of the linear, low-molecular-weight dextran synthesized by a D-glucosyltransferase (Gtf-S3) of *Streptococcus sobrinus*. *Carbohydr Polym* 16:342-353.
105. Moulis C, Joucla G, Harrison D, Fabre E, Potocki-Véronèse G, Monsan P, Remaud-Siméon M (2006) Understanding the polymerization mechanism of glycoside-hydrolase family 70 glucansucrases. *J Biol Chem* 281:31254-31267.
106. Ebert KH, Schenk G (1968) Mechanisms of biopolymer growth: the formation of dextran and levan. *Adv Enzymol Relat Areas Mol Biol* 30:179-221.
107. Albenne C, Skov LK, Mirza O, Gajhede M, Feller G, D' Amico S, André G, Potocki-Véronèse G, van der Veen BA, Monsan P, Remaud-Siméon M (2004) Molecular basis of the amylose-like polymer formation catalyzed by *Neisseria polysaccharea* amylosucrase. *J Biol Chem* 279:726-734.

108. Skov LK, Mirza O, Sprogøe D, Dar I, Remaud-Siméon M, Albenne C, Monsan P, Gajhede M (2002) Oligosaccharide and sucrose complexes of amylosucrase. Structural implications for the polymerase activity. *J Biol Chem* 277:47741-47747.
109. Albenne C, Skov LK, Tran V, Gajhede M, Monsan P, Remaud-Siméon M, André-Leroux G (2007) Towards the molecular understanding of glycogen elongation by amylosucrase. *Proteins* 66:118-126.
110. Devlamynck T, te Poele EM, Meng X, van Leeuwen S, Dijkhuizen L (2016) Glucansucrase Gtf180-ΔN of *Lactobacillus reuteri* 180: Enzyme and reaction engineering for improved glycosylation of non-carbohydrate molecules. *Appl Microbiol Biotechnol* 100:7529-7539.
111. Robyt JF, Walseth TF (1978) The mechanism of acceptor reactions of *Leuconostoc mesenteroides* B-512F dextransucrase. *Carbohydr Res* 61:433-445.
112. Robyt JF, Eklund SH (1983) Relative, quantitative effects of acceptors in the reaction of *Leuconostoc mesenteroides* B-512F dextransucrase. *Carbohydr Res* 121:279-286.
113. Fu DT, Robyt JF (1990) Acceptor reactions of maltodextrins with *Leuconostoc mesenteroides* B-512FM dextransucrase. *Arch Biochem Biophys* 283:379-387.
114. Monsan PF, Ouarné F (2009) Oligosaccharides derived from sucrose. Prebiotics and probiotics science and technology 293-336 (Charalampopoulos D, Rastall RA, Eds.) Springer New York.
115. Koepsell HJ, Tsuchiya HM, Hellman NN, Kazenko A, Hoffman CA, Sharpe ES, Jackson RW (1953) Enzymatic synthesis of dextran: acceptor specificity and chain initiation. *J Biol Chem* 200:793-801.
116. Moulis C, Medina GV, Suwannarangsee S, Monsan P, Remaud-Siméon M, Potocki-Véronèse G (2008) One-step synthesis of isomalto-oligosaccharide syrups and dextrans of controlled size using engineered dextransucrase. *Biocat Biotrans* 26:141-151.
117. Rycroft CE, Jones MR, Gibson GR, Rastall RA (2001) A comparative in vitro evaluation of the fermentation properties of prebiotic oligosaccharides. *J Appl Microbiol* 91:878-887.
118. Díez-Municio M, Herrero M, Jimeno ML, Olano A, Moreno FJ (2012) Efficient synthesis and characterization of lactulosucrose by *Leuconostoc mesenteroides* B-512F dextransucrase. *J Agric Food Chem* 60:10564-10571.
119. Côté GL (2009) Acceptor products of alternansucrase with gentiobiose. Production of novel oligosaccharides for food and feed and elimination of bitterness. *Carbohydr Res* 344:187-190.
120. Bertrand A, Morel S, Lefoulon F, Rolland Y, Monsan P, Remaud-Simeon M (2006) *Leuconostoc mesenteroides* glucansucrase synthesis of flavonoid glucosides by acceptor reactions in aqueous-organic solvents. *Carbohydr Res* 341:855-863.
121. Woo HJ, Kang HK, Nguyen TTH, Kim GE, Kim YM, Park JS, Kim D, Cha J, Moon YH, Nam SH, Xia YM, Kimura A, Kim D (2012) Synthesis and characterization of ampelopsin glucosides using dextransucrase from *Leuconostoc mesenteroides* B-1299CB4: Glucosylation enhancing physicochemical properties. *Enzyme Microb Technol* 51:311-318.
122. Kim GE, Kang HK, Seo ES, Jung SH, Park JS, Kim DH, Kim DW, Ahn SA, Sunwoo C, Kim D (2012) Glucosylation of the flavonoid, astragaloside by *Leuconostoc mesenteroides* B-512FMCM

- dextranucrase acceptor reactions and characterization of the products. *Enzyme Microb Technol* 50:50-56.
123. Meulenbeld GH, Zuilhof H, van Veldhuizen A, van den Heuvel RH, Hartmans S (1999) Enhanced (+)-catechin transglucosylating activity of *Streptococcus mutans* GS-5 glucosyltransferase-D due to fructose removal. *Appl Environ Microbiol* 65:4141-4147.
 124. Overwin H, Wray V, Hofer B (2015) Flavonoid glucosylation by non-Leloir glycosyltransferases: formation of multiple derivatives of 3,5,7,3',4'-pentahydroxyflavane stereoisomers. *Appl Microbiol Biotechnol* 99:9565-9576.
 125. Meulenbeld GH, Hartmans S (2000) Transglycosylation by *Streptococcus mutans* GS-5 glucosyltransferase-D: Acceptor specificity and engineering of reaction conditions. *Biotechnol Bioeng* 70:363-369.
 126. Moon YH, Lee JH, Ahn JS, Nam SH, Oh DK, Park DH, Chung HJ, Kang S, Day DF, Kim D (2006) Synthesis, structure analyses, and characterization of novel epigallocatechin gallate (EGCG) glycosides using the glucansucrase from *Leuconostoc mesenteroides* B-1299CB. *J Agric Food Chem* 54:1230-1237.
 127. Seo ES, Kang J, Lee JH, Kim GE, Kim GJ, Kim D (2009) Synthesis and characterization of hydroquinone glucoside using *Leuconostoc mesenteroides* dextranucrase. *Enzyme Microb Technol* 45:355-360.
 128. Yoon SH, Fulton DB, Robyt JF (2010) Enzymatic synthesis of L-DOPA α -glycosides by reaction with sucrose catalyzed by four different glucansucrases from four strains of *Leuconostoc mesenteroides*. *Carbohydr Res* 345:1730-1735.
 129. Malbert Y, Pizzut-Serin S, Massou S, Cambon E, Laguerre S, Monsan P, Lefoulon F, Morel S, André I, Remaud-Simeon M (2014) Extending the structural diversity of α -flavonoid glycosides with engineered glucansucrases. *ChemCatChem* 6:2282-2291.
 130. Moon YH, Lee JH, Jhon DY, Jun WJ, Kang SS, Sim J, Choi H, Moon JH, Kim D (2007) Synthesis and characterization of novel quercetin- α -glucopyranosides using glucansucrase from *Leuconostoc mesenteroides*. *Enzyme Microb Technol* 40:1124–1129.
 131. Overwin H, Wray V, Seeger M, Sepulveda-Boza S, Hofer B (2016) Flavanone and isoflavone glucosylation by non-Leloir glycosyltransferases. *J Biotech* 233:121-128.
 132. Su D, Robyt JF (1993) Control of the synthesis of dextran and acceptor-products by *Leuconostoc mesenteroides* B-512FM dextranucrase. *Carbohydr Res* 248:339-348.
 133. Brink LES, Tramper J, Luyben KCAM, Van 't Riet K (1988) Biocatalysis in organic media. *Enzyme Microb Technol* 10:736-743.
 134. Girard E, Legoy MD (1999) Activity and stability of dextranucrase from *Leuconostoc mesenteroides* NRRL B-512F in the presence of organic solvents. *Enzyme Microb Technol* 24:425-432.
 135. Meng X, Dobruchowska JM, Gerwig GJ, Kamerling JP, Dijkhuizen L (2015) Synthesis of oligo- and polysaccharides by *Lactobacillus reuteri* 121 reuteransucrase at high concentrations of sucrose. *Carbohydr Res* 414:85-92.

136. Wenzel TJ, van den Berg MA, Visser W, van den Berg JS, Steensma HY (1992) Characterization of *Saccharomyces cerevisiae* mutant lacking the E1 α subunit of the pyruvate dehydrogenase complex. *Eur J Biochem.* 209:697-705.
137. te Poele EM, Valk V, Devlamynck T, van Leeuwen S, Dijkhuizen L (2017) Catechol glucosides act as donor/acceptor substrates of glucansucrase enzymes of *Lactobacillus reuteri*. *Appl Microbiol Biotechnol* 101:4495-4505.
138. te Poele EM, Grijpstra P, van Leeuwen SS, Dijkhuizen L (2016) Glucosylation of catechol with the GtfA glucansucrase enzyme from *Lactobacillus reuteri* and sucrose as donor substrate. *Bioconjug Chem* 27:937-946.
139. De Winter K, Dewitte G, Dirks-Hofmeister ME, De Laet S, Pelantova H, Kren V, Desmet T (2015) Enzymatic glycosylation of phenolic antioxidants: Phosphorylase-mediated synthesis and characterization. *J Agric Food Chem* 63:10131-10139.
140. Prodanovic R, Milosavic N, Jovanovic S, Cirkovic T, Vujcic Z, Jankov R (2006) Stabilization of α -glucosidase in organic solvents by immobilization on macroporous poly(GMA-co-EGDMA) with different surface characteristics. *J Serb Chem Soc* 71:339-347.
141. Graebin NG, Schöffner JDN, Andrades DD, Hertz PF, Ayub MA, Rodrigues RC (2016) Immobilization of glycoside hydrolase families GH1, GH13, and GH70: State of the art and perspectives. *Molecules* 21:1074.
142. Karav S, Cohen JL, Barile D, de Moura Bell JM (2017) Recent advances in immobilization strategies for glycosidases. *Biotechnol Prog* 33:104-112.
143. Alcalde M, Plou FJ, Gómez de Segura A, Remaud-Simeon M, Willemot RM, Monsan P, Ballesteros A (1999) Immobilization of native and dextran-free dextransucrases from *L. mesenteroides* NRRL B-512F for the synthesis of glucooligosaccharides. *Biotechnol Tech* 13 749:755.
144. Kaboli H, Reilly PJ (1980) Immobilization and properties of *Leuconostoc mesenteroides* dextransucrase. *Biotechnol Bioeng* 22:1055-1069.
145. Monsan P, Lopez A (1981) On the production of dextran by free and immobilized dextransucrase. *Biotechnol Bioeng* 23:2027-2037.
146. Gomez de Segura A, Alcalde M, Yates M, Rojas-Cervantes ML, Lopez-Cortes N, Ballesteros A, Plou FJ (2004) Immobilization of dextransucrase from *Leuconostoc mesenteroides* NRRL B-512F on Eupergit C Supports. *Biotechnol Prog* 20:1414-1420.
147. Kothari D, Baruah R, Goyal A (2012) Immobilization of glucansucrase for the production of gluco-oligosaccharides from *Leuconostoc mesenteroides*. *Biotechnol Lett* 34:2101-2106.
148. Tanriseven A, Dogan S (2002) Production of isomalto-oligosaccharides using dextransucrase immobilized in alginate fibres. *Proc Biochem* 37:1111-1115.
149. Verhaeghe T, De Winter K, Berland M, De Vreese R, D'hooghe M, Offmann B, Desmet T (2016) Converting bulk sugars into prebiotics: semi-rational design of a transglucosylase with controlled selectivity. *Chem Commun* 52:3687-3689.
150. Nestl BM, Hauer B (2014) Engineering of flexible loops in enzymes. *ACS Catal* 4:3201-3211.

References

151. Liang C, Zhang Y, Jia Y, Wang W, Li Y, Lu S, Jin JM, Tang SY (2016) Engineering a carbohydrate-processing transglycosidase into glycosyltransferase for natural product glycodiversification. *Sci Reports* 6:21051.
152. Buchholz K, Seibel J (2003) Isomaltooligosaccharides. *Oligosaccharides in Food and Agriculture* 63-75 (Eggleston G, Cote GL, Eds.), Oxford University Press, Washington DC.
153. Buchholz K, Noll-Borchers M, Schwengers D (1998) Production of leucrose by dextranucrase. *Starch* 50:162-164.
154. Lina BA, Jonker D, Koziarowski G (2002) Isomaltulose (palatinose): A review of biological and toxicological studies. *Food Chem Toxicol* 40:1375-1381.
155. Hellmuth H, Wittrock S, Kralj S, Dijkhuizen L, Hofer B, Seibel J (2008) Engineering the glucansucrase GtfR enzyme reaction and glycosidic bond specificity: Toward tailor-made polymer and oligosaccharide products. *Biochemistry* 47:6678-6684.
156. Kelly RM, Dijkhuizen L, Leemhuis H (2009) Starch and α -glucan acting enzymes, modulating their properties by directed evolution. *J Biotechnol* 140:184-193.
157. Leemhuis H, Kelly RM, Dijkhuizen L (2009) Directed evolution of enzymes: Library screening strategies. *IUBMB Life* 61:222-228.
158. Turner NJ (2009) Directed evolution drives the next generation of biocatalysts. *Nat Chem Biol* 5:567-573.
159. Seibel J, Hellmuth H, Hofer B, Kicinska AM, Schmalbruch B (2006) Identification of new acceptor specificities of glycosyltransferase R with the aid of substrate microarrays. *ChemBioChem* 7:310-320.
160. Ojha S, Mishra S, Kapoor S, Chand S (2013) Synthesis of hexyl α -glucoside and α -polyglucosides by a novel *Microbacterium* isolate. *Appl Microbiol Biotechnol* 97:5293-5301.
161. Desmet T, Soetaert W (2012) Broadening the synthetic potential of disaccharide phosphorylases through enzyme engineering. *Proc Biochem* 47:11-17.
162. Monsan P, Remaud-Siméon M, André I (2010) Transglucosidases as efficient tools for oligosaccharide and glucoconjugate synthesis. *Curr Opin Microbiol* 13:293-300.
163. Yoon SH, Robyt JF (2002) Synthesis of acarbose analogues by transglycosylation reactions of *Leuconostoc mesenteroides* B-512FMC and B-742CB dextranucrases. *Carbohydr Res* 337:2427-2435.
164. Kim YMM, Yeon MJ, Choi NSS, Chang YHH, Jung MY, Song JJ, Kim JS (2010) Purification and characterization of a novel glucansucrase from *Leuconostoc lactis* EG001. *Microbiol Res* 165:384-391.
165. Auriol D, Nalin R, Robe P, Lefevre F (2012) Phenolic compounds with cosmetic and therapeutic applications. EP2027279.
166. Van Geel-Schutten GH, Faber E, Smit E, Bonting K, Smith M, Ten Brink B, Kamerling J, Vliegthart J, Dijkhuizen L (1999) Biochemical and structural characterization of the glucan and fructan exopolysaccharides synthesized by the *Lactobacillus reuteri* wildtype strain and by mutant strains. *Appl Environ Microbiol* 65:3008-3014.
167. Mayer RM (1987) Dextranucrase: a glycosyltransferase from *Streptococcus sanguis*. *Methods Enzymol* 138:649-661.

168. De Winter K, Cerdobbel A, Soetaert W, Desmet T (2011) Operational stability of immobilized sucrose phosphorylase: continuous production of α -glucose-1-phosphate at elevated temperatures. *Proc Biochem* 46:2074-2078.
169. Seo ES, Lee JH, Park JY, Kim D, Han HJ, Robyt JF (2005) Enzymatic synthesis and anti-coagulant effect of salicin analogs by using the *Leuconostoc mesenteroides* glucansucrase acceptor reaction. *J Biotechnol* 117:31-38.
170. Van Leeuwen SS, Leeflang BR, Gerwig GJ, Kamerling JP (2008) Development of a ^1H NMR structural-reporter-group concept for the primary structural characterisation of α -D-glucans. *Carbohydr Res* 343:1114-1119.
171. Bock K, Thøgersen H (1982) Nuclear magnetic resonance spectroscopy of mono- and oligosaccharides. *Annu Rep NMR Spectrosc* 13:2-57.
172. De Winter K, Verlinden K, Kren V, Weignerova L, Soetaert W, Desmet T (2013) Ionic liquids as cosolvents for glycosylation by sucrose phosphorylase: balancing acceptor solubility and enzyme stability. *Green Chem* 15:1949-1955.
173. Laane C, Boeren S, Vos K, Veeger C (1987) Rules for optimization of biocatalysis in organic solvents. *Biotech Bioeng* 30:81-87.
174. Carrea G (1984) Biocatalysis in water-organic solvent two-phase systems. *Trends Biotechnol* 2:102-106.
175. Eggers DK, Blanch HW, Prausnitz JM (1989) Extractive catalysis: Solvent effects on equilibria of enzymatic reactions in two-phase systems. *Enzyme Microb Technol* 11:84-89.
176. Hajipour S, Sarkaki A, Farbood Y, Eidi A, Mortazavi P, Valizadeh Z (2016) Effect of gallic acid on dementia type of Alzheimer disease in rats: Electrophysiological and histological studies. *Basic Clin Neurosci* 7:97-106.
177. Ortega-Arellano HF, Jimenez-Del-Rio M, Velez-Pardo C (2013) *Dmp53*, *basket* and *drICE* gene knockdown and polyphenol gallic acid increase life span and locomotor activity in a *Drosophila* Parkinson's disease model. *Genet Mol Biol* 36:608-615.
178. Demarche P, Junghanns C, Mazy N, Agathos SN (2012) Design-of-experiment strategy for the formulation of laccase biocatalysts and their application to degrade bisphenol A. *N Biotechnol* 30:96-103.
179. Brash JL, Horbett TA (1995) Proteins at interfaces: an overview. American Chemical Society pp. 1-23.
180. Kondo A, Urabe T (1995) Relationship between molecular states (conformation and orientation) and activities of α -amylase adsorbed on ultrafine silica particles. *Appl Microbiol Biotechnol* 43:801-807.
181. Hommes G, Gasser CA, Howald CB, Goers R, Schlosser D, Shahgaldian P, Corvini PF (2012) Production of a robust nanobiocatalyst for municipal wastewater treatment. *Bioresour Technol* 115:8-15.
182. Mateo C, Grazú V, Pessela BC, Montes T, Palomo JM, Torres R, López-Gallego F, Fernández-Lafuente R, Guisán JM (2007) Advances in the design of new epoxy supports for enzyme immobilization-stabilization. *Biochem Soc Trans* 35:1593-1601.

References

183. Li XD, Wu J, Jia DC, Wan YH, Yang N, Qiao M (2016) Preparation of cross-linked glucoamylase aggregates immobilization by using dextrin and xanthan gum as protecting agents. *Catalysts* 6, DOI:10.3390/catal6060077.
184. De Winter K, Soetaert W, Desmet T (2012) An imprinted cross-linked enzyme aggregate (iCLEA) of sucrose phosphorylase: Combining improved stability with altered specificity. *Int J Mol Sci* 13:11333-11342.
185. Geuns J (2003) Stevioside. *Phytochemistry* 64:913-921.
186. Goyal SK, Samsher, Goyal RK (2010) Stevia (*Stevia rebaudiana*) a bio-sweetener: a review. *Int J Food Sci Nutr* 61:1-10.
187. Puri M, Sharma D, Tiwari AK (2011) Downstream processing of stevioside and its potential applications. *Biotechnol Adv* 29:781-791.
188. DuBois GE, Prakash I (2012) Non-caloric sweeteners, sweetness modulators, and sweetener enhancers. *Annu Rev Food Sci Technol* 3:353-380.
189. Yadav SK, Guleria P (2012) Steviol glycosides from *Stevia*: biosynthesis pathway review and their application in foods and medicine. *Crit Rev Food Sci Nutr* 52:988-998.
190. Brandle JE, Starratt AN, Gijzen M (1998) *Stevia rebaudiana*: Its agricultural, biological, and chemical properties. *Can J Plant Sci* 78:527-536.
191. Ceunen S, Geuns JMC (2013) Steviol glycosides: chemical diversity, metabolism, and function. *J Nat Prod* 76:1201-1228.
192. Risso D, Morini G, Pagani L, Quagliariello A, Giuliani C, De Fanti S, Sazzini M, Luiselli D, Tofanelli S (2014) Genetic signature of differential sensitivity to stevioside in the Italian population. *Genes Nutr* 9:401.
193. Wölwer-Rieck U (2012) The leaves of *Stevia rebaudiana* (Bertoni), their constituents and the analyses thereof: a review. *J Agric Food Chem* 60:886-895.
194. Li X, Staszewski L, Xu H, Durick K, Zoller M, Adler E (2002) Human receptors for sweet and umami taste. *Proc Natl Acad Sci USA* 99:4692-4696.
195. Nelson G, Hoon MA, Chandrashekar J, Zhang Y, Ryba NJ, Zuker CS (2001) Mammalian sweet taste receptors. *Cell* 106:381-390.
196. Ohtani K, Aikawa Y, Fujisawa Y, Kasai R, Tanaka O, Yamasaki K (1991) Solubilization of steviolbioside and steviolmonoside with gamma-cyclodextrin and its application to selective syntheses of better sweet glycosides from stevioside and rubusoside. *Chem Pharm Bull (Tokyo)* 39:3172-3174.
197. van Leeuwen SS, Kralj S, Gerwig GJ, Dijkhuizen L, Kamerling JP (2008) Structural analysis of bioengineered α -D-glucan produced by a triple mutant of the glucansucrase GTF180 enzyme from *Lactobacillus reuteri* strain 180: generation of $(\alpha 1 \rightarrow 4)$ linkages in a native $(1 \rightarrow 3)(1 \rightarrow 6)$ - α -D-glucan. *Biomacromolecules* 9:2251-2258.
198. Box G, Wilson K (1951) On the experimental attainment of optimum conditions (with discussion). *J R Stat Soc Series B* 13:1-45.
199. Box G, Behnken D (1960) Some new three level designs for the study of quantitative variables. *Technometrics* 2:455-475.
200. JMP®, Version 12. SAS Institute Inc., Cary, NC, 1989-2007.

201. LeadIT 2.1.8. (2014) BioSolveIT GmbH.
202. Upreti M, Smit JP, Hagen EJ, Smolenskaya VN, Prakash I (2012) Single crystal growth and structure determination of the natural 'high potency' sweetener rebaudioside A. *Cryst Growth Des* 12:990-993.
203. SeeSAR 3.3. (2015) BioSolveIT GmbH.
204. Schrödinger L (2013) The PyMOL Molecular Graphics System, Version 1.6.x.
205. Damásio MH, Costell E (1991) Analisis sensorial descriptivo: Generacion de descriptores y seleccion de catadores. *Rev Agroquim Y Tecnol Aliment* 31:165-178.
206. Amerine MA, Pangborn RM, Roessler EB (1965) Principles of sensory evaluation of food. Academic Press.
207. Schiffman SS, Sattely-Miller EA, Bishay IE (2007) Time to maximum sweetness intensity of binary and ternary blends of sweeteners. *Food Qual Prefer* 18:405-415.
208. Jamieson P (2008) The sugarfree toolbox – Bulk ingredients and intense sweeteners. *Manuf Confect* 88:33-46.
209. Fujimaru T, Park JH, Lim J (2012) Sensory characteristics and relative sweetness of tagatose and other sweeteners. *J Food Sci* 77:323-328.
210. Tukey JW (1953) The problem of multiple comparisons. Princeton University.
211. Games P, Howell J (1976) Pairwise multiple comparison procedures with unequal N's and/or variances: a Monte Carlo study. *J Educ Stat* 1:113-125.
212. Prakash I, DuBois GE, Clos JF, Wilkens KL, Fosdick LE (2008) Development of Rebiana, a natural, non-caloric sweetener. *Food Chem Toxicol* 46:75-82.
213. World Health Organization (2007) The challenge of obesity in the WHO European Region and the strategies for response. <http://www.who.int>
214. Field AE, Coakley EH, Must A, Spadano JL, Laird N, Dietz WH, Rimm E, Colditz GA (2001) Impact of overweight on the risk of developing common chronic diseases during a 10-year period. *Arch Intern Med* 161:1581-1586.
215. Gregg EW, Cheng YJ, Cadwell BL, Imperatore G, Williams DE, Flegal KM, Narayan KM, Williamson DF (2005) Secular trends in cardiovascular disease risk factors according to body mass index in US adults. *JAMA* 293:1868-1874.
216. Calle EE, Rodriguez C, Walker-Thurmond K, Thun MJ (2003) Overweight, obesity, and mortality from cancer in a prospectively studied cohort of US adults. *N Engl J Med* 348:1625-1638.
217. Te Morenga LA, Mann J, Mallard S (2013) Dietary sugars and body weight: systematic review and meta-analyses of randomised controlled trials and cohort studies. *BMJ* 346:e7492.
218. Sun YH (2008) Health concern, food choice motives, and attitudes toward healthy eating: The mediating role of food choice motives. *Appetite* 51:42-49.
219. Bearth A, Cousin ME, Siegrist M (2014) The consumer's perception of artificial food additives: Influences on acceptance, risk and benefit perceptions. *Food Qual Prefer* 38:14-23.
220. Faus I (2000) Recent developments in the characterization and biotechnological production of sweet-tasting proteins. *Appl Microbiol Biotechnol* 53:145-151.

References

221. Liu HM, Sugimoto N, Akiyama T, Maitani T (2000) Constituents and their sweetness of food additive enzymatically modified licorice extract. *J Agr Food Chem* 48: 6044-6047.
222. Murata Y, Yoshikawa S, Suzuki YA, Sugiura M, Inui H, Nakano Y (2006) Sweetness characteristics of the triterpene glycosides in *Siraitia grosvenori*. *J Jpn Soc Food Sci* 53:527-533.
223. Prawitt D, Monteilh-Zoller MK, Brixel L, Spangenberg C, Zabel B, Fleig A, Penner R (2003) TRPM5 is a transient Ca²⁺-activated cation channel responding to rapid changes in [Ca²⁺]_i. *Proc Natl Acad Sci USA* 100:15166-15171.
224. Colsool B, Schraenen A, Lemaire K, Quintens R, Van Lommel L, Segal A, Owsianik G, Talavera K, Voets T, Margolskee RF, Kokrashvili Z, Gilon P, Nilius B, Schuit FC, Vennekens R (2010) Loss of high-frequency glucose-induced Ca²⁺ oscillations in pancreatic islets correlates with impaired glucose tolerance in *Trpm5*^{-/-} mice. *Proc Natl Acad Sci USA* 107:5208-5213.
225. Philippaert K, Pironet A, Mesuere M, Sones W, Vermeiren L, Kerselaers S, Pinto S, Segal A, Antoine A, Gysemans C, Laureys J, Lemaire K, Gilon P, Cuypers E, Tytgat J, Mathieu C, Schuit F, Rorsman P, Talavera K, Voets T, Vennekens R (2017) Steviol glycosides enhance pancreatic beta-cell function and taste sensation by potentiation of TRPM5 channel activity. *Nat Commun* 8:14733.
226. Sips NCAP, Vercauteren RLM (2011). Sweetener compositions with reduced bitter off taste and methods of preparing. WO 2011143465.
227. Ciucanu I, Kerek F (1984) A simple and rapid method for the permethylation of carbohydrates. *Carbohydr Res* 131:209-217.
228. Kamerling JP, Gerwig GJ (2007) Strategies for the structural analysis of carbohydrates. In Kamerling JP, Boons GJ, Lee YC, Suzuki A, Taniguchi N, Voragen AGJ (Eds), *Comprehensive Glycoscience - From Chemistry to Systems Biology*, Elsevier Ltd, Oxford, Vol. 2, pp1-68.
229. Levitt MH, Freeman R, Frenkiel T (1982) Broad-band heteronuclear decoupling. *J Magn Reson* 47:328-330.
230. Musa A, Gasmalla MAA, Miao M, Zhang T, Aboshora W, Eibaid A, Jiang B (2014) Separation and structural characterization of tri-glucosyl-stevioside. *J Acad Ind Res* 2:593-598.
231. Musa A, Miao M, Gasmalla MAA, Zhang T, Eibaid A, Aboshora W, Jiang B (2015) Effect of shaking velocity on mono-glycosyl-stevioside productivity via alternansucrase acceptor reaction. *J Mol Catal B: Enzym* 116:106-112.
232. Broers NJ, Boer VM, Lawrence AG (2015) Diterpene production in *Yarrowia*. WO2015011209.
233. Tufvesson P, Lima-Ramos J, Nordblad M, Woodley JM (2011) Guidelines and cost analysis for catalyst production in biocatalytic processes. *Org Process Res Dev* 15:266-274.
234. Bai Y, van der Kaaij RM, Woortman AJJ, Jin Z, Dijkhuizen L (2015) Characterization of the 4,6- α -glucanotransferase GTFB enzyme of *Lactobacillus reuteri* 121 isolated from inclusion bodies. *BMC Biotechnol* 15:49.

235. Jørgensen OB, Karlsen LG, Nielsen NB, Pedersen S, Rugh S (1988) A new immobilized glucose isomerase with high productivity produced by a strain of *Streptomyces murinus*. *Starch Stärke* 40:307-313.
236. Kobayashi M, Nagasawa T, Yamada H (1992) Enzymatic synthesis of acrylamide: a success story not yet over. *Trends Biotechnol* 10:402-408.
237. Yoon S, Mukerjea R, Robyt JF (2003) Specificity of yeast (*Saccharomyces cerevisiae*) in removing carbohydrates by fermentation. *Carbohydr Res* 338:1127-1132.
238. Hahn JJ, Evans JC, Myerson AS, Oolman T, Rhonemus TA, Tyler CA, Storo KM (2008) Method of producing purified rebaudioside A compositions using solvent/antisolvent crystallization. WO2008091547.
239. Liu Y, Di D, Bai Q, Li J, Chen Z, Lou S, Ye H (2011) Preparative separation and purification of rebaudioside A from steviol glycosides using mixed-mode macroporous adsorption resins. *J Agr Food Chem* 59:9629-9636.
240. Rozzell JD (1999) Commercial scale biocatalysis: myths and realities. *Bioorg Med Chem* 7:2253-2261.
241. Prakash I, Clos JF, Chaturvedula VSP (2012) Stability of rebaudioside A under acidic conditions and its degradation products. *Food Res Int* 48:65-75.
242. Musa A, Miao M, Gasmalla MAA, Zhang T, Eibaid A, Aboshora W, Jiang B (2014) Stability of stevioside and glucosyl-stevioside under acidic conditions and its degradation products. *J Food Nutr Res* 2:198-203.
243. Gong Q, Bell LN (2013) Degradation kinetics of rebaudioside A in various buffer solutions. *Int J Food Sci Tech* 48:2500-2505.
244. Lang H (1948) Simplified approach to preliminary cost estimates. *Chem Eng* 55:112.
245. Fox M, Akkerman C, Straatsma H, de Jong P (2010) Energy reduction by high dry matter concentration and drying. *Spray drying*, NIZO Food Research, pages 6-8.
246. Horowitz RM, Gentili B (1963) Dihydrochalcone derivatives and their use as sweetening agents. US3087821.
247. Borrego F, Castillo J, Benavente-García O, Del Rio JA (1991) Application potential of the citrus origin sweetener neohesperidin dihydrochalcone. *Intl Food Ingredients* 2:23-26.
248. Frydman A, Weissshaus O, Huhman DV, Sumner LW, Bar-Peled M, Lewinsohn E, Fluhr R, Gressel J, Eyal Y (2005) Metabolic engineering of plant cells for biotransformation of hesperidin into neohesperidin, a substrate for production of the low-calorie sweetener and flavor enhancer NHDC. *J Agric Food Chem* 53:9708-9712.
249. Roowi S, Crozier A (2012) Flavonoids in tropical Citrus species. *J Agric Food Chem* 60:12217-12225.
250. She G, Wang S, Liu B (2011) Dihydrochalcone glycosides from *Oxytropis myriophylla*. *Chem Central J* 5:71-73.
251. Perez Gutierrez RM, Garcia Campoy AH, Muñoz Ramirez A (2016) Properties of flavonoids isolated from the bark of *Eysenhardtia polystachya*, and their effect on oxidative stress in streptozotocin-induced diabetes mellitus in mice. *Oxid Med Cell Longev*, DOI:10.1155/2016/9156510.

References

252. DuBois GE, Crosby GA, Stephenson RA (1981) Dihydrochalcone sweeteners. A study of the atypical temporal phenomena. *J Med Chem* 24:408-428.
253. Schiffman SS, Sattely-Miller EA, Graham BG, Booth BJ, Gibes KM (2000) Synergism among ternary mixtures of fourteen sweeteners. *Chem Senses* 25:131-140.
254. Schiffman SS, Booth BJ, Carr BT, Losee ML, Sattely-Miller EA, Graham BG (1995) Investigation of synergism in binary mixtures of sweeteners. *Brain Res Bull* 38:105-120.
255. Engel LD, Stagnitti G (1997) Flavor modifying composition. WO1996017527.
256. Felisaz D, Jacquier Y (1999) Taste masking powders for pharmaceuticals. WO1999027915.
257. Felisaz D, Sinet N, Thieblemont C (2007) Powdered sweetener for human nutrition. WO2006012763.
258. Sun B, Tang L, Lu W, Chen Z, Yi Y, Wu B (2012) Sweetener composition. WO2011066754.
259. Abraham J, Mathew F (2014) Taste masking of paediatric formulation: A review on technologies, recent trends and regulatory aspects. *Int J Pharm Pharm Sci* 6:12-19.
260. Shi Q, Song XF, Fu JL, Su CY, Xia XM, Song EQ, Song Y (2015) Artificial sweetener neohesperidin dihydrochalcone showed antioxidative, anti-inflammatory and anti-apoptosis effects against paraquat-induced liver injury in mice. *Int Immunopharmacol* 29:722-729.
261. Su CY, Xia XM, Shi Q, Song XF, Fu JL, Xiao CX, Chen HJ, Lu B, Sun ZY, Wu SM, Yang SY, Li XG, Ye XL, Song EQ, Song Y (2015) Neohesperidin dihydrochalcone versus CCl₄-induced hepatic injury through different mechanisms: the implication of free radical scavenging and Nrf2 activation. *J Agric Food Chem* 63:5468-5475.
262. Choi JM, Yoon BS, Lee SK, Hwang JK, Ryang R (2007) Antioxidant properties of neohesperidin dihydrochalcone: inhibition of hypochlorous acid-induced DNA strand breakage, protein degradation, and cell death. *Biol Pharm Bull* 30:324-330.
263. Xia XM, Fu JL, Song XF, Shi Q, Su CY, Song EQ, Song Y (2015) Neohesperidin dihydrochalcone down-regulates MyD88-dependent and -independent signaling by inhibiting endotoxin-induced trafficking of TLR4 to lipid rafts. *Free Radic Biol Med* 89:522-532.
264. Daly K, Darby AC, Hall N, Nau A, Bravo D, Shirazi-Beechey SP (2014) Dietary supplementation with lactose or artificial sweetener enhances swine gut *Lactobacillus* population abundance. *Br J Nutr* 111:S30-S35.
265. Benavente-García O, Castillo J, Del Baño MJ, Lorente J (2001) Improved water solubility of neohesperidin dihydrochalcone in sweetener blends. *J Agric Food Chem* 49:189-191.
266. Caccia F, Dispenza R, Fronza G, Fuganti C, Malpezzi L, Mele A (1998) Structure of neohesperidin dihydrochalcone/ β -cyclodextrin inclusion complex: NMR, MS, and X-ray spectroscopic investigation. *J Agric Food Chem* 46:1500-1505.
267. Cho JS, Yoo SS, Cheong TK, Kim MJ, Kim Y, Park KH (2000) Transglycosylation of neohesperidin dihydrochalcone by *Bacillus stearothermophilus* maltogenic amylase. *J Agric Food Chem* 48:152-154.
268. Sharma OP, Bhat TK (2009) DPPH antioxidant assay revisited. *Food Chem* 113:1202-1205.
269. Maltese F, Erkelens C, Van der Kooy F, Choi YH, Verpoorte R (2009) Identification of natural epimeric flavone glycosides by NMR spectroscopy. *Food Chem* 116:575-579.

Dankwoord

Een doctoraat is nooit het werk van de promovendus alleen, al zeker niet wanneer het gaat over een gezamenlijk doctoraat. Ik heb het geluk gehad om onderzoek te mogen doen in twee landen, twee universiteiten én een pilot plant. Er is waarschijnlijk niemand die de afgelopen 4 jaar meer gereisd heeft van Gent naar het Verre Noorden en omgekeerd. En er is waarschijnlijk niemand die beter weet waar de beste koffie en lekkerste hamburgers te vinden zijn op de schier eindeloze A6 doorheen Flevoland. Gelukkig heb ik me altijd thuis gevoeld in zowel Gent als Groningen, de gezelligste steden van respectievelijk België en Nederland. Daarom is het heel passend om een aantal mensen te bedanken die meegeholpen hebben aan mijn doctoraat maar ook aan het gevoel van thuiskomen dat ik altijd ervaar nadat ik weer eens ettelijke uren in de auto heb versleten.

Eerst en vooral zou ik graag mijn promotoren, prof. Lubbert Dijkhuizen en prof. Wim Soetaert, bedanken. Enerzijds om mij voldoende vertrouwen te schenken om te doen wat ik dacht dat het beste was, met als gevolg enkele successen maar ook veel mislukkingen en, daaraan gekoppeld, veel leermomenten. Daarnaast ook om twee uitstekende doch verschillende voorbeelden te zijn van de ondernemende wetenschapper, iets waar ik veel van opgestoken heb. Mijn dank gaat ook uit naar de leden van de leescommissie, prof. Remko Boom, prof. Gert-Jan Euverink, prof. Dick Janssen, en prof. John Van Camp, voor het kritisch nalezen van mijn thesis.

Aangezien ik de eerste twee jaren van mijn doctoraat doorgebracht heb in Groningen en er bovendien niets boven Groningen gaat, moet ik dit dankwoord wel verderzetten met de mensen die ik in de Parel van het Noorden heb ontmoet. Eerst en vooral moet ik Evelien te Poele bedanken voor de dagelijkse begeleiding gedurende deze eerste twee jaren, inclusief gezamenlijk HPLC-gevloek, en de vruchtbare samenwerking nadien. Wat mij altijd het meest gecharmeerd heeft aan de Microbiële Fysiologie-groep is de ongedwongen en multiculturele sfeer die er heerste, en natuurlijk de vrijdagse borrels. Het was een plezier om een kantoorruimte te delen met Yuxiang, Ana, en Markus. Het ventileren van onze gelijkaardige frustraties liet me toe om alles te relativiseren en niet op te geven. Een speciaal woord van dank gaat uit naar Xiangfeng, wiens onderzoek het dichtst aansloot bij het mijne. Jouw kennis over glucansucrases was onovertroffen, net

als je vermogen om onvermoeibaar nieuwe enzymmutanten te produceren. Structuurbepaling vormde een essentieel deel van mijn doctoraat en was niet mogelijk geweest zonder de hulp van experts prof. Hans Kamerling, dr. Gerrit Gerwig en dr. Sander van Leeuwen. Ook bedankt voor het kritisch nalezen van mijn manuscripten. Het lab werd al die tijd draaiende gehouden door Pieter die nooit te verlegen was om iedereen, mezelf inclusief, te wijzen op hun tekortkomingen, waarvoor mijn excuses en dank. Laura, bedankt voor jouw luisterend oor, zowel binnen als buiten het lab. Jouw vriendschap en opgewektheid vormden belangrijke steunpilaren gedurende al deze jaren. Joana, als baken van rust en kalmte vormde je tevens een vat vol levenswijsheden en enzymknowhow. Bedankt ook voor het herhaaldelijk uitlenen van buffers wanneer ik vanuit Gent naar Groningen kwam om vlug een aantal experimenten te doen. Lara en Ana, twee handen op één buik waarmee ik veel plezier heb beleefd maar ook moeilijkere momenten heb gedeeld, bedankt hiervoor. En dan zou ik bijna HaJö vergeten: ik spreek voor velen als ik zeg dat jouw humor een typisch grijze Groningse dag in één klap veel zonniger kon maken. Ik mag zeker ook Bea, Manon en later Anmara niet vergeten te bedanken voor de altijd vriendelijke behulpzaamheid bij allerhande administratieve rompslomp. Ook Hien, Huifang, Justyna, Elena, Mirjan, Alicia, Maarten, Jelle, Cecile, Geralt en Vincent: bedankt voor de goeie sfeer op het lab! Daarnaast wil ik ook enkele mensen van buiten het lab bedanken: Guti, wij vormden een onnavolgbaar duo op de flanken van VVK Groningen Zaterdag 2 en hebben samen menig verdediging geterroriseerd, tenminste als we niet geblesseerd waren. Natuurlijk wil ik ook de andere medespelers bedanken voor de altijd welgekomen ontspanning op donderdag en zaterdag. Vele vrijdagavonden, soms ook zaterdagavonden, heb ik doorgebracht in etablissementen zoals Papa Joe, Ribhouse Bronco, Chupitos, Het Feest en mijn favoriete Grieks eetcafé Fortuna. Bedankt aan iedereen die hier bij was: Javi, Joost en alle anderen die al vermeld zijn.

Dit brengt me bij mijn periode in Gent die ik deels gependeed heb in het lab van Bio Base Europe Pilot Plant (BBEPP), deels in het lab van InBio. Het was niet evident om na twee jaar in Groningen het onderzoek eigenlijk opnieuw op te starten. De mensen van BBEPP die het nauwst betrokken waren bij mijn

onderzoek waren Rakesh, bedankt om mij te helpen met de fermentaties, Emile, bedankt voor de discussies met betrekking tot DSP, en An, bedankt om mij bij te staan bij de HPLC-analyses. Ook een dankjewel aan alle anderen die altijd klaar stonden om mijn vragen te beantwoorden op de meest ongeschikte momenten. Natuurlijk moet ik vooral Koen bedanken: dankzij jouw inzet en werklust is mijn thesis sterker en completer geworden! Het doet me plezier dat we nu opnieuw collega's zijn. Daarnaast ben ik ook dankbaar voor de productieve samenwerking met Davy, Allison en Griet van SensoLab in het kader van het Finesweet-project. De resulterende data maken van mijn thesis een veel mooier geheel. Naar het einde van mijn doctoraat toe begon ik ook meer tijd door te brengen in het lab van InBio. Het was vreemd om na vier jaar terug te zijn op de plek waar het voor mij allemaal ooit begon en (opnieuw) vele nieuwe gezichten te zien. Maar ook hier was de sfeer in het lab en vooral in de Happy Side fantastisch! Robin, Veerle, Mol, Yatti, Nico, Marilyn, Lisa, Sofie, Sophie, Anke, Gilles, Isabelle, Anneleen en Barbara: jullie waren allen heel behulpzaam wanneer ik weer eens in de war was over de lokale labgewoontes en hebben ervoor gezorgd dat ik me ook bij InBio onmiddellijk thuis voelde. Bedankt hiervoor en veel succes met jullie doctoraten! In het bijzonder wil ik Dominique bedanken voor het verlichten van mijn kopzorgen bij al het gedoe rond het administratieve aspect van het gezamenlijk doctoraat.

Het wordt veel gezegd maar is daarom niet minder waar: Mijn ouders zijn altijd heel ondersteunend geweest in al de beslissingen die ik de laatste jaren genomen heb, niet alleen financieel maar zeker ook door middel van veel goede raad. Ook de grote volumes meeneemstoofvlees werden erg geapprecieerd! In die zin hebben ze misschien wel het meest bijgedragen aan het afwerken van dit doctoraat. Bedankt hiervoor!

Tenslotte wil ik ook Marta bedanken voor alle steun en liefde de afgelopen drie jaar. We hebben ons doctoraat ongeveer in dezelfde periode afgewerkt en de resulterende wetenschappelijke discussies hebben veel bijgedragen aan dit werk. Maar vooral bedankt om er te zijn tijdens de moeilijke momenten, mijn culturele horizon te verbreden en me een beter mens te maken. Merci!

Over de jaren heen heb ik veel gemijmerd over hoe een mogelijk dankwoord er zou kunnen uitzien. Nu het eindelijk is neergeschreven betekent dit dat het einde van een mooie periode nabij is. Nogmaals merci aan iedereen voor al de mooie herinneringen!

Tim

26 september 2017

Curriculum vitae

Tim Devlamynck (° 12 January 1990)

Education

- 2015 - 2017 **PhD student**, Faculty of Bioscience Engineering, Ghent University, Ghent, Belgium
- 2013 - 2015 **PhD student**, Groningen Biomolecular Sciences and Biotechnology Institute, University of Groningen, Groningen, Netherlands
- 2008 - 2013 **Master in Bioscience Engineering**, option Chemistry and Bioprocess Technology, Faculty of Bioscience Engineering, Ghent University, Ghent, Belgium
- 2006 - 2008 **Latin-Sciences**, Sint-Jozefsinstituut-College, Torhout, Belgium
- 2002 - 2006 **Latin**, Margareta-Maria-Instituut, Kortemark, Belgium

List of publications

te Poele EM, Devlamynck T, Jäger M, Gerwig GJ, Van de Walle D, Dewettinck K, Hirsch AKH, Kamerling JP, Soetaert W, Dijkhuizen L (2017) Glucansucrase (mutant) enzymes from *Lactobacillus reuteri* 180 efficiently transglucosylate *Stevia* component rebaudioside A, resulting in a superior taste. Sci Reports. Submitted for publication.

te Poele EM, Valk V, Devlamynck T, van Leeuwen S, Dijkhuizen L (2017) Catechol glucosides act as donor/acceptor substrates of glucansucrase enzymes of *Lactobacillus reuteri*. Appl Microbiol Biotechnol 101:4495-4505.

Devlamynck T, te Poele EM, Meng X, van Leeuwen S, Dijkhuizen L (2016) Glucansucrase Gtf180-ΔN of *Lactobacillus reuteri* 180: Enzyme and reaction

engineering for improved glycosylation of non-carbohydrate molecules. *Appl Microbiol Biotechnol* 100:7529-7539.

De Winter K, Desmet T, Devlamynck T, Van Renterghem L, Verhaeghe T, Pelantová H, Křen V, Soetaert W (2014) Biphasic catalysis with disaccharide phosphorylases: chemoenzymatic synthesis of α -D-glucosides using sucrose phosphorylase. *Org Process Res Dev* 18:781-787.